Novel role of the AT-HOOK MOTIF NUCLEAR LOCALIZED 15 gene in Arabidopsis meristem activity and longevity

Rahimi, A.

Novel role of the *AT-HOOK MOTIF NUCLEAR LOCALIZED 15* gene in Arabidopsis meristem activity and longevity

Arezoo Rahimi

Arezoo Rahimi

Novel role of the *AT-HOOK MOTIF NUCLEAR LOCALIZED 15* gene in Arabidopsis meristem activity and longevity

PhD Thesis, Leiden University, 2020

This work was performed in the Molecular and Developmental Genetics department at the Institute of Biology Leiden of Leiden University, The Netherlands.

Cover designed by Arezoo Rahimi

Printed by Gildeprint, Enschede, The Netherlands

Novel role of the *AT-HOOK MOTIF NUCLEAR LOCALIZED 15* gene in Arabidopsis meristem activity and longevity

Proefschrift

Ter verkrijging van
de graad van Doctor aan de Universiteit Leiden,
op gezag van de Rector Magnificus Prof. Mr. C.J.J.M. Stolker,
volgens besluit van het College voor Promoties
te verdedigen op dinsdag 1 september 2020
klokke 11.15 uur

door

Arezoo Rahimi
Geboren te Dehgolan, Iran
18th January 1987

Thesis committee

Promotors:	Prof. dr. R. Offringa
	Prof. dr. P.J.J. Hooykaas
Promotiecommissie:	Prof. dr . G. P. van Wezel
	Prof. dr . J. Memelink
	Dr. F. Lens (LU gast UD/Naturalis)
	Prof. R. Immink (Wageningen University & Research)
	Dr. K. Kajala (Universiteit Utrecht)

In memory of my father,

To my mother for her endless Love
And to my hero, Omid

Contents

Chapter 1

General introduction

Arezoo Rahimi[1] **and Remko Offringa**[1]

[1]Plant Developmental Genetics, Institute of Biology Leiden, Leiden University, Sylviusweg 72, 2333 BE Leiden, Netherlands

Unlike animals, higher plants have the unique ability to continuously produce new tissues and organs in the apical and lateral direction throughout their life span via proliferation of pluripotent stem cells organized in niches called meristems. As sessile organisms, this allows plants to replace organs that are lost due to pathogen attack or herbivory, and also to adapt their architecture or developmental program in response to (adverse) abiotic environmental signals. The stem cells in meristems self-renew through asymmetric cell division, producing a daughter cell that maintains stem-cell identity and a second daughter cell that differentiates into a more specialized cell type (Soyars et al., 2016).

In angiosperm plants, two stem-cell niches are generated during embryogenesis: the shoot apical meristem (SAM) and root apical meristem (RAM). These apical meristems produce primary meristems such as the protoderm, which gives rise to the outside cell layer or epidermis of the plant; the procambium, which produces the xylem and phloem for water and nutrient transport, respectively; and the cambium, responsible for secondary growth controlling the thickness of stems and roots. All aboveground organs of the plant are produced by the SAM or by so-called axillary meristems (AMs) that arise in axils of leaves, whereas the RAM produces the cell layers of the main root, including the pericycle stem-cell layer, which produces the lateral roots, and thus determines the branching of the plant root system (Uchida and Torii, 2019).

During growth and development of the plant, the position of new organs or tissues within the plant body depends on the activity and communication between the different plant meristems. In this chapter, we review the current knowledge about the mechanisms controlling initiation, development, and activity of meristems.

The role of the shoot apical meristem in growth and development

The post-embryonic formation of all aerial plant parts depends on the activity of the SAM. The SAM in Arabidopsis is divided into four different zones: 1) the central zone (CZ), 2) the peripheral zone (PZ), 3) the rib meristem (RM) also referred to as organizing center (OC) and 4) the rib zone (RZ), which is located below the OC and produces the internal part of the stem (Fig. 1). The CZ consists of pluripotent stem cells that by continuous division maintain the stem cell niche, and displace daughter cells into the PZ, where the lateral organs such as leaves or flowers are formed. Slow stem cell divisions in the CZ also displace daughter cells downwards into the RM/OC. The OC controls stem-cell proliferation in the CZ and differentiation in the PZ and in this way maintains the function and organization of the SAM (Murray et al., 2012; Soyars et al., 2016).

Previous genetic studies have shown that the specification and maintenance of stem cells in the SAM is regulated by many factors, including transcriptional regulators, receptor kinases, miRNAs, small peptides, epigenetic marks, and plant hormones (Dodsworth, 2009; Bustamante et al., 2016; Somssich et al., 2016). *CLAVATA3 (CLV3)* and *WUSCHEL (WUS)*, are key factors that help the SAM to stay functional and organized. Arabidopsis plants mutated in *WUS* have no functional SAM. The spatial feedback loop between the WUS homeodomain transcription factor and the CLV3/CLV1 peptide ligand/receptor kinase maintains the cell identity in the OC. *WUS* is expressed in the OC, and can induce *CLV3* expression by moving to the CZ. In turn, the CLV3 peptide moves back to the OC where it

represses *WUS* expression by binding to the CVL1 receptor kinase (Somssich et al., 2016). Two main plant hormones, cytokinin and auxin, play an important role in the SAM regulatory network. Cytokinin (CK) is essential for continuous cell division in meristematic tissues, as it activates both *WUS* and *CLV3* expression, enabling *WUS* induction independent of the *CLV* pathway via the type-B ARABIDOPSIS RESPONSE REGULATOR transcription factors (type-B ARRs). Auxin, through its directional intercellular transport by the PIN FORMED (PIN) auxin efflux carriers, promotes cell differentiation and formation of lateral organs such as leaves and flowers (Reinhardt et al., 2000; Murray et al., 2012). Besides its role in organ initiation, auxin helps to maintain a balance between stem-cell activity and organ formation by regulating the CK signaling suppressing type-A ARRs, mediated by the AUXIN RESPONSE FACTOR (ARF) transcription factor MONOPTEROS (MP/ARF5). MP directly represses the expression of the type-A *ARR7* and *ARR15* genes, which subsequently enhances CK signaling (Zhao et al., 2010). At the same time, MP represses CK signaling by inducing the expression of the *ARABIDOPSIS HISTIDINE PHOSPHOTRANSFER PROTEIN 6* (*AHP6*) gene (Besnard et al., 2014).

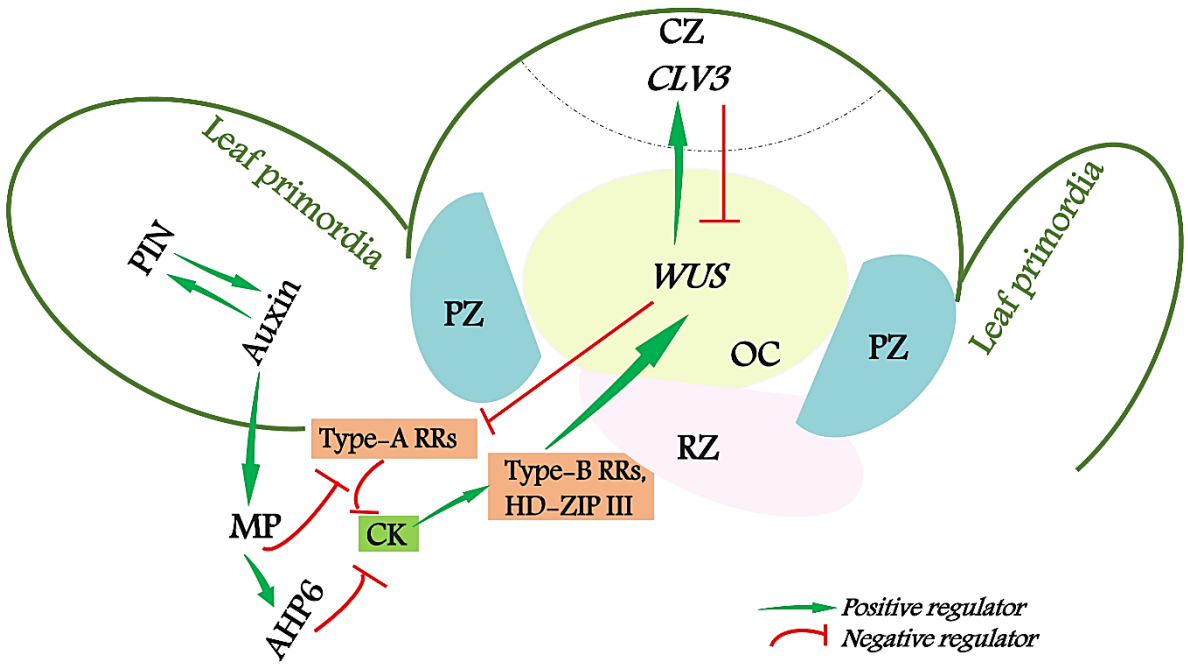

Figure 1. Main elements controlling shoot apical meristem (SAM) activity. The CLV3 peptide is expressed in the central zone (CZ) consisting of pluripotent stem cells. *WUS* is expressed in the organizing center (OC) and activates *CLV3* expression by moving to the CZ. CLV3 moves back to the OC, where negative feedback signaling by binding to the CLV1 receptor kinase represses *WUS* expression. The hormone cytokinin (CK) activates type-B ARRs, which by binding to the class III homeodomain–leucine zipper (HD-ZIP III) transcription factors promote *WUS* expression. WUS itself negatively regulates type-A ARRs (a negative regulator of CK signaling) in order to maintain CK signaling. Auxin in turn modulates stem-cell activity by repressing type-A ARR and inducing AHP6 expression through the ARF transcription factor MP/ARF5.

Post-embryonic shoot development in plants progresses through several distinct developmental phases, starting with the juvenile vegetative, and followed successively by the adult vegetative and the reproductive phases (Fig. 2). The transitions between these developmental phases are regulated mainly in the SAM, as in each phase the SAM produces new organs with different morphological features (Poethig, 2013). The SAM produces morphogenetic units called phytomers in the vegetative phase consisting of a stem, a node, and a leaf, with an axillary meristem (AM) in the axil of the leaf. AMs constitute another shoot meristem that can act as a SAM. They are thought to originate from the SAM and play an important role in secondary shoot production (branches) (Grbić and Bleecker, 2000; Wang et al., 2018). Upon floral transition, the SAM gradually matures into an inflorescence meristem (IM), initially producing phytomers with leaf-like bracts, and when fully matured phytomers with one or more flowers (Park et al., 2014; Wang et al., 2018). Upon successful fertilization, these flowers eventually develop into fruits with seeds.

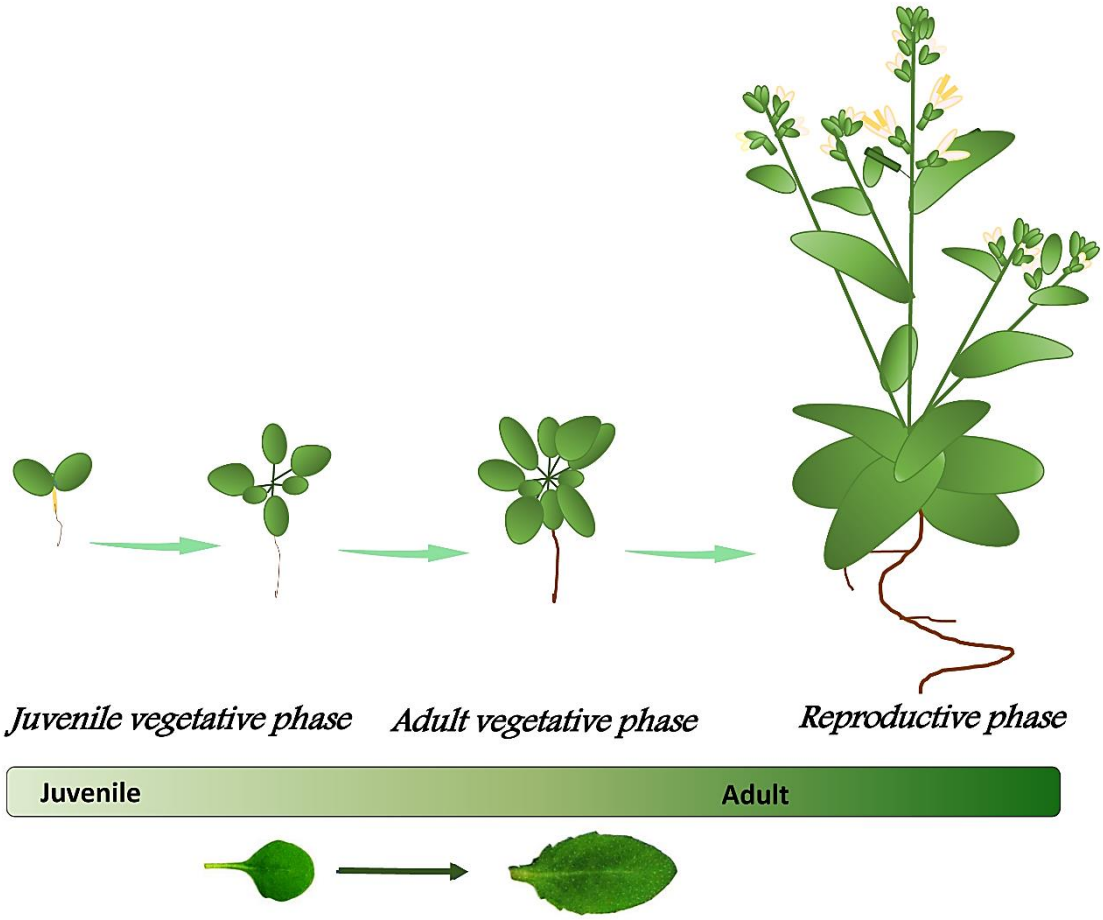

Figure 2. The two main developmental phase transitions in Arabidopsis. After germination, the seedling enters the vegetative phase, with the SAM and RAM responsible for organogenesis. The plant gradually goes through roughly three distinct developmental phases. The vegetative phase of growth is divided into a juvenile and an adult phase. Plant size and mass rapidly increase during the vegetative phase. Arabidopsis is a typical model plant in which, through leaf morphology, the juvenile phase is distinguishable from the adult phase (juvenile leaves are small and round in shape, with no trichomes on the abaxial side; in contrast, adult leaves are serrated and large, with trichomes produced on the abaxial side). In the juvenile vegetative phase, the plant is incompetent to flower, but during the adult vegetative phase the plant becomes flower competent and this starts its transition to the reproductive phase, in which the SAM becomes an IM giving rise to stems with bracts and flowers instead of leaves.

The juvenile-to-adult vegetative phase transition

In the juvenile vegetative phase, most plants are not competent to flower. Therefore, flowering requires the transition from juvenile to adult vegetative development, which is referred to as the vegetative phase change (VPC) (Poethig, 2013). The VPC is one of the most striking examples of a developmental switch that has a substantial impact on plant fitness and biomass (Demura and Ye, 2010). In many plants, the VPC coincides with distinguishable morphological changes such as changes in leaf shape or internode length, leaf position (phyllotaxis), the time interval between two consecutive (plastochron) leaf initiation events, or the appearance of trichomes on the abaxial leaf surface. These changes eventually result in the production of both juvenile and adult internodes or leaves on the same plant, which is known as heteroblasty (Huijser and Schmid, 2011; Poethig, 2013). In perennial woody plants, heteroblasty can be clearly observed, since these plants show a long juvenile period (Zotz et al., 2011; Huijser and Schmid, 2011). However, most of our knowledge on the molecular mechanisms governing this process is limited to Arabidopsis, since the majority of molecular genetic studies have focused on this annual model plant. In Arabidopsis, the VPC coincides with the production of larger and eventually serrated leaves that have a higher length:width ratio and develop trichomes on the abaxial leaf side (Telfer et al., 1997; Wu and Poethig, 2006; Poethig, 2013; Lee, 2000).

miRNAs, SPLs, and gibberellic acid regulate the juvenile-to-adult phase transition

The VPC is regulated by various endogenous factors that interact with environmental factors such as photoperiod, light intensity, and temperature. Studies in Arabidopsis have shown that two microRNAs (miR156 and miR157), a class of noncoding RNAs of 20–24 nucleotides involved in post-transcriptional regulation of gene expression, and their *SQUAMOSA PROMOTER BINDING PROTEIN-LIKE* (*SPL*) target genes play a crucial role in the VPC (Fig. 2) (Poethig, 1990; Lee, 2000; Huijser and Schmid, 2011; Poethig, 2013; Usami et al., 2009; He et al., 2018). Other studies have shown that miR156/157-regulated *SPL* genes are also drivers of the VPC in maize (Chuck et al., 2011) and a number of other herbaceous (Fu et al., 2012; Salinas et al., 2012; Shikata et al., 2012; Xie et al., 2012; Zhang et al., 2011) and woody plants (Wang et al., 2011).

Overexpression of *miR156* results in a prolonged juvenile phase, which has been observed in many plants including Arabidopsis (Schwab et al., 2005; Shikata et al., 2012; Fornara and Coupland, 2009; Wu et al., 2009b), rice (Xie et al., 2012), tomato (Zhang et al., 2011), and poplar (Wang et al., 2011). *miR156* differs from *miR157* in three nucleotides, but the overexpression phenotype of *miR157* is quite similar to that of *miR156* (Gandikota et al., 2007; Xu et al., 2016). The expression of the *miR156*/*miR157* genes is high at the young seedling stage, but gradually decreases as plant development progresses (He et al., 2018), leading to increased abundance of the SPL transcription factors (Fig. 3). Eleven of the seventeen *SPL* genes in Arabidopsis contain the *miR156/miR157* complementary sequence, but only six of those (*SPL2/9/10/11/13/15)* are involved in the VPC (Gandikota et al., 2007; Xu et al., 2016). miR156 and miR157 repress the *SPL* transcripts by direct binding, causing translational repression (He et al., 2018). In contrast to overexpression of *miR156* or *miR157*,

which reduces SPL abundance, SPL levels can be enhanced by introducing into the plant a miRNA-resistant gene version (*r-SPL*), in which the miR156/157 target site has been mutated. Alternatively, the same can be achieved by lowering miR156 abundance by overexpression of a miRNA target-site mimic (*35S:MIM156*) or by generating *mir156* loss-of-function mutations. In all cases, enhanced SPL abundance results in precocious appearance of adult traits and early flowering (Smith et al., 2009; Xu et al., 2016). Taken together, it can be concluded that miR156 and miR157 have a central role in the regulation of the VPC.

Together with a gradual decrease in *miR156*/*miR157* expression during shoot maturation, the expression of another miRNA gene, *miR172*, gradually increases (Fig. 3). The expression of *miR172* is low during the juvenile phase and increases during the VPC, since SPLs act as transcriptional activators of the *miR172* gene. miR172 promotes the development of trichomes on the abaxial side of leaves by repressing the expression of the *APETALA2-LIKE* (*AP2-like*) transcription factors *TARGET OF EARLY ACTIVATION TAGGED1* (*TOE1*) and *TOE2* (Aukerman and Sakai, 2003; Wu et al., 2009a) (Fig. 3). In addition, SPLs promote other adult leaf traits such as elongation and serration independent of miR172. However, the genes that act downstream of SPLs and TOE1/TOE2 during the VPC have remained unidentified until now (Fig. 3).

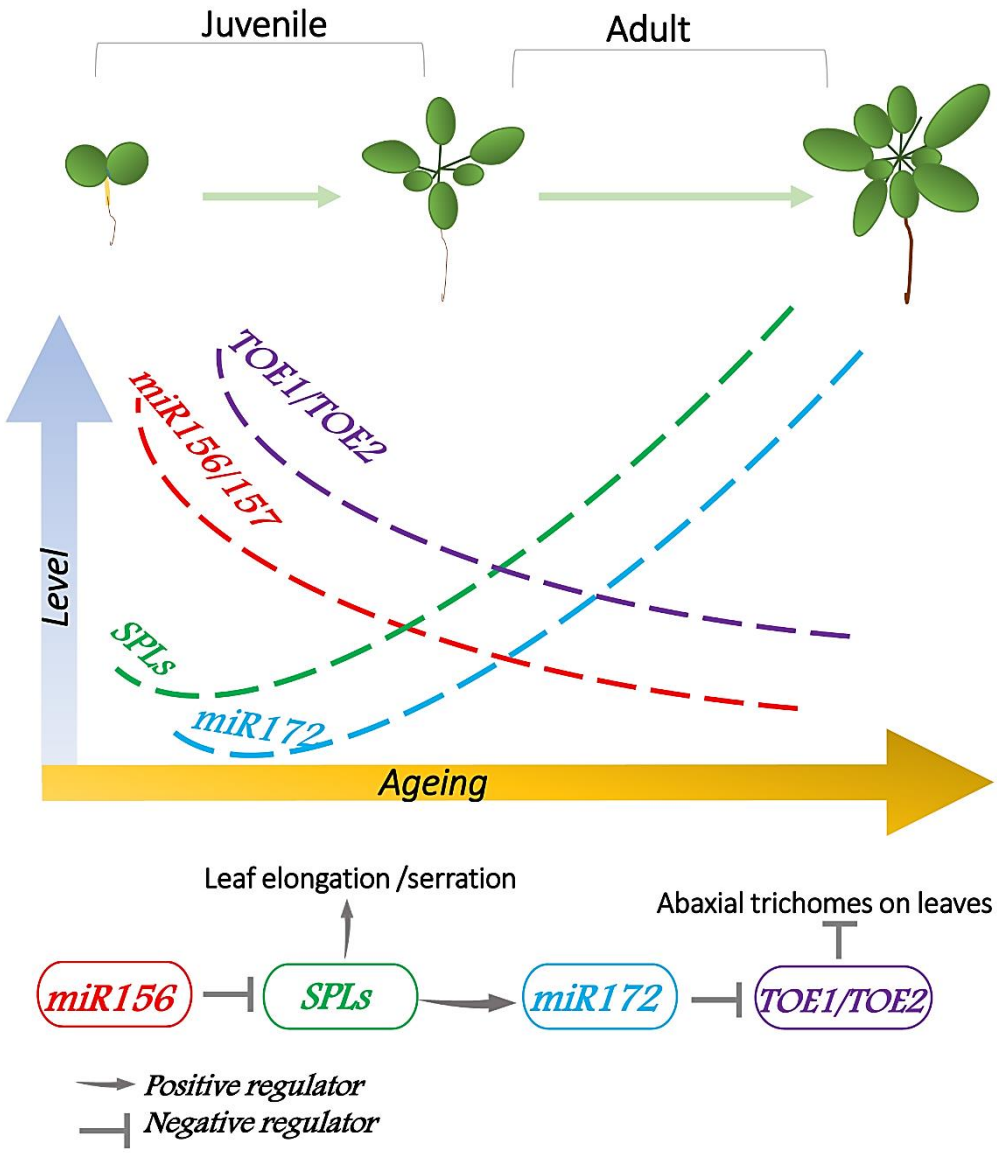

Figure 3. Regulation of the vegetative phase change in Arabidopsis. In early Arabidopsis development, levels of *miR156/157* (master regulator) are high in order to promote juvenile vegetative growth in seedlings. *miR156/157* levels (dotted red line) steadily decrease, allowing transcription factor production by *SPL* target genes (dotted green line) to increase gradually, and resulting in the appearance of adult leaf morphology. At the same time, the SPL transcription factors directly induce the expression of *miR172* (dotted blue line), which results in the suppression of the TOE1 and TOE2 transcription factors (dotted purple line), allowing trichome formation on the abaxial side of leaves.

Besides the miRNAs and their SPL targets, other endogenous factors such as the phytohormone gibberellic acid (GA) are involved in the VPC. In Arabidopsis, exogenous application of GA can accelerate the appearance of adult vegetative traits such as abaxial trichomes (Telfer et al., 1997; Park et al., 2017). In contrast, Arabidopsis GA-insensitive mutants or mutants deficient in GA biosynthesis show prolonged juvenile vegetative development. GA affects the adult phase by promoting the expression of some *SPL* genes, but no effect was observed on *miR156* expression (Fornara and Coupland, 2009; Galvão et al., 2012; Jung et al., 2012). GA therefore seems to promote SPL protein abundance, and as a consequence the VPC, in a miRNA-independent manner.

The vegetative-to-reproductive phase transition

The vegetative-to-reproductive phase transition involves the induction of flowering and plays a central role in the context of important agronomic traits such as plant biomass and seed- and fruit productivity. In fruit and seed crops, flowering should occur at the correct time when the environmental conditions are suitable to ensure maximal reproductive success (Jung and Müller, 2009). For the majority of plant species, transition to the reproductive phase or flowering occurs when they are in the adult phase. In these plants, flowering time largely depends on the duration of the juvenile phase. Some plants flower quickly after the transition to the adult phase, but other plants stay in the adult vegetative phase for a while before flowering.

The switch to the reproductive phase involves integrating multiple endogenous and environmental cues such as GA or the age pathway and photoperiod or vernalization, respectively (Fig. 4) (Amasino, 2010; Turnbull, 2011; Song et al., 2013). This involves a large number of genes that all act in a gene regulatory network (GRN) to coordinate the response to all these cues (Amasino, 2010; Turnbull, 2011; Song et al., 2013). In this GRN, *SUPPRESSOR OF CONSTANS1* (*SOC1*), *FLOWERING LOCUS T* (*FT*), *FLOWERING LOCUS C* (*FLC*), the *SPLs*, and *CONSTANS* (*CO*) are also known as floral pathway integrator genes, influencing flowering by integrating the different environmental and endogenous signaling pathways (Amasino and Michaels, 2010; Amasino, 2009; Andrés and Coupland, 2012; Hwang et al., 2019).

Regarding the transition from the vegetative to the reproductive phase in response to photoperiod, there are three main types of plants: i) short-day plants, in which a shorter photoperiod promotes flowering; ii) long-day plants, in which a long photoperiod promotes flowering; and iii) day-neutral plants, in which flowering does not depend on photoperiod (Song et al., 2013). Arabidopsis is a typical long-day plant with the B-box transcription factor CO at the core of the photoperiod pathway. Its abundance is up-regulated through light signaling in the leaf at the post-translational level (Fig. 4) (Turnbull, 2011; Song et al., 2013). CO performs its role by directly binding to the *FT* gene to activate its expression. The FT protein acts as a florigen signal that is transported from the leaf through the phloem to the SAM. In the SAM, FT interacts with the bZIP transcription factor FD. Together, FT and FD form a floral activator complex that activates the transcription of several flowering-promoting genes, including *SOC1* (Fig. 4), that switch the fate of the SAM to IM (Turnbull, 2011; Song et al., 2013; Jung et al., 2016; Abe et al., 2019).

Many plants in temperate climate regions have evolved to acquire reproductive activity by prolonged cold exposure through a process known as vernalization. A central node in the vernalization pathway is the MADS-box transcription factor FLC (Fig. 4), which acts as a potent repressor of flowering (Amasino and Michaels, 2010; Kim and Sung, 2014). FLC affects flowering by suppressing the *FT* and *SPL* genes in leaves and the *FD* and *SOC1* genes in the SAM (Fig. 4) (Deng et al., 2011; Matsoukas et al., 2012). Thus, FLC represses the flowering pathways in both leaf and meristem. Prolonged cold exposure leads to stable silencing of *FLC* expression by local chromatin modification and, subsequently, the induction of flowering (Kim and Sung, 2014). Besides chromatin modification, alternative splicing (Mahrez et al., 2016) and post-translational protein stabilization (Kwak et al., 2016) mechanisms have been shown to regulate FLC abundance at the molecular level.

Among flowering pathways, the GA pathway is an important endogenous pathway that controls the switch to the reproductive phase independent of the photoperiod (Yu et al., 2012; Davière and Achard, 2013). The control of flowering time by GA depends on GA biosynthesis, signaling, and degradation. GA-deficient mutants, either defective in GA biosynthesis or with higher GA degradation levels, show delayed flowering (Jung et al., 2012; Yu et al., 2012). DELLA proteins are central regulatory hubs in GA signaling-induced flowering. In this signal transduction, binding of GA to its receptor GIBBERELLIN INSENSITIVE DWARF1 (GID1) results in a conformational change that allows GID1 to bind to DELLA proteins and to form a GA–GID1–DELLA complex. The GA–GID1–DELLA complex subsequently promotes DELLA degradation by the 26S proteasome. (Silverstone and Pui, 1997; Griffiths et al., 2006; Sun, 2010; Galvão et al., 2012). GA signaling induces flowering mainly by promoting the expression of the *SPL* and *SOC1* genes (Fig. 4) (Jung et al., 2012, 2011; Fornara and Coupland, 2009).

In addition to the critical regulatory role of miR156/157 and miR172 in the VPC, these microRNAs also act as key players in the plant age-dependent floral pathway (Poethig, 2013). Also here, the age-related reduction in *miR156* expression leads to increasing levels of SPL transcription factors, which subsequently induce flowering by activating the transcription of *SOC1* and several other floral-promoting genes in the SAM (Fig. 4). Activation of *miR172* by SPL proteins in leaves leads to repression of a sub-family of *APATELA2* (AP2)-like target genes that are repressors of flowering (Wang et al., 2011; Wu and Poethig, 2006; Andrés and Coupland, 2012; Wu et al., 2009b). Thus, miR156/157 and miR172 have opposite effects on flowering time, as overexpression of *miR156* delays flowering time, whereas overexpression of *miR172* accelerates flowering (Aukerman and Sakai, 2003; Huijser and Schmid, 2011; Poethig, 2013). Molecular genetic studies have shown that the ageing pathway is highly integrated into other flowering-time pathways (Wang, 2014).

APETALA1 (*AP1*) and *LEAFY* (*LFY*) are key floral-meristem identity genes that act downstream of the floral integrator SOC1 and eventually convert the vegetative SAM to an IM (Andrés and Coupland, 2012; Matsoukas et al., 2012; Blümel et al., 2015). The photoperiod-regulated FT–FD complex is directly involved in the transcriptional activation of *SOC1* in the SAM, and the central floral integrator SOC1 subsequently promotes flowering through activation of both floral-meristem genes *AP1* and *LFY* (Fig. 4) (Turnbull, 2011; Song et al., 2013).

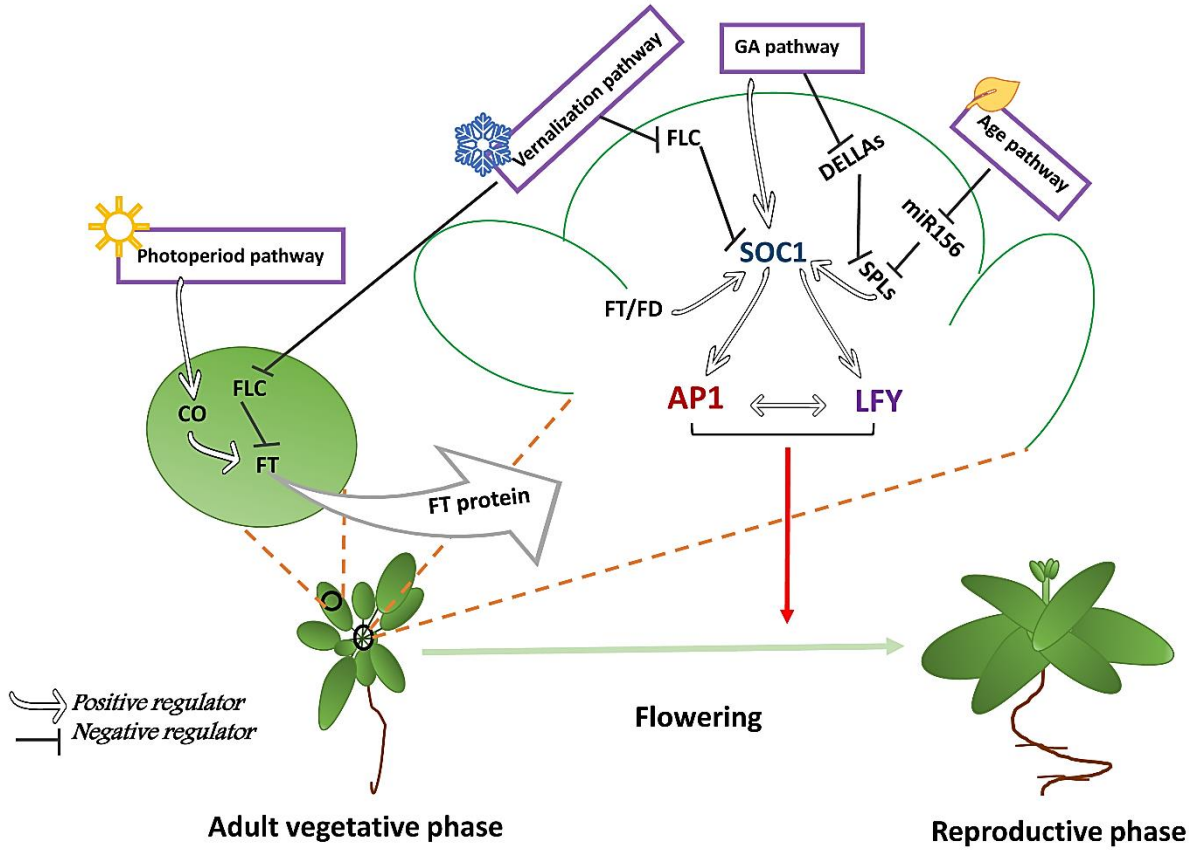

Figure 4. A simplified model of the gene regulatory network comprising the four pathways controlling flowering in Arabidopsis. In the photoperiod pathway, long days lead to CO accumulation in leaves, which induces FT expression. The FT protein travels through the phloem from the leaves to the SAM to interact with FD and activate *SOC1* and as a result subsequently *AP1* and *LFY*. In the vernalization pathway, cold treatment leads to stable repression of the *FLC* gene. The MADS-box protein FLC determines the cold-period-dependent timing of flowering by repression of the floral integrator genes *FT*, *FD* and *SOC1*. In the age-dependent pathway, a gradual reduction in *miR156* allows SPL abundance to increase, which activates *SOC1* and other floral integrators (not shown). Finally, the GA pathway promotes flowering independently by activation of *SOC1* and *SPL* genes. Subsequently, all four pathways help with transcriptional regulation of the floral integrators *FT* and *SOC1*, which promote *AP1* and *LFY* expression. *AP1* and *LFY* are required to complete the floral transition.

Axillary meristem formation and outgrowth

The ability to continue producing new organs throughout life is one of the unique post-embryonic features in plants. However, once the SAM is converted to IM, it will only produce a defined number of stems with flowers before its activity ceases, and its activity will be taken over by AMs that can act as SAM to establish secondary shoots (branches) (Pautler et al., 2013).

Genetic and physiological studies have identified several genes and plant hormones involved in AM formation (Scofield et al., 2018; Balkunde et al., 2017). Most of the key genes in regulating AM formation are transcription factors that were identified through phenotypic defects of loss-of-function mutants in the encoding genes. In Arabidopsis, the transcription factor *LATERAL SUPPRESSOR* (*LAS*) is required for AM formation, as shown by the *las* loss-of-function mutant that is no longer able to produce lateral shoots. *LAS* is florigenic, and

it migrates from the SAM toward the leaf axil (Greb et al., 2003). The putative transcription factors LAX PANICLE 1 (LAX1) and LAX PANICLE 2 (LAX2) interact with each other and are involved in AM formation in rice as *lax1* and *lax2* mutants both produce less AMs (Oikawa and Kyozuka, 2009; Tabuchi et al., 2011). Mutations in the *REVOLUTA* (*REV*) gene, encoding a class III homeodomain/leucine zipper TF (HD-ZIP III), reduce AM formation in Arabidopsis (Otsuga et al., 2001). The *REGULATOR OF AXILLARY MERISTEMS* (*RAX*) genes (*RAX1*, *RAX2*, and *RAX3*), encoding MYB-like transcription factors, are specifically expressed at the center of the leaf axil, and their loss of function affects AM formation in Arabidopsis and tomato (Keller et al., 2006). And lastly, cytokinin and auxin are two important plant hormones involved in AM formation (Wang et al., 2014a, 2014b).

The AMs can undergo immediate outgrowth or initially develop into dormant axillary buds. The latter may then grow out, leading to the formation of lateral shoots. In Arabidopsis and many other plants, plant shape and biomass are highly influenced by axillary bud outgrowth (referred to as branching) during plant growth and development. Branching is considered one of the most important agronomic traits. The identification of genes controlling branching has provided tools for genetic manipulation to improve plant architecture and enhance yield in crops.

In the last decade, significant progress has been made in understanding the regulation of bud outgrowth and branching. Whether buds are dormant or growth out is influenced by a wide range of internal factors and environmental cues such as light quality, shoot apex damage, and availability of nutrients (Kim et al., 2010; Djennane et al., 2014; Rameau et al., 2015).

Plant hormones are the most important internal factors that regulate shoot branching. Extensive studies have been performed on understanding hormone-regulated bud outgrowth. Auxin was the first plant hormone that has been shown to suppress the outgrowth of axillary buds. Classical decapitation experiments have shown that the SAM inhibits bud outgrowth, since its removal allows the lateral buds to grow out to secondary shoots. Apical dominance can be recovered, however, by applying auxin to the decapitated shoot, showing that auxin provided by the shoot tip suppresses bud outgrowth and promotes apical dominance (De Smet and Jürgens, 2007; Domagalska and Leyser, 2011; Waldie and Leyser, 2018) (Fig. 5). Unlike auxin, cytokinin directly promotes axillary bud outgrowth (Fig. 5). It has been shown that either overexpression of genes encoding enzymes mediating cytokinin biosynthesis *ISOPENTENYLTRANSFERASE* (*IPTs*) or exogenous cytokinin application triggers bud outgrowth (Ferguson and Beveridge, 2009; Domagalska and Leyser, 2011; Waldie and Leyser, 2018). Strigolactones (SLs) are a recently discovered class of plant hormones with a specific role in bud outgrowth. SLs inhibit bud outgrowth and branching (Fig. 5) in Arabidopsis and other species (rice, pea, tomato, and petunia). It was shown that the *MORE AXILLARY GROWTH MAX* genes (*MAX1*, *3*, *4*, *5*) in Arabidopsis and *MAX* orthologs *RAMOSUS* (*RMS*) *1, 2, 3, 5, 6* in pea, *DWARF* (*D*) *10, 17, 27* in rice and *DECREASED APICAL DOMINANCE* (*DAD*) *1*, *2*, *3* in petunia are involved in SL biosynthesis, and that mutants in these genes showed increased shoot branching compared to the wild type (Johnson et al., 2006). Auxin stimulates SL biosynthesis by up-regulation of the responsible genes (Foo et al., 2005). Therefore, SL biosynthesis may be part of the apical-dominance-promoting and bud outgrowth-inhibiting auxin pathway (Fig. 5). Furthermore, SL regulates

shoot branching by rapidly modulating auxin transport. (Shinohara et al., 2013). Two other phytohormones, GA and ABA, are considered bud-outgrowth inhibitors (Rameau et al., 2015; Gonzalez-Grandio et al., 2017; Yao and Finlayson, 2015). BRC1, by promoting the expression of *HOMEOBOX PROTEIN* (*HB*) *21*, *40*, and *53* mediates ABA accumulation and Several other genes have been identified to be involved in shoot branching. Among these, *TEOSINTE BRANCHED 1* (*TB1*) is known as a key gene that controls branching in maize. TB1 acts as a bud-outgrowth repressor, as the maize *tb1* mutant shows high tiller and aerial branch production. Mutation in the *TB1* orthologues *OsTB1* in rice or *BRANCHED 1* (*BRC1*) in Arabidopsis and pea also increase shoot branching (Aguilar-Martínez et al., 2007; Braun et al., 2012; Martín-Trillo et al., 2011; Minakuchi et al., 2010). The *BRC1/TB1* genes encode a protein belonging to the TCP transcription-factor family, which is specifically expressed in axillary buds and required for bud-outgrowth inhibition and branch repression (Gonzalez-Grandio et al., 2017). BRC1 is a key target of hormonal signaling (Fig. 5) (Dun et al., 2012). Overall, all of the factors mentioned above together control bud outgrowth with BRC1 at a central position (Fig. 5) (Seale et al., 2017).

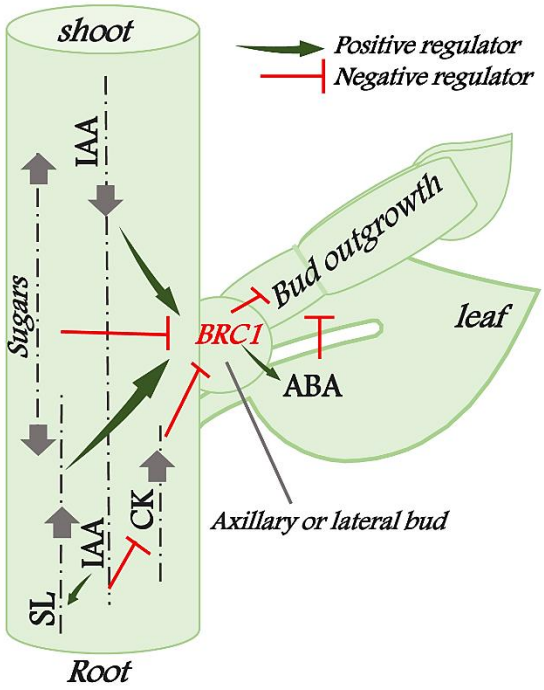

Figure 5. Hormonal signals control lateral bud outgrowth via BRC1. Hormones and nutrition control bud outgrowth. *BRC1* has a central role by interacting with different phytohormones. CK and sugars repress *BRC1*. Auxin represses CK either by repressing *IPT* genes or by promoting SL biosynthesis. In addition, BRC1 promotes ABA accumulation, which in turn suppresses bud development and outgrowth.

Axillary-meristem maturation and plant longevity

Plant longevity is defined as the period in which plants remain viable. Plant longevity has long been considered an essential trait for ecology, agronomy, and economy. However, the mechanisms regulating longevity in plants are mostly unknown. AMs, like the SAM, undergo phase changes. Upon flowering in Arabidopsis and many annual plants, when the SAM changes to an IM, vegetative development from AMs is highly suppressed (Amasino, 2009; Davies and Gan, 2012) and all energy is funneled toward reproductive activities (Thomas, 2013). The majority of AMs in axils of Arabidopsis leaves do not show vegetative development and immediately become IMs, and after producing a few cauline leaves are converted to flower meristems. However, in some Arabidopsis ecotypes such as Sy-0 this early maturation of the AMs is prevented, as some are maintained in the vegetative phase (Poduska et al., 2003). This heterochronic change of AM phase identity in Sy-0 leads to the formation of aerial rosettes in the axils of stem leaves, and significantly increases longevity and extends the period during which the plant is able to produce seed (Poduska et al., 2003). A dominant allele of the *FLC* gene has been suggested to underlie the increased life span of Sy-0 (Poduska et al., 2003). In addition, it has been shown that a double mutant of the Arabidopsis flowering-time genes *SOC1* and *FRUITFULL* (*FUL*) also shows enhanced vegetative development from AMs, leading to an increased life span (Melzer et al., 2008). FLC has previously been shown to negatively regulate *SOC1* and other flowering-time genes in the SAM (Deng et al., 2011; Matsoukas et al., 2012). However, our understanding of the mechanisms by which FLC keeps the AMs in the vegetative phase during floral transition is still limited.

Plants display a wide range of life cycles, varying from a few weeks for several annual species up to several thousands of years for some perennial species. In conjunction with their life span, plants have evolved two opposing growth habits. Many species are monocarpic, as they senesce and die after producing offspring once, even under appropriate growth conditions. By contrast, polycarpic plants do not die after flowering and typically produce multiple successful offspring over several consecutive years during their life history. All annual plants—but very few perennial plants—are monocarpic. Monocarpic perennials grow for many years, but die after producing offspring once (Munné-Bosch, 2008; Thomas, 2013).

The fate of AMs plays a critical role in the opposing growth habits of monocarpic and polycarpic plants. In contrast to the conversion of all AMs to inflorescences and the eventual death of the plant body in monocarpic plants (Fig. 6), polycarpic plants maintain a number of AMs in the vegetative state after a successful round of offspring production. In this way polycarpic plants prolong their life span, with their maintained vegetative AMs producing new shoots during the next growing season (Fig. 6) (Amasino, 2009). In some polycarpic plants, however, all AMs do change to the reproductive phase. Still, vegetative development is maintained by reversing some IMs to the vegetative state under specific environmental conditions (Tooke et al., 2005). Many plants, such as petunia and tomato, can maintain some AMs in the vegetative state during flowering and, therefore, they can stay alive for a few years when grown as perennials in year-round tropical conditions (e.g. in greenhouses), but generally they are grown as annual plants because they cannot survive the cold temperature during the winter. However, these plants have a considerably longer life span compared to the typical annuals that only stay alive until the end of the reproductive phase.

The existence of both mono- and polycarpic species within many plant genera implies that the transition between polycarpic and monocarpic growth habit might be associated with relatively small genetic changes. In fact, the switch between mono- and polycarpy is considered as the most common growth form transition in angiosperms (Amasino, 2009). However, despite considerable interest in understanding the molecular mechanisms controlling the switch between mono- and polycarpy, only a few genes have yet been identified that are involved in the offspring-linked death in monocarpic plants and the survival of polycarpic plants even after multiple rounds of offspring production.

Consistent with the central position of the vegetative-to-reproductive phase transition in determining the life history of a plant, the key regulators of this phase transition play an important role in regulating the vegetative activity of AMs during the reproductive phase. Indeed, the perennial life history in close relatives of Arabidopsis, such as *Arabis alpina*, relies on not all AMs converting to IMs in a single growing season. Some meristems undergo floral transition in spring, while several AMs are maintained in the vegetative state, allowing subsequent cycles of growth during the next growing season.

Studies in Brassicaceae species have recently started to reveal the genetic basis that differentiates between the monocarpic and polycarpic growth habit. The *FLC* MADS-box gene ortholog *PERPETUAL FLOWERING1* (*PEP1*) in the conditionally polycarpic perennial *A. alpina* controls the temperature-dependent switch from polycarpic to monocarpic growth (Wang et al., 2009). PEP1 blocks the vegetative-to-reproductive transition of meristems, resulting in continued vegetative development. Still, low-temperature-induced chromatin modifications (during winter) lead to repression of *PEP1* transcription and subsequently to flowering (in spring). However, the low temperature only transiently suppresses the expression of *PEP1*, as restoration of the chromatin modifications at the *PEP1* locus to their original levels after the cold period leads to reactivation of *PEP1*, causing the dormant meristems or the new meristems produced during the reproductive phase in *A. alpina* to maintain the vegetative fate. The outgrowth of these meristems during the next growth season supports a subsequent cycle growth (Wang et al., 2009). Lack of epigenetic memory at the *PEP1* locus after a cold period thus explains the temperature-dependent polycarpic life history of *A. alpina*. It has been shown that the Arabidopsis double mutant in the flowering genes *SOC1* and *FUL* shows a perennial-like lifestyle (Melzer et al., 2008). Interestingly, the PEP1-induced polycarpic behavior of *A. alpina* was also shown to be caused by suppression of *AaSOC1* expression (Bergonzi et al., 2013). This indicates that advances in the understanding of molecular mechanisms behind monocarpic life strategies can help to elucidate how polycarpic plants survive after multiple rounds of flowering.

The temperature-dependent polycarpic life history of *A. alpina* is also controlled by the age-dependent pathway. Unlike in Arabidopsis, the decrease in miR156 levels is uncoupled with miR172 in *A. alpina*, whereas the expression of *miR172* is up-regulated by cold temperatures independently of miR156 (Bergonzi et al., 2013). The induction of miR172 by low temperatures leads to the repression of the *APETALA2*-like transcription factor gene *PEP2*. PEP2 positively regulates PEP1 expression, thus providing negative feedback to the floral transition by promoting the maintenance of the vegetative identity in AMs. The decline in miR156 levels is essential for flowering in cold-treated *A. alpina* plants, as only AMs with low miR156 levels transit to the reproductive phase (Bergonzi et al., 2013), indicating that

polycarpic life history in *A. alpina* is also dependent on miR156 levels in AMs, this serving as a distant pathway independent of the vernalization pathway. Recently it was reported that cold exposure is not able to induce flowering in an *A. alpina spl15* loss-of-function mutant (Hyun et al., 2019), indicating that the different floral pathway integrator genes act in parallel to control polycarpic behavior in *A. alpina*.

Cardamine flexuosa is another polycarpic close relative of Arabidopsis. Its polycarpic life history is mediated by cold temperatures, but unlike *A. alpina*, the age-decreased miR156 is associated with an increase in miR172 levels independent of cold temperature , which causes repression of its target *TOE1* and subsequently leads to repression of *CfPEP1* expression (Zhou et al., 2013a). This indicates that polycarpic behavior in Brassicaceae is controlled through distinct mechanisms.

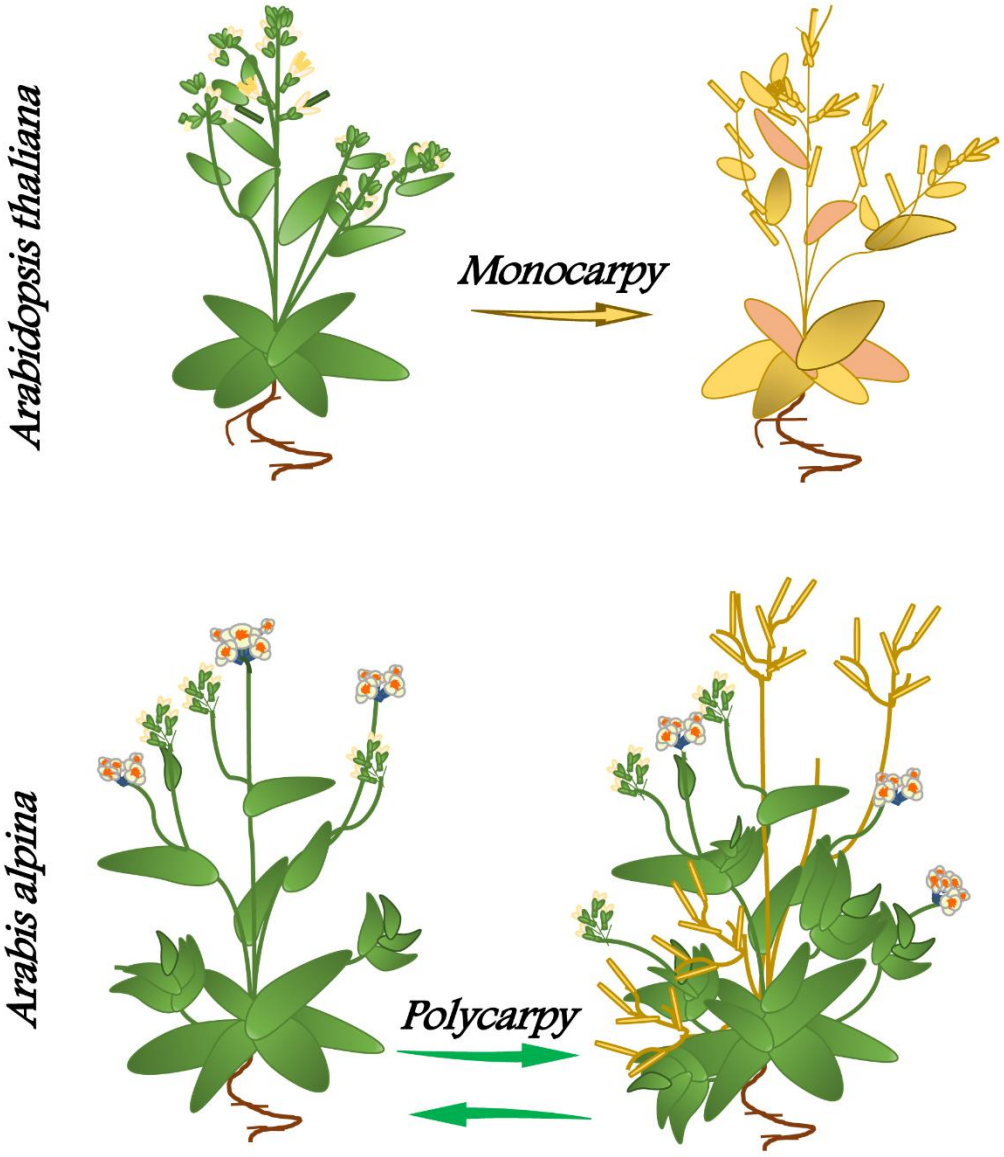

Figure 6. Monocarpic versus polycarpic life histories

Vascular meristems and primary and secondary growth

The evolution of vascular tissues composed of xylem and phloem for transport of various molecules such as water, nutrients, and other growth and defense factors between different tissue and organs has allowed higher plants to increase in size, and thus to outcompete smaller plants for light and nutrients. Vascular tissues also play an essential role in physical strength and resilience to wind and gravity. The vascular tissues connect all the plant organs by their conductive function, from the root tip to the various organs in the shoot. The xylem mediates the long-distance transport from root to shoot, such as water and solute minerals. In contrast, multiple signaling molecules and photosynthetic products are distributed throughout the entire plant by the phloem.

Vascular tissues in higher plants undergo two distinct growth phases during plant life history: primary and secondary growth. In young stems, the primary growth stage includes a number of vascular bundles. Each of these bundles contains procambium, primary phloem, and primary xylem (Fig. 7). After primary vascular growth, the procambium and its neighboring interfascicular parenchyma cells in stems are converted into the cambium, forming a ring of meristematic cells that in parallel to the production of phloem and xylem, respectively facing out and inside of the stem, promotes secondary growth of the stem. (Fig. 7) (Jouannet et al., 2015; Ragni and Greb, 2018). Apart from the mechanical support, this delivers through increased stem thickness, secondary growth plays a critical role in plant development as it also enhances the transport capacity of the stem by producing specialized cell types belonging to the phloem and xylem. However, in many flowering plants, especially monocots, all procambial cells eventually differentiate into non-meristematic vascular tissues during primary growth, and therefore cambium formation and secondary growth do not take place all.

Procambium and cambium formation

Procambium and cambium are a pool of stem cells formed in vascular plants that continuously generates the major plant vascular tissues, xylem and phloem, via asymmetric periclinal cell divisions. The basic characteristics and activity of procambium and cambium are very similar, and this is why they are considered the same set of vascular stem cells at different developmental stages. For instance, both in procambium and cambium, xylem is produced toward the inside and phloem toward the outside. However, cambium stem cells are usually more active than the ones in the procambium (Jouannet et al., 2015).

The SAM is the source of all primary vasculature system, containing several bundles. Each bundle includes procambium as a stem-cell provider between the phloem and the xylem (Fig. 7) (Jouannet et al., 2015). Cells located in the interfascicular region (the area between two bundles) gradually differentiate to parenchyma cells (Fig. 7). The cambium cylinder is generated from the procambium, by gradual fate change of interfascicular parenchyma cells to cambial cells, (Fig. 7). The cambium zone includes two parts: the division zone and the differentiation zone. The meristematic cells are located in vascular cambium named with vascular stem cells. These cells divide in two different directions, known as radial division toward xylem and phloem, which is responsible for stem diameter growth (Chiang and Greb, 2019). The extent of cambium activity can determine the number of xylem and phloem cells.

Once cells acquire a phloem or xylem identity, they elongate and expand their growth and eventually some cells undergo programmed cell death (Siedlecka et al., 2008). Environmental cues such as temperature, photoperiod, and water- and nutrient availability influence cambium activity. Many details about the factors and mechanisms behind cambium activity, regulation, and maintenance are still unknown.

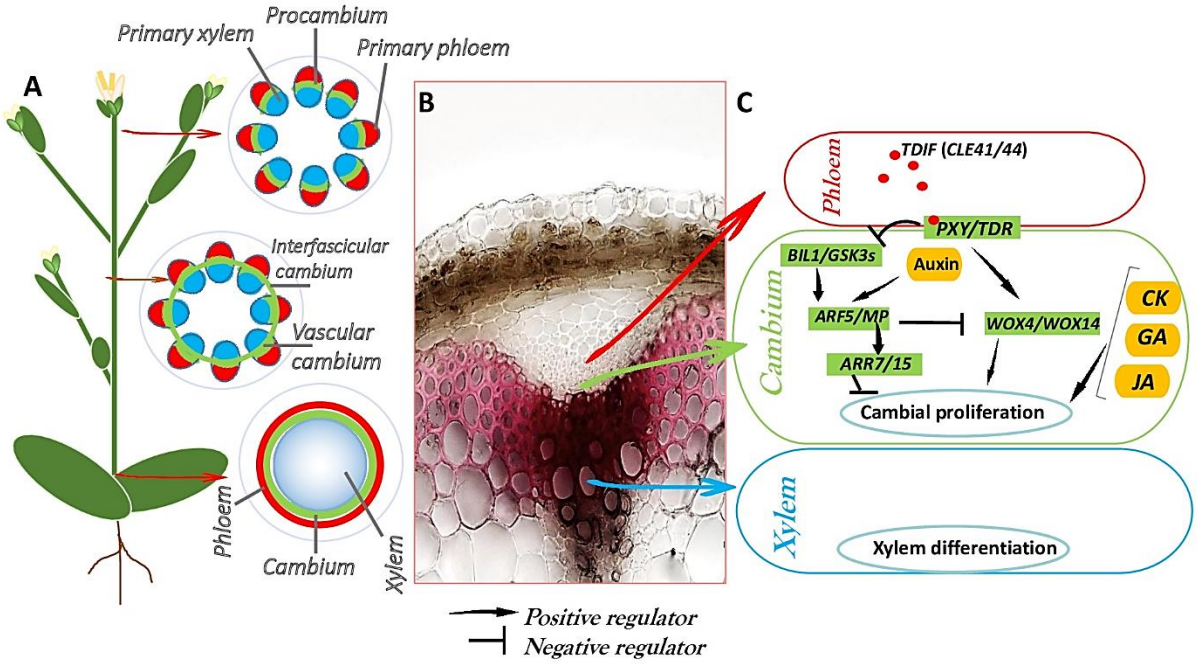

Figure 7. Dynamic nature of vascular cambium in the Arabidopsis inflorescence stem. (**A**) Schematic representation of an Arabidopsis plant with cross sections of the top-, middle- and bottom part of inflorescence stem showing different stages of vascular development. Very young stems from the top of the plant develop vascular bundles containing phloem, procambium, and xylem. In the middle part of the stem, cambial cell activity forms a ring of cambium extending into the interfascicular region. At the bottom, secondary phloem and xylem are formed as a consequence of cambium activity. (**B**) Bright field image of a lignin stained cross section of a middle part of an inflorescence stem showing the vascular bundle. (**C**) Hormonal and transcriptional control of vascular-cambium activity: the PXY receptor-like kinase, is activated by binding of the TDIF peptide ligand (red dots) synthesized in the phloem, and this induces *WOX4* transcription, which promotes cell proliferation in the cambium. PXY also promotes cambium activity by repressing *BIL1*expression and thus the auxin-dependent negative feed-back on cambial cell division. The plant hormones CK, jasmonate and GA all positively regulate cambium activity.

Hormonal and peptide signaling in secondary growth

Phytohormones are known to be involved in cambium regulation in parallel to environmental factors. The instrumental role of auxin in cambium regulation has been described in several reports. Auxin transport toward root from its source at the SAM affects cambium activity. In the stem of trees, auxin is highly accumulated in the cambium. Its levels are gradually decreased in cell types that are far from the cambium area (Tuominen et al., 1997; Aloni, 2013), suggesting the important role of auxin in cambium activity. However, no clear close correlation has been observed by now between auxin levels in the cambium and their effect

on cambium activity (Nilsson et al., 2008). A recent report showed that local auxin maximum in roots plays a role in promoting xylem identity (Smetana et al., 2019).

Cytokinin has a central role in procambium/cambium initiation and development. Depending on side-chain structure, cytokinins are classified into four different groups (tZ-type, cis-zeatin-type, isopentenyladenine (iP)-type, and aromatic cytokinins). The most active cytokinins (iP-type and tZ-type) are synthesized by isopentenyltransferases (*IPTs*). Arabidopsis encodes eight *IPT* genes (*IPT1*, *3*, *4*, *5*, *6*, *7*, *8*) that mediate cytokinin biosynthesis (Miyawaki et al., 2004; Kakimoto, 2001). The Arabidopsis *ipt1*, *3*, *5*, *7* quadruple mutant shows no cambium activity and, subsequently, no secondary growth (Matsumoto-Kitano et al., 2008), whereas overexpressing *IPT7* in Populus strongly increases secondary growth and biomass in the stem (Immanen et al., 2016). The *LONELY GUY* (*LOG*) gene family is known to be involved in cytokinin homeostasis. LOG proteins can convert conjugated inactive forms of cytokinin to the active forms through different pathways. Interestingly, the expression of *LOG* genes in rice is required for meristem activity and maintenance. *Lonely guy (log)* mutant in rice shows defects in shoot meristem maintenance, resulting in abnormal branching patterns (Kurakawa et al., 2007). In hybrid aspen trees, high expression of *CYTOKININ DEHYDROGENASE 2* (*CKX2*) encoding a cytokinin-degrading enzyme reduces cytokinin levels and, concomitantly, secondary growth in the stem (Nieminen et al., 2008). Cytokinin's critical role in cambium dynamics and proliferation is less clear, and its key upstream and downstream partners remain elusive.

Other hormones and their effect on cambium dynamics, development, and secondary growth have often been discussed in different reports. Overexpression of gibberellin 20-oxidase (GA biosynthesis) increases the secondary growth in hybrid aspen (Mauriat and Moritz, 2009). In contrast, Arabidopsis GA biosynthesis mutants show an opposite effect on cambium activity in the hypocotyl (Ragni et al., 2011). Other hormones, such as jasmonic acid, brassinosteroids, strigolactones, and ethylene, positively regulate the cambium (Sehr et al., 2010; Ibañes et al., 2009; Hayward et al., 2009).

In addition to the hormonal pathways regulating secondary growth, peptide signaling constitutes another facet of the cambium regulatory system that plays an important role in secondary growth. The TDIF–PXY–WOX signaling pathway is the best-studied signaling pathway that controls cambium activity. The TRACHEARY ELEMENT DIFFERENTIATION INHIBITORY FACTOR (TDIF) peptide ligand encoded by the *CLAVATA3 (CLV3)/EMBRYO SURROUNDING REGIONRELATED 41 (CLE41)* and *CLE44* genes is synthesized in the phloem and diffuses through the apoplastic space to the cambium cells, where it binds to its cognate receptor PHLOEM INTERCALATED WITH XYLEM (PXY) (Fig. 7) (Etchells and Turner, 2010; Hirakawa et al., 2010). The PXY/TDIF complex regulates procambium/cambium cell division, inhibits xylem cell differentiation and is important for vascular-tissue patterning (Etchells and Turner, 2010; Fisher and Turner, 2007). The *WUSCHEL RELATED HOMEOBOX4 (WOX4)* and *WOX14* genes are downstream targets of PXY/TDIF, and they positively regulate the vascular cell division (Fig. 7) (Etchells et al., 2013; Hirakawa et al., 2010; Etchells et al., 2015; Kucukoglu et al., 2017). In Arabidopsis *wox4* or *wox14* single mutants cambium cell activity and -division rate is affected. In fact, a more substantial effect was observed in the *wox4 wox14* double mutant, surprisingly without any effect on vascular organization (Etchells et al., 2013). The WOX4

and WOX14 transcription factors promote stem cell proliferation by interacting with the GRAS-domain transcription factor HAIRY MERISTEM 4 (HAM4) (Zhou et al., 2015). In addition, PXY promotes the proliferation of cambium cells by repression of *BRASSINOSTEROID-INSENSITIVE 2-LIKE 1* (*BIL1*) expression (Fig. 7) independent of *WOX4/14.* The BIL1 protein kinase was shown to phosphorylate MP/ARF5 and thereby enhance its inhibitory effect on cambium activity in the Arabidopsis stem and hypocotyl. The Arabidopsis *bil1* mutant showed increased cambial activity and subsequently vascular-tissue production. Interestingly, BIL1-MP/ARF5 signaling acts by activation of the A-type *ARABIDOPSIS RESPONSE REGULATOR (ARR)* genes *ARR7* and *ARR15* (Fig. 7), encoding known negative regulators of cytokinin signaling (Han et al., 2018).

The role of AT-hook-motif nuclear proteins in plant development

All plant species, from the moss *Physcomitrella patens* to monocot and dicot plants whose genomes have been sequenced, contain highly conserved *AT-HOOK MOTIF NUCLEAR LOCALIZED (AHL)* genes (Rensing et al., 2008; Kaul et al., 2000; Paterson et al., 2009; Goff et al., 2002; Tuskan et al., 2006; Zhao et al., 2014). The high conservation of this family among land plants suggests the important role of AHL in plant growth and development. However, our knowledge about the exact role of this family in terms of biological function is limited.

AHL proteins contain two different conserved units: the AT-hook motif and plant- and a prokaryote-conserved (PPC) domain. They bind to the minor groove of DNA in AT-rich areas via the AT-hook motif, which contains an Arg-Gly-Arg conserved palindromic core. This binding occurs when the DNA backbone interacts with the AT-hook core via the side chain of an arginine residue inserted into the minor groove of the DNA (Huth et al., 1997). The second important functional unit of AHL proteins is the PPC domain—120 amino acid in length—which exists in bacteria and archaea as a single protein that forms a trimer (Fujimoto et al., 2004; Lin et al., 2007). Among land plants, the PPC domain has been identified in AHL proteins, where it is located in the carboxyl end. The PPC domain is responsible for AHL's nuclear localization and physical protein–protein interaction with other AHLs or common transcription factors (Fujimoto et al., 2004; Street et al., 2008; Zhao et al., 2013a).

The Arabidopsis genome encodes 29 AHL proteins with either one or two AT-hook DNA-binding motifs (Fujimoto et al., 2004; Matsushita et al., 2007; Zhao et al., 2014). *AHL* family members are involved in different aspects of growth and development in Arabidopsis, including flowering time, flower development, vascular-tissue differentiation, hypocotyl growth, and hormonal regulation (Weigel et al., 2000; Jin et al., 2011; Gallavotti et al., 2011; Street et al., 2008; Zhao et al., 2014; Zhou et al., 2013b; Matsushita et al., 2007). Overexpression of *AHL18* and *AHL22* delay flowering time (Street et al., 2008; Xiao et al., 2009; Yun et al., 2012; Xu et al., 2013), *SUPPRESSOR OF PHYTOCHROMEB-4 (SOB3/AHL29), ESCAROLA (ESC/AHL27),* and *AHL22* control the hypocotyl elongation of light-grown seedlings (Street et al., 2008; Xiao et al., 2009), overexpression of *SOB3/AHL27* and *ESC/AHL29* results in bigger organs such as leaves, flowers, and fruit (Street et al., 2008), overexpression of *AHL25* and *AHL15* maintains the negative feedback of *GA 3-oxidase* involve in GA biosynthesis (Matsushita et al., 2007), *AHL18* modulates primary root

architecture (Širl et al., 2020), *SOB3/AHL27* and *AHL20* regulate plant innate immune responses (Lim et al., 2007; Lu et al., 2010), and *AHL15*, *AHL19* and *AHL20* are involved in embryogenesis (Karami et al., 2020).
The absence of clear phenotypes in single and double Arabidopsis *ahl* loss-of-function mutants suggests a high functional redundancy among *AHL* genes. Therefore, most reports about this family and its effects come from overexpression of these genes in Arabidopsis (Street et al., 2008; Xiao et al., 2009; Zhao et al., 2013). High levels of functional redundancy across the AHL genes can be overcome by deleting six conserved amino acids at the core of the PPC domain. Removal of this region in AHL29 confers a dominant-negative effect when expressed in wild-type Arabidopsis, suggesting a possible interaction among AHLs with themselves and also other transcription factors by forming different protein complexes (Zhao et al., 2013b).
In animals, most AT-hook proteins are localized to MARs (Fusco and Fedele, 2007), where they are generally associated with proteins that modulate chromatin architecture (Fusco and Fedele, 2007). Matrix attachment regions (MARs) are DNA sequences rich in AT nucleotides that interact with the nuclear matrix or protein network inside the nucleus. MARs regulate gene expression by organizing chromatin at a higher order (Heng et al., 2004; Girod et al., 2007; Wilson and Coverley, 2013). Also plant AHL proteins were shown to preferentially bind to the AT-rich sequences in MARs (Morisawa et al., 2000; Fujimoto et al., 2004; Xu et al., 2013). Some evidence exists showing that AHL proteins function by altering the organization of the chromatin structure (Lim et al., 2007; Ng et al., 2009; Yun et al., 2012; Xu et al., 2013). It was recently shown that *AHL15* overexpression extensively re-organizes the chromatin configuration (Karami et al., 2020). In addition, it has been demonstrated that AHL proteins repress the transcription of several essential developmental regulatory genes, possibly through modulation of the epigenetic code in the vicinity of their DNA-binding regions (Lim et al., 2007; Ng et al., 2009; Yun et al., 2012). Despite the progress mentioned above with regard to AHL function in Arabidopsis, the exact molecular mechanism behind their role in plant development remains elusive.

Outline of this thesis

In **chapter 2** of this thesis we confirmed that *AHL15* acts as an AM maturation suppressor, resulting in plant longevity extension. *ahl15* loss-of-function accelerates AM maturation. Conversely, high expression of *AHL15* suppresses AM maturation and induces polycarpic features in monocarpic Arabidopsis and tobacco. Interestingly, in short-day grown Arabidopsis with promoted longevity, the expression of *AHL15* was quite high in AMs. Our genetic studies indicate the crucial role of *AHL15* in suppressing axillary-meristem maturation and promoting plant longevity, directly downstream of *SOC1*, *FUL*, and upstream of GA.
More-detailed analyses revealed that *AHL15* is not only and specifically involved in suppressing AM maturation, but that interestingly, the protein rather has a crucial role in an earlier development phase transitions. In **chapter 3**, we verified that *ahl15* loss-of-function leads to early VPC and flowering. A dramatic delay in the VPC and flowering was observed

upon *AHL15* overexpression in Arabidopsis and tobacco. Tissue-specific expression of *AHL15* in the SAM and in young leaves confirmed the direct and indirect role of AHL15 in phase change and flowering in Arabidopsis. Furthermore, we found that AHL15 represses *SPLs* independent of miR156 (master regulator of VPC). AHLs and SPLs suppress each other in a negative feedback manner, since the effect of SPLs on VPC turned out to be mediated by repression of *AHL* expression. Our findings indicate genetic interaction between AHLs and SPLs in controlling the VPC.

We also noticed that *AHL15* overexpression surprisingly affects secondary growth in Arabidopsis. In **chapter 4**, we showed that *AHL15* plays a central role in inducing vascular-cambium activity downstream of *SOC1* and *FUL* and upstream of the *IPT* cytokinin biosynthesis genes. Overexpression of *AHL15* lead to extensive secondary xylem production in Arabidopsis. In contrast, *ahl15* loss-of-function plants showed significant reduction in cambium activity and xylem production. By tracking the expression pattern of *AHL15*, we confirmed that *AHL15* is specifically expressed in the intra- and interfascicular parts of the vascular cambium. By expressing *AHL15* under a cambium-specific promoter (*pPXY:AHL15*), we verified that cambium-specific enhancement of *AHL15* expression is sufficient to promote cambium activity and enhance xylem formation.

References

Abe, M., Kosaka, S., Shibuta, M., Nagata, K., Uemura, T., Nakano, A., and Kaya, H. (2019). Transient activity of the florigen complex during the floral transition in arabidopsis thaliana. Development **146**: 171504.

Aguilar-Martínez, J.A., Poza-Carrión, C., and Cubas, P. (2007). Arabidopsis BRANCHED1 acts as an integrator of branching signals within axillary buds. Plant Cell **19**: 458–472.

Aloni, R. (2013). The role of hormones in controlling vascular differentiation. Plant Cell Monogr. **20**: 99–139.

Amasino, R. (2009). Floral induction and monocarpic versus polycarpic life histories. Genome Biol. **10**: 228.

Amasino, R. (2010). Seasonal and developmental timing of flowering. Plant J. **61**: 1001–1013.

Amasino, R.M. and Michaels, S.D. (2010). The timing of flowering. Plant Physiol. **154**: 516–520.

Andrés, F. and Coupland, G. (2012). The genetic basis of flowering responses to seasonal cues. Nat. Rev. Genet. **13**: 627–639.

Aukerman, M.J. and Sakai, H. (2003). Regulation of flowering time and foral organ identity by a microRNA and its APETALA2 -like target genes. Genetics **15**: 2730–2741.

Balkunde, R., Kitagawa, M., Xu, X.M., Wang, J., and Jackson, D. (2017). SHOOT MERISTEMLESS trafficking controls axillary meristem formation, meristem size and organ boundaries in Arabidopsis. Plant J. **90**: 435–446.

Bergonzi, S., Albani, M.C., Ver Loren van Themaat, E., Nordström, K.J. V, Wang, R., Schneeberger, K., Moerland, P.D., and Coupland, G. (2013). Mechanisms of age-dependent response to winter temperature in perennial flowering of Arabis alpina. Science **340**: 1094–1097.

Besnard, F. et al. (2014). Cytokinin signalling inhibitory fields provide robustness to phyllotaxis. Nature **505**: 417–421.

Blümel, M., Dally, N., and Jung, C. (2015). Flowering time regulation in crops—what did we learn from Arabidopsis? Curr. Opin. Biotechnol. **32**: 121–129.

Braun, N. et al. (2012). The pea TCP transcription factor PsBRC1 acts downstream of strigolactones to control shoot branching. Plant Physiol. **158**: 225–238.

Bustamante, M., Matus, J.T., and Riechmann, J.L. (2016). Genome-wide analyses for dissecting gene regulatory networks in the shoot apical meristem. J. Exp. Bot. **67**: 1639–1648.

Chiang, M.H. and Greb, T. (2019). How to organize bidirectional tissue production? Curr. Opin. Plant Biol. **51**: 15–21.

Chuck, G.S. et al. (2011). Overexpression of the maize Corngrass1 microRNA prevents flowering, improves digestibility, and increases starch content of switchgrass. Proc. Natl. Acad. Sci. **108**: 17550–15555.

Davière, J.-M. and Achard, P. (2013). Gibberellin signaling in plants. Development **140**: 1147–1151.

Davies, P.J. and Gan, S. (2012). Towards an integrated view of monocarpic plant senescence. Russ. J. Plant Physiol. **59**: 467–478.

Demura, T. and Ye, Z.-H. (2010). Regulation of plant biomass production. Curr. Opin. Plant Biol. **13**: 299–304.

Deng, W., Ying, H., Helliwell, C.A., Taylor, J.M., Peacock, W.J., and Dennis, E.S. (2011). FLOWERING LOCUS C (FLC) regulates development pathways throughout the life cycle of Arabidopsis. Proc. Natl. Acad. Sci. **2011**: 1–6.

Djennane, S., Hibrand-Saint Oyant, L., Kawamura, K., Lalanne, D., Laffaire, M., Thouroude, T., Chalain, S., Sakr, S., Boumaza, R., Foucher, F., and Leduc, N. (2014). Impacts of light and temperature on shoot branching gradient and expression of strigolactone synthesis and signalling genes in rose. Plant, Cell Environ. **37**: 742–757.

Dodsworth, S. (2009). A diverse and intricate signalling network regulates stem cell fate in the shoot apical meristem. Dev. Biol. **336**: 1–9.

Domagalska, M.A. and Leyser, O. (2011). Signal integration in the control of shoot branching. Nat. Rev. Mol. Cell Biol. **12**: 211–221.

Dun, E.A., Germain, A. de Saint, Rameau, C., and Beveridge, C.A. (2012). Antagonistic action of

strigolactone and cytokinin in bud outgrowth control. Plant Physiol. **158**: 487–498.
Etchells, J.P., Mishra, L.S., Kumar, M., Campbell, L., and Turner, S.R. (2015). Wood formation in trees is increased by manipulating PXY-regulated cell division. Curr. Biol. **25**: 1050–1055.
Etchells, J.P., Provost, C.M., Mishr, L., and Turner, S.R. (2013). WOX4 and WOX14 act downstream of the PXY receptor kinase to regulate plant vascular proliferation independently of any role in vascular organisation. Dev. **140**: 2224–2234.
Etchells, J.P. and Turner, S.R. (2010). The PXY-CLE41 receptor ligand pair defines a multifunctional pathway that controls the rate and orientation of vascularcell division. Development **137**: 767–774.
EVERT, R.F. (2006). Esau's Plant Anatomy, 3rd edition.
Ferguson, B.J. and Beveridge, C.A. (2009). Roles for auxin, cytokinin, and strigolactone in regulating shoot branching. Plant Physiol. **149**: 109.135475.
Fisher, K. and Turner, S. (2007). PXY, a Receptor-like Kinase Essential for Maintaining Polarity during Plant Vascular-Tissue Development. Curr. Biol. **17**: 1061–1066.
Foo, E., Bullier, E., Goussot, M., Foucher, F., Rameau, C., and Beveridge, C.A. (2005). The branching gene RAMOSUS1 mediates interactions among two novel signals and auxin in pea. Plant Cell **17**: 464–474.
Fornara, F. and Coupland, G. (2009). Plant phase transitions make a SPLash. Cell **138**: 625–627.
Fu, C., Sunkar, R., Zhou, C., Shen, H., Zhang, J.-Y., Matts, J., Wolf, J., Mann, D.G.J., Stewart, C.N., Tang, Y., and Wang, Z.-Y. (2012). Overexpression of miR156 in switchgrass (Panicum virgatum L.) results in various morphological alterations and leads to improved biomass production. Plant Biotechnol. J. **10**: 443–452.
Fujimoto, S., Matsunaga, S., Yonemura, M., Uchiyama, S., Azuma, T., and Fukui, K. (2004). Identification of a novel plant MAR DNA binding protein localized on chromosomal surfaces. Plant Mol. Biol. **56**: 225–239.
Fusco, A. and Fedele, M. (2007). Roles of HMGA proteins in cancer. Nat. Rev. Cancer **7**: 899–910.
Gallavotti, A., Malcomber, S., Gaines, C., Stanfield, S., Whipple, C., Kellogg, E., and Schmidt, R.J. (2011). BARREN STALK FASTIGIATE1 is an AT-hook protein required for the formation of maize ears. Plant Cell **23**: 1756–1771.
Galvão, V.C., Horrer, D., Küttner, F., and Schmid, M. (2012). Spatial control of flowering by DELLA proteins in Arabidopsis thaliana. Development **139**: 4072–4082.
Gandikota, M., Birkenbihl, R.P., Höhmann, S., Cardon, G.H., Saedler, H., and Huijser, P. (2007). The miRNA156/157 recognition element in the 3' UTR of the Arabidopsis SBP box gene SPL3 prevents early flowering by translational inhibition in seedlings. Plant J. **49**: 683–693.
Girod, P., Nguyen, D., Calabrese, D., Puttini, S., Martinet, D., Regamey, A., Saugy, D., Beckmann, J.S., Bucher, P., and Mermod, N. (2007). Genome-wide prediction of matrix attachment regions that increase gene expression in mammalian cells. Nat. Methods **4**: 747–753.
Goff, S.A. et al. (2002). A draft sequence of the rice genome (Oryza sativa L. ssp. japonica). Science (80-.). **296**: 92–100.
Gonzalez-Grandio, E., Pajoro, A., Franco-Zorrilla, J.M., Tarancon, C., Immink, R.G.H., and Cubas, P. (2017). Abscisic acid signaling is controlled by a BRANCHED1/HD-ZIP i cascade in Arabidopsis axillary buds. Proc. Natl. Acad. Sci. U. S. A. **114**: E245–E254.
Grbić, V. and Bleecker, A.B. (2000). Axillary meristem development in Arabidopsis thaliana. Plant J. **21**: 215–223.
Greb, T., Clarenz, O., Schafer, E., Muller, D., Herrero, R., Schmitz, G., and Theres, K. (2003). Molecular analysis of the LATERAL SUPPRESSOR gene in Arabidopsis reveals a conserved control mechanism for axillary meristem formation. Genes Dev. **17**: 1175–1187.
Griffiths, J., Murase, K., Rieu, I., Zentella, R., Zhang, Z.L., Powers, S.J., Gong, F., Phillips, A.L., Hedden, P., Sun, T.P., and Thomas, S.G. (2006). Genetic characterization and functional analysis of the GID1 gibberellin receptors in Arabidopsis. Plant Cell **18**: 3399–3414.
Han, S., Cho, H., Noh, J., Qi, J., Jung, H.J., Nam, H., Lee, S., Hwang, D., Greb, T., and Hwang, I. (2018). BIL1-mediated MP phosphorylation integrates PXY and cytokinin signalling in secondary

growth. Nat. Plants **4**: 605–614.

Hayward, A., Stirnberg, P., Beveridge, C., and Leyser, O. (2009). Interactions between auxin and strigolactone in shoot branching control. Plant Physiol. **151**: 400–412.

He, J., Xu, M., Willmann, M.R., McCormick, K., Hu, T., Yang, L., Starker, C.G., Voytas, D.F., Meyers, B.C., and Poethig, R.S. (2018). Threshold-dependent repression of SPL gene expression by miR156/miR157 controls vegetative phase change in Arabidopsis thaliana. PLoS Genet. **14**: 1007337.

Heng, H.H.Q., Goetze, S., Ye, C.J., Liu, G., Stevens, J.B., Bremer, S.W., Wykes, S.M., Bode, J., and Krawetz, S. (2004). Chromatin loops are selectively anchored using scaffold/matrix-attachment regions. J. Cell Sci. **117**: 999–1008.

Hirakawa, Y., Kondo, Y., and Fukuda, H. (2010). TDIF peptide signaling regulates vascular stem cell proliferation via the WOX4 homeobox gene in Arabidopsis. Plant Cell **22**: 2618–2629.

Huijser, P. and Schmid, M. (2011). The control of developmental phase transitions in plants. Development **138**: 4117–4129.

Huth, J.R., Bewley, C.A., Nissen, M.S., Evans, J.N.S., Reeves, R., Gronenborn, A.M., and Clore, G.M. (1997). The solution structure of an HMG-I(Y)-DNA complex defines a new architectural minor groove binding motif. Nat. Struct. Biol. **4**: 657–665.

Hwang, K., Susila, H., Nasim, Z., Jung, J.Y., and Ahn, J.H. (2019). Arabidopsis ABF3 and ABF4 Transcription Factors Act with the NF-YC Complex to Regulate SOC1 Expression and Mediate Drought-Accelerated Flowering. Mol. Plant **12**: 489–505.

Hyun, Y., Vincent, C., Tilmes, V., Bergonzi, S., Kiefer, C., Richter, R., Martinez-Gallegos, R., Severing, E., and Coupland, G. (2019). Plant science: A regulatory circuit conferring varied flowering response to cold in annual and perennial plants. Science (80-.). **363**: 409–412.

Ibañes, M., Fàbregas, N., Chory, J., and Caño-Delgadob, A.I. (2009). Brassinosteroid signaling and auxin transport are required to establish the periodic pattern of Arabidopsis shoot vascular bundles. Proc. Natl. Acad. Sci. U. S. A. **106**: 13630–13635.

Immanen, J. et al. (2016). Cytokinin and auxin display distinct but interconnected distribution and signaling profiles to stimulate cambial activity. Curr. Biol. **26**: 1990–1997.

Jin, Y. et al. (2011). An AT-hook gene is required for palea formation and floral organ number control in rice. Dev. Biol. **359**: 277–88.

Johnson, X., Brcich, T., Dun, E.A., Goussot, M., Haurogné, K., Beveridge, C.A., and Rameau, C. (2006). Branching genes are conserved across species. Genes controlling a novel signal in pea are coregulated by other long-distance signals. Plant Physiol. **142**: 1014–1026.

Jouannet, V., Brackmann, K., and Greb, T. (2015). (Pro)cambium formation and proliferation: Two sides of the same coin? Curr. Opin. Plant Biol. **23**: 54–60.

Jung, C. and Müller, A.E. (2009). Flowering time control and applications in plant breeding. Trends Plant Sci. **14**: 563–573.

Jung, J.-H., Seo, P.J., Kang, S.K., and Park, C.-M. (2011). miR172 signals are incorporated into the miR156 signaling pathway at the SPL3/4/5 genes in Arabidopsis developmental transitions. Plant Mol. Biol. **76**: 35–45.

Jung, J., Ju, Y., Seo, P.J., Lee, J., Park, C., and Genomics, P. (2012). The SOC1-SPL module integrates photoperiod and gibberellic acid signals to control flowering time in Arabidopsis. Plant J. **69**: 577–588.

Jung, J.H., Lee, H.J., Ryu, J.Y., and Park, C.M. (2016). SPL3/4/5 Integrate Developmental Aging and Photoperiodic Signals into the FT-FD Module in Arabidopsis Flowering. Mol. Plant **9**: 1647–1659.

Kakimoto, T. (2001). Identification of plant cytokinin biosynthetic enzymes as dimethylallyl diphosphate:ATP/ADP isopentenyltransferases. Plant Cell Physiol. **42**: 677–685.

Karami, O., Rahimi, A., Mak, P., Horstman, A., Boutilier, K., Compier, M., Van der Zaal, B., and Offringa, R. (2020). An Arabidopsis AT-hook motif nuclear protein mediates somatic-to-embryonic cell fate conversion coinciding with genome duplication. bioRxiv. **Nature com**: https://www.biorxiv.org/content/10.1101/2020.01.03.

Kaul, S. et al. (2000). Analysis of the genome sequence of the flowering plant Arabidopsis thaliana. Nature **408**: 796–815.

Kim, D.-H. and Sung, S. (2014). Genetic and epigenetic mechanisms underlying vernalization. Arabidopsis Book **12**: e0171.

Kim, H.K., Van Oosterom, E., Dingkuhn, M., Luquet, D., and Hammer, G. (2010). Regulation of tillering in sorghum: Environmental effects. Ann. Bot. **106**: 57–67.

Kucukoglu, M., Nilsson, J., Zheng, B., Chaabouni, S., and Nilsson, O. (2017). WUSCHEL-RELATED HOMEOBOX4 (WOX4)-like genes regulate cambial cell division activity and secondary growth in Populus trees. New Phytol. **215**: 642–657.

Kurakawa, T., Ueda, N., Maekawa, M., Kobayashi, K., Kojima, M., Nagato, Y., Sakakibara, H., and Kyozuka, J. (2007). Direct control of shoot meristem activity by a cytokinin-activating enzyme. Nature **445**: 652–655.

Kwak, J.S., Son, G.H., Kim, S.I., Song, J.T., and Seo, H.S. (2016). Arabidopsis HIGH PLOIDY2 Sumoylates and stabilizes flowering locus C through Its E3 ligase activity. Front. Plant Sci.

Lee, H. (2000). The AGAMOUS-LIKE 20 MADS domain protein integrates floral inductive pathways in Arabidopsis. Genes Dev. **14**: 2366–2376.

Lim, P.O., Kim, Y., Breeze, E., Koo, J.C., Woo, H.R., Ryu, J.S., Park, D.H., Beynon, J., Tabrett, A., Buchanan-Wollaston, V., and Nam, H.G. (2007). Overexpression of a chromatin architecture-controlling AT-hook protein extends leaf longevity and increases the post-harvest storage life of plants. Plant J. **52**: 1140–1153.

Lin, L., Nakano, H., Nakamura, S., Uchiyama, S., Fujimoto, S., Matsunaga, S., Kobayashi, Y., Ohkubo, T., and Fukui, K. (2007). Crystal structure of pyrococcus horikoshii PPC protein at 1.60 Å resolution. Proteins Struct. Funct. Genet. **67**: 505–507.

Lu, H., Zou, Y., and Feng, N. (2010). Overexpression of AHL20 negatively regulates defenses in Arabidopsis. J. Integr. Plant Biol. **52**: 801–808.

Mahrez, W., Shin, J., Muñoz-Viana, R., Figueiredo, D.D., Trejo-Arellano, M.S., Exner, V., Siretskiy, A., Gruissem, W., Köhler, C., and Hennig, L. (2016). BRR2a Affects Flowering Time via FLC Splicing. PLoS Genet. **12**: 1005924.

Martín-Trillo, M., Grandío, E.G., Serra, F., Marcel, F., Rodríguez-Buey, M.L., Schmitz, G., Theres, K., Bendahmane, A., Dopazo, H., and Cubas, P. (2011). Role of tomato BRANCHED1-like genes in the control of shoot branching. Plant J. **67**: 701–714.

Matsoukas, I.G., Massiah, A.J., and Thomas, B. (2012). Florigenic and antflorigenic signaling in plants. Plant Cell Physiol. **53**: 1827–1842.

Matsumoto-Kitano, M., Kusumoto, T., Tarkowski, P., Kinoshita-Tsujimura, K., Václavíková, K., Miyawaki, K., and Kakimoto, T. (2008). Cytokinins are central regulators of cambial activity. Proc. Natl. Acad. Sci. U. S. A. **105**: 20027–20031.

Matsushita, A., Furumoto, T., Ishida, S., and Takahashi, Y. (2007). AGF1, an AT-hook protein, is necessary for the negative feedback of AtGA3ox1 encoding GA 3-oxidase. Plant Physiol. **143**: 1152–1162.

Mauriat, M. and Moritz, T. (2009). Analyses of GA20ox- and GID1-over-expressing aspen suggest that gibberellins play two distinct roles in wood formation. Plant J. **58**: 989–1003.

Melzer, S., Lens, F., Gennen, J., Vanneste, S., Rohde, A., and Beeckman, T. (2008). Flowering-time genes modulate meristem determinacy and growth form in Arabidopsis thaliana. Nat. Genet. **40**: 1489–1492.

Minakuchi, K., Kameoka, H., Yasuno, N., Umehara, M., Luo, L., Kobayashi, K., Hanada, A., Ueno, K., Asami, T., Yamaguchi, S., and Kyozuka, J. (2010). FINE CULM1 (FC1) works downstream of strigolactones to inhibit the outgrowth of axillary buds in rice. Plant Cell Physiol. **51**: 1127–1135.

Miyawaki, K., Matsumoto-Kitano, M., and Kakimoto, T. (2004). Expression of cytokinin biosynthetic isopentenyltransferase genes in Arabidopsis: Tissue specificity and regulation by auxin, cytokinin, and nitrate. Plant J. **37**: 128–138.

Morisawa, G., Han-Yama, A., Moda, I., Tamai, A., Iwabuchi, M., and Meshi, T. (2000). AHM1, a

novel type of nuclear matrix-localized, MAR binding protein with a single AT hook and a J domain-homologous region. Plant Cell **12**: 1903–1916.

Munné-Bosch, S. (2008). Do perennials really senesce? Trends Plant Sci. **13**: 216–220.

Murray, J.A.H., Jones, A., Godin, C., and Traas, J. (2012). Systems analysis of shoot apical meristem growth and development: Integrating hormonal and mechanical signaling. Plant Cell **24**: 3907–3919.

Ng, K.-H., Yu, H., and Ito, T. (2009). AGAMOUS controls GIANT KILLER, a multifunctional chromatin modifier in reproductive organ patterning and differentiation. PLoS Biol. **7**: e1000251.

Nieminen, K. et al. (2008). Cytokinin signaling regulates cambial development in poplar. Proc. Natl. Acad. Sci. U. S. A. **105**: 20032–20037.

Nilsson, J., Karlberg, A., Antti, H., Lopez-Vernaz, M., Mellerowicz, E., Perrot-Rechenmann, C., Sandberg, G., and Bhalerao, R.P. (2008). Dissecting the molecular basis of the regulation of wood formation by auxin in hybrid aspen. Plant Cell **20**: 843–855.

Oikawa, T. and Kyozuka, J. (2009). Two-step regulation of LAX PANICLE1 protein accumulation in Axillary meristem formation in rice. Plant Cell **21**: 1095–1108.

Park, J., Oh, D., Dassanayake, M., Nguyen, K.T., Ogas, J., and Choi, G. (2017). Gibberellin signaling requires chromatin remodeler PICKLE to promote vegetative growth and phase transitions. Plant Physiol. **173**: 1463–1474.

Park, S.J., Eshed, Y., and Lippman, Z.B. (2014). Meristem maturation and inflorescence architecture — lessons from the Solanaceae. Curr. Opin. Plant Biol. **17**: 70–77.

Paterson, A.H. et al. (2009). The Sorghum bicolor genome and the diversification of grasses. Nature **457**: 551–556.

Pautler, M., Tanaka, W., Hirano, H.Y., and Jackson, D. (2013). Grass meristems I: Shoot apical meristem maintenance, axillary meristem determinacy and the floral transition. Plant Cell Physiol. **54**: 313–324.

Poduska, B., Humphrey, T., Redweik, A., and Grbić, V. (2003). The synergistic activation of FLOWERING LOCUS C by FRIGIDA and a new flowering gene AERIAL ROSETTE 1 underlies a novel morphology in arabidopsis. Genetics **163**: 1457–1465.

Poethig, R.S. (1990). Phase change and the regulation of shoot morphogenesis in plants. Science (80-.). **250**: 923–930.

Poethig, R.S. (2013). Vegetative phase change and shoot maturation in plants. Curr. Top. Dev. Biol. **105**: 125–152.

Ragni, L. and Greb, T. (2018). Secondary growth as a determinant of plant shape and form. Semin. Cell Dev. Biol. **79**: 58–67.

Ragni, L., Nieminen, K., Pacheco-Villalobos, D., Sibout, R., Schwechheimer, C., and Hardtke, C.S. (2011). Mobile gibberellin directly stimulates Arabidopsis hypocotyl xylem expansion. Plant Cell **23**: 1322–1336.

Rameau, C., Bertheloot, J., Leduc, N., Andrieu, B., Foucher, F., and Sakr, S. (2015). Multiple Pathways Regulate Shoot Branching. Front. Plant Sci. **5**: 00741.

Reinhardt, D., Mandel, T., and Kuhlemeier, C. (2000). Auxin regulates the initiation and radial position of plant lateral organs. Plant Cell **12**: 507–518.

Rensing, S.A. et al. (2008). The Physcomitrella genome reveals evolutionary insights into the conquest of land by plants. Science (80-.). **319**: 64–69.

Salinas, M., Xing, S., Höhmann, S., Berndtgen, R., and Huijser, P. (2012). Genomic organization, phylogenetic comparison and differential expression of the SBP-box family of transcription factors in tomato. Planta **235**: 1171–1184.

Schwab, R., Palatnik, J.F., Riester, M., Schommer, C., Schmid, M., and Weigel, D. (2005). Specific effects of microRNAs on the plant transcriptome. Dev. Cell **8**: 517–527.

Scofield, S., Murison, A., Jones, A., Fozard, J., Aida, M., Band, L.R., Bennett, M., and Murray, J.A.H. (2018). Coordination of meristem and boundary functions by transcription factors in the SHOOT MERISTEMLESS regulatory network. Dev. **145**: 157081.

Seale, M., Bennett, T., and Leyser, O. (2017). BRC1 expression regulates bud activation potential but

is not necessary or sufficient for bud growth inhibition in arabidopsis. Dev. **144**: 1661–1673.
Sehr, E.M., Agusti, J., Lehner, R., Farmer, E.E., Schwarz, M., and Greb, T. (2010). Analysis of secondary growth in the Arabidopsis shoot reveals a positive role of jasmonate signalling in cambium formation. Plant J. **63**: 811–822.
Shikata, M., Yamaguchi, H., Sasaki, K., and Ohtsubo, N. (2012). Overexpression of Arabidopsis miR157b induces bushy architecture and delayed phase transition in Torenia fournieri. Planta **236**: 1027–1035.
Shinohara, N., Taylor, C., and Leyser, O. (2013). Strigolactone can promote or inhibit shoot branching by triggering rapid depletion of the auxin efflux protein PIN1 from the plasma membrane. PLoS Biol. **11**: e1001474.
Siedlecka, A., Wiklund, S., Péronne, M.A., Micheli, F., Leśniewska, J., Sethson, I., Edlund, U., Richard, L., Sundberg, B., and Mellerowicz, E.J. (2008). Pectin methyl esterase inhibits intrusive and symplastic cell growth in developing wood cells of Populus. Plant Physiol. **146**: 554–565.
Silverstone, A.L. and Pui, Y. (1997). The new RGA locus encodes a negative regulator of gibberellin response in Arabidopsis thaliana. Genetics **146**: 1087–1109.
Širl, M., Šnajdrová, T., Gutiérrez-Alanís, D., Dubrovsky, J.G., Vielle-Calzada, J.P., Kulich, I., and Soukup, A. (2020). At-hook motif nuclear localised protein 18 as a novel modulator of root system architecture. Int. J. Mol. Sci. **21**: 1–19.
De Smet, I. and Jürgens, G. (2007). Patterning the axis in plants - auxin in control. Curr. Opin. Genet. Dev. **17**: 337–343.
Smetana, O. et al. (2019). High levels of auxin signalling define the stem-cell organizer of the vascular cambium. Nature **565**: 485–489.
Smith, M.R., Willmann, M.R., Wu, G., Berardini, T.Z., Möller, B., Weijers, D., and Poethig, R.S. (2009). Cyclophilin 40 is required for microRNA activity in Arabidopsis. Proc. Natl. Acad. Sci. **106**: 5424–5429.
Somssich, M., Je, B. Il, Simon, R., and Jackson, D. (2016). CLAVATA-WUSCHEL signaling in the shoot meristem. Dev. **143**: 3238–3248.
Song, Y.H., Ito, S., and Imaizumi, T. (2013). Flowering time regulation: photoperiod- and temperature-sensing in leaves. Trends Plant Sci. **18**: 575–583.
Soyars, C.L., James, S.R., and Nimchuk, Z.L. (2016). Ready, aim, shoot: Stem cell regulation of the shoot apical meristem. Curr. Opin. Plant Biol. **29**: 163–168.
Street, I.H., Shah, P.K., Smith, A.M., Avery, N., and Neff, M.M. (2008). The AT-hook-containing proteins SOB3/AHL29 and ESC/AHL27 are negative modulators of hypocotyl growth in Arabidopsis. Plant J. **54**: 1–14.
Sun, T. -p. (2010). Gibberellin-GID1-DELLA: A Pivotal Regulatory Module for Plant Growth and Development. Plant Physiol. **154**: 567–570.
Tabuchi, H. et al. (2011). LAX PANICLE2 of rice encodes a novel nuclear protein and regulates the formation of axillary meristems. Plant Cell **23**: 3276–3287.
Telfer, A., Bollman, K.M., and Poethig, R.S. (1997). Phase change and the regulation of trichome distribution in Arabidopsis thaliana. Development **124**: 645–654.
Thomas, H. (2013). Senescence , ageing and death of the whole plant. New Phytol.: 12047.
Tooke, F., Ordidge, M., Chiurugwi, T., and Battey, N. (2005). Mechanisms and function of flower and inflorescence reversion. J. Exp. Bot. **56**: 2587–2599.
Tuominen, H., Puech, L., Fink, S., and Sundberg, B. (1997). A radial concentration gradient of indole-3-acetic acid is related to secondary xylem development in hybrid aspen. Plant Physiol. **115**: 577–585.
Turnbull, C. (2011). Long-distance regulation of flowering time. J. Exp. Bot. **62**: 4399–43413.
Tuskan, G.A. et al. (2006). The genome of black cottonwood, Populus trichocarpa (Torr. & Gray). Science (80-.). **313**: 1596–1604.
Uchida, N. and Torii, K.U. (2019). Stem cells within the shoot apical meristem: identity, arrangement and communication. Cell. Mol. Life Sci. **76**: 1067–1080.

Usami, T., Horiguchi, G., Yano, S., and Tsukaya, H. (2009). The more and smaller cells mutants of Arabidopsis thaliana identify novel roles for SQUAMOSA PROMOTER BINDING PROTEIN-LIKE genes in the control of heteroblasty. Development **136**: 955–964.

Waldie, T. and Leyser, O. (2018). Cytokinin targets auxin transport to promote shoot branching. Plant Physiol. **177**: 803–818.

Wang, B., Smith, S.M., and Li, J. (2018). Genetic Regulation of Shoot Architecture. Annu. Rev. Plant Biol. **69**: 437–468.

Wang, J.-W. (2014). Regulation of flowering time by the miR156-mediated age pathway. J. Exp. Bot. **65**: 4723–4730.

Wang, J.-W., Park, M.Y., Wang, L.-J., Koo, Y., Chen, X.-Y., Weigel, D., and Poethig, R.S. (2011). miRNA control of vegetative phase change in trees. PLoS Genet. **7**: e1002012.

Wang, Q., Kohlen, W., Rossmann, S., Vernoux, T., and Theres, K. (2014a). Auxin depletion from the leaf axil conditions competence for axillary meristem formation in Arabidopsis and tomato. Plant Cell **26**: 2068–2079.

Wang, R., Farrona, S., Vincent, C., Joecker, A., Schoof, H., Turck, F., Alonso-Blanco, C., Coupland, G., and Albani, M.C. (2009). PEP1 regulates perennial flowering in Arabis alpina. Nature **459**: 423–427.

Wang, Y., Wang, J., Shi, B., Yu, T., Qi, J., Meyerowitz, E.M., and Jiao, Y. (2014b). The stem cell niche in leaf axils is established by auxin and cytokinin in Arabidopsis. Plant Cell **26**: 2055–2067.

Weigel, D. et al. (2000). Activation tagging in Arabidopsis. Plant Physiol. **122**: 1003–1013.

Wilson, R.H.C. and Coverley, D. (2013). Relationship between DNA replication and the nuclear matrix. Genes Cells **18**: 17–31.

Wu, G., Park, M.Y., Conway, S.R., Wang, J.-W., Weigel, D., and Poethig, R.S. (2009a). The sequential action of miR156 and miR172 regulates developmental timing in Arabidopsis. Cell **138**: 750–759.

Wu, G., Park, M.Y., Conway, S.R., Wang, J.W., Weigel, D., and Poethig, R.S. (2009b). The Sequential Action of miR156 and miR172 Regulates Developmental Timing in Arabidopsis. Cell **138**: 750–759.

Wu, G. and Poethig, R.S. (2006). Temporal regulation of shoot development in Arabidopsis thaliana by miR156 and its target SPL3. Development **133**: 3539–3547.

Xiao, C., Chen, F., Yu, X., Lin, C., and Fu, Y.-F. (2009). Over-expression of an AT-hook gene, AHL22, delays flowering and inhibits the elongation of the hypocotyl in Arabidopsis thaliana. Plant Mol. Biol. **71**: 39–50.

Xie, K., Shen, J., Hou, X., Yao, J., Li, X., Xiao, J., and Xiong, L. (2012). Gradual increase of miR156 regulates temporal expression changes of numerous genes during leaf development in rice. Plant Physiol. **158**: 1382–1394.

Xu, M., Hu, T., Zhao, J., Park, M.-Y., Earley, K.W., Wu, G., Yang, L., and Poethig, R.S. (2016). Developmental functions of miR156-regulated SQUAMOSA PROMOTER BINDING PROTEIN-LIKE (SPL) genes in Arabidopsis thaliana. PLoS Genet. **12**: e1006263.

Xu, Y., Wang, Y., Stroud, H., Gu, X., Sun, B., Gan, E.-S., Ng, K.-H., Jacobsen, S.E., He, Y., and Ito, T. (2013). A matrix protein silences transposons and repeats through interaction with retinoblastoma-associated proteins. Curr. Biol. **23**: 345–350.

Yao, C. and Finlayson, S.A. (2015). Abscisic acid is a general negative regulator of arabidopsis axillary bud growth. Plant Physiol. **169**: 611–626.

Yu, S., Galvão, V.C., Zhang, Y.-C., Horrer, D., Zhang, T.-Q., Hao, Y.-H., Feng, Y.-Q., Wang, S., Schmid, M., and Wang, J.-W. (2012). Gibberellin regulates the Arabidopsis floral transition through miR156-targeted SQUAMOSA promoter binding-like transcription factors. Plant Cell **24**: 3320–32.

Yun, J., Kim, Y.-S., Jung, J.-H., Seo, P.J., and Park, C.-M. (2012). The AT-hook motif-containing protein AHL22 regulates flowering initiation by modifying FLOWERING LOCUS T chromatin in Arabidopsis. J. Biol. Chem. **287**: 15307–16.

Zhang, X., Zou, Z., Zhang, J., Zhang, Y., Han, Q., Hu, T., Xu, X., Liu, H., Li, H., and Ye, Z. (2011). Over-

expression of sly-miR156a in tomato results in multiple vegetative and reproductive trait alterations and partial phenocopy of the sft mutant. FEBS Lett. **585**: 435–439.

Zhao, J., Favero, D.S., Peng, H., and Neff, M.M. (2013a). Arabidopsis thaliana AHL family modulates hypocotyl growth redundantly by interacting with each other via the PPC/DUF296 domain. Proc. Natl. Acad. Sci. **110**: E4688–E4697.

Zhao, J., Favero, D.S., Peng, H., and Neff, M.M. (2013b). Arabidopsis thaliana AHL family modulates hypocotyl growth redundantly by interacting with each other via the PPC/DUF296 domain. Proc. Natl. Acad. Sci. U. S. A. **110**: E4688–E4697.

Zhao, J., Favero, D.S., Qiu, J., Roalson, E.H., and Neff, M.M. (2014). Insights into the evolution and diversification of the AT-hook Motif Nuclear Localized gene family in land plants. BMC Plant Biol. **14**: 266.

Zhao, Z., Andersen, S.U., Ljung, K., Dolezal, K., Miotk, A., Schultheiss, S.J., and Lohmann, J.U. (2010). Hormonal control of the shoot stem-cell niche. Nature **465**: 1089–1092.

Zhou, C.-M., Zhang, T.-Q., Wang, X., Yu, S., Lian, H., Tang, H., Feng, Z.-Y., Zozomova-Lihová, J., and Wang, J.-W. (2013a). Molecular basis of age-dependent vernalization in Cardamine flexuosa. Science **340**: 1097–1100.

Zhou, J., Wang, X., Lee, J.-Y., and Lee, J.-Y. (2013b). Cell-to-cell movement of two interacting AT-hook factors in Arabidopsis root vascular tissue patterning. Plant Cell **25**: 187–201.

Zotz, G., Wilhelm, K., and Becker, A. (2011). Heteroblasty—A Review. Bot. Rev. **77**: 109–151.

Chapter 2

A suppressor of axillary meristem maturation promotes longevity in flowering plants

Omid Karami[1], Arezoo Rahimi[1], Majid Khan[1,5], Marian Bemer[3], Rashmi R. Hazarika[4], Patrick Mak[1,6], Monique Compier[1,7] Vera van Noort[2,4] and Remko Offringa[1,*]

Nature Plants (2020)

[1] Plant Developmental Genetics and [2] Bioinformatics and Genomics, Institute of Biology Leiden, Leiden University, Sylviusweg 72, 2333 BE Leiden, The Netherlands

[3] Laboratory of Molecular Biology and B.U. Bioscience, Wageningen University & Research, Droevendaalsesteeg 1, 6708 PB Wageningen, The Netherlands

[4] KU Leuven, Centre of Microbial and Plant Genetics, Kasteelpark Arenberg 20, B-3001 Leuven, Belgium.

[5] Present address: Institute of Biotechnology and Genetic Engineering (IBGE), University of Agriculture Peshawar, Peshawar, Pakistan

[6] Present address: Sanquin Plasma Products BV, Dept. Product Development, Plesmanlaan 125, 1066 CX Amsterdam, The Netherlands

[7] Present address: Rijk Zwaan, Burgemeester Crezeelaan 40, 2678 KX De Lier, The Netherlands

[*] Email: r.offringa@biology.leidenuniv.nl

Abstract

Post embryonic development and longevity of flowering plants are for a large part determined by the activity and maturation state of stem cell niches formed in the axils of leaves, the so-called axillary meristems (AMs) (Grbić and Bleecker, 2000; Wang et al., 2018). The genes that are associated with AM maturation and underlie the differences between monocarpic (reproduce once and die) annual and the longer-lived polycarpic (reproduce more than once) perennial plants are still largely unknown. Here we identify a new role for the Arabidopsis *AT-HOOK MOTIF CONTAINING NUCLEAR LOCALIZED 15* (*AHL15*) gene as a suppressor of AM maturation. Loss of *AHL15* function accelerates AM maturation, whereas ectopic expression of *AHL15* suppresses AM maturation and promotes longevity in monocarpic Arabidopsis and tobacco. Accordingly, in Arabidopsis grown under longevity-promoting short day conditions, or in polycarpic *Arabidopsis lyrata*, expression of *AHL15* is upregulated in AMs. Together our results indicate that *AHL15* and other *AHL* clade-A genes play an important role, directly downstream of flowering genes (*SOC1*, *FUL*) and upstream of the flowering promoting hormone gibberellic acid, in suppressing AM maturation and extending the plant's lifespan.

Keywords: Axillary meristems (AMs), *AHL* genes, monocarpic, polycarpic, *Arabidopsis*, tobacco

Introduction

Plant architecture and -longevity are dependent on the activity of stem cell groups called meristems. The primary shoot and root apical meristem of a plant are established during early embryogenesis and give rise to respectively the shoot- and the root system during post-embryonic development. In flowering plants, post-embryonic shoot development starts with a vegetative phase, during which the primary shoot apical meristem (SAM) produces morphogenetic units called phytomers consisting of a stem (internode) subtending a node with a leaf and a secondary or axillary meristem (AM) located in the axil of the leaf (Grbić and Bleecker, 2000; Wang et al., 2018). Both the SAM and these AMs undergo a maturation process. Like the SAM, young immature AMs are vegetative and when activated they produce leaves, whereas in plant species such as Arabidopsis partially matured AMs produce a few cauline leaves before they fully mature into inflorescence meristems (IMs) and start developing phytomers comprising a stem subtending one or more flowers (Park et al., 2014; Wang et al., 2018).

The maintenance of vegetative development after flowering is an important determinant of plant longevity and -life history. Monocarpic plants, such as the annuals *Arabidopsis thaliana* (Arabidopsis) or *Nicotiana tabacum* (tobacco), complete their life cycle in a single growing season. The AMs that are established during the vegetative phase initially produce leaves. Upon floral transition, however, all AMs rapidly convert into IMs producing secondary and tertiary inflorescences with bracts and flowers, thus maximizing offspring production before the plant's life ends with senescence and death. The number of leaves and bracts produced by an AM is thus a measure for its maturation state upon activation. By contrast, many other flowering plant species are polycarpic perennials, such as the close Arabidopsis relative *Arabidopsis lyrata*. Under permissive growth conditions, they can live and flower for more than two growing seasons. As some AMs are maintained in the vegetative state, this allows polycarpic plants to produce new shoots after seed set and the subsequent activation of these AMs by the appropriate growth conditions before the start of the next growing season (Munné-Bosch, 2008; Amasino, 2009). Despite considerable interest in the molecular basis of plant life history, the proposed molecular mechanisms determining the difference in loss or maintenance of vegetative development after flowering between respectively monocarpic or polycarpic plants are still largely based on our extensive knowledge on the control of flowering in Arabidopsis and closely related species. From these studies, the MADS box proteins SUPPRESSOR OF OVEREXPRESSION OF CONSTANS 1 (SOC1) and FRUITFULL (FUL) have been identified as key promotors of flowering and monocarpic growth, and FLOWERING LOCUS C (FLC) as their upstream cold-sensitive inhibitor (Melzer et al., 2008; Amasino, 2009; Kiefer et al., 2017). However, the factors that maintain vegetative development after flowering, and thereby allow polycarpic growth, are still elusive.

Here we present evidence that the Arabidopsis *AT-HOOK MOTIF COINTAINING NUCLEAR LOCALIZED 15* (*AHL15*) gene plays an important role in the control of AM maturation and extending the plant's lifespan.

Results and discussion

AHL15 forms a clade (clade-A) with 14 other *AHL* genes in Arabidopsis that encode nuclear proteins containing a single N-terminal DNA binding AT-hook motif and a C-terminal Plants and Prokaryotes Conserved (PPC) domain (Supplementary Fig. 1a and Fig. 1a). The PPC domain was previously shown to contribute to the physical interaction with other AHL or nuclear proteins (Zhao et al., 2013). *AHL15* homologs have been implicated in several aspects of plant growth and development in Arabidopsis, including hypocotyl growth and leaf senescence (Street et al., 2008; Xiao et al., 2009; Zhao et al., 2013), flower development (Ng et al., 2009), and flowering time(Xiao et al., 2009; Yun et al., 2012).
In contrast to other *ahl* mutants (Xiao et al., 2009), *ahl15* loss-of-function mutant plants (Supplementary Fig. 1b-e) flowered at the same time and developed the same number of rosette leaves before flowering as wild-type plants, both under short day (SD) and long day (LD) conditions (Fig. 1d,e). After bolting, however, the AMs located in the axils of rosette leaves (rosette AMs) of *ahl15* mutant plants produced less additional rosette leaves compared to those in wild-type plants (Fig. 2a,e and Fig. 3a-c). More detailed analysis showed that this reduction in additional rosette leaf production in *ahl15* plants was not caused by a delayed outgrowth of rosette AMs into axillary buds or to early floral transition, but rather to a reduction in the vegetative activity of these buds (Fig. 4a,b). Following the floral transition, the *ahl15* rosette AMs produced the same number of cauline leaves (Fig. 3d) and flowers (Supplementary Fig. 2a) as the wild type (Col-0). However, the cauline branches produced by the aerial AMs on *ahl15* inflorescences developed less cauline leaves (Fig. 3e) and flowers/fruits (Supplementary Fig. 2b) compared to those produced by wild-type inflorescences, resulting in a significant reduction of the total number of cauline leaves and flowers on *ahl15* inflorescences. Introduction of the *pAHL15:AHL15* genomic clone into the *ahl15* mutant background restored both the rosette and cauline leaf as well as the flower and fruit numbers to wild-type levels (Fig. 2e and Fig 3a-e, Supplementary Fig. 2b), confirming that the phenotypes were caused by *ahl15* loss-of-function. GUS staining of plants carrying a *pAHL15:GUS* promoter:reporter fusion showed that *AHL15* is expressed in AMs (Fig. 2b,c) and young axillary buds (Fig. 2d). Together these results suggested a novel role for *AHL15* in controlling AM maturation.

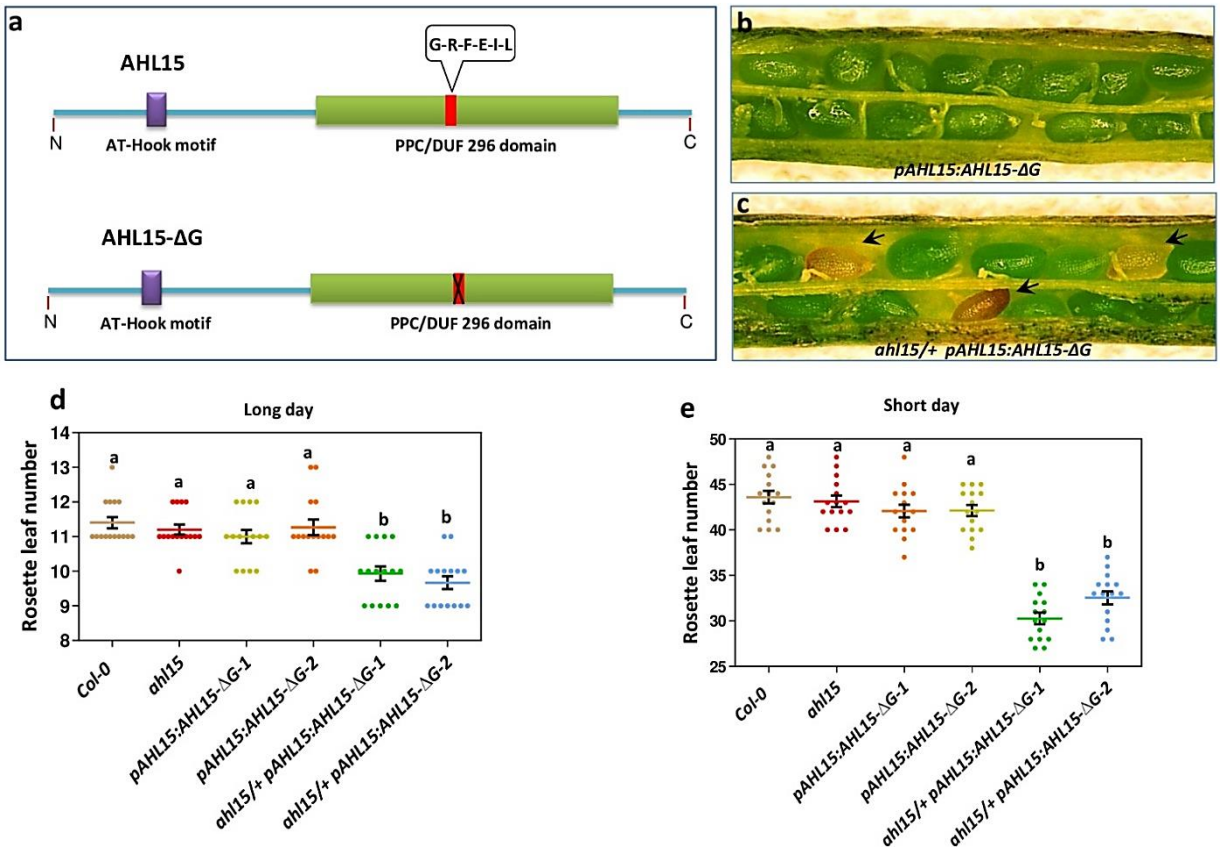

Fig. 1| Expression of a dominant negative AHL15-ΔG mutant protein. Expression of a dominant negative AHL15-ΔG mutant protein in the Arabidopsis *ahl15* mutant background causes early flowering and impairs seed development. **a**. The schematic domain structure of AHL15 and the dominant negative AHL15-ΔG version, in which six-conserved amino-acids (Gly-Arg-Phe-Glu-Ile-Leu, red box) are deleted from the C-terminal PPC domain. **b**. Wild-type seed development in *pAHL15:AHL15-ΔG* siliques. **c**. Aberrant seed development (arrowheads) in *ahl15/+ pAHL15:AHL15-ΔG* siliques (observed in 3 independent *pAHL15:AHL15-ΔG* lines crossed with the ahl15 mutant). Similar results were obtained in three independent experiments. **d**, **e**. The number of rosette leaves produced by the SAM in wild-type, *ahl15*, *pAHL15:AHL15-ΔG* and *ahl15/+ pAHL15:AHL15-ΔG* plants grown in long day (LD, **d**) or short day (SD, **e**) conditions. Two independent transgenic lines (1 and 2) were used in each experiment. Dots in d and e indicate the rosette leaf number per plant (n=15 biologically independent plants), horizontal lines the mean and error bars the s.e.m. Letters (a, b, c) indicate statistically significant differences ($P < 0.01$), as determined by a one-way ANOVA with a Tukey's HSD post hoc test.

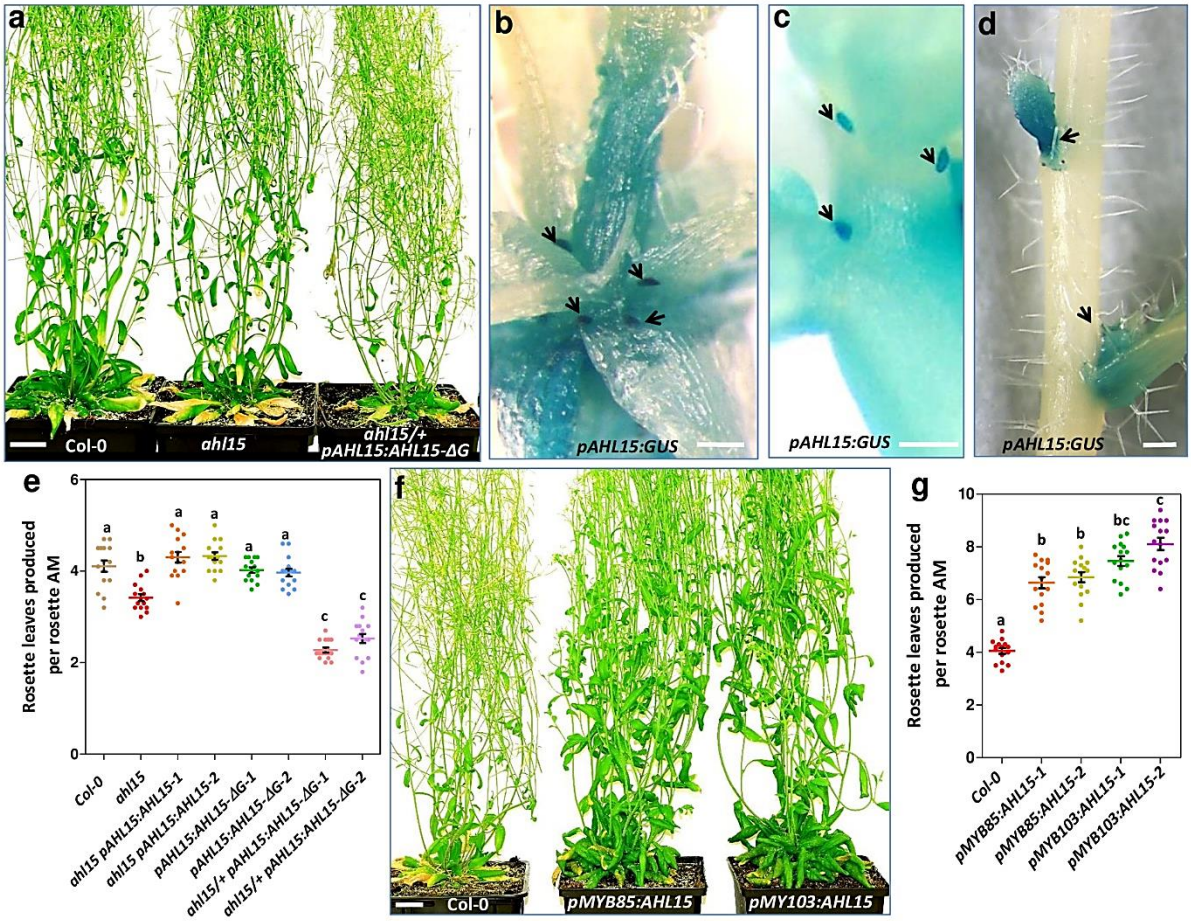

Fig. 2 | *AHL15* represses AM maturation in Arabidopsis. (**a**) Shoot phenotypes of fifty-day-old flowering wild-type (left**),** *ahl15* (middle) and *ahl15/+ pAHL15:AHL15-ΔG* mutant (right) plants. (**b-d**) *pAHL15:GUS* expression in rosette AMs (arrow heads in **b**), aerial AMs located on a young inflorescence stem (arrow heads in **c**) and in activated axillary buds on an inflorescence stem (arrow heads in **d**) of a flowering plant. (**e**) The rosette leaves produced per rosette AM in fifty-day-old wild-type, *ahl15*, *ahl15 pAHL15:AHL15*, *pAHL15:AHL15-ΔG* and *ahl15/+ pAHL15:AHL15-ΔG* plants. (**f**) Shoot phenotype of a sixty-day-old flowering wild-type (left), *pMYB85:AHL15* (middle) or *pMYB103:AHL15* (right) plant. (**g**) The rosette leaves produced per rosette AM in sixty-day-old wild-type, *pMYB85:AHL15* or *pMYB103:AHL15* plants. Dots in **e** and **g** indicate the number of rosette leaves per plant (n=15 biologically independent plants) per line, horizontal lines indicate the mean, and error bars the SEM. Letters (a, b, c) indicate statistically significant differences ($p < 0.01$), as determined by a one-way ANOVA with a Tukey's HSD post hoc test. The P values are provided in Supplementary Tables 3 and 4. Plants were grown under long day conditions (LD). Size bars indicate 2 cm in **a, f** and **1** mm in **b-c**. The leaf production per rosette AM in **e** and **g** was determined for two independent transgenic lines (1 and 2).

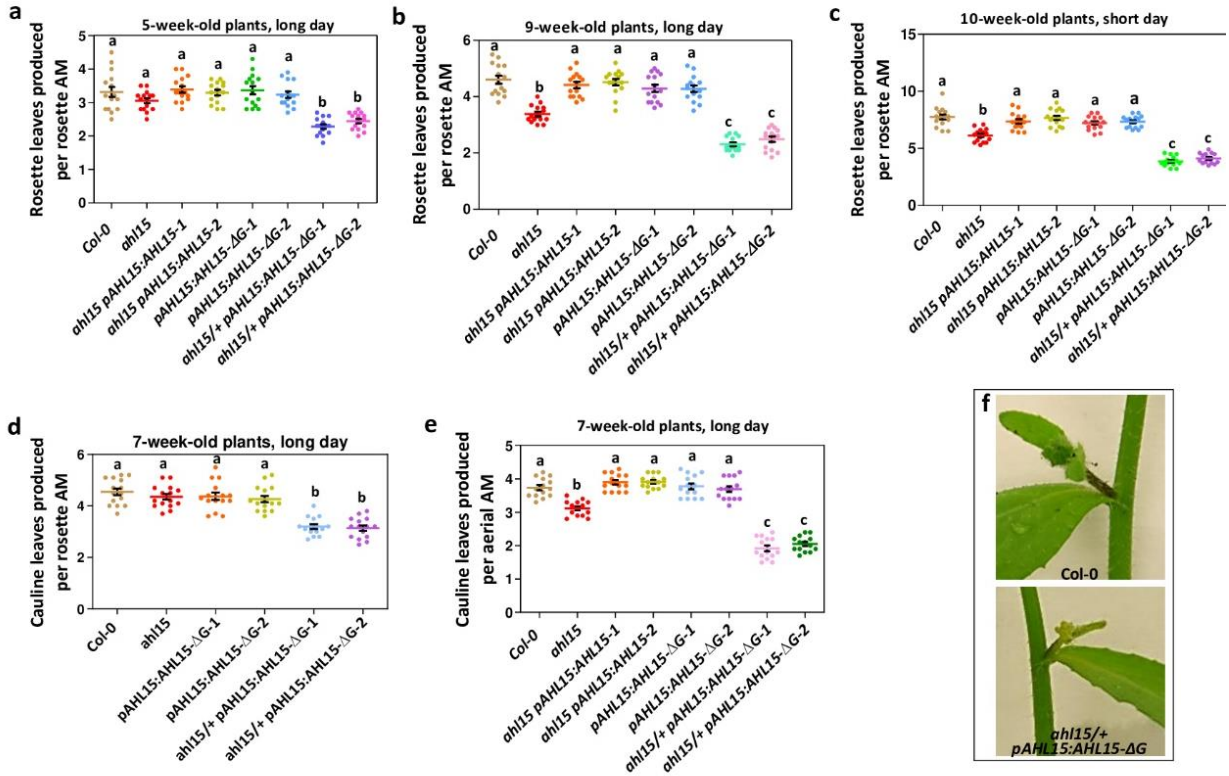

Fig. 3 | *AHL15* and other clade A *AHL* genes represses AM maturation in Arabidopsis. a, **b**. The number of rosette leaves produced per rosette AM of wild-type, *ahl15*, *ahl15 pAHL15:AHL15*, *pAHL15:AHL15-ΔG* and *ahl15/+ pAHL15:AHL15-ΔG* plants 5 (**a**), 9 (**b**), or 10 weeks (**c**) after germination in long day (LD, **a**,**b**) or short day (SD, **c**) conditions. **d**, **e**. The number of cauline leaves produced by rosette AMs (**d**) or by aerial AMs (**e**) of 7-week-old wild-type, *ahl15*, *ahl15 pAHL15:AHL15*, *pAHL15:AHL15-ΔG* and *ahl15/+ pAHL15:AHL15-ΔG* plants. Dots in **a-e** indicate rosette or cauline leaf number per AM per plant (n=15 biologically independent plants), horizontal lines the mean, and error bars the s.e.m. Letters (a, b, c) indicate statistically significant differences ($P < 0.01$), as determined by a one-way ANOVA with a Tukey's HSD post hoc test. The P values are provided in Supplementary Tables 8–12. **f**. A lateral inflorescence with cauline leaves formed on the first inflorescence node of a wild-type (top) or *ahl15/+ pAHL15:AHL15-ΔG* plant (bottom).

AHL proteins interact with each other through their PPC domain and with other non-AHL proteins through a conserved six-amino-acid (GRFEIL) region in the PPC domain. Expression of an AHL protein without the GRFEIL region leads to a dominant negative effect, as it generates a non-functional complex that is unable to modulate transcription (Zhao et al., 2013). Expression of a deletion version of AHL15 lacking the GRFEIL region under control of the *AHL15* promoter (*pAHL15:AHL15-ΔG*) in the wild-type background (n=20) resulted in fertile plants (Fig. 1a,b) that showed normal AM maturation (Fig. 2e and Fig. 3). In the heterozygous *ahl15* loss-of-function background, however, *pAHL15:AHL15-ΔG* expression induced early flowering (Fig. 1d,e, Fig. 4b), resulting in a strong reduction of rosette and cauline leaf production by AMs (Fig. 2a,e, Fig. 3a-f, Fig. 4a). Homozygous *ahl15 pAHL15:AHL15-ΔG* progeny were never obtained, and defective seeds present in siliques of *ahl15/+ pAHL15:AHL15-ΔG* plants suggest that this genetic combination is embryo lethal (Fig. 1b,c). The significantly stronger phenotypes observed for *ahl15/+ pAHL15:AHL15-ΔG* plants are in line with the dominant negative effect of AHL15-ΔG expression overcoming the functional redundancy among Arabidopsis clade A *AHL* family members (Street et al., 2008; Xiao et al., 2009; Zhao et al., 2013)

Based on the observation that the flowering time and the number of rosette leaves before bolting was the same for wild-type and *ahl15* loss-of-function plants, but not for *ahl15/+ pAHL15:AHL15-ΔG* plants, we speculated that other *AHL* clade A family members are more active in the SAM, whereas *AHL15* more strongly acts on AM maturation. To test this, we overexpressed a fusion protein between AHL15 and the rat glucocorticoid receptor under control of the constitutive Cauliflower Mosaic Virus *35S* promoter (*p35S:AHL15-GR*). This rendered the nuclear import and thereby the activity of the ectopically expressed AHL15-GR fusion inducible by dexamethasone (DEX). Untreated *p35S:AHL15-GR* plants showed a wild-type phenotype (Fig. 5b,c), but after spraying flowering *p35S:AHL15-GR* plants with DEX, rosette AMs produced significantly more rosette and cauline leaves (Fig. 5a-c). Interestingly, spraying *p35S:AHL15-GR* plants before flowering also significantly delayed their floral transition (Fig. 5d), indicating that ectopically expressed AHL15 can also suppress maturation of the SAM. In turn, overexpression of the Arabidopsis *AHL* family members *AHL19*, *AHL20*, *AHL27* and *AHL29*, as well as the putative *AHL15* orthologs from *Brassica oleracea* and *Medicago truncatula* in Arabidopsis resulted in similar morphological changes as observed for *p35S:AHL15-GR* plants after DEX treatment. The overexpression plants produced more rosette and cauline leaves during flowering (Fig. 6a,b), supporting the idea that there is functional redundancy among *AHL* clade A family members and that the ability to control either SAM or AM maturation depends on the spatio-temporal expression of the corresponding genes.

In contrast to the observed growth arrest and death of two-month-old Arabidopsis plants grown under long day (LD) conditions (Fig. 7d), four-month-old short day (SD) grown Arabidopsis plants continued to grow after the first cycle of flowering, as aerial AMs on the last-formed lateral branches produced new rosette leaves (Fig. 7a and Fig. 8). However, SD grown *ahl15* mutant plants did not show this renewed vegetative growth and died, whereas *ahl15 pAHL15:AHL15* plants grew like wild type under these conditions (Fig. 7a and Fig. 8). GUS staining of *pAHL15:GUS* plants revealed that *AHL15* expression was strongly enhanced in young lateral inflorescences, axils of cauline leaves and rosette branches in SD conditions

compared to LD conditions (Fig. 7b,c and Fig. 9), indicating that *AHL15* expression is day-length sensitive, and confirming the important role of this gene in extending the lifespan of Arabidopsis under SD conditions.

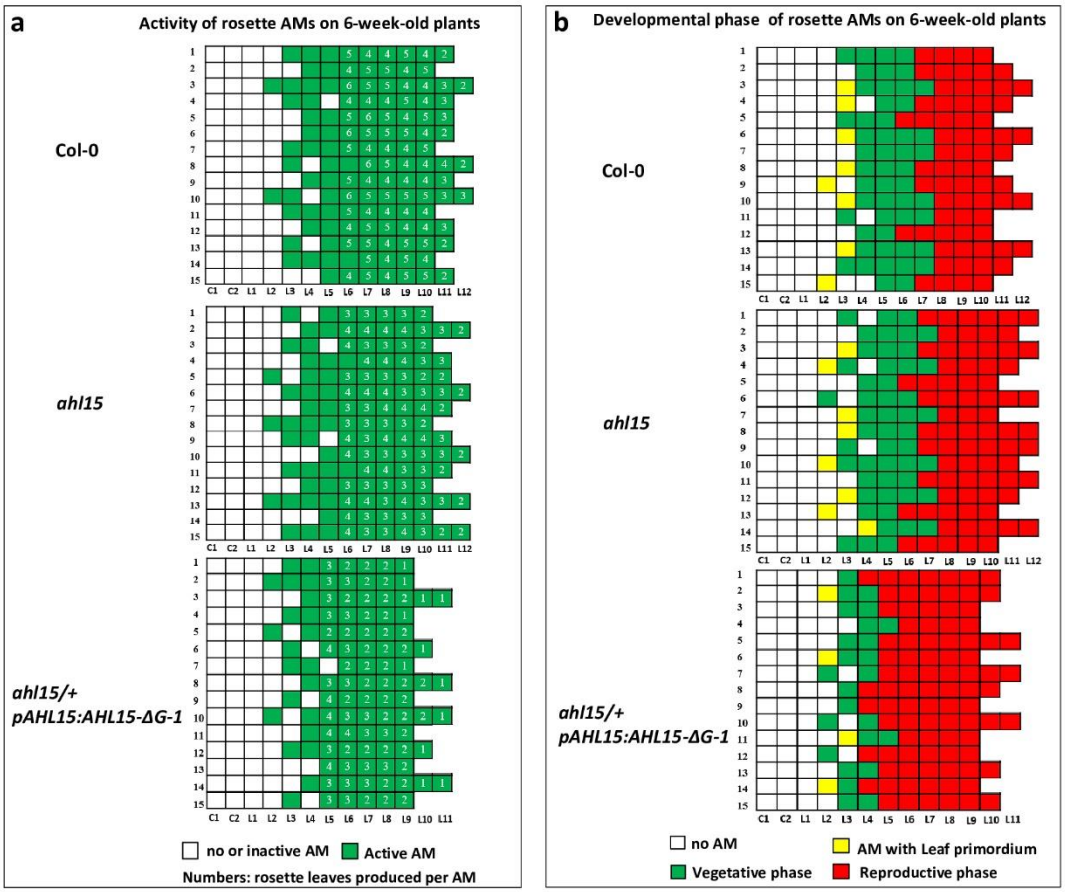

Fig. 4 | *Arabidopsis AHL* genes enhance the vegetative activity and suppress the floral transition of rosette AMs. a. Schematic representation of the vegetative activity of rosette AMs of six-week-old wild-type, *ahl15* and *ahl15/+ pAHL15:AHL15-ΔG-1* plants. Each row represents a single plant, and each square represents an individual AM in a cotyledon axil (C1 and C2) or in a rosette leaf axils (L1 to L12). The numbers within a square represent the number of rosette leaves produced by a rosette AM. A green square indicates a leaf axil with an active AM, as indicated by bud outgrowth or leaf development, and a white square indicates a leaf axil without an (active) AM. **b**. Developmental phase of the rosette AMs of six-week-old wild-type, *ahl15* and *ahl15/+ pAHL15:AHL15-ΔG-1* plants. White, yellow, green or red squares indicate axils without (active) AM, or rosette AMs with at least one visible leaf primordium, producing rosette leaves (vegetative) or producing cauline leaves or flowers (reproductive), respectively. Plants in **a** and **b** were grown in LD conditions.

Growing Arabidopsis plants under SD conditions significantly delays flowering (Andrés and Coupland, 2012), and this might thus indirectly enhance the repressing effect of AHL15 on AM maturation and extending the lifespan. In order to assess AHL15 function independently of day length and flowering time, we expressed *AHL15* under control of the *MYB85* or *MYB103* promoters, which are highly active in Arabidopsis rosette nodes and aerial axillary buds (Fig. 10a) (Ko et al., 2004). In LD conditions, *pMYB85:AHL15* and *pMYB103:AHL15* plants flowered at the same time as wild-type plants, but their AMs produced significantly more rosette and cauline leaves compared to those in wild-type plants (Fig. 2f,g and Fig. 10b,c). Moreover, after flowering and seed set, when wild-type plants senesced and died, *pMYB85:AHL15* and *pMYB103:AHL15* rosette and aerial AMs produced new rosette leaves, which allowed these plants to continue to grow and generate new flowers and seeds (Fig.

7d,e). Also senesced *p35S:AHL15-GR* plants carrying fully ripened siliques started new aerial vegetative development on lateral secondary inflorescences after DEX treatment, and ultimately produced new inflorescences from the resulting rosettes (Fig. 11a). Interestingly, the development of vegetative shoots from AMs formed on rosette and aerial nodes after reproduction also contributes to the polycarpic growth habit of *Arabis alpina* or *Cardamine flexuosa* plants[15,16]. Our results indicate that increased expression of *AHL15* in late stages of development promotes longevity by inducing a polycarpic-like growth habit in Arabidopsis, with an important difference that AMs that remain vegetative do not show dormancy.

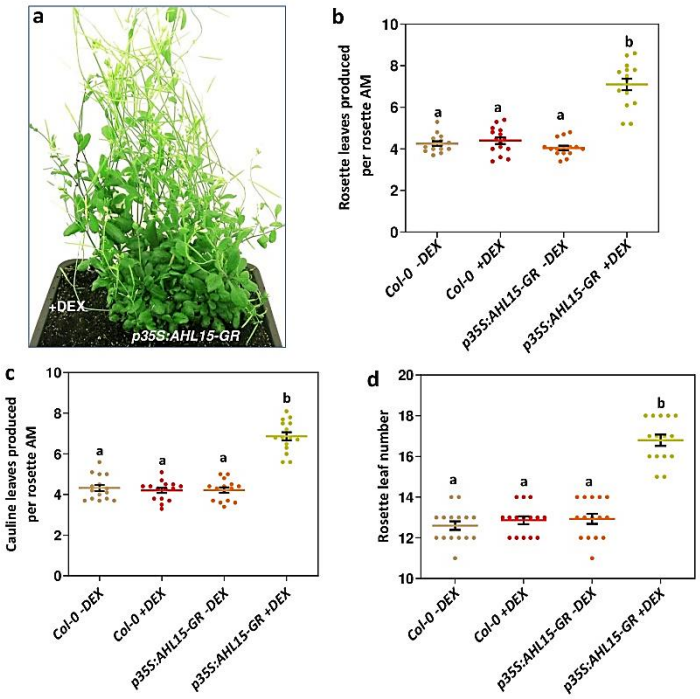

Fig. 5 | *AHL15* overexpression delays floral transition of the SAM and represses AM maturation. **a**. Shoot phenotype of a flowering 7-week-old *35S:AHL15-GR* plant that was DEX-treated upon bolting (5 weeks old). **b**, **c**. Number of rosette leaves (**b**) or cauline leaves (**c**) produced by rosette AMs of 7-week-old mock-treated wild-type, DEX-treated wild-type, mocktreated *35S:AHL15-GR* and DEX-treated *35S:AHL15-GR* plants. Plants were DEX-treated upon bolting (5 weeks old) and scored 2 weeks later. **d**. The number of rosette leaves produced by the SAM in mock-treated wild-type, DEX-treated wild-type, mock-treated *35S:AHL15-GR* and DEX-treated *35S:AHL15-GR* plants. Non-flowering (3-week-old) plants were treated and the SAM-produced rosette leaves were counted after bolting. Dots in **b**-**d** indicate number of leaves (per AM or SAM) per plant (n=15 biologically independent plants), horizontal lines the mean, and error bars the s.e.m. Letters (a, b, c) indicate statistically significant differences ($P < 0.01$), as determined by a one-way ANOVA with a Tukey's HSD post hoc test. Plants were grown in LD conditions.

To determine whether heterologous *AHL15* expression could induce similar developmental changes in a monocarpic plant species from a different family, we introduced the *35S:AHL15-GR* construct into tobacco. Wild-type and *p35S:AHL15-GR* tobacco plants were allowed to grow and set seeds without DEX treatment. After seed harvesting, all leaves and side branches were removed, and the bare lower parts of the primary stems were either mock- or DEX treated. Whereas stems of wild-type and mock-treated *p35S:AHL15-GR* plants did not show any growth, the AMs on DEX-treated *p35S:AHL15-GR* tobacco stems resumed vegetative growth, eventually leading to a second cycle of flowering and seed set (Fig. 7f). Continued DEX treatment after each subsequent cycle of seed harvesting efficiently induced vegetative growth and subsequent flowering and seed set, allowing the *p35S:AHL15-GR* tobacco plants to survive for more than 3 years (Fig. 11b). This result confirmed the conclusion from previous overexpression experiments (Fig. 7d,e, Fig. 5 and Fig. 11a) that enhanced *AHL15* expression facilitates polycarpic-like growth by keeping some AMs in the vegetative state after flowering.

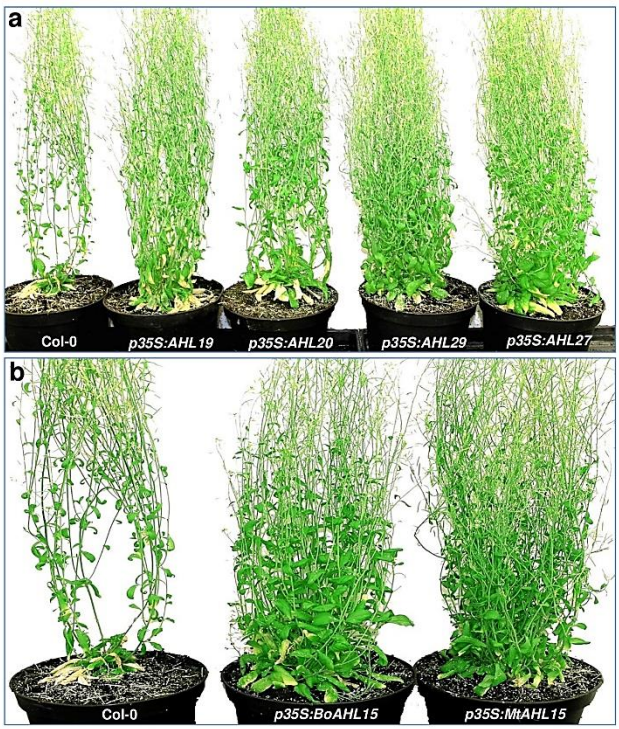

Fig. 6 | Overexpression of *Arabidopsis AHL15* paralogs or putative orthologs represses AM maturation in *Arabidopsis*. Overexpression of *Arabidopsis AHL15* paralogs or putative orthologs represses AM maturation in *Arabidopsis*. (**a** and **b**) Wild-type (Col-0) or transgenic 7-week-old *Arabidopsis* plants overexpressing *Arabidopsis AHL19*, *AHL20*, *AHL27* and *AHL29* (**a**), or the putative *AHL15* orthologs from *Brassica oleracea* (*BoAHL15*) or *Medicago trunculata* (*MtAHL15*) (**b**). For **a** and **b** similar results were obtained in two independent experiments. Plants were grown in LD conditions. For presentation purposes, the original background of the images was replaced by a homogeneous white background

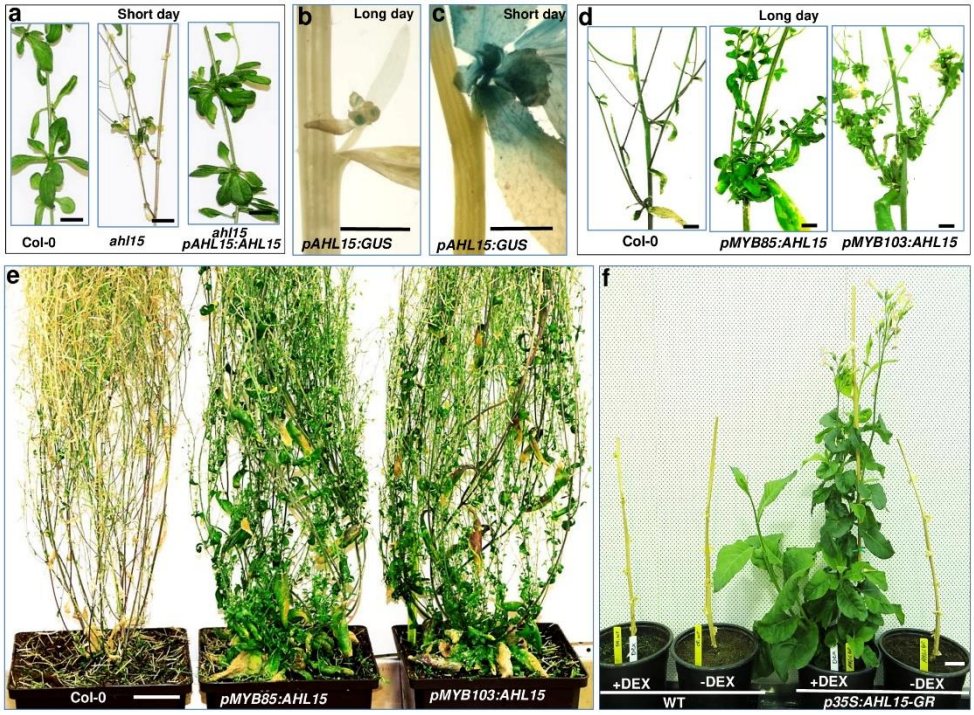

Fig. 7 | *AHL15* promotes longevity in *Arabidopsis* and tobacco. a, Rosette leaves produced by aerial AMs in 4-month-old wild-type (left) and *ahl15 pAHL15:AHL15* (right) plants, but not in *ahl15* mutant plants (middle), grown under SD conditions. **b**,**c**, *pAHL15:GUS* expression in a lateral inflorescence of a 9-week-old plant grown under LD conditions (**b**) and a 4-month-old plant grown under SD conditions (**c**). **d**, Lateral aerial nodes without and with rosette leaves in 4-month-old wild-type (left), *pMYB85:AHL15* (middle) and *pMYB103:AHL15* (right) plants grown under LD conditions. **e**, Phenotype of 4-month-old wild-type (Col-0, left), *pMYB85:AHL15* (middle) and *pMYB103:AHL15* (right) plants grown under LD conditions. **f**, Growth response following DEX treatment in bare stems of 5-month-old wild-type (WT, left) and *35S:AHL15-GR* (right) tobacco plants grown under LD conditions. Scale bars, 1 cm in **a**–**d**, 2 cm in **b** and 5 cm in **c**.

Fig. 8 | *AHL15* enhances the longevity of short day-grown *Arabidopsis* plants. Phenotype of 5-month-old wild-type (Col-0, left), *ahl15* (middle) and *ahl15 pAHL15:AHL15* (right) plants. The plants were grown in SD conditions.

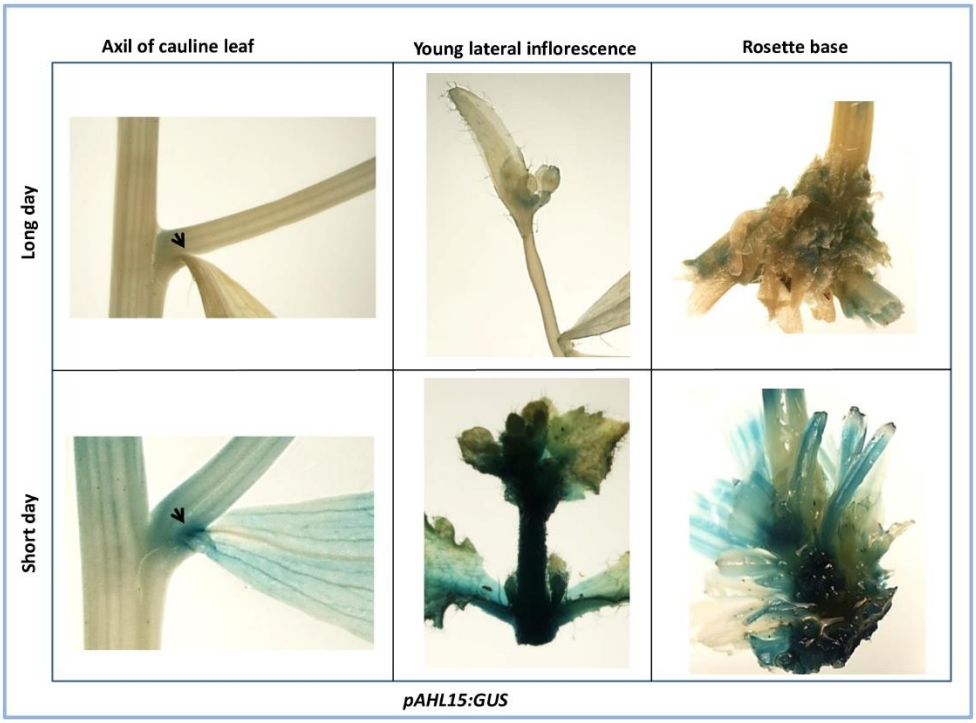

Fig. 9 | *AHL15* expression is day length sensitive. Expression of the *pAHL15:GUS* reporter in the axil of a cauline leaf (left, arrowheads),Young lateral inflorescence (middle) and rosette base (right) of a 9-week-old plant grown in LD conditions (top) or a 4-month-old plant grown under SD conditions (bottom). Similar results were obtained in two independent experiments.

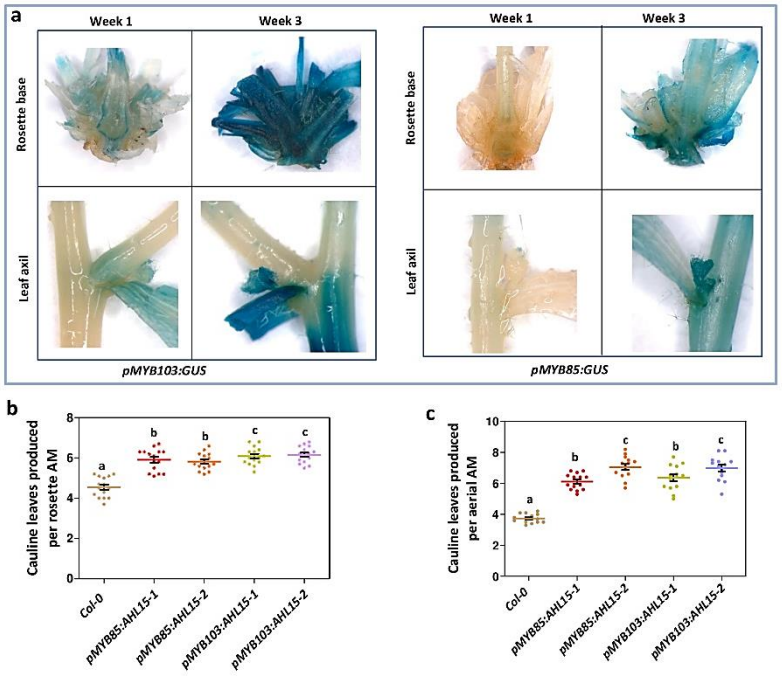

Fig. 10 | *AHL15* overexpression in the rosette base and leaf axils delays AM maturation in *Arabidopsis*. a. Expression of *pMYB58:GUS* and *pMYB103:GUS* reporters in the rosette base (top) or leaf axils (bottom) of *Arabidopsis* plants respectively one or three weeks after flowering, as monitored by histochemical GUS staining. **b**, **c**. The number of cauline leaves produced by rosette AMs (**b**) or aerial AMs (**c**) of 6-week-old (**b**) or 7-week-old (**c**) wild-type, *pMYB85:AHL15* or *pMYB103:AHL15* plants grown in LD conditions. Dots in **b** and **c** indicate number of cauline leaves produced per AM per plant (n=15 biologically independent plants), horizontal lines indicate the mean, and error bars the s.e.m. Letters (a, b, c) indicate statistically significant differences ($P < 0.01$), as determined by a one-way ANOVA with a Tukey's HSD post hoc test.

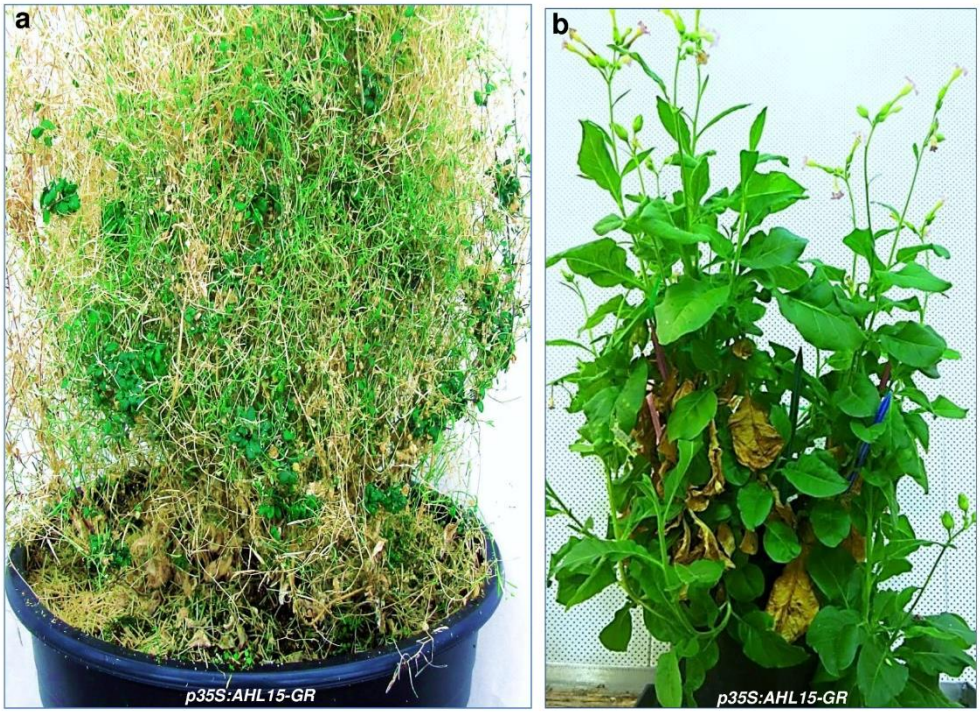

Fig. 11 | *AHL15* overexpression promotes longevity in *Arabidopsis* and tobacco. a. Renewed vegetative growth on aerial branches of a 5-month-old *Arabidopsis 35S:AHL15-GR* plant, 4 weeks after spraying with 20 µM DEX. Similar results were obtained in three independent experiments. **b**. Efficient production of leaves and inflorescences in a 3-year-old *35S::AHL15-GR* tobacco plant, 3 weeks after treatment with 30 µM DEX, following 6 previous cycles of DEX-induced seed production. Plants in **a** and **b** were grown in LD condition.

,

Previously, loss-of-function of both *SOC1* and *FUL* in Arabidopsis was reported to suppress AM maturation, resulting in polycarpic-like growth (Melzer et al., 2008). We found that the aerial rosette formation that is normally observed in the *soc1 ful* double mutant was significantly reduced in *soc1 ful ahl15* triple mutant plants (Fig. 12a, b). Moreover, the polycarpic features of the *soc1 ful* double mutant were lost in the *ahl15* mutant background, as *soc1 ful ahl15* plants senesced and died following seed set, just like wild-type Arabidopsis. Expression analysis by qRT-PCR (Fig. 12c) or by using the *pAHL15:GUS* reporter (Fig. 12d,e) showed that *AHL15* was indeed strongly upregulated in *soc1 ful* inflorescence nodes and lateral inflorescences. Previous studies have revealed that the expression of *SOC1* is positively regulated by LD conditions. Moreover, SOC1 was shown to bind to the *AHL15* upstream and downstream regions (Chr3, 20603158-20604316 and 20610947-20612012), which both contain a canonical CArG box (CC[A/T]6GG) (Fig. 12f) (Lee and Lee, 2010; Immink et al., 2012; Tao et al., 2012). This together with our own data suggested that *AHL15* expression is repressed by SOC1 in LD conditions (Fig. 7b), and that unrepressed AHL15 activity in the *soc1 ful* background explains the aerial rosette formation and the polycarpic-like growth of mutant plants. To check whether the CArG-box containing regions could also be bound by FUL, we used stem fragments containing axillary nodes of *pFUL:FUL-GFP ful* plants to perform ChIP. Subsequent qPCR revealed significant enrichment for the upstream and downstream regions (Fig. 12g), indicating that FUL can repress *AHL15* expression by directly binding to these regions. To further confirm that FUL and SOC1 can bind the CArG-boxes in the *AHL15* up- and downstream regions, we performed Electrophoretic Mobility Shift Assay (EMSA) experiments. Probe fragments containing the corresponding regulatory regions (frag 1 and frag 3), or these regions with a mutated CArG-box (frags 1m and 3m), were tested with SOC1 and FUL homo- and heterodimers. The SOC1/FUL heterodimer could bind to both regulatory fragments, but this binding was reduced when the CArG-box was mutated in frag 1m and even completely abolished in frag 3m (Fig. 12h), providing additional evidence for the importance of the CArG-boxes for the binding of SOC1 and FUL. The SOC1 homodimer showed the same results, while the FUL homodimer did not show binding (Supplementary Fig. 3).

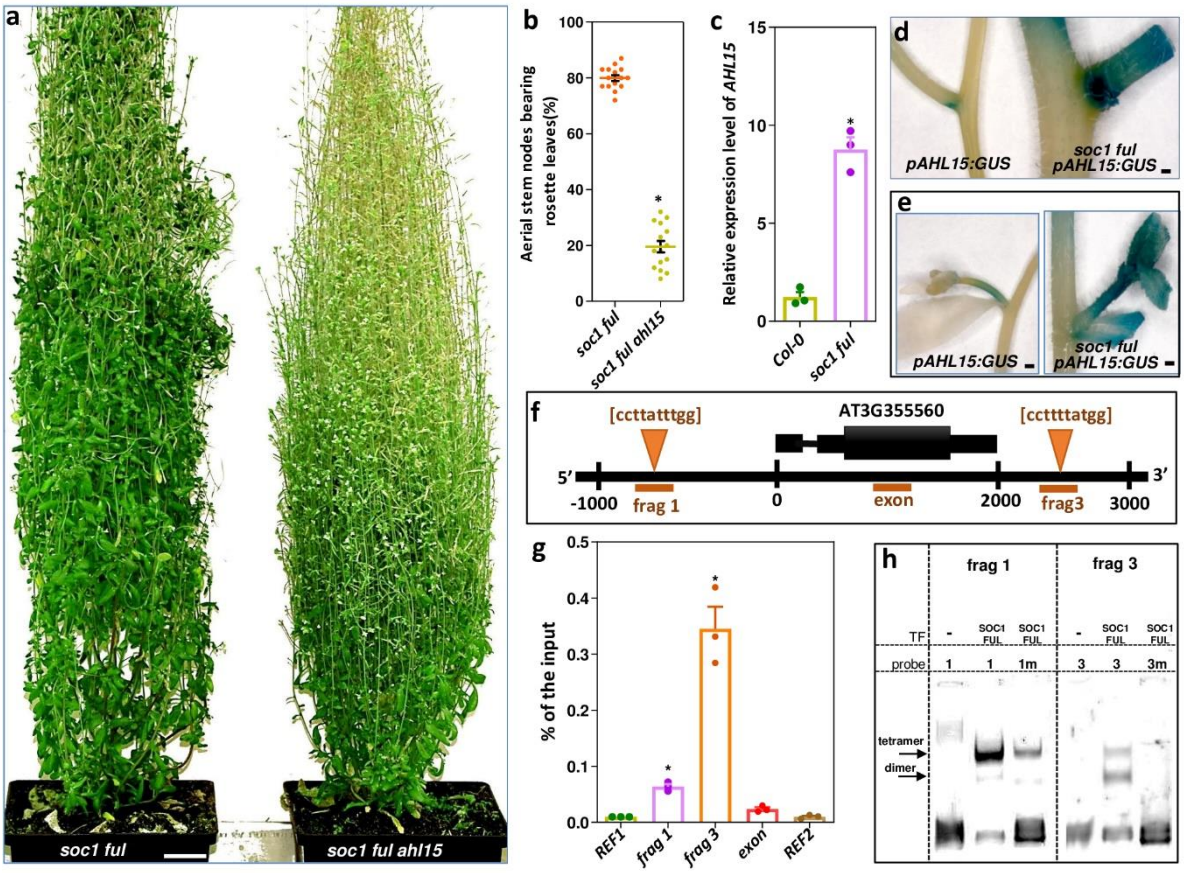

Fig. 12 | *AHL15* is essential for suppression of AM maturation in the *Arabidopsis soc1 ful* mutant. a, A 3-month-old *soc1 ful* double-mutant plant with numerous aerial rosettes (left) and a *soc1 ful ahl15* triple-mutant plant with a limited number of aerial rosettes (right), both grown under LD conditions. **b**, Percentage of aerial stem nodes bearing rosette leaves in 3-month-old *soc1 ful* and *soc1 ful ahl15* plants. Dots indicate the percentage per plant (n = 10 biologically independent plants), horizontal lines the mean and error bars indicate s.e.m. The asterisk indicates a significant difference ($P < 0.001$) as determined by two-sided Student's t-test. **c**, qPCR analysis of *AHL15* expression in secondary inflorescence nodes of wild-type (Col-0) and *soc1 ful* plants 2 weeks after flowering. Dots indicate the values of three biological replicates per plant line, bars indicate the mean and error bars indicate s.e.m. The asterisk indicates a significant difference ($P < 0.001$) as determined by two-sided Student's t-test. **d**,**e**, *pAHL15:GUS* expression in an inflorescence node (**d**) and a secondary inflorescence (**e**) in wild-type (left) or a *soc1 ful* mutant (right) background. **f**, *AHL15* gene model with canonical CArG-boxes located in the upstream (frag 1) and downstream (frag 3) regions, but not in the exon fragment that was used as control (exon). The *AHL15* coding region is indicated by a thick black bar, exons by intermediate black bars and the position of the intron by a black line. **g**, Graph showing ChIP–qPCR results from *FUL-GFP ap1 cal* secondary inflorescence nodes using an anti-green fluorescent protein antibody. Enrichment of fragments was calculated as a percentage of the input sample. ref1 and ref2 are reference fragments (see Methods), while other fragments are also indicated in the gene model. Dots indicate the values of three biological replicates, bars the means and error bars indicate s.e.m. Asterisks indicate significant differences with ref1 and ref2 ($P < 0.001$) as determined by two-sided Student's t-test. Exact P values are provided in Supplementary Table 5. **h**, Binding of the transcription factors (TFs) SOC1 and FUL to regulatory regions near *AHL15*. Left: EMSA of promoter frag 1 with a wild-type (1) or mutated (m1) CArG-box. Right: EMSA of downstream frag 3 with a wild-type (3) or mutated (3 m) CArG-box. Shifting of the probe, indicating binding, occurred through either a tetramer (top band) or dimer (bottom band). Scale bars, 2 cm in **a** and 1 mm in **d**,**e**.

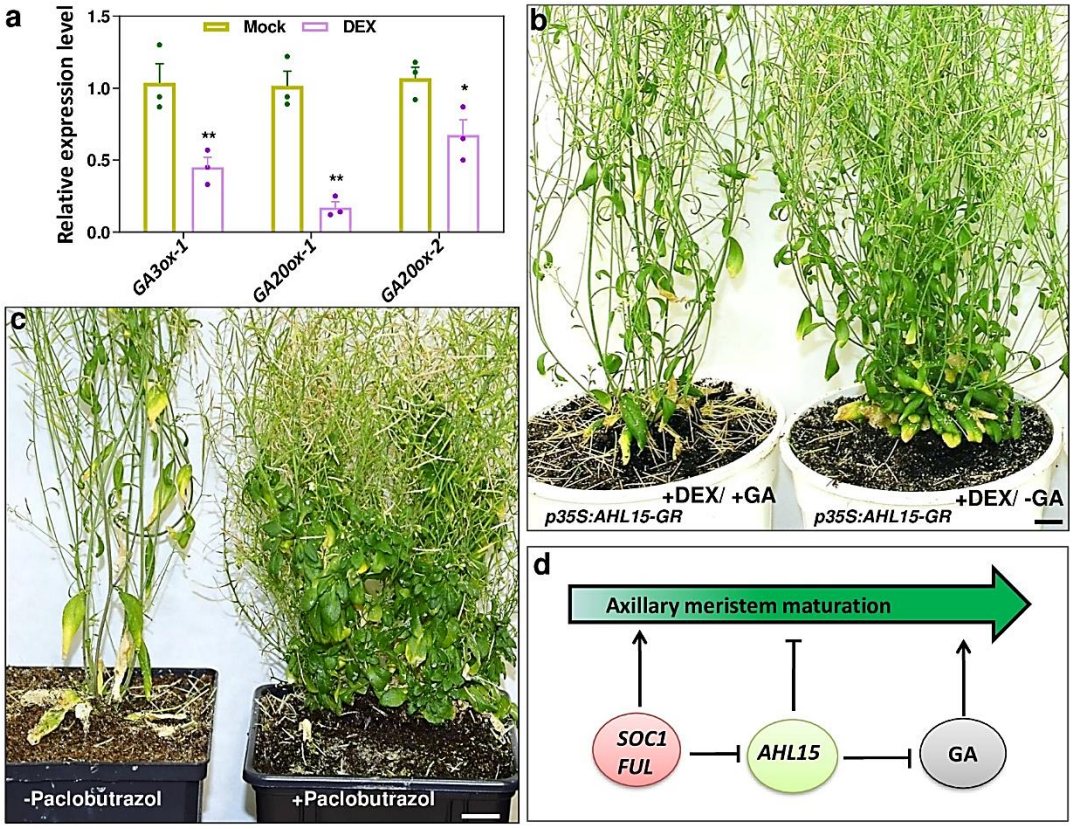

Fig. 13 | AHL15 delays AM maturation in part by suppression of GA biosynthesis. a, Relative expression level of GA biosynthesis genes *GA3OX1*, *GA20OX1* and *GA20OX2* by qPCR analysis in the basal regions of 1-week-old *35S:AHL15-GR* inflorescences 1 day after spraying with either water (mock) or 20 μM DEX. Dots indicate the values of three biological replicates per plant line, bars indicate the mean and error bars indicate s.e.m. Asterisks indicate significant differences from mock-treated plants (*P < 0.05, **P < 0.01), as determined by two-sided Student's *t*-test. **b**, Shoot phenotype of 3-month-old *p35S:AHL15-GR* plants that were DEX sprayed at 5 weeks of age and subsequently sprayed 1 week later with either 10 μM GA4 (+GA) or water (–GA). **c**, Shoot phenotype of 3-month-old wild-type *Arabidopsis* plants that were sprayed 6 weeks earlier with either water (–Paclobutrazol) or 3 μM paclobutrazol (+Paclobutrazol). Plants in **b**,**c** were grown under LD conditions; scale bars, 2 cm. **d**, Proposed model for the key role of *AHL15* (and other *AHL* clade-A genes) in controlling AM maturation downstream of flowering genes *SOC1* and *FUL* and upstream of GA biosynthesis. Blunt-ending lines indicate repression, arrows indicate promotion.

SOC1 and FUL are known as central floral integrators, as they integrate the different environmental and endogenous signaling pathways that influence flowering (Ko et al., 2004; Lee and Lee, 2010; Matsoukas et al., 2012). They promote flowering through activation of the floral meristem genes *APETALA1* (*AP1*) and *LEAFY* (*LFY)*(Turnbull, 2011; Song et al., 2013), and of genes involved in the biosynthesis of the plant hormone gibberellic acid (GA) (Andrés et al., 2014). GA plays an important role in the promotion of flowering through activation of *SOC1* and the *SQUAMOSA PROMOTER BINDING PROTEIN-LIKE* (*SPL*) genes (Yu et al., 2012; Wang, 2014). Interestingly, AHL15 and AHL25 also control GA biosynthesis by direct binding to the promoter of *GA3-oxidase1* (*GA3OX1*), which encodes an enzyme required for GA biosynthesis (Matsushita et al., 2007). We therefore investigated the relationship between GA biosynthesis and AHL15 in the control of AM maturation. qPCR analysis showed that the expression of *GA3OX1*, *GA20OX1* and *GA20OX2*, genes, encoding rate limiting enzymes in the last steps of the GA biosynthetic pathway (Huang et

al., 1998; Rieu et al., 2008; Andrés et al., 2014), was down-regulated in DEX-treated *35S:AHL15-GR* inflorescence nodes (Fig. 13a). In line with the down-regulation of GA biosynthesis, GA application to DEX-treated flowering *p35S:AHL15-GR* plants resulted in a remarkable repression of vegetative AM activity (Fig. 13b). In turn, treatment of flowering wild-type Arabidopsis plants by paclobutrazol, a potent inhibitor of GA biosynthesis, prevented AM maturation, resulting in the aerial rosette leaf formation and enhanced longevity (Fig. 13c). Based on our findings, we postulate that *AHL15* acts downstream of SOC1 and FUL as central repressor of AM maturation, and that AHL15 prevents AM maturation in part by suppressing GA biosynthesis (Fig. 13d). Interestingly, the polycarpic behavior of *Arabis alpina* was shown to be based on age-dependent suppression of *AaSOC1* expression[15] and GA levels (Tilmes et al., 2019) and, like in our model (Fig. 13d), *AHL* genes might also link these two regulatory pathways facilitating polycarpic growth in *Arabis alpina*.

The existence of both mono- and polycarpic species within many plant genera indicates that life history traits have changed frequently during evolution (Amasino, 2009). *AHL* clade-A gene families can be found in both monocarpic and polycarpic plant species (Supplementary Fig. 4a) (Zhao et al., 2014), and expression of the *AHL* clade-A gene family could therefore provide a mechanism by which a plant species attains a polycarpic growth habit. A comparison of the gene family size in representative species of 3 plant families did however not show significant gene deletion or duplication events linked to respectively the monocarpic or polycarpic growth habit (Supplementary Fig. 4b). This suggests that a switch from monocarpic to polycarpic habit or vice versa could possibly be mediated by a change in gene regulation.

To find support for this, we compared the *AHL* gene family of Arabidopsis with that of its close polycarpic relative *Arabidopsis lyrata* (Remington et al., 2015). The *A. thaliana* and *A. lyrata* genomes both encode 15 AHL clade-A proteins, among which the orthologous pairs can clearly be identified based on amino acid sequence identity (Supplementary Fig. 5). We hypothesized that the polycarpic habit of *A. lyrata* might be associated with enhanced *AHL* clade-A gene expression leading to the maintenance of basal AMs in the vegetative state during flowering (Fig. 14a). Expression analysis of individual *AHL* clade-A genes in Arabidopsis showed that the expression of the majority of these genes, including *AHL15*, *AHL19*, and *AHL20*, was decreased in rosette nodes of *A. thaliana* flowering plants compared to 2-week-old seedlings (Fig. 14b). In contrast, the expression of 5 members of the *AHL* gene family (*AHL15*, *AHL17*, *AHL19*, *AHL20* and *AHL27)* was significantly higher in rosette nodes of flowering *A. lyrata* plants compared to seedlings (Fig. 14c). These data are in line with our hypothesis and suggest that the different life-history strategies in *A. thaliana* and *A. lyrata* might be associated with the differential regulation of *AHL* genes in AMs.

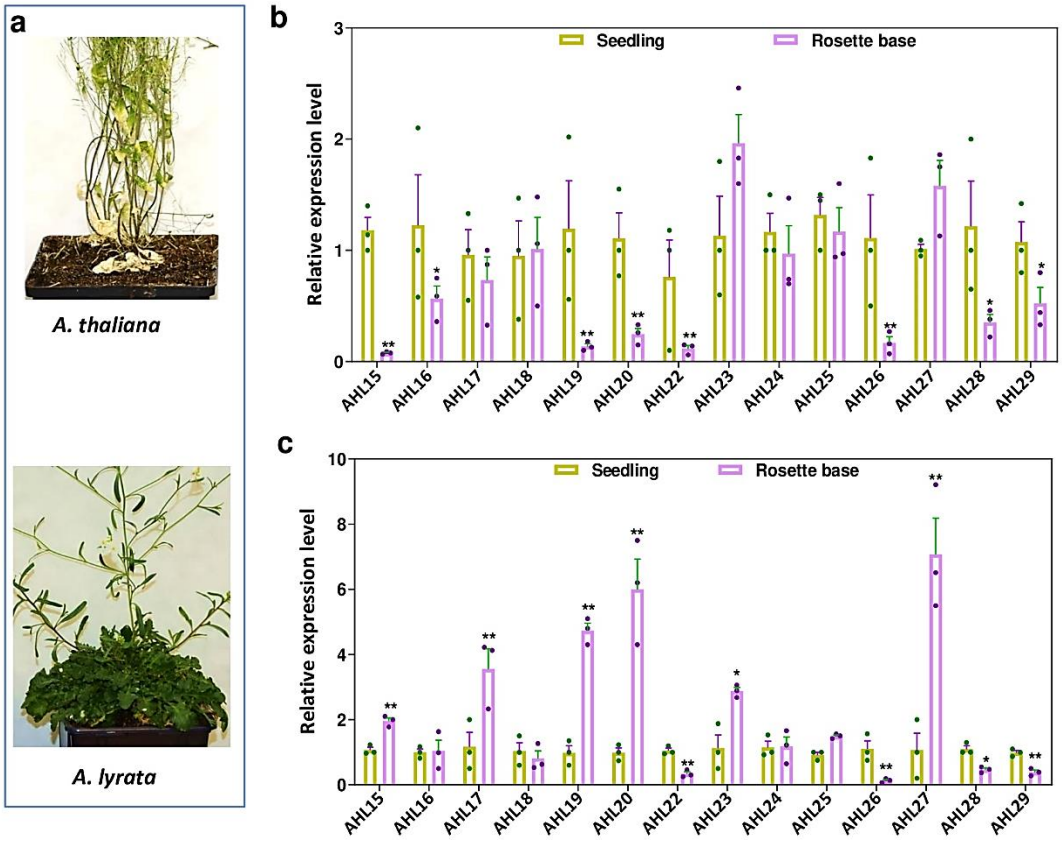

Fig. 14 | Expression of clade-A *AHL* genes in seedlings or in the rosette base of flowering *Arabidopsis* or *A. lyrata* plants. a. Shoot phenotype of a 3-month-old *Arabidopsis* (upper panel) or a 4-month-old *A. lyrata* (lower panel) plant grown in LD conditions. **b**, **c**. qPCR analysis of the expression of clade-A *AHL* genes in 2-week-old seedlings or in the rosette base of 2-monthold flowering plants of *A. thaliana* (**b**) or *A. lyrata* (**c**). Dots in **b** and **c** indicate relative expression levels per experiment (n=3 biologically independent replicates), bars indicate the mean, and error bars indicate the s.e.m. Asterisks indicate significant differences from mock-treated plants (* $p<0.05$, ** $p<0.01$, *** $p<0.001$), as determined by a two-sided Student's *t*-test.

Conclusion

In conclusion, our data provide evidence for a novel role for *AHL15* and other *AHL* clade-A genes in suppressing AM maturation and enhancing plant longevity. Arabidopsis plants with enhanced *AHL15* expression show polycarpic-like growth, but their vegetative AMs lack the dormancy that is characteristic for the reproductive cycles in perennial plants (e.g. *A. lyrata* and *A. alpina*). The importance of the SOC1/FUL-AHL-GA pathway in perennial life history therefore requires further confirmation. Although the exact mode of action of AHL proteins is largely unknown, they are characterized as DNA-binding proteins, and like AT-hook proteins in animals they seem to act through chromatin remodeling (Lim et al., 2007; Ng et al., 2009). It has been shown that AHL22 represses *FLOWERING LOCUS T* (*FT*) expression by binding to the *FT* promoter where it possibly modulates the epigenetic signature around its binding region (Yun et al., 2012). Detailed studies on the chromatin configuration by approaches such as chromosome conformation capture technologies (Dekker et al., 2013)

should provide more insight into the mode of action of these plant-specific AT-Hook motif proteins. One of the objectives of our future research will be to unravel the molecular mechanisms by which these proteins influence plant development.

Methods

Plant material, growth conditions and phenotyping

All Arabidopsis mutant- and transgenic lines used in this study are in Columbia (Col-0) background. The *ahl15* (SALK_040729) T-DNA insertion mutant and the previously described *soc1-6 ful-7* double mutant (Wang et al., 2009) were obtained from the Nottingham Arabidopsis Stock Centre (NASC). Seeds were planted directly into soil in pots and germinated at 21°C, 65% relative humidity and a 16 hours (long day: LD) or 8 hours (short day: SD) photoperiod. When seedlings were 10 days old, they were thinned to one seedling per pot by cutting the hypocotyls. To score for phenotypes such as longevity, Col-0 wild-type, mutant or transgenic plants were transferred to larger pots about 3 weeks after flowering. *Nicotiana tabacum* cv SR1 Petit Havana (tobacco) plants were grown in medium-sized pots at 25°C, 70% relative humidity and a 16 hours photoperiod. For dexamethasone (DEX, Sigma-Aldrich) treatment, Arabidopsis and tobacco plants were sprayed with 20 and 30 µM DEX, respectively. To test the effect of GA on AHL15-GR activation by DEX treatment, 35-day-old flowering *p35S:AHL15-GR* plants were first sprayed with 20 µM DEX, followed 1 week later by spraying with 10 µM GA4 (Sigma-Aldrich). The production of rosette leaves, cauline leaves, flowers or fruits per rosette or aerial AM of 5-, 7-, 9- or 10-week-old plants was determined by dividing the total number of leaves or fruits produced by the number of active rosette or aerial AMs per plant. For the flowering time the number of rosette leaves produced by the SAM were counted upon bolting.

Plasmid construction and transgenic Arabidopsis lines

To generate the different *promoter:AHL15* gene fusions, the complete *AHL15* (AT3G55560) genomic fragment from ATG to stop codon was amplified from genomic DNA of Arabidopsis ecotype Columbia (Col-0) using PCR primers Gateway-AHL15-F and -R (Supplementary Table 1). The resulting fragment was inserted into pDONR207 via a BP reaction. LR reactions were carried out to fuse the *AHL15* coding region downstream of the *35S* promotor in destination vector pMDC32 (Karimi et al., 2007). Subsequently, the *35S* promoter was excised with *Kpn*I and *Sph*I and replaced by the Gateway cassette (*ccdB* flanked by *attP* sequences) amplified from pMDC164(Karimi et al., 2007) by the *Kpn*I and *Sph*I flanked primers (Supplementary Table 1), resulting in plasmid pGW-AHL15. To generate the constructs *pFD:AHL15*, *pMYB85:AHL15*, *pMYB103:AHL15* and *pAHL15:AHL15*, 3 kb regions upstream of the ATG start codon of the genes *FD* (AT4G35900), *MYB85* (AT4G22680), *MYB103* (AT1G63910) and *AHL15* were amplified from ecotype Columbia (Col-0) genomic DNA using the forward (F) and reverse (R) PCR primers indicated in Supplementary Table 1. The resulting fragments were first inserted into pDONR207 by BP reaction, and subsequently cloned upstream of the *AHL15* genomic

fragment in destination vector pGW-AHL15 by LR reaction. To generate the *pAHL15:GUS*, *pMYB85:GUS* and *pMYB103:GUS* reporter constructs, the corresponding promotor fragments were cloned upstream of the *GUS* gene in destination vector pMDC164 by LR reaction. To generate the *pAHL15:AHL15-ΔG* construct, a synthetic *Kpn*I-*Spe*I fragment containing the *AHL15* coding region lacking the sequence encoding the Gly-Arg-Phe-Glu-Ile-Leu amino acids in the C-terminal region (BaseClear, Leiden, NL) was used to replace the corresponding coding region in the *pAHL15:AHL15* construct. To construct *35S::AHL15-GR*, a synthetic *Pst*I-*Xho*I fragment containing the *AHL15-GR* fusion (Shine Gene Molecular Biotech, see Supplementary File. 1) was used to replace the *BBM-GR* fragment in binary vector pSRS031 (Passarinho et al., 2008). To generate the other overexpression constructs, the full-length cDNA clones of *AHL19* (AT3G04570), *AHL20* (AT4G14465), *AHL27* (AT1G20900) and *AHL29* (AT1G76500) from Arabidopsis Col-0, *AC129090* from *Medicago trunculata cv* Jemalong (*MtAHL15*), and *Bo-Hook1* (AM057906) from *Brassica oleracea* var *alboglabra* (*BoAHL15*) were used to amplify the open reading frames using primers indicated in Supplementary Table 1. The resulting fragments were cloned into plasmid pJET1/blunt (GeneJET™ PCR Cloning Kit, #K1221), and subsequently transferred as *Not*I fragments to binary vector pGPTV 35S-FLAG (Becker et al., 1992). All binary vectors were introduced into *Agrobacterium tumefaciens* strain AGL1 by electroporation (den Dulk-Ras and Hooykaas, 1995) and Arabidopsis Col-0 and *ahl15* plants were transformed using the floral dip method (Clough and Bent, 1998).

Tobacco transformation

Round leaf discs were prepared from the lamina of 3rd and 4th leaves of 1-month-old soil grown tobacco plants. The leaf discs were surface sterilized by three washes with sterile water followed by incubation in 10% chlorine solution for 20 minutes, and by 4 to 5 subsequent washes with sterile water (Baltes et al., 2014). The surface sterilized leaf discs were syringe infiltrated with an overnight acetosyringone (AS)-induced culture of *Agrobacterium tumefaciens* strain AGL1 containing binary vector pSRS031 (grown to OD_{600}= 0.6 in the presence of 100 µM AS) carrying the *35S::AHL15-GR* construct, and co-cultivated for 3 days in the dark on co-cultivation medium (CCM), consisting of full strength MS medium (Murashige and Skoog, 1962) with 3% (w/v) sucrose (pH 5.8) solidified with 0.8 % (w/v) Diachin agar and supplemented with 2mg/l BAP, 0.2mg/l NAA and 40mg/l AS. After co-cultivation, the explants were transferred to CCM supplemented with 15mg/l phosphinothricin (ppt) for selection and 500mg/l cefotaxime to kill *Agrobacterium*. Regeneration was carried out at 24°C and 16 hours photoperiod. The regenerated transgenic shoots were rooted in big jars containing 100 ml hormone free MS medium with 15mg/l ppt and 500 mg/l cefotaxime. The rooted transgenic plants were transferred to soil and grown in a growth room at 25°C, 75% relative humidity and a 16 hours photoperiod. All the transgenic plants were checked for the presence of the T-DNA insert by PCR, using genomic DNA extracted from leaf tissues by the CTAB method (Doyle, 1990).

Histochemical staining and microscopy

Histochemical staining of transgenic lines for β-glucuronidase (GUS) activity was performed as described previously (Anandalakshmi et al., 1998). Tissues were stained for 4 hours at

37°C, followed by chlorophyll extraction and rehydration by incubation for 10 minutes in a graded ethanol series (75, 50, and 25 %). GUS stained tissues were observed and photographed using a LEICA MZ12 microscope equipped with a LEICA DC500 camera.

Quantitative real-time PCR (qPCR) analysis

RNA isolation was performed using a NucleoSpin® RNA Plant kit (MACHEREY-NAGEL). For qPCR analysis, 1 µg of total RNA was used for cDNA synthesis with the iScript™ cDNA Synthesis Kit (BioRad). PCR was performed using the SYBR-Green PCR Master mix (SYBR® Premix Ex Taq™, Takara) and a CFX96 thermal cycler (BioRad). The Pfaffl method was used to determine relative expression levels (Pfaffl, 2001). Expression was normalized using *β-TUBULIN-6* and *EF1-ALPHA* as reference genes. Three biological replicates were performed, with three technical replicates each. The primers used are described in Supplementary Table 2.

ChIP-qPCR experiment

For the ChIP-qPCR analysis, three independent samples were harvested from secondary inflorescence nodes of *pFUL:FUL-GFP ful* plants and processed as described in (Mourik et al., 2015; Balanzà et al., 2018). Primer sequences used for the ChIP-qPCR are detailed in Supplementary Table 2.

EMSA experiment

The EMSA was performed as described before (Bemer et al., 2017). The sequences of the probes are detailed in Supplementary Table 2.

***AHL* clade-A gene family data retrieval**

The nucleotide and amino acid sequences for *AHL* clade-A genes in *A. thaliana* (*AtAHLs*) were retrieved by Biomart from Ensembl Plants (plants.ensembl.org/index.html). For our study we selected 15 additional species from 3 major plant families, i.e. Brassicaceae, Solanaceae and Fabaceae. Initially more species were included, but some were excluded from the analysis (e.g. *Arabis alpina*) for reasons described below. The amino acid sequences of *A. thaliana*, *A. lyrata*, *Brassica oleracea*, *Brassica rapa*, *Solanum lycopersicum*, *Solanum tuberosum*, *Medicago truncatula* and *Glycine max* were downloaded from Ensembl Plants (ftp://ftp.ensemblgenomes.org). The genomes of *Nicotiana tabacum*, *Capsicum annuum*, *Brassica napus* were downloaded from NCBI Genome (ftp://ftp.ncbi.nih.gov/genomes/) and the genomes of *Phaseolus vulgaris*, *Capsella rubella*, *Capsella grandiflora*, *Boechera stricta* and *Eutrema salsugineum* were downloaded from Phytozome (https://phytozome.jgi.doe.gov/pz/portal.html).

Building of profile HMMs and hmmer searches

The whole protein sequences of the Arabidopsis *AHL* clade-A genes were used as a query and BLASTP (Altschup et al., 1990) with an e-value set at 0.001 was used to search for *AHL* clade-A genes in the other plant genomes. Only BLASTP hits >70% coverage and 70% sequence identity with intact single AT-Hook motif and PPC domain were used for building profile Hidden Markov Models (HMMs). We used MAFFT software (Katoh et al., 2002)

with FF-NS-i algorithm for construction of seed alignments. The alignments were manually inspected to remove any doubtful sequences. To increase the specificity of the search, columns with many gaps or low conservation were excluded using the trimAl software (Capella-gutiérrez et al., 2009). We applied a strict non-gap percentage threshold of 80% or similarity score lower than 0.001 such that at least 30% of the columns were conserved. At this point several species were excluded (e.g. *Arabis alpina*), because of extensive gaps in the sequence alignment. Profile HMMs were built from the Multiple Sequence Alignment (MSA) aligned fasta files using hmmbuild and subsequent searches against the remaining 16 genomes was carried out using hmmsearch from the HMMER 3.1b1 package (Eddy, 2011). AHL proteins in plants consist of two closely resembling clades; Clade-A and Clade-B. AHL sequences were classified to the Clade-A family based on a comparison with Clade-B AHL sequences, where a hit with lower e-value for either Clade-A or Clade-B would correctly place the sequence in the corresponding clade (e.g. low e-value for Clade A would place the sequence in Clade-A and vice-versa).

Phylogenetic reconstruction and reconciliation

Phylogenetic analysis was carried out using both Maximum Likelihood (ML) with PhyML(Guindon and Gascuel, 2003) and Bayesian Inference implementing the Markov Chain Monte Carlo (MCMC) algorithm with MrBayes (Ronquist and Huelsenbeck, 2003). For Bayesian inference, we specified the number of substitution types (nst) equal to 6 and the rate variation (rates) as invgamma. Invgamma states that a proportion of the sites are invariable while the rate for the remaining sites are drawn from a gamma distribution. These settings are equivalent to the GTR + I + gamma model. Two independent analysis (nruns=2) of 4 chains (3 heated and one cold) were run simultaneously for at least 10 million generations, sampling every 1000 generations. Burn-in was set as 25%. For Clade-A AHLs the simulations were run for 10 million generations, sampling every 1000 generations and convergence was reached at 0.016. For ML analysis, we used the default amino acid substitution model LG and the number of bootstrap replicates was specified as 100.

Tree resolving, rearrangement, and reconciliation was carried out using NOTUNG software (Liebert et al., 2000). NOTUNG uses duplication/loss parsimony to fit a gene (protein) tree to a species tree. The species tree was obtained using PhyloT (http://phylot.biobyte.de/index.html) which generates phylogenetic trees based on the NCBI taxonomy. Tree editing/manipulations were performed using the R packages APE (Paradis et al., 2004) and GEIGER (Harmon et al., 2008). We applied a strict threshold for rearrangement of 90%. After the rearrangement, we performed the reconciliation of the gene (protein) tree with the species tree.

Reconstruction of evolutionary scenario using Dollo parsimony method

Dollo parsimony principles are commonly exploited for two-state character traits. To classify branches as either gene-losses or gene-gains, we used Dollo parsimony method, which allows for an unambiguous reconstruction of ancestral character states, as it is based on the assumption that a complex character that has been lost during evolution of a particular lineage cannot be regained.

References

Altschup, S.F., Gish, W., Pennsylvania, T., and Park, U. (1990). Basic Local Alignment Search Tool 2Department of Computer Science. J. Mol. Biol. **215**: 403–410.

Amasino, R. (2009). Floral induction and monocarpic versus polycarpic life histories. Genome Biol. **10**: 228.

Anandalakshmi, R., Pruss, G.J., Ge, X., Marathe, R., Mallory, A.C., Smith, T.H., and Vance, V.B. (1998). A viral suppressor of gene silencing in plants. Proc. Natl. Acad. Sci. U. S. A. **22**: 13079--13084.

Andrés, F. and Coupland, G. (2012). The genetic basis of flowering responses to seasonal cues. Nat. Rev. Genet. **13**: 627–639.

Andrés, F., Porri, A., Torti, S., Mateos, J., Romera-Branchat, M., García-Martínez, J.L., Fornara, F., Gregis, V., Kater, M.M., and Coupland, G. (2014). SHORT VEGETATIVE PHASE reduces gibberellin biosynthesis at the Arabidopsis shoot apex to regulate the floral transition. Proc. Natl. Acad. Sci. **111**: E2760-9.

Balanzà, V., Martínez-Fernández, I., Sato, S., Yanofsky, M.F., Kaufmann, K., Angenent, G.C., Bemer, M., and Ferrándiz, C. (2018). Genetic control of meristem arrest and life span in Arabidopsis by a FRUITFULL-APETALA2 pathway. Nat. Commun. **9**: /s41467-018-03067-5.

Baltes, N.J., Gil-Humanes, J., Cermak, T., Atkins, P. a, and Voytas, D.F. (2014). DNA replicons for plant genome engineering. Plant Cell **26**: 151163.

Becker, D., Kemper, E., Schell, J., and Masterson, R. (1992). New plant binary vectors with selectable markers located proximal to the left T-DNA border. Plant Mol. Biol. **20**: 1195–1197.

Bemer, M., Van Mourik, H., Muiño, J.M., Ferrándiz, C., Kaufmann, K., and Angenent, G.C. (2017). FRUITFULL controls SAUR10 expression and regulates Arabidopsis growth and architecture. J. Exp. Bot. **68**: 3391–3403.

Capella-gutiérrez, S., Silla-martínez, J.M., and Gabaldón, T. (2009). trimAl : a tool for automated alignment trimming in large-scale phylogenetic analyses. Bioinformatics **25**: 1972–1973.

Clough, S.J. and Bent, F. (1998). Floral dip: a simplified method for Agrobacterium-mediated transformation of Arabidopsis thaliana. Plant J. **16**: 735–743.

Dekker, J., Marti-Renom, M.A., and Mirny, L.A. (2013). Exploring the three-dimensional organization of genomes: Interpreting chromatin interaction data. Nat. Rev. Genet. **14**: 390-403.

Doyle, J.J. (1990). Isolation of plant DNA from fresh tissue. Focus (Madison). **12**: 13–15.

den Dulk-Ras, A. and Hooykaas, P.J. (1995). Electroporation of Agrobacterium tumefaciens. Methods Mol. Biol. **55**: 63–72.

Eddy, S.R. (2011). Accelerated Profile HMM Searches. PLoS Comput. Biol. **7**.

Grbić, V. and Bleecker, A.B. (2000). Axillary meristem development in Arabidopsis thaliana. Plant J. **21**: 215–223.

Guindon, S. and Gascuel, O. (2003). A simple, fast, and accurate algorithm to estimate large phylogenies by maximum likelihood. Syst. Biol. **5**.

Harmon, L.J., Weir, J.T., Brock, C.D., Glor, R.E., Challenger, W., and Science, A. (2008). GEIGER : investigating evolutionary radiations. Bioinformatics **24**: 129–131.

Huang, S., Raman, A.S., Ream, J.E., Fujiwara, H., Cerny, R.E., and Brown, S.M. (1998). Overexpression of 20-Oxidase confers a gibberellin- overproduction phenotype in Arabidopsis. Plant Physiol. **118**: 773–781.

Immink, R.G.H., Posé, D., Ferrario, S., Ott, F., Kaufmann, K., Valentim, F.L., de Folter, S., van der Wal, F., van Dijk, A.D.J., Schmid, M., and Angenent, G.C. (2012). Characterization of SOC1's central role in flowering by the identification of its upstream and downstream regulators. Plant Physiol. **160**: 433–449.

Karimi, M., Depicker, A., and Hilson, P. (2007). Recombinational cloning with plant gateway vectors.

Plant Physiol. **145**: 1144–1154.

Katoh, K., Misawa, K., Kuma, K., and Miyata, T. (2002). MAFFT : a novel method for rapid multiple sequence alignment based on fast Fourier transform. Nucleic Acids Res. **30**: 3059–3066.

Kiefer, C., Severing, E., Karl, R., Bergonzi, S., Koch, M., Tresch, A., and Coupland, G. (2017). Divergence of annual and perennial species in the Brassicaceae and the contribution of cis-acting variation at FLC orthologues. Mol. Ecol. **26**: 3437–3457.

Ko, J., Han, K., Park, S., and Yang, J. (2004). Plant Body Weight-Induced Secondary Growth in Arabidopsis and Its Transcription Phenotype Revealed by Whole-Transcriptome Profiling 1 [w]. Plant Physiol. **135**: 1069–1083.

Lee, J. and Lee, I. (2010). Regulation and function of SOC1 , a flowering pathway integrator. J. Exp. Bot. **61**: 2247–2254.

Liebert, M.A., Chen, K., Durand, D., Farach-colton, M., and Al, C.E.T. (2000). NOTUNG : A Program for Dating Gene Duplications. J. Comput. Biol. **7**: 429–447.

Lim, P.O., Kim, Y., Breeze, E., Koo, J.C., Woo, H.R., Ryu, J.S., Park, D.H., Beynon, J., Tabrett, A., Buchanan-Wollaston, V., and Nam, H.G. (2007). Overexpression of a chromatin architecture-controlling AT-hook protein extends leaf longevity and increases the post-harvest storage life of plants. Plant J. **52**: 1140–1153.

Matsoukas, I.G., Massiah, A.J., and Thomas, B. (2012). Florigenic and antflorigenic signaling in plants. Plant Cell Physiol. **53**: 1827–1842.

Matsushita, A., Furumoto, T., Ishida, S., and Takahashi, Y. (2007). AGF1, an AT-hook protein, is necessary for the negative feedback of AtGA3ox1 encoding GA 3-oxidase. Plant Physiol. **143**: 1152–1162.

Melzer, S., Lens, F., Gennen, J., Vanneste, S., Rohde, A., and Beeckman, T. (2008). Flowering-time genes modulate meristem determinacy and growth form in Arabidopsis thaliana. Nat. Genet. **40**: 1489–1492.

Mourik, H. Van, Muiño, J.M., Pajoro, A., Angenent, G.C., and Kaufmann, K. (2015). Characterization of In Vivo DNA-Binding Events of Plant Transcription Factors by ChIP-seq : Experimental Protocol and Computational Analysis. Methods Mol Biol **1284**: 93–121.

Munné-Bosch, S. (2008). Do perennials really senesce? Trends Plant Sci. **13**: 216–220.

Murashige, T. and Skoog, F. (1962). A Revised Medium for Rapid Growth and Bio Assays with Tobacco Tissue Cultures. Physiol. Plant. **15**: 473–497.

Ng, K.-H., Yu, H., and Ito, T. (2009). AGAMOUS controls GIANT KILLER, a multifunctional chromatin modifier in reproductive organ patterning and differentiation. PLoS Biol. **7**: e1000251.

Paradis, E., Claude, J., and Strimmer, K. (2004). APE : Analyses of Phylogenetics and Evolution in R language. Bioinformatics **20**: 289–290.

Park, S.J., Eshed, Y., and Lippman, Z.B. (2014). Meristem maturation and inflorescence architecture — lessons from the Solanaceae. Curr. Opin. Plant Biol. **17**: 70–77.

Passarinho, P., Ketelaar, T., Xing, M., van Arkel, J., Maliepaard, C., Hendriks, M.W., Joosen, R., Lammers, M., Herdies, L., den Boer, B., van der Geest, L., and Boutilier, K. (2008). BABY BOOM target genes provide diverse entry points into cell proliferation and cell growth pathways. Plant Mol. Biol. **68**: 225–237.

Pfaffl, M.W. (2001). A new mathematical model for relative quantification in real-time RT-PCR. Nucleic Acids Res. **29**: e45--e45.

Remington, D.L., Figueroa, J., and Rane, M. (2015). Timing of shoot development transitions affects degree of perenniality in Arabidopsis lyrata (Brassicaceae). BMC Plant Biol. **15**: 1–13.

Rieu, I., Ruiz-Rivero, O., Fernandez-Garcia, N., Griffiths, J., Powers, S.J., Gong, F., Linhartova, T., Eriksson, S., Nilsson, O., Thomas, S.G., Phillips, A.L., and Hedden, P. (2008). The gibberellin biosynthetic genes AtGA20ox1 and AtGA20ox2 act, partially redundantly, to promote growth and development throughout the Arabidopsis life cycle. Plant J. **53**: 488–504.

Ronquist, F. and Huelsenbeck, J.P. (2003). MrBayes 3 : Bayesian phylogenetic inference under mixed models. Bioinformatics **19**: 1572–1574.

Song, Y.H., Ito, S., and Imaizumi, T. (2013). Flowering time regulation: photoperiod- and

temperature-sensing in leaves. Trends Plant Sci. **18**: 575–583.

Street, I.H., Shah, P.K., Smith, A.M., Avery, N., and Neff, M.M. (2008). The AT-hook-containing proteins SOB3/AHL29 and ESC/AHL27 are negative modulators of hypocotyl growth in Arabidopsis. Plant J. **54**: 1–14.

Tao, Z., Shen, L., Liu, C., Liu, L., Yan, Y., and Yu, H. (2012). Genome-wide identification of SOC1 and SVP targets during the floral transition in Arabidopsis. Plant J. **70**: 549–561.

Tilmes, V., Mateos, J.L., Madrid, E., Vincent, C., Severing, E., Carrera, E., López-Díaz, I., and Coupland, G. (2019). Gibberellins Act Downstream of Arabis PERPETUAL FLOWERING1 to Accelerate Floral Induction during Vernalization . Plant Physiol. **180**: 1549–1563.

Turnbull, C. (2011). Long-distance regulation of flowering time. J. Exp. Bot. **62**: 4399–43413.

Wang, B., Smith, S.M., and Li, J. (2018). Genetic Regulation of Shoot Architecture. Annu. Rev. Plant Biol. **69**: 437–468.

Wang, J.-W. (2014). Regulation of flowering time by the miR156-mediated age pathway. J. Exp. Bot. **65**: 4723–4730.

Wang, J.-W., Czech, B., and Weigel, D. (2009). miR156-regulated SPL transcription factors define an endogenous flowering pathway in Arabidopsis thaliana. Cell **138**: 738–749.

Xiao, C., Chen, F., Yu, X., Lin, C., and Fu, Y.-F. (2009). Over-expression of an AT-hook gene, AHL22, delays flowering and inhibits the elongation of the hypocotyl in Arabidopsis thaliana. Plant Mol. Biol. **71**: 39–50.

Yu, S., Galvão, V.C., Zhang, Y.-C., Horrer, D., Zhang, T.-Q., Hao, Y.-H., Feng, Y.-Q., Wang, S., Schmid, M., and Wang, J.-W. (2012). Gibberellin regulates the Arabidopsis floral transition through miR156-targeted SQUAMOSA promoter binding-like transcription factors. Plant Cell **24**: 3320–32.

Yun, J., Kim, Y.-S., Jung, J.-H., Seo, P.J., and Park, C.-M. (2012). The AT-hook motif-containing protein AHL22 regulates flowering initiation by modifying FLOWERING LOCUS T chromatin in Arabidopsis. J. Biol. Chem. **287**: 15307–16.

Zhao, J., Favero, D.S., Peng, H., and Neff, M.M. (2013). Arabidopsis thaliana AHL family modulates hypocotyl growth redundantly by interacting with each other via the PPC/DUF296 domain. Proc. Natl. Acad. Sci. **110**: E4688–E4697.

Zhao, J., Favero, D.S., Qiu, J., Roalson, E.H., and Neff, M.M. (2014). Insights into the evolution and diversification of the AT-hook Motif Nuclear Localized gene family in land plants. BMC Plant Biol. **14**: 266.

Acknowledments
We thank Kim Boutilier and Thomas Greb for critical comments on the manuscript.

Author contribution
O.K. and R.O. conceived and supervised the project; O.K. and A.R. performed respectively 50% and 40% of the Arabidopsis experiments. All authors designed experiments and analyzed and interpreted results; O.K. and A.R. performed the majority of the Arabidopsis experiments; M.B., P.M., and M.C. contributed to the Arabidopsis experiments; M.K. generated and analyzed the tobacco lines; R.R.H. and V.N. analysed the *AHL* gene families in different mono- and polycarpic plant species, O.K., A.R and R.O. wrote the manuscript; All authors read and commented on versions of the manuscript.

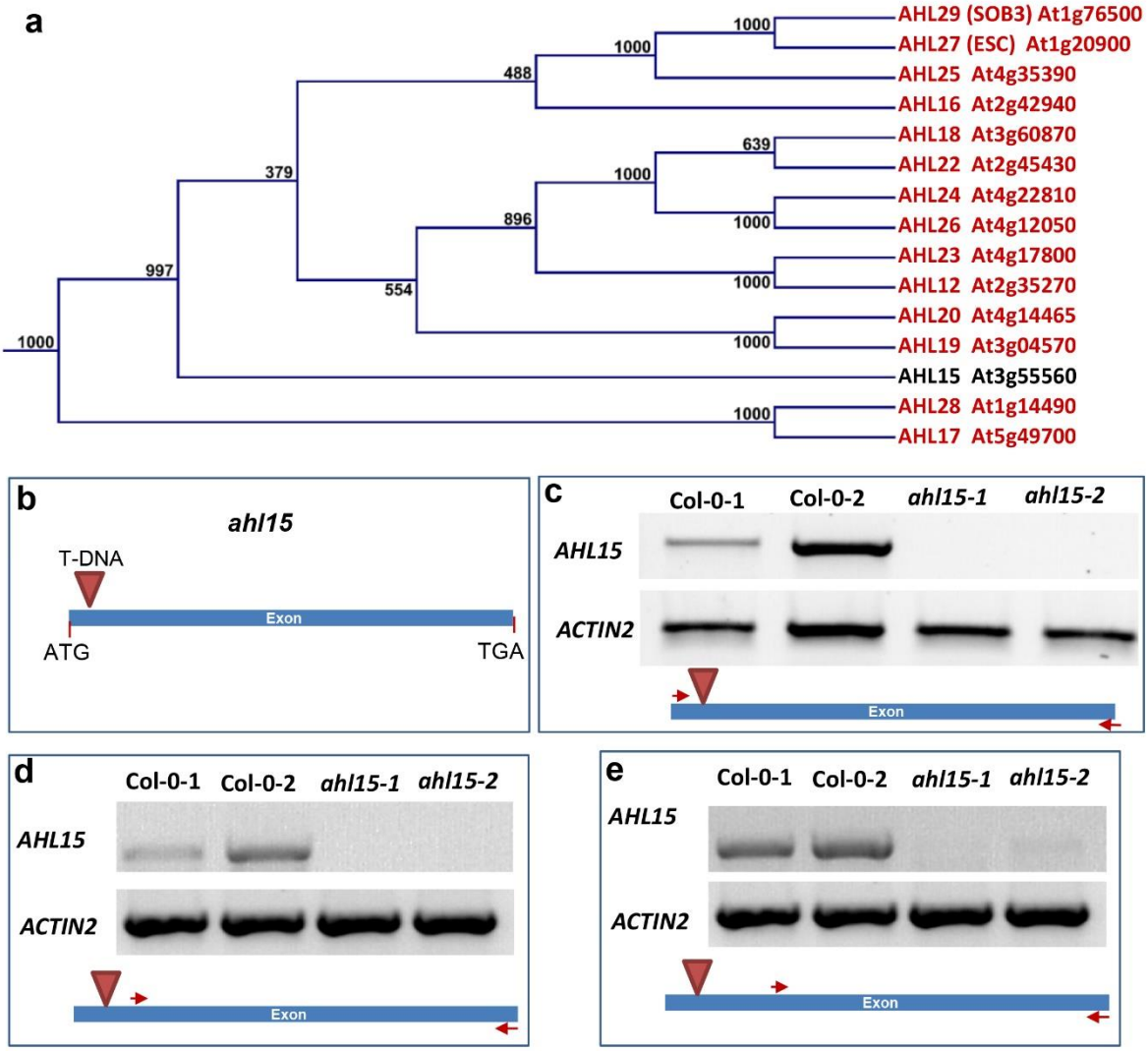

Supplementary Fig. 1 | The Arabidopsis clade-A AHL protein and gene family. (**a**) A phylogenetic tree of part of the Arabidopsis AHL protein family showing all clade-A AHL proteins containing a single At-Hook domain, including AHL15. (**b**) Location of the T-DNA insertion in the intronless *AHL15* gene, resulting in the *ahl15* loss-of-function mutant allele used for this research. (**c-e**) Duplicate RT-PCR detection of full-length *AHL15* coding sequence (CDS) (**c**), from 64bp downstream of the ATG until the end of the CDS (**d**) and from 197bp downstream of the ATG until end of the CDS (**e**) in wild-type Arabidopsis (Col-0) but not in the *ahl15* mutant. The *ACTIN2* was used as a positive control. The primers used for RT-PCR are described in Supplementary Table 2.

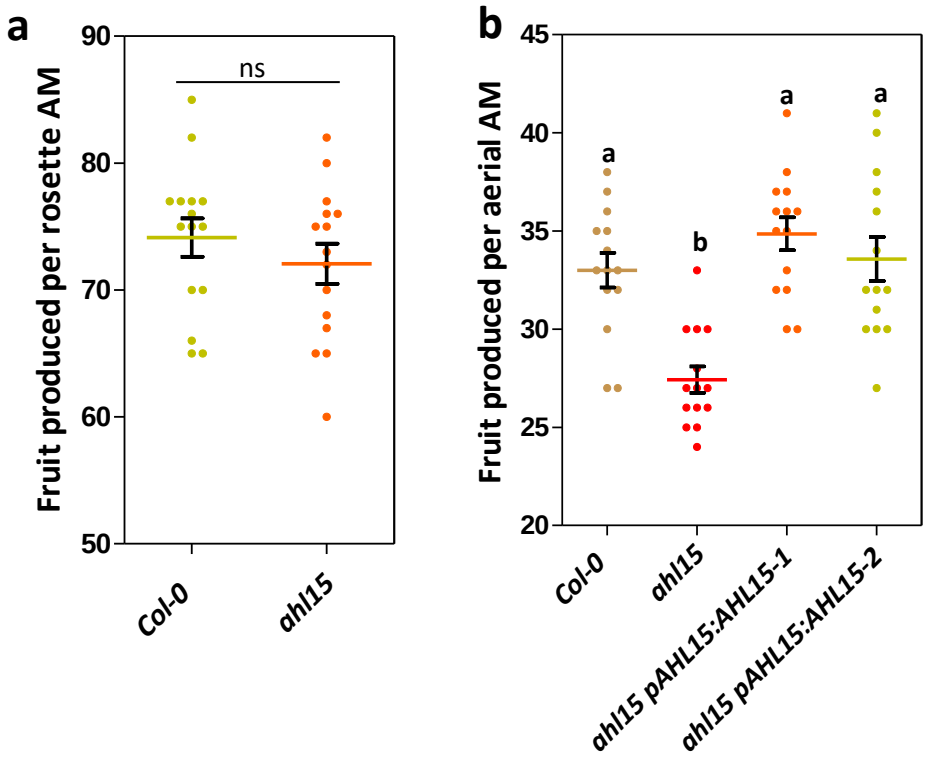

Supplementary Fig. 2 | Repression of AM maturation by *AHL15* leads to increased flower and fruit production in Arabidopsis. (**a**) The number of fruits produced by the rosette AMs of 7-week-old wild-type or *ahl15* plants. Dots indicate number of fruits produced per AM per plant (n=15 biologically independent plants), horizontal lines indicate the mean, and error bars the SEM. ns indicates no significant difference ($p < 0.05$), as determined by a two-sided Student's *t*-test. The P values are provided in Supplementary Table 18. (**b**) The number of fruits produced by the aerial AMs of 7-week-old wild-type, *ahl15* or *ahl15 pAHL15:AHL15* plants. Dots indicate number of fruits produced per AM per plant (n=15 biologically independent plants), horizontal lines indicate the mean, and error bars the SEM. Letters (a, b) indicate statistically significant differences ($p < 0.01$), as determined by a one-way ANOVA with a Tukey's HSD post hoc test.

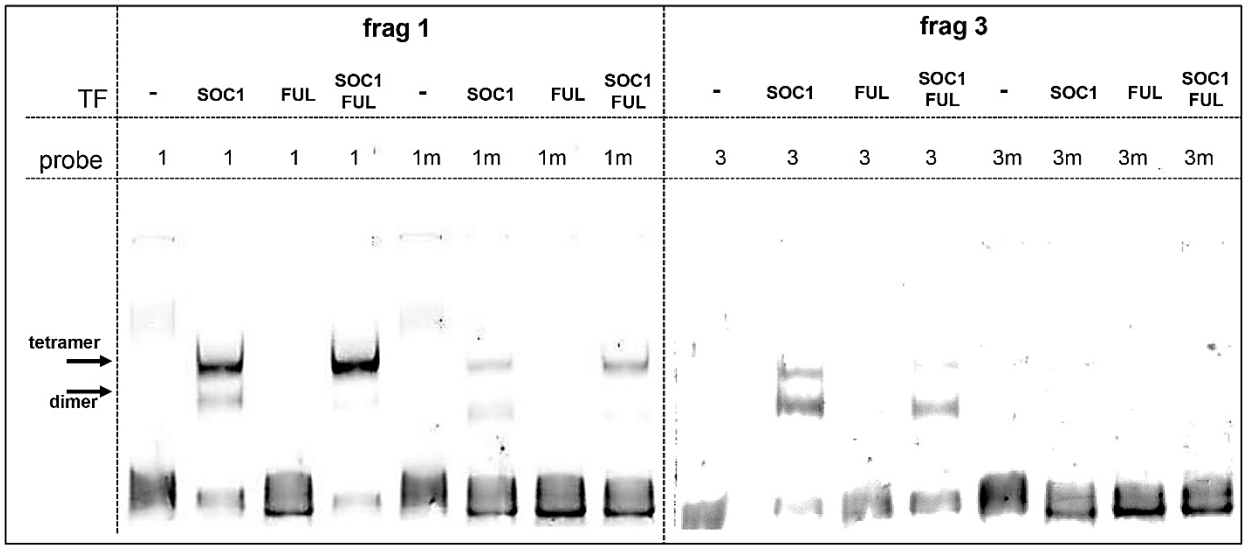

Supplementary Fig. 3. Binding of SOC1 and FUL to regulatory regions near *AHL15*. Left panel: EMSA of promoter fragment 1 with a wild-type (1) or mutated (m1) CArG-box. Right panel: EMSA of downstream fragment 3 with a wild-type (3) or mutated (3m) CArG-box. Shifting of the probe, indicating binding, occurs either by a tetramer (upper band) or dimer (lower band).

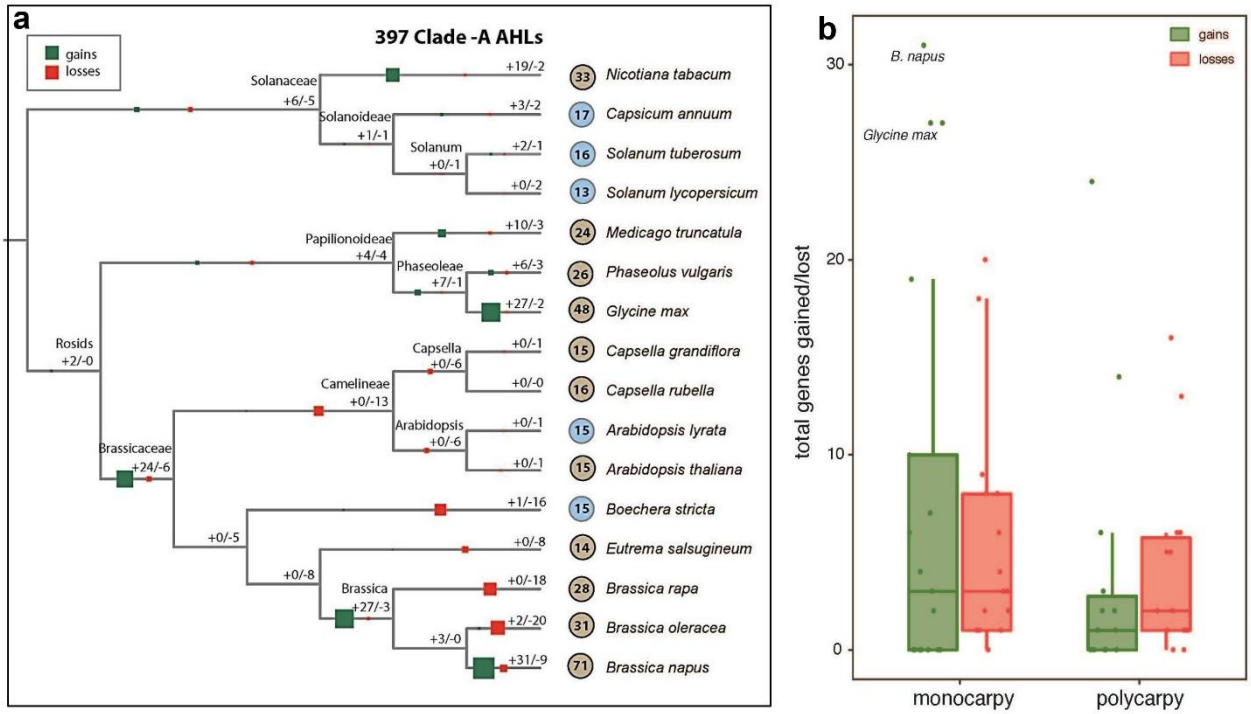

Supplementary Figure 4. Evolutionary history of the Clade-A *AHL* gene family in relation to the monocarpic and polycarpic plant growth habit. (**a**) Reconciliation of the gene (protein) tree with the species tree of 16 selected dicot plant species with either a monocarpic (light brown circled number) or a polycarpic (light blue circled number) life history strategy. The tree topology was extracted from the NCBI taxonomy database. For each tree node, the number of gained genes (+) is indicated by the size of the green box, and the number of lost genes (-) by the size of the red box. The total number of *AHL* genes for each plant species is indicated by the circled number. (**b**) The distribution of total Clade-A *AHL* gene gains and losses for monocarpy or polycarpy in (**a**) have been summarized as box-plots. The character state of each ancestor was determined for the presence (polycarpy) or absence (monocarpy) of polycarpic growth habit using Dollo's parsimony principle. Horizontal bars indicate median values , boxes demarcate 1st and 3rd quartiles, and whiskers delineate minimum (within 1.5 times Inter Quartile Range (IQR) below 1st quartile) and maximum (within 1.5 times IQR above 3rd quartile) values. The dots in the box-plots indicate all the ancestral states and current species for which the total gene gains/losses were estimated (n = 11 monocarpic species and 5 polycarpic species). The outlier species are labelled with the species name. The outlier species are labelled with the species name.

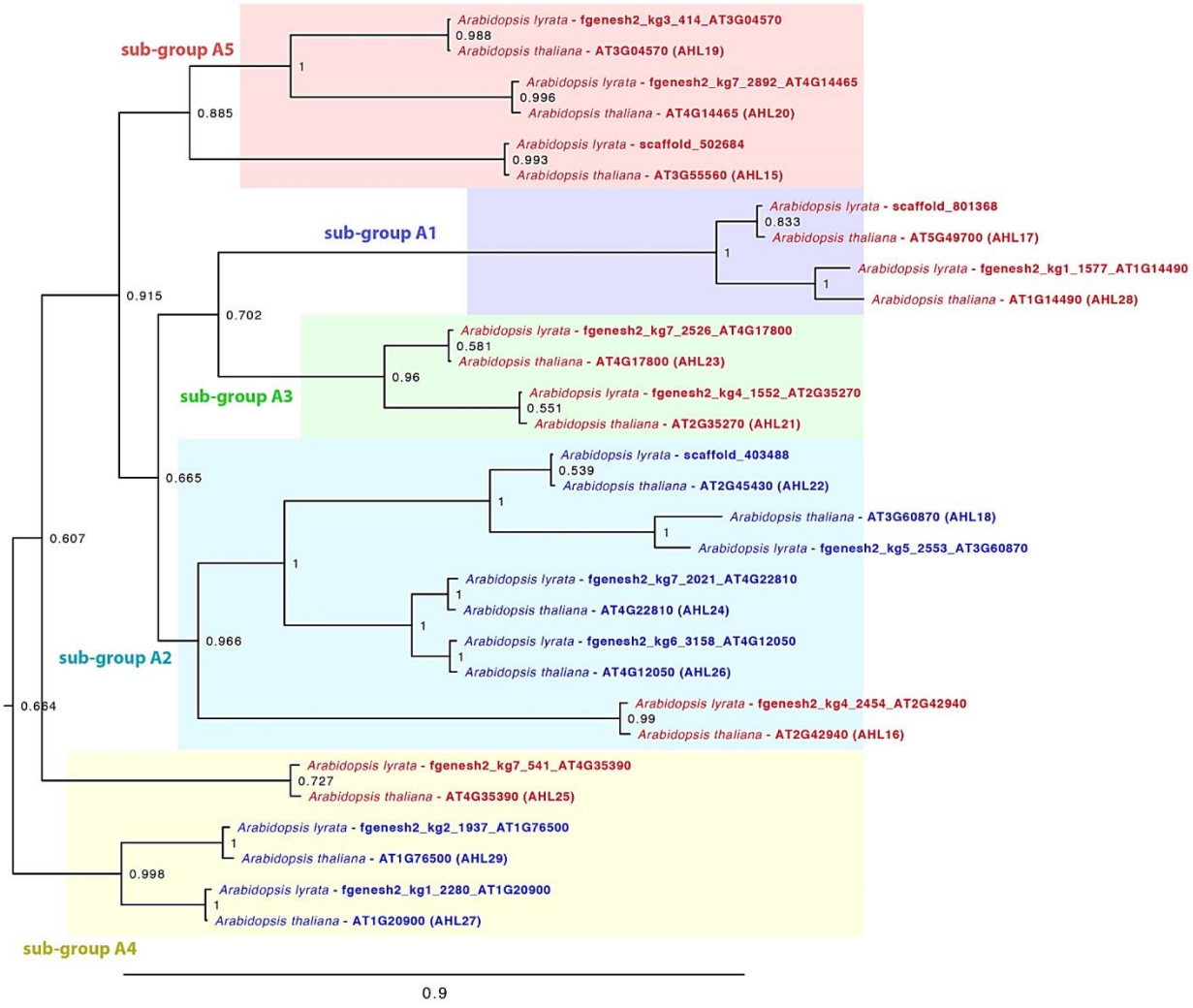

Supplementary Fig. 5 | Phylogenetic tree of *A. thaliana* and *A. lyrata* clade-A AHL proteins. The tree shows 15 one-to-one orthologous pairs between the two species.

Supplementary Table 1: PCR primers used for cloning and genotyping

Name*	Sequence (5' to 3')	Purpose
Gateway-AHL15-F	GGGGACAAGTTTGTACAAAAAAGCAGGCTCGATGGCGAATCCTTGGTGGGT	*pGW-AHL15* construct
Gateway-AHL15-R	GGGGACCACTTTGTACAAGAAAGCTGGGTAATACGAAGGAGGAGCACGAG	
ccdB gene +KpnI-F	CGGGTACCGCTATCGAACCACTTTGTAC	Amplify *ccdB* gene
ccdB gene +SphI-R	GACTGCAAGTCACGTCGGCAG	
pAHL15:AHL15-F	GGGGACAAGTTTGTACAAAAAAGCAGGCTCGACACTCCTCTGTGCCACATT	*pAHL15:AHL15* construct
pAHL15:AHL15-R	GGGGACCACTTTGTACAAGAAAGCTGGGTATCTTTTTTTCTTCTCTAATGG	
pFD:AHL15-F	GGGGACAAGTTTGTACAAAAAAGCAGGCTGGCCCTCTCTACTTGATTTAG	*pFD:AHL15* construct
pFD:AHL15-R	GGGGACCACTTTGTACAAGAAAGCTGGGTATGGAAAAGAGAACAGAAGTGAAC	
pMYB85:AHL15-F	GGGGACAAGTTTGTACAAAAAAGCAGGCTGGTGGGGTGTTGAAATGTCAC	*pMYB85:AHL15* construct
pMYB85:AHL15-R	GGGGACCACTTTGTACAAGAAAGCTGGGTATAAATACTATATAGAAATGATATG	
pMYB103:AHL15-F	GGGGACAAGTTTGTACAAAAAAGCAGGCTTTCTATTGCTCCTCCTTAAAGG	*pMYB103:AHL15* construct
pMYB103:AHL15-R	GGGGACCACTTTGTACAAGAAAGCTGGGTAGATTAGTAGCTCCTCAAAGTAAC	
p35S:AHL29-F	ATAAGAATGCGGCCGCGACGGTGGTTACGATCAATC	*p35S:AHL29* construct
p35S:AHL29-R	ATAGTTTAGCGGCCGCCTAAAAGGCTGGTCTTGGTG	
p35S:AHL20 –F	ATAAGAATGCGGCCGCGCAAACCCTTGGTGGACGAAC	*p35S:AHL20* construct
p35S:AHL20-R	ATAGTTTAGCGGCCGCTCAGTAAGGTGGTCTTGCGT	
p35S:AHL27-F	ATAAGAATGCGGCCGCGAAGGCGGTTACGAGCAAGG	*p35S:AHL27* construct
p35S:AHL27-R	ATAGTTTAGCGGCCGCTTAAAAAGGTGGTCTTGAAG	
p35S: BoAHL15-1-F	ATAAGAATGCGGCCGCGCGAATCCTTGGTGGGTAGA	*p35S:BoAHL15* construct
p35S: BoAHL15-1-R	ATAGTTTAGCGGCCGCTCAATATGAAGGAGGACCAC	
p35S: MtAHL15-F	ATAAGAATGCGGCCGCTCGAATCGATGGTGGAGTGG	*p35S: MtAHL15* construct
p35S: MtAHL15-R	ATAGTTTAGCGGCCGCTCAATATGGAGGTGGATGTG	
p35S:AHL19-F	GGGGACAAGTTTGTACAAAAAAGCAGGCTCGATGGCGAATCCATGGTGGAC	*p35S:AHL19* construct
p35S:AHL19-R	GGGGACCACTTTGTACAAGAAAGCTGGGTAAACAAGTAGCAACTGACTGG	
SALK_040729-F	GTCGGAGAGCCATCAACACCA	*ahl15* genotyping
SALK_040729-R	CGACGACCCGTAGACCCGGATC	
soc1-6 -F	AAAGGATGAGGTTTCAAGCG	*soc1-6* genotyping
soc1-6 -R	ATGTGATTCCACAAAAGGCC	
ful-7-F	TTTCCGCCTTCTCTCGTTGTG	*ful-7 genotyping*

*, F: forward; R: reverse

Supplementary Table 2: PCR primers used for qRT-PCR and RT-PCR

Name*	Sequence (5' to 3')	Purpose
qAHL15-F	AAGAGCAGCCGCTTCAACTA	*qRT-PCR AHL15*
qAHL15-R	TGTTGAGCCATTTGATGACC	
qAHL16-F	CCAGCTTCATCAGGAGCAAT	*qRT-PCR AHL16*
qAHL16-R	ATGCAGCCATGAGAACAACA	
qAHL17-F	GTCCACTTATTTCGGCAGGA	*qRT-PCR AHL17*
qAHL17-R	TACCCCACACGACTCTCCTC	
qAHL18-F	ACACGGACGGTTTGAGATTC	*qRT-PCR AHL18*
qAHL18-R	GCCTCTCGTAAGATGCGTTT	
qAHL19-F	CTCTAACGCGACTTACGAGAGATT	*qRT-PCR AHL19*
qAHL19-R	ATATTATACACCGGAAGTCCTTGGT	
qAHL20-F	CAAGGCAGGTTTGAAATCTTATCT	*qRT-PCR AHL20*
qAHL20-R	TAGCGTTAGAGAAAGTAGCAGCAA	
qAHL22-F	AGCTGGAGCGGTTGCTAATA	*qRT-PCR AHL22*
qAHL22-R	CAGCTGGCAATTGAACAGAA	
qAHL23-F	TTGTGACGCTACAAGGAACG	*qRT-PCR AHL23*
qAHL23-R	AAACGAAGCTGCAATCACAA	
qAHL24-F	TGGTTGGAGGAAGCGTAGTT	*qRT-PCR AHL24*
qAHL24-R	GCTTGTTGCTGATGTTGCAG	
qAHL25-F	GCAAACGCAGTTTATGATAGGTTAC	*qRT-PCR AHL25*
qAHL25-R	ATTCCAAGATTGTAGAAAGCAACAC	
qAHL26-F	GGTGGGACCTTTGTTGTGTT	*qRT-PCR AHL26*
qAHL26-R	TGCCATAGCTTGTTGCTGTC	
$_{R1}$AHL15-F	ATGGCGAATCCTTGGTGGGTAG	*RT-PCR$_1$ AHL15*
$_{R1}$AHL15-R	TCAATACGAAGGAGGAGCACGAG	
$_{R}$ACTIN2-F	TGAGACCTTTAACTCTCCCGCTA	*RT-PCR ACTIN2*
$_{R}$ACTIN2-R	TGATTTCTTTGCTCATACGGTCA	
$_{R2}$AHL15-F	TCAGCT CCT TCT TTGCACCAC	*RT-PCR$_2$ AHL15*
$_{R2}$AHL15-R	ATACGAAGGAGGAGCACGAGG	
$_{R3}$AHL15-F	AAGAACAGAACAGCAGAGACG	*RT-PCR$_3$ AHL15*
$_{R3}$AHL15-R	TCAATACGAAGGAGGAGCACG	
qβ-TUBULIN-6-F	TGGGAACTCTGCTCATATCT	*qRT-PCR AHL15*
qβ-TUBULIN-6-R	GAAAGGAATGAG GTTCACTG	
QEF1ALPHA-F	TGAGCACGCTCTTCTTGCTTTCA	*qRT-PCR EF1alpha*
QEF1ALPHA-R	GGTGGTGGCATCCATCTTGTTACA	
ChIP REF1-F	TCTCCGACCTTTCTTCACACCCATTCC	*ChIP-qPCR REF1*
ChIP REF1-R	CTGAGAACTTGCTTACTTGATAGACTC	
ChIP REF2-F	GCTATCCACAGGTTAGATAAAGGAG	*ChIP-qPCR REF2*
ChIP REF2-R	GGACTAGATTTGAGGAAAGGAAGGA	
ChIP frag1-F	TGTCACACCACTCTCTTTGCA	*ChIP-qPCR frag1*
ChIP frag1-R	AATAATGGTTACTGAAAACGTACA	
ChIP exon-F	TCCAGAGCCATGTTCTTGAG	*ChIP-qPCR exon*
ChIP exon-R	GCTGACGCAGAGTAACATTAG	
ChIP frag3-F	TTGGATCTTTGGCATTGTCTC	*EMSA-PCR frag3*
ChIP frag3-F	TGCTACGGAGTTTAGTCATCA	
EMSA frag1-F	TGTCACACCACTCTCTTTGCA	*PCR frag1*
EMSA frag1-R	AATAATGGTTACTGAAAACGTACA	
EMSA exon-F	TCCAGAGCCATGTTCTTGAG	*PCR exon*
EMSA exon-R	GCTGACGCAGAGTAACATTAG	
EMSA frag3-F	TTGGATCTTTGGCATTGTCTC	*PCR frag3*
EMSA frag3-F	TGCTACGGAGTTTAGTCATCA	
EMSA frag1 sequence	TGTCACACCACTCTCTTTGCATATAATCCAAAACATATATGGGTTAATGAATTTTC AAAAAATAACAGCCCTTATTTGGATCTTACAATAAATGTACGTTTTCAGTAACCA TTATT	
EMSA mutated frag1 sequence	TGTCACACCACTCTCTTTGCATATAATCCAAAACATATATGGGTTAATGAATTTTC AAAAAATAACAGCCCTTCCTTGGATCTTACAATAAATGTACGTTTTCAGTAACCA TTATT	
EMSA exon sequence	TTGGATCTTTGGCATTGTCTCTGGTCTTAAATATCCCTTTTATGGTATATCAAAAA AACATGAGTACGGAATATATGGTCCCATGATGACTAAACTCCGTAGCA	

EMSA frag3 sequence	TTGGATCTTTGGCATTGTCTCTGGTCTTAAATATCCCCTCCATGGTATATCAAAAA AACATGAGTACGGAATATATGGTCCCATGATGACTAAACTCCGTAGCA
EMSA mutated frag3 sequence	TCCAGAGCCATGTTCTTGAGATTGCTACGGGAGCTGACGTGGCGGAAAGCTTAA ACGCCTTTGCTCGTAGACGCGGCCGGGGCGTTTCGGTGCTGAGCGGTAGTGGTTT GGTTACTAATGTTACTCTGCGTCAGC

*, F: forward; R: reverse.

Chapter 3

miR156-independent repression of the ageing pathway by longevity-promoting AHL proteins in Arabidopsis

Arezoo Rahimi[1], Omid Karami[1] and Remko Offringa[1]

[1]Plant Developmental Genetics, Institute of Biology Leiden, Leiden University, Sylviusweg 72, 2333 BE Leiden, Netherlands

Abstract

Plants age by transition through distinct developmental phases, with the juvenile- to adult vegetative and the adult vegetative to reproductive phase change as two consecutive important post-embryonic phase transitions. During the transition from the juvenile- to adult vegetative phase, also known as the vegetative phase change (VPC), many plants undergo specific morphological and physiological changes. In the model plant *Arabidopsis thaliana* (Arabidopsis), for example, the VPC is marked by clear heteroblastic changes in leaf shape and size and the appearance of trichomes on the abaxial side of leaves. The VPC and the vegetative to reproductive transition are promoted by the SQUAMOSA PROMOTOR BINDING PROTEIN-LIKE (SPL) family of transcription factors and repressed by miR156 and miR157 that target the *SPL* transcripts. Here we present data that the plant longevity promoting AT-HOOK MOTIF NUCLEAR LOCALIZED protein 15 (AHL15) and family members also repress the SPL-driven ageing pathway. Arabidopsis *ahl* loss-of-function mutants showed an accelerated VPC and flowering time, whereas *AHL15* overexpression dramatically delayed the VPC and flowering time in both Arabidopsis and *Nicotiana tabacum*. Expression analysis and tissue-specific *AHL15* overexpression revealed that *AHL15* affects the VPC and flowering time directly through its expression in the shoot apical meristem and young leaves. In addition, we found evidence that AHL15 represses *SPL* gene expression in a miR156/157-independent manner. The juvenile traits of *spl* loss-of-function mutants appeared to be dependent on the enhanced expression of the *AHL15* gene, providing evidence for a reciprocal negative feedback between *AHL15* and *SPL* genes. Antagonistically to AHLs, SPLs promote axillary meristem (AM) maturation and thus prevent vegetative growth from these meristems by repressing *AHL15* expression. Taken together, our results place AHL15 and family members at a central position in the SPL-driven ageing pathway as suppressors of the VPC, flowering time and AM maturation.

Keywords: Vegetative Phase Change, *AHL* genes, *SPL* genes, *miR156/miR157*, Arabidopsis

Introduction

Plant development progresses through several distinct developmental phases, starting with embryogenesis and followed successively by the juvenile vegetative, adult vegetative, reproductive and gametophytic phase. In the juvenile vegetative phase, the plant is not competent to flower. Therefore, flowering requires the transition from juvenile to adult vegetative development, which is referred to as the vegetative phase change (VPC). The VPC generally leads to plant morphological changes such as increased internode length, adventitious root production and changes in leaf size and shape and trichome distribution, a situation also known as heteroblasty (Huijser and Schmid, 2011). In *Arabidopsis*, leaf heteroblasty provides a clear indicator of the VPC. Juvenile leaves have smooth margins, are rounder (length/width), and lack abaxial trichomes, whereas adult leaves have serrated margins, are more elongated (length/width ratio) and have abaxial trichomes (Telfer et al., 1997).

Compared to the adult-to-reproductive phase transition, which is one of the key-traits in crops, much less is known about the molecular mechanisms that mediate the juvenile-to-adult transition. However, recent progress in *Arabidopsis thaliana* (Arabidopsis) has demonstrated that microRNAs (miRNAs) miR156, miR157, and miR172, are major regulators of the juvenile-to-adult transition in Arabidopsis and other plant species (Poethig, 2013; Teotia and Tang, 2015). During the Arabidopsis life cycle the gradual decrease in *miR156/miR157* expression results in increased expression of the *SQUAMOSA-PROMOTER BINDING PROTEIN-LIKE (SPL) miR156/miR157* target genes. SPL transcription factors, in turn, promote the adult developmental program at the shoot apical meristem (SAM), resulting in the transition from juvenile to adult leaf production and eventually from vegetative to reproductive development (Wang et al., 2009; Wu et al., 2009; He et al., 2018). The gradual decrease of *miR156/miR157* expression during shoot maturation is accompanied by an SPL-induced gradual increase in *miR172* expression. miR172 promotes the development of trichomes on the abaxial side of leaves by repressing the expression of the APETALA2-LIKE (AP2-like) transcription factors TARGET OF EARLY ACTIVATION TAGGED1 (TOE1) and TOE2 (Wu et al., 2009). In addition, SPLs promote the other adult leaf traits such as leaf elongation and leaf serration independent of miR172. However, the genes that act downstream of SPLs and TOE1/TOE2 in juvenile-and-adult transition remain unidentified.

In eukaryotes, a wide range of DNA binding proteins have been identified that bind to the minor groove of DNA by a small AT-hook motif (Reeves, 2010). AT-hook proteins are considered as chromatin architectural factors involved in a diverse array of crucial cellular processes, including cell growth, -differentiation, -transformation, -proliferation, -death, and DNA replication and repair, by regulating chromatin remodelling, and gene transcription (Reeves, 2010; Sgarra et al., 2010; Ozturk et al., 2014). The Arabidopsis genome encodes 29 AT-Hook motif nuclear-Localized (AHL) proteins that containing either one or two AT-hook domains and a Plant and Prokaryote Conserved (PPC) domain (Fujimoto et al., 2004; Matsushita et al., 2007; Street et al., 2008; Zhao et al., 2013). These AHL proteins have been shown to be implicated in several aspects of plant growth and development, including hypocotyl growth (Street et al., 2008; Xiao et al., 2009; Zhao et al., 2013), root vascular

tissue differentiation (Zhou et al., 2013), flower development (Ng et al., 2009), flowering time (Street et al., 2008; Xiao et al., 2009; Yun et al., 2012; Xu et al., 2013). Based on mutants and protein-protein interaction studies, the AHL family members have been proposed to bind AT-rich DNA regions as hetero-multimeric complexes. These AHL complexes use the AT-hook domains to anchor to AT-rich DNA regions and recruit other transcription factors through their interacting PPC domains (Zhao et al., 2013). In addition, it has been shown that AHL proteins repress transcription of several key developmental regulatory genes, possibly through modulation of the epigenetic code in the vicinity of their DNA binding regions (Lim et al., 2007; Ng et al., 2009; Yun et al., 2012). Some evidence has been obtained that AHL proteins function by altering the organization of the chromatin structure (Lim et al., 2007; Ng et al., 2009; Yun et al., 2012; Xu et al., 2013). However, since this plant-specific class of nuclear proteins has only been studied more recently, their exact mode of action is still elusive.

Recently, we have shown that the *AHL15* gene and other *AHL* family members are important for embryogenesis (Karami et al., 2020b) and that they promote plant longevity by delaying axillary meristem (AM) maturation (Karami et al., 2020a, chapter 2). In view of the seemingly antagonistic effect of *AHL15* and its family members on the plant ageing pathway, we here studied their possible role in the regulation of the VPC and flowering time. Our analyses in Arabidopsis and *Nicotiana tabacum* (tobacco) showed that *AHL15* overexpression prolongs the juvenile vegetative phase and delays flowering, whereas *ahl15* loss of function results in precocious appearance of adult vegetative traits. A more detailed analysis indicated that AHL15 delays developmental phase changes by repressing *SPL* gene expression in a miRNA-independent manner. We further show that in turn *AHL15* expression is repressed through feedback regulation by the SPLs.

Results

AHL genes delay the vegetative phase change and flowering time

When studying plants overexpressing *AHL15* (*p35S:AHL15*), we noticed that they initially produced much smaller rosette leaves than wild-type plants with a low number of adaxial trichomes (not shown), and that leaves produced three to four weeks later were similar in size to the first juvenile leaves of wild-type plants (Fig. 1A, B). More detailed analysis showed that *p35S:AHL15* plants produced leaves with a reduced length/width ratio (Fig. 1C) and had a significantly delayed VPC, as indicated by an increased number of leaves without abaxial trichomes, both under short day (SD) and long day (LD) conditions (Fig. 1D, E). By contrast, *ahl15* loss-of-function mutants developed leaves with a slightly increased length/width ratio with the VPC occurring 1 to 2 plastochrons earlier (Fig. 1A-E). Introduction of a *pAHL15:AHL15* genomic clone into the *ahl15* mutant background resulted again in wild-type leaf development (Fig. 1A-E), indicating that the phenotypes were caused by *ahl15* loss-of-function. *AHL15* is part of a large gene family in Arabidopsis, where it clusters together with two close homologs *AHL19* and *AHL20* (Chapter 2). In line with the previously reported high degree of functional redundancy between *AHL* genes (Street et al., 2008; Xiao et al., 2009; Zhao et al., 2013), *ahl15 ahl19 p35S:amiRAHL20* triple mutant plants showed a stronger increase in the leaf length/width ratio compared to the *ahl15* single or *ahl15 ahl19* double

mutant. However, the timing of the VPC was comparable with that of the single or *ahl15 ahl19* double mutant plants under both SD and LD conditions (Fig. 1A-E).

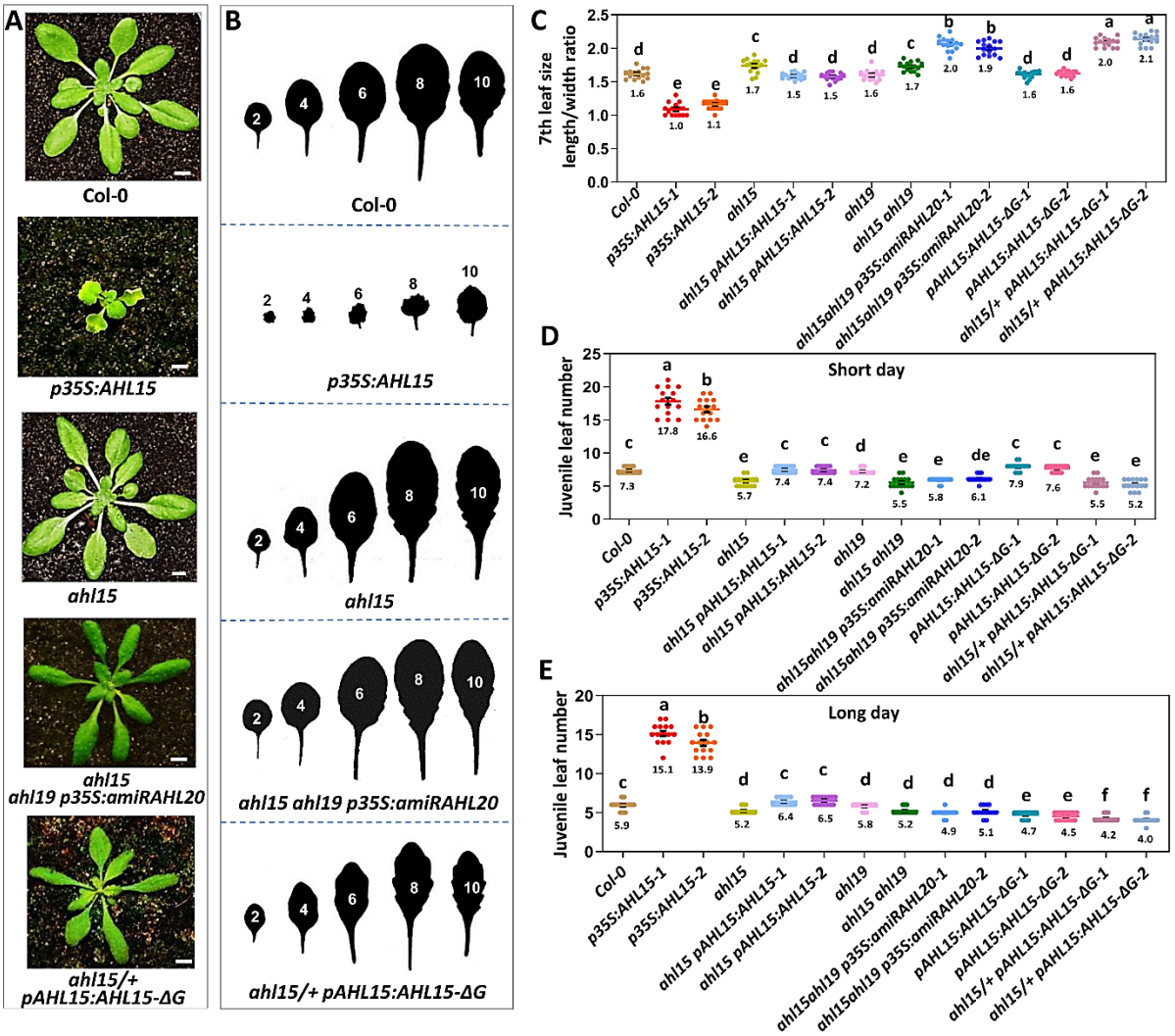

Figure 1. *AHL15* and family members delay the vegetative phase change in Arabidopsis. (**A**) The rosette phenotype of 5-week-old wild-type (Col-0), *p35S:AHL15*, *ahl15*, *ahl15 ahl19 p35S:amiRAHL20*, or *ahl15/+ pAHL15:AHL15-ΔG* plants grown under short-day (SD) conditions. Size bars indicate 1 cm. (**B**) Shape of the successive rosette leaves of 7-week-old of wild-type, *p35S:AHL15*, *ahl15 ahl19 p35S:amiRAHL20*, or *ahl15/+ pAHL15:AHL15-ΔG* plants grown under SD. (**C**) The length:width ratio of the 7 th leaf of 7-week-old wild-type, *p35S:AHL15*, *ahl15*, *ahl15 pAHL15:AHL15*, *ahl19*, *ahl15 ahl19*, *ahl15 ahl19 p35S:amiRAHL20*, *pAHL15:AHL15-ΔG* and *ahl15/+ pAHL15:AHL15-ΔG* plants grown under SD. (**D** and **E**) The juvenile leaf number (leaves without abaxial trichomes) in wild-type, *p35S:AHL15*, *ahl15*, *ahl15 pAHL15:AHL15*, *ahl19*, *ahl15 ahl19*, *ahl15 ahl19 p35S:amiRAHL20*, *pAHL15:AHL15-ΔG* and *ahl15/+ pAHL15:AHL15-ΔG* plants grown under SD (**D**) and under long day (**E**). Coloured dots in C-E indicate length:width ratio (**C**) and the number of leaves without abaxial trichomes (**D**,**E**) per plant (n=15 biologically independent plants) per line, horizontal line and the number below this line indicate the mean and error bars indicate the s.e.m. **C-E** Different letters indicate statistically significant differences ($P < 0.01$) as determined by one-way ANOVA with Tukey's honest significant difference post hoc test.

Previously, we have shown that expression of a mutant version of AHL15 lacking the conserved GRFEIL motif in the PPC domain under control of the *AHL15* promoter in the heterozygous mutant background (*ahl15+/-pAHL15:AHL15-ΔG*) leads to a dominant-negative effect that allows to overcome the functional redundancy between *AHL* genes (Karami et al., 2020a, chapter 2). Expression of *pAHL15:AHL15-ΔG* in the wild-type background only led to an acceleration of the VPC under LD conditions (Fig. 1A-E). However, ahl15/+ *pAHL15:AHL15-ΔG* plants showed the highest increase in leaf length/width ratio and also the strongest enhancement in timing of the VPC under LD conditions compared to wild type or to other *ahl* mutant lines (Fig. 1A-E). Since Arabidopsis plants require the VPC before they can shift to the reproductive phase, we also monitored the flowering time of our mutant lines. Our previous analysis already showed that *ahl15/+ pAHL15:AHL15-ΔG* plants flowered significantly earlier, as quantified by the number rosette leaves developed until flowering, under both LD and SD conditions compared to wild-type plants (Karami et al., 2020a, chapter 2). Further analysis showed that the single *ahl15* and *ahl19* loss-of-function mutations did not significantly affect flowering time, whereas *ahl15 ahl19 p35S:amiRAHL20* triple mutant plants showed a significant reduction in flowering time only under SD conditions (Supplementary Fig. 1A-C). In contrast, *p35S:AHL15* plants showed a significant delay of flowering under both SD and LD conditions (Supplementary Fig. 1A-C). These results indicate that *AHL* genes are important determinants of the VPC and, most likely as a result, also of the vegetative to reproductive phase transition (Supplementary Fig. 1A-C).

We also analysed the effect of *AHL15* overexpression on the same developmental phase changes in tobacco, a plant species from a different family, using available *p35S:AHL15-GR* tobacco lines (Karami et al., 2020a, chapter 2). In contrast to mock-treated *p35S:AHL15-GR* tobacco plants, which showed wild-type leaf development with three round juvenile leaves preceding the production of the typically larger and longer adult leaves, DEX-treated *p35S:AHL15-GR* plants formed many small, round juvenile leaves (Supplementary Fig. 2A). By spraying these plants once per week with DEX, the shoot apical meristem continued to produce small juvenile leaves, and plants could be kept in the juvenile vegetative state for more than a year, resulting in highly branched and bushy plants (Supplementary Fig. 2B and C). In contrast, *p35S:AHL15-GR* control plants that were not treated with DEX developed normally and flowered after two-month (not shown). This result indicates that *AHL15* overexpression can also strongly delay, if not prevent the VPC and flowering in a non-brassicaceae plant species, such as tobacco.

AHL15 delays the VPC through its expression in the SAM and in leaf primordia

To further understand the role of *AHL* genes in these developmental switches, we analysed the expression dynamics of *AHL15* and its close homologs *AHL19* and *AHL20* during the VPC. Quantitative RT-PCR (qPCR) experiments showed that expression of the three *AHL* genes was negatively correlated with shoot age, as expression of all three genes was higher in the shoot apex and young leaves of 1- or 2-week-old seedlings grown under short day (SD) conditions, and then significantly declined in these tissues in 3-week-old seedlings (Fig. 2A). This is in line with the timing of the VPC, which for Arabidopsis ecotype Col-0 has been reported to occur at 17-20 days after germination (DAG) under SD conditions (Xu et al.,

2016). Similarly, analysis of *AHL15* expression in leaves and shoot apices using *pAHL15:GUS* reporter lines showed that *AHL15* was expressed throughout the shoot at 7 and 12 DAG (week 1 and week 2), that its expression declined in the shoot apical meristem (SAM) at 12 DAG, but that at 17 DAG (week 3) its expression was off or severely reduced in respectively the SAM or the new-formed leaves (Fig, 2B). The gene expression dynamics of *AHL15* and its close homologs supports their role in maintaining vegetative juvenile traits and thus suppressing the VPC.

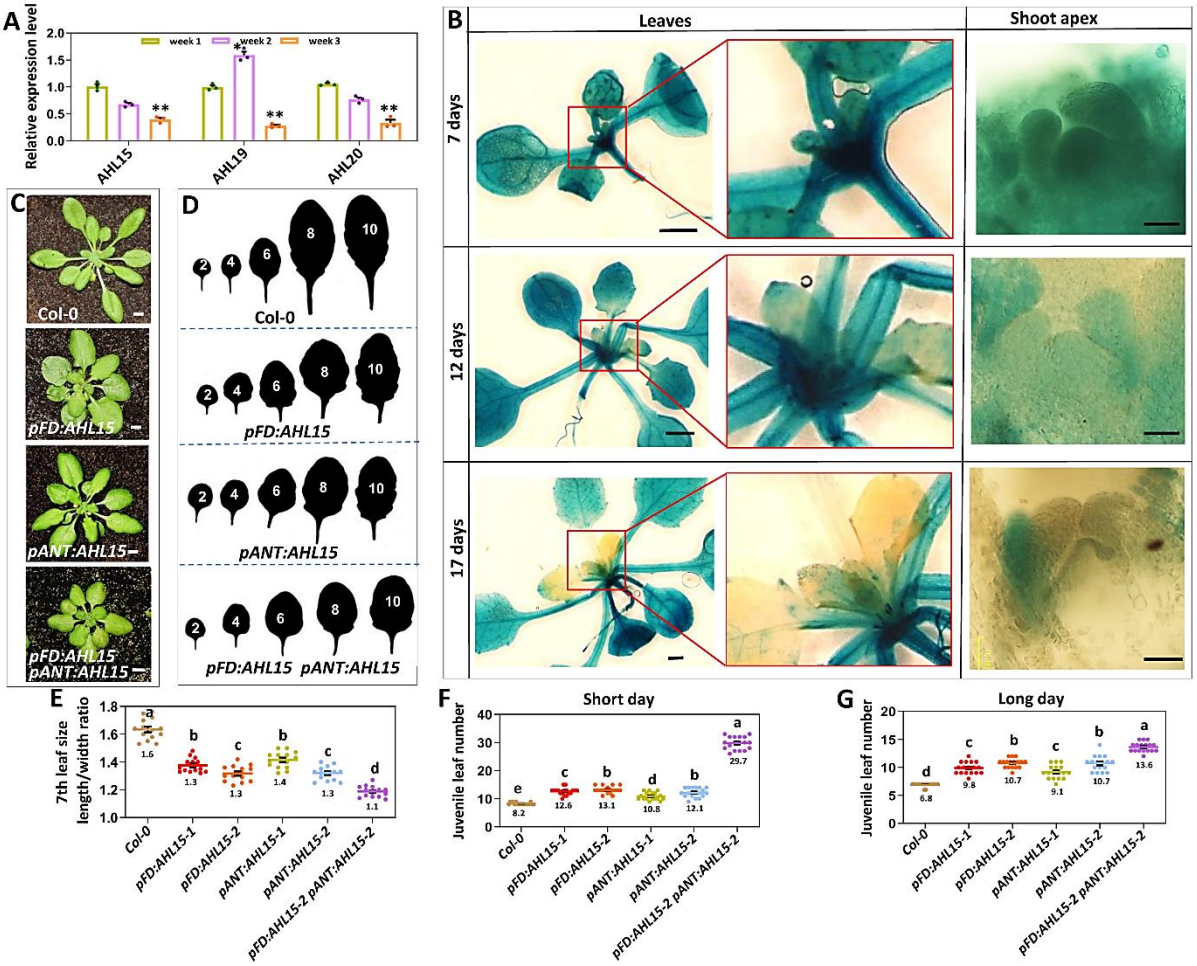

Figure 2. *AHL15* expression in the SAM and leaf primordia delays the VPC. (**A**) The relative expression level of *AHL15*, *AHL19*, and *AHL20* in the shoot apex and young leaves of 1, 2, and 3 week-old seedlings grown under SD conditions. Dots indicate the values of three biological replicates per plant line, bar indicates the mean, and error bars the s.e.m. The asterisk indicates a significant difference (*P< 0.05, **P< 0.01), as determined by a two-sided Student's *t*-test. (**B**) Histochemical staining for GUS activity in 7-, 12-, and 17-day-old *pAHL15:GUS* seedlings. Images show overview of leaves (left two rows) and details shoot apex (right row). (**C**) The rosette phenotype of 5-week-old wild-type (Col-0), *pFD:AHL15*, *pANT:AHL15* and *pFD:AHL15 pANT:AHL15* plants grown under SD conditions. (**D**) Shape successive rosette leaves of 7-week-old of wild-type, *pFD:AHL15*, *pANT:AHL15* and *pFD:AHL15 pANT:AHL15* plants grown under SD. (**E**) The length:width ratio of the 7 th leaf of 7-week-old wild-type, *pFD:AHL15*, *pANT:AHL15* and *pFD:AHL15 pANT:AHL15* plants grown under SD. (**F** and **G**) The juvenile leaf number (leaves without abaxial trichomes) in wild-type, *pFD:AHL15*, *pANT:AHL15*, and *pFD:AHL15 pANT:AHL15* plants grown under SD. (**F**) and under LD (**G**). Colored dots in **E-G** indicate length:width ratio (**E**) and the number of leaves without abaxial trichomes (**F**,**G**) per plant (n = 15 biologically independent plants) per line, horizontal line and the number below this line indicate the mean and error bars indicate the s.e.m. **E-G** Different letters indicate statistically significant differences (P < 0.01) as determined by one-way ANOVA with Tukey's honest significant difference post hoc test. Size bars indicate 1 cm in **C** and **B** (left panel) and 50 µm **B** (right panel).

Previous studies have shown that the VPC is regulated by both internal factors at the SAM (Fouracre and Scott Poethig, 2019) and peripheral organ-derived signals (Yang et al., 2011, 2013; Yu et al., 2013). During the VPC *AHL15* remains expressed in the peripheral organs, but its expression is reduced in the SAM and newly formed organs, suggesting that its expression in these tissues is most relevant for its function. To confirm this, we expressed *AHL15* under the control of the *FLOWERING LOCUS D* (*pFD*) and *AINTEGUMENTA* (*pANT*) promoters, which are predominantly active in the SAM and in young leaf primordia (Yamaguchi et al., 2016; Fouracre and Scott Poethig, 2019). Expression of *AHL15* under these promotors significantly delayed the VPC, as indicated by the reduced length/width ratio of the leaves and increased number of leaves lacking abaxial trichomes (Fig. 2C-G), and also delayed the flowering time (Supplementary Fig. 3A and B) under both SD and LD conditions. Combining both *pFD:AHL15* and *pANT:AHL15* constructs in one plant line led to a further delay of the VPC (Fig. 2C-G) and flowering time (Supplementary Fig. 3A and B). This additive effect can be explained by the slightly different but overlapping activities of the selected promoters (Yamaguchi et al., 2016; Fouracre and Scott Poethig, 2019). These results indicate that *AHL15*-induced delay in the VPC and flowering time is achieved through its expression in the SAM and leaf primordia, and not by its expression in older leaves (Fig. 2B).

AHL proteins repress *SPL* gene expression in a miR156/miR157-independent manner

In Arabidopsis, the VPC is mediated by a gradual decrease in *miR156*/*miR157* expression, which increases the expression of the *SPL* miR156/miR157 target genes. *SPL* genes in turn promote the adult developmental program in the SAM, resulting in the production of adult instead of juvenile leaves and eventually in the initiation of flowering (Wang et al., 2009; Wu et al., 2009). One possible mode of action of AHL proteins might be that they suppress *SPL* expression by enhancing the *miR156*/*miR157* pathway. A comparison of the expression of several *SPL* genes (*SPL2*, *SPL9*, *SPL10*, *SPL11*, *SPL13*, and *SPL15*) known to promote the VPC (Xu et al., 2016) by qPCR showed that the transcript levels of *SPL2*, *SPL9*, *SPL13*, and *SPL15* were significantly upregulated in shoots of 3-week-old *ahl15/+ pAHL15:AHL15-ΔG* mutant compared to wild-type seedlings (Fig. 3A), and that only *SPL2* expression was higher in 2-week-old mutant seedling (Fig. 3A). This is in line with the timing of the VPC and the dynamics of *AHL* gene expression (Fig 2A, B), and indicates that AHL proteins repress the expression of *SPL2*, *SPL9*, *SPL13*, and *SPL15* during this period.

The fact that not all six *SPL* genes tested were simultaneously upregulated in the *ahl15/+ pAHL15:AHL15-ΔG* mutant background suggested that AHLs repress *SPL* expression independent of the *miR156*/*miR157* pathway. Indeed, *pmiR156A:GUS*, *pmiR156B:GUS*, and *pmiR156D:GUS* reporters (Yu et al., 2015) did not show a major change in expression upon AHL15 activation by DEX treatment in the *p35S:AHL15-GR* background (Supplementary. Fig, 4A). Also qPCR analysis showed that miR156/157 levels were not significantly different in 2- or 3-week-old wild-type or *ahl15/+ pAHL15:AHL15-ΔG* seedlings grown under juvenile phase prolonging SD conditions (Fig. 3B). In addition, when testing the expression of six miR156/miR157-insensitive *pSPL:rSPL-GUS* reporters (e.g., *rSPL2*, *rSPL9*, *rSPL10*, *rSPL11*, *rSPL13*, *rSPL15*) (Xu et al., 2016) in the *p35S:AHL15-GR* background, the expression of *rSPL2*, *rSPL9*, *rSPL13*, and *rSPL15* appeared to be down-regulated by DEX treatment (Fig. 3C). Together these results indicate that AHL proteins suppress the

expression of specific *SPL* genes involved in the VPC in a miR156/miR157-independent manner.

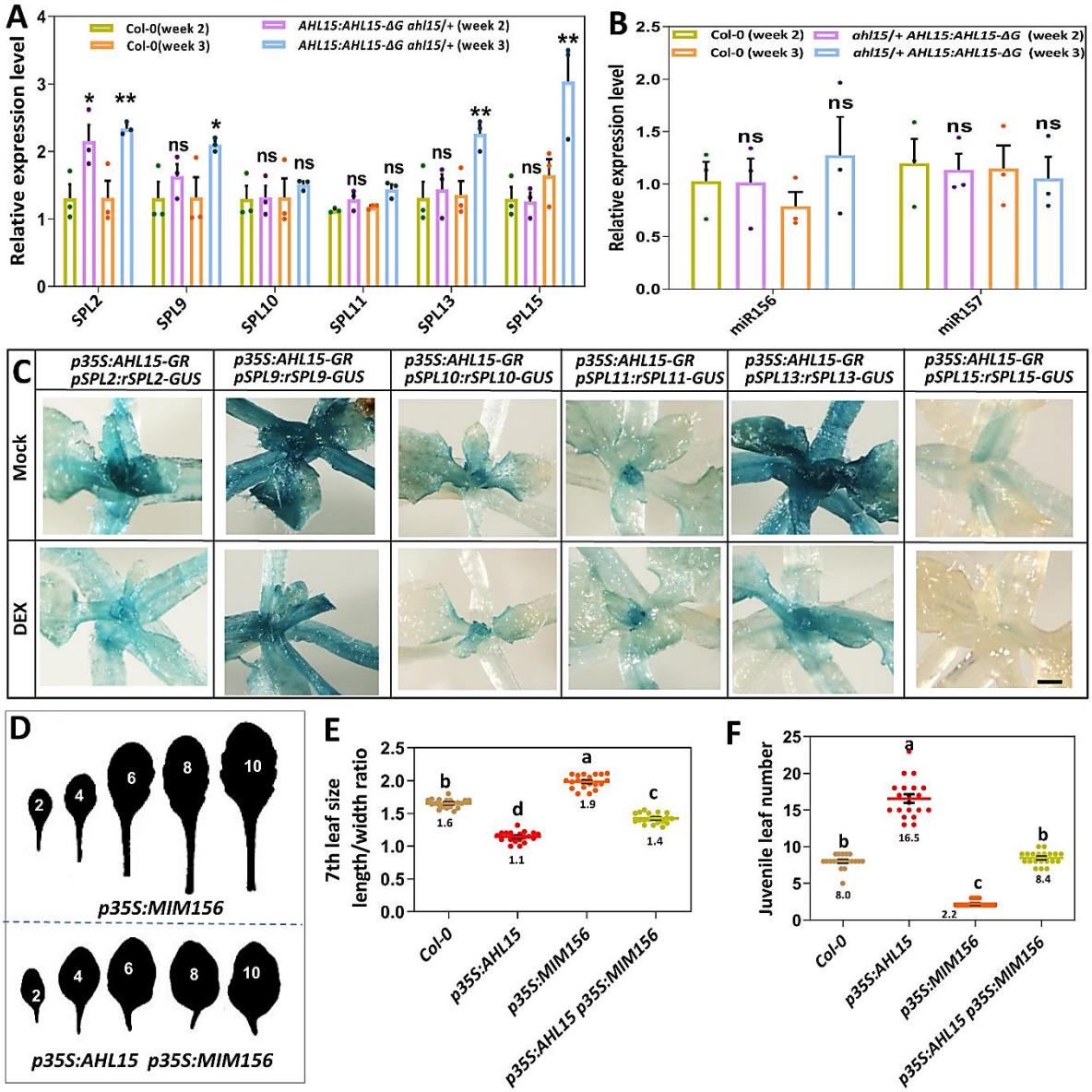

Figure 3. AHL15 represses *SPL* gene expression in a miRNA-independent manner. (**A, B**) The relative expression level of *SPL2, SPL9, SPL10, SPL11, SPL13,* and *SPL15* (**A**) or *miR156* and *miR157* (**B**) in the shoot apex and young leaves of 2- and 3-week-old wild-type and *ahl15/+ pAHL15:AHL15-ΔG* plants grown under SD conditions. (Dots indicate the values of three biological replicates per plant line, the bar indicates the mean and error bars indicate the s.e.m. Asterisks indicate significant differences from wild type (Col-0, *P < 0.05, **P < 0.01, ns = not significant or P ≥ 0.05), as determined by a two-sided Student's *t*-test. In **B,** values were normalized to the value in wild-type in week 2. (**C**) Histochemical staining for GUS activity in 10-day-old shoot apex and young leaves of water (mock) or 20 µM DEX (+DEX) treated (for 2 days) *p35S:AHL15-GR* plants expressing the miR156 resistant *pSPL9:rSPL9-GR, pSPL2:rSPL2-GUS, pSPL9:rSPL9-GUS, pSPL10:rSPL10-GUS, pSPL11:rSPL11-GUS, pSPL13:rSPL13-GUS* or *pSPL15:rSPL15-GUS* reporter grown under LD conditions. Size bars indicate 1 mm. (**D**) Shape of the successive rosette leaves of 7-week-old *p35S:MIM156* or *p35S:AHL15 p35S:MIM156* plants grown under SD conditions. (**E, F**) The length:width ratio of the 7 th leaf (**E**) or The juvenile leaf number (leaves without abaxial trichomes) (**F**) of 7-week-old wild-type, *p35S:MIM156, p35S:AHL15* or *p35S:AHL15 p35S:MIM156* plants grown under SD conditions. Colored dots indicate length:width ratio (**E**) or the number of leaves without abaxial trichomes (**F**) per plant (n = 15 biologically independent plants) per line, horizontal line and the number below this line indicate the mean and error bars indicate the s.e.m. Different letters indicate statistically significant differences (P < 0.01) as determined by a one-way ANOVA with Tukey's honest significant difference post hoc test.

In plants overexpressing a target mimic of *miR156* (*p35S:MIM156*) *SPL* expression is enhanced (Franco-Zorrilla et al., 2007), resulting in the accelerated appearance of adult leaves (Fig. 3D-F) and early flowering (Supplementary Fig. 5A and B). *AHL15* overexpression negated the precocious appearance of adult vegetative traits (Fig. 3D-F) and early flowering (Supplementary Fig. 5A and B) of *p35S:MIM156* plants, bringing these traits back to or close to wild-type levels. In the reverse experiment where the *p35S:AHL15* construct was introduced into the *p35S:miR156* background having low SPL levels, we observed a remarkably additive effect on the vegetative phase transition and flowering time (Supplementary Fig. 6A and B). The results of both experiments support our model that AHL15 and family members suppresses *SPL* gene expression in a miR156/miR157-independent manner.

SPLs promote the vegetative phase change in part by repressing *AHL15* expression

During the VPC in 2-week-old Arabidopsis seedlings, increasing SPL levels (Wang et al., 2009) coincided with downregulation of *AHL15*, *AHL19* and *AHL20* (Fig 1A, B). This led us to hypothesize that the SPL transcription factors are mediating down-regulation of *AHL* gene expression. Based on this hypothesis, we expected *AHL* expression to be downregulated in Arabidopsis lines with elevated SPL levels (e.g. *p35S:MIM156* or *pSPL9:rSPL9*) and to be upregulated in Arabidopsis lines with reduced SPL levels (e.g. *p35S:miR156* or *spl* loss-of-function mutants). qPCR analysis indeed showed that the expression of *AHL15* and *AHL20* was significantly reduced in one-week-old *p35S:MIM156* seedlings compared to wild-type seedlings (Fig. 4A). In line with this result, expression of the *pAHL15*:*GUS* reporter was reduced in one-week-old seedlings of the *p35S:MIM156* line compared to wild-type seedlings (Fig. 4B), or in DEX-treated *pSPL9:rSPL9-GR* seedlings compared to mock-treated seedlings (Fig. 4C). In contrast, expression of the *pAHL15:GUS* reporter seemed rather enhanced in two-week-old *p35S:miR156* seedlings compared to wild-type seedlings (Fig. 4D).

Based on our hypothesis, the delayed VPC and flowering phenotypes of plants with reduced SPL levels (e.g. the *spl9 spl15* double loss-of-function mutant and *p35S:miR156*; Wu et al., 2009) would be dependent on the elevated expression of functional *AHL* genes. The *ahl15* loss-of-function mutation in the *ahl15 spl9 spl15* triple mutant indeed partially rescued the delayed VPC phenotypes of the *spl9 spl15* double mutant. The length/width ratio of *ahl15 spl9 spl15* leaves was almost restored to wild-type levels, and the VPC of *ahl15 spl9 spl15* plants was significantly accelerated compared to that of *spl9 spl15* double mutant plants, both in SD and in LD conditions (Fig. 4E-G). Introduction of the *p35S:miR156* line in the *ahl15* loss-of-function background also rescued the delay in VPC induced by *miR156* overexpression back to wild type levels, even in heterozygous *ahl15/+ 35S:miR156* plants. Since we could not exclude that the T-DNA insertion in the *ahl15* mutant silenced the *p35S:miR156* construct (Daxinger et al., 2008), we placed the *miR156* gene under control of the *FD* promotor (*pFD:miR156*) and introduced the resulting construct into the *ahl15* mutant and wild-type background. The delay in VPC caused by *FD* promotor-controlled *miR156* expression in the wild-type background was significantly reduced in the *ahl15* background both under SD and LD conditions (Fig. 4F-H). These results indicate that a functional *AHL15* gene is required for the delay in VPC in plants with reduced SPL levels. Together the data

confirms our hypothesis that the repression of *AHL*s in the SAM and flower primordia is mediated by SPLs, either indirectly or directly by binding of these transcription factors to the *AHL* regulatory regions.

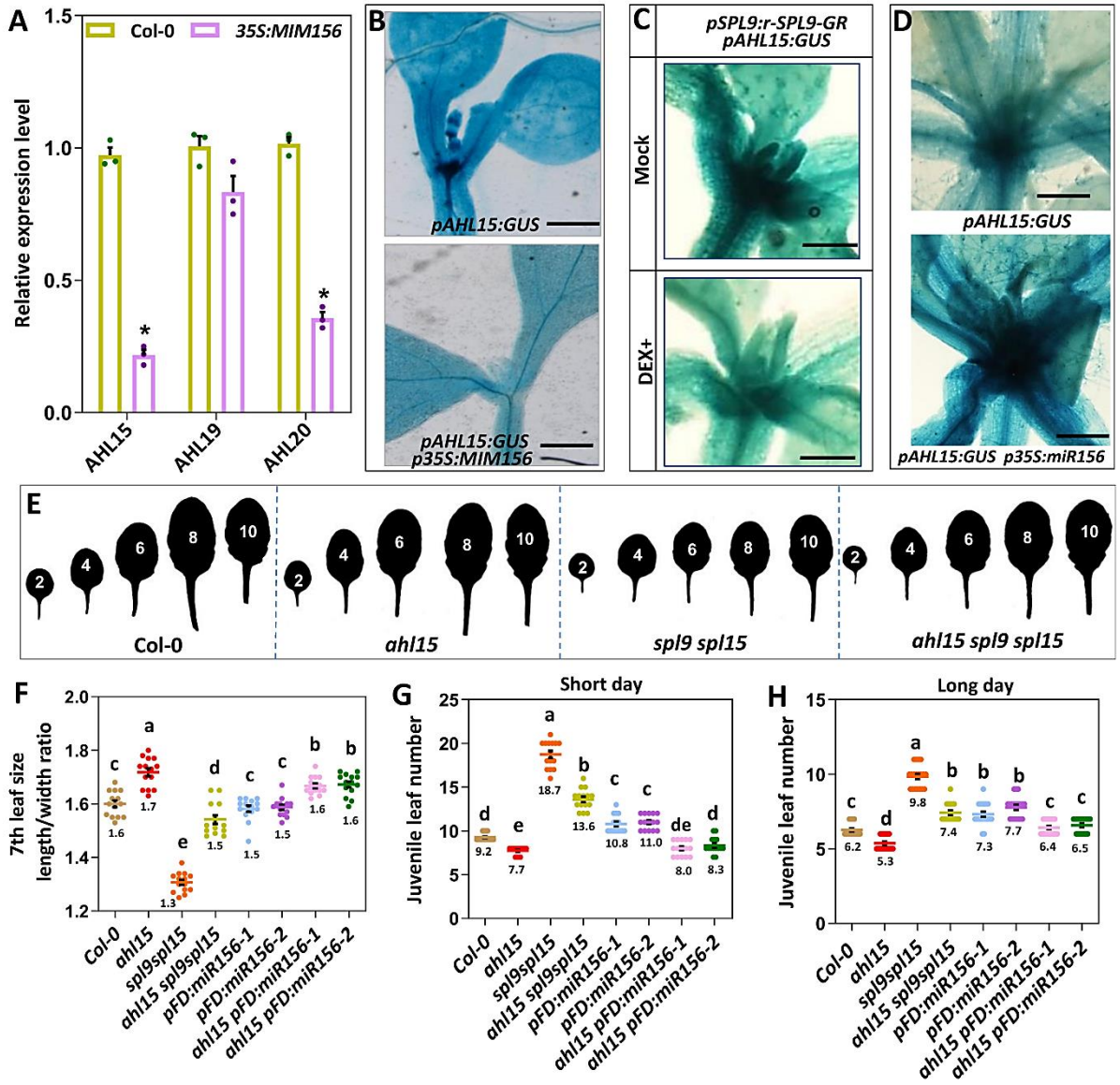

Figure 4. SPLs promote the VPC by repressing *AHL15* expression. (**A**) Relative expression level of *AHL15*, *AHL19* and *AHL20* in the shoot apex and young leaves of 2-week-old wild-type or *p35S:MIM156* seedlings grown under LD conditions. Dots indicate the values of three biological replicates per plant line, the bar indicates the mean, and error bars the s.e.m Asterisks indicate a significant difference ($p < 0.01$), as determined by a two-sided Student's *t*-test. (**B-D**) Histochemical staining for GUS activity in 8-day-old *pAHL15:GUS* (top) or *p35S:MIM156 pAHL15:GUS* (bottom) seedlings (**B**), 10-day-old water (mock) or 20 µM DEX (+DEX) treated *pAHL15:GUS p35S:SPL9-GR* seedlings (**C**), or 15-day-old wild-type (top) or *p35S:miR156* (bottom) seedlings (**D**) grown under LD conditions. (**E**) Shape of the successive rosette leaves of 7-week-old wild-type, *ahl15*, *spl9 spl15* and *ahl15 spl9 spl15* plants grown under SD conditions. Size bars indicate 1 mm. (**F**) The length:width ratio of the 7th leaf of 7-week-old wild-type, *ahl15*, *spl9 spl15* and *ahl15 spl9 spl15* plants grown under SD conditions. (**G**, **H**) The juvenile leaf number (leaves without abaxial trichomes) in wild-type, *ahl15*, *spl9 spl15* and *ahl15 spl9 spl15* plants grown under SD (**G**) or LD (**H**) conditions. Colored dots in **F**-**H** indicate length:width ratio of the 7th leaf (**F**) or the number of leaves without abaxial trichomes (**G**,**H**) per plant (n = 15 biologically independent plants) per line, horizontal line and the number below this line indicate the mean and error bars indicate the s.e.m. Different letters indicate statistically significant differences ($P < 0.01$) as determined by one-way ANOVA with Tukey's honest significant difference post hoc test.

In contrast to the VPC results presented above, the *ahl15* loss-of-function mutation had no or only a marginal effect on the delayed flowering of the *spl9 spl15* or *pFD:miR156* plants (Supplementary Fig. 7). It should be noted, however, that *ahl15* single or *ahl15 ahl19* double mutant plants show a wild-type flowering time, and that only *ahl15 ahl19 p35S:amiRAHL20* triple mutant or the *ahl15/+ pAHL15:AHL15-ΔG* dominant negative mutant plants flower significantly earlier compared to wild type (Supplementary Fig. 1, Karami et al., 2020, Chapter 2). This indicates that not *AHL15* but other redundantly acting *ALH* genes, such as *AHL20* (Fig 4A), are the prime targets for repression by SPLs in the promotion of flowering.

SPLs promote reproductive identity of axillary meristems by repressing *AHL15* expression

Our previous results have shown that *AHL15* does play a central role in axillary meristem (AM) maturation, i.e. the switch from vegetative to reproductive identity (Karami et al., 2020a, chapter 2). Overexpression of *AHL15* (*p35S:AHL15* or *pMYB:AHL15*) repressed AM maturation, leading to their prolonged vegetative activity and resulting in the formation of aerial rosettes from inflorescence nodes. Such aerial rosettes are not formed on wild-type Arabidopsis (Col-0) plants grown under LD conditions (Supplementary Fig. 8A and B), but can be induced by growing plants under SD conditions or by mutating the *SOC1* and *FUL* genes encoding transcription factors that suppress *AHL15* expression. We have demonstrated that the aerial rosette phenotype is dependent on a functional *AHL15* gene (Karami et al., 2020a, chapter 2). Interestingly, the AMs in the axils of cauline leaves of the *spl9 spl15* mutant or *p35S:miR156* (or *pFD:miR156*) overexpression plants also produced aerial rosettes (Supplementary Fig. 8A and B), revealing a yet unidentified role for SPLs in promoting the vegetative to reproductive transition of AMs. Introduction of *spl9 spl15* or *pFD:miR156* in the *ahl15* loss-of-function mutant background strongly reduced the aerial rosette formation phenotype of both mutant lines (Fig. 5A and B), indicating that *AHL15* function is important for the frequent aerial rosette formation in *spl9 spl15* and *pFD:miR156* plants, which is completely absent in wild-type and *ahl15* plants when grown under the same LD conditions (Karami et al., 2020b, Chapter 2). In line with the role of the SPL transcription factors as *AHL* repressors, *AHL15* expression was significantly increased in *spl9 spl15* and *p35S:miR156* AMs compared to wild-type AMs (Fig. 5C and D). Based on these results, we concluded that *AHL15* acts downstream of the *SPL* genes, and that repression of *AHL15* by SPLs in wild-type plants promotes the reproductive identity of AMs, whereas under conditions where SPL activity is reduced (e.g. in *p35S:miR156* or *spl9 spl15* plants) elevated *AHL15* expression enhances the vegetative activity of AMs, resulting in the formation of aerial rosettes.

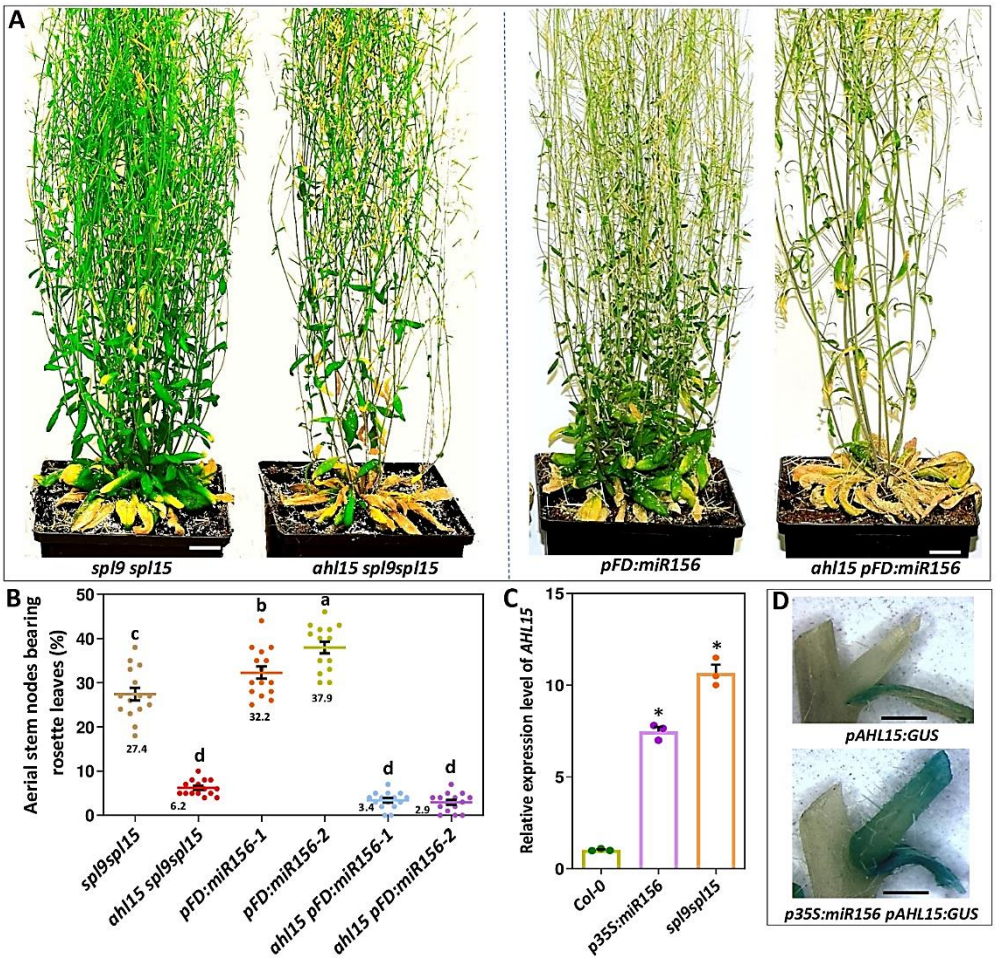

Figure 5. SPLs promote reproductive identity of axillary meristems by repressing *AHL15*. (**A**) Phenotype of 3-month-old *spl9 spl15*, *ahl15 spl9 spl15*, *pFD:miR156* or *pFD:miR156 ahl15* plants grown under LD conditions. (**B**) Percentage of the aerial stem nodes bearing rosette leaves in 3-month-old *spl9 spl15*, *ahl15 spl9 spl15*, *pFD:miR156*, *ahl15 pFD:miR156* plants grown under LD conditions. Please note that wild-type and *ahl15* stem nodes do not form rosette leaves under these conditions. Colored dots indicate the percentage per plant (n = 15 biologically independent plants) per line, horizontal line indicates the mean and error bars indicate the s.e.m. Different letters indicate statistically significant differences ($P < 0.01$) as determined by one-way ANOVA with Tukey's honest significant difference post hoc test. (**C**) The relative expression level of *AHL15* in aerial stem nodes of wild-type, *p35S:miR156* or *spl9 spl15* plants 2 weeks after flowering. Dots indicate the values of three biological replicates per plant line, horizontal line and the number below this line indicate the mean and error bars indicate the s.e.m . The asterisk indicates a significant difference ($p < 0.01$), as determined by a two-sided Student's *t*-test. (**C**) Histochemical staining for GUS activity in inflorescence nodes of six-week-old wild-type and *p35S:miR156* plants grown under LD conditions. Size bars indicate 1 cm in A and 50 mm in **D**.

Discussion

Plants during their lifetime progress through distinct consecutive developmental phases, starting with embryogenesis and followed by respectively the juvenile-, adult- and reproductive phase. What drives and regulates the transition from one developmental phase to another is a longstanding fundamental question in plant developmental biology. In Arabidopsis and several other plants, the transition from the juvenile to adult phase (VPC) and from the adult to reproductive phase (flowering) has been shown to be driven by the ageing pathway. In this pathway, the SPL transcription factors promote phase transitions, and miR156 and miR157 repress these transitions by targeting the *SPL* transcripts (Poethig, 2013; Teotia and Tang, 2015). Previously we have shown that Arabidopsis *AHL15* and its paralogs enhance plant longevity by delaying maturation of AMs (Karami et al., 2020a). Here we show that AHL proteins interfere with the ageing pathway by repressing *SPL* gene expression in a miRNA-independent manner, and that in turn *AHL15* expression is repressed through feedback regulation by the SPLs. In addition, we show that this reciprocal negative feedback loop between *AHL* and *SPL* genes not only regulates the VPC and flowering but also AM maturation and thus controls plant longevity and -life history.

AHL genes delay the VPC

Although the adult vegetative to reproductive phase change is agronomically most important, the VPC also has a strong impact on plant fitness and biomass, not in the least because it determines the balance between vegetative growth and reproductive development (Demura and Ye, 2010). Although the timing of the VPC can be influenced by environmental factors such as photoperiod, light intensity and temperature, this developmental switch is mainly regulated by endogenous genetic components (Poethig, 2013). Studies in Arabidopsis have revealed that the gradual decline in the expression of miR156/miR157 increases the abundance of the SPL transcription factors, which promote the VPC (Poethig, 2013; Teotia and Tang, 2015). The change in leaf morphology during the VPC is accompanied by a reduced expression of *AHL15* and close homologs in the SAM and young leaves, which is in line with the repression of *AHL* genes by SPLs.

Recently, it has been reported that these internal factors at the SAM maintain the juvenile phase during early shoot development, but that the SAM plays a relatively minor role in the regulation of leaf identity at later stages of the VPC (Fouracre and Poethig, 2019). The fact that *ahl* loss-of-function plants (*ahl15/+ pAHL15:AHL15-ΔG*) immediately form adult leaves, and that *p35S:AHlL15* seedlings form multiple juvenile leaves confirm that AHLs belong to the internal factors in the SAM that maintain the juvenile phase in early shoot development. However, when we overexpressed *AHL15* specifically in young leaf primordia this also delayed the VPC, which is in line with the observation that the VPC is regulated by peripheral organ-derived signaling (Yang et al., 2011, 2013; Yu et al., 2013) and that AHL15 can control the VPC both internally at the SAM and through leaf-derived signalling (Poethig, 2013; Teotia and Tang, 2015).

Our analysis showed that AHL15 represses the expression of *SPL* genes in a miR156/miR157-independent manner. Previous studies have shown that the abundance of miR156/miR157 is highly declined (about 90%) at the shoot apex of Arabidopsis seedlings in

a two weeks period, whereas the level of the most SPLs remained constant or even slightly increased during this period (Xu et al., 2016). We showed that the level of *SPL2, SPL9, SPL13,* and *SPL15* are significantly higher at the shoot apex of *ahl15* loss-of-function compared to wild-type plants, whereas the level of miR156/miR157 did not change between wild-type or *ahl15* loss-of-function mutant plants. This clearly indicates that the maintained repression of SPL expression is mediated by AHL15 independent of miR156/157. How AHL15 represses *SPL* genes remains unknown. AHL15 might directly bind to the *SPL* loci. However, preliminary yeast one-hybrid assays did not provide an indication for direct binding of AHL15 to the promoter regions of *SPL* (data not shown). Recently, we have shown that AHL15 overexpression suppresses the biosynthesis of the plant hormone gibberellic acid (GA) (Karami et al., 2020a). Since DELLA proteins, the degradation targets of GA signalling, have been shown to repress *SPL* expression (Yu et al., 2012), AHL15 may repress *SPLs* by reducing GA biosynthesis and thus stabilizing the DELLA proteins (Supplementary Figure 9).

Previously, it has been shown that SPLs promote trichome development on the abaxial side of leaves partially by repressing the AP2-like transcription factors TOE1 and TOE2 (Wu et al., 2009). How SPLs promote the other adult leaf traits such as leaf elongation and leaf serration was not known until now. In this study, we showed that the promotion of adult traits, including leaf elongation and trichomes on the abaxial side of leaves, by SPLs is contributed by the repression of *AHL* genes, as the delay in the juvenile-to-adult transition by miR156 requires AHL15. Thus, we suggest a reciprocal negative feedback loop between SPL and AHL (Fig. 6), and although we do not know whether AHLs and SPLs regulate each other's expression directly or indirectly, our findings provide a new advance in the understanding of the regulation of VPC.

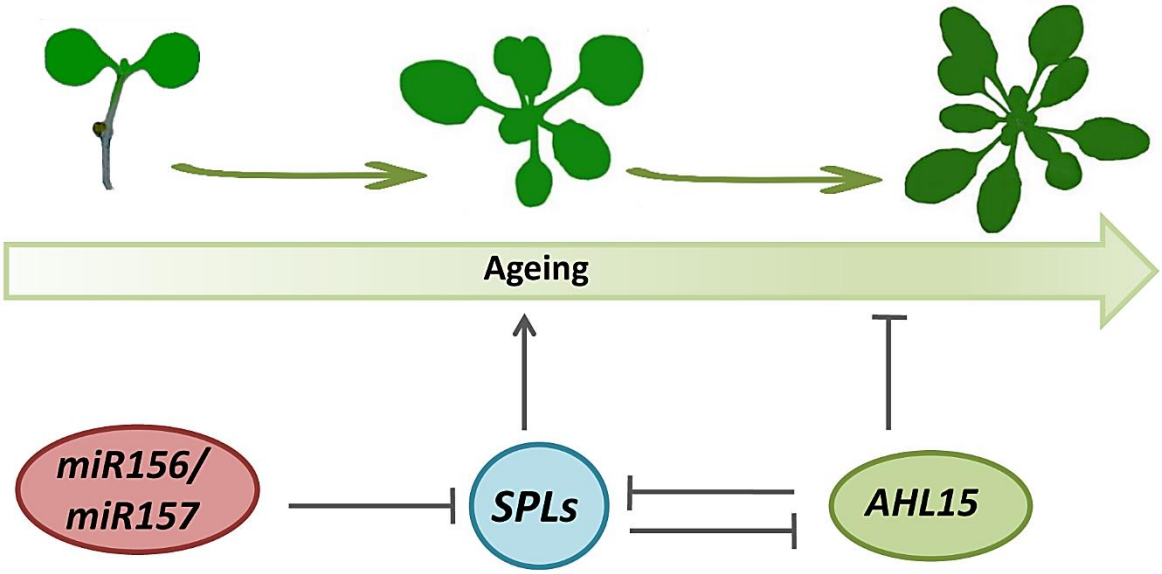

Figure.6 Proposed model for the role of AHL15 and family members in the regulation of plant ageing. Following their germination, high expression of *miR156* and *AHL15* and family members keeps seedlings in the juvenile vegetative phase by suppressing the expression of the ageing promoting SPL transcription factors. When seedlings get older, gradual down-regulation of *miR156* elevates SPL abundance, which in turn promotes the juvenile to adult phase transition (VPC) by stimulating plant ageing in part by downregulating AHLs. Negative feed-back between AHLs and SPLs moderates plant ageing. Arrows indicate activation, and blunted lines indicate repression.

AHL genes delay flowering time

The switch from vegetative growth to flowering is a major developmental transition in plants. Two decades of genetic and physiological studies have led to the identification a number of pathways controlling flowering, including the photoperiod pathway, the vernalization pathway, the GA pathway, and the age pathway (Supplementary Fig. 9) (Turnbull, 2011; Matsoukas et al., 2012; Song et al., 2013). In this work, we have revealed that *AHL15* and close homologs are involved in the control of flowering time. We showed that overexpression *AHL15* causes extremely late flowering. The late-flowering phenotypes were also observed in overexpression of *AHL18*, *AHL22*, *AHL27*, and *AHL29* (Street et al., 2008; Xiao et al., 2009; Yun et al., 2012; Xu et al., 2013). However, these overexpression phenotypes did not reflect the normal function of these genes since no effect or relatively small effects were on flowering time observed in single loss-of-function mutants of these genes. Thus, the role of these AHLs and other members of the AHL family in the control flowering time has remained elusive until now. Our results showed, however, that loss-of-function of *AHL15* and close homologs does promote flowering time, indicating an important role for these genes in regulating the vegetative to reproductive phase change.

An increase in SPL proteins levels promotes the flowering time by activating the transcription of *SOC1* and several other floral-promoting genes at the SAM (Wang et al., 2009; Yu et al., 2012). Consistent with delay in the flowering time by targeted expression of *AHL15* in the SAM, we postulate that AHL15-suppressed flowering time at the SAM is contributed by the repression of SPLs at the SAM (Supplementary Fig. 9). FLOWERING LOCUS T (FT) that is produced in leaves and is transported as a florigen signal from the leaves to the SAM (Supplementary Fig. 9), triggers the flowering by activating the

transcription of several flowering-promoting genes (Abe et al., 2005; Corbesier et al., 2007). It has been shown that overexpression of *AHL22* delays flowering time in Arabidopsis by repressing *FT* in leaves (Yun et al., 2012). Consistent with delay in the flowering time by targeted expression of AHL15 in leaves, the AHL15-suppressed flowering time through leaves is might be also contributed to repression of *FT* (Supplementary Fig. 9). Interestingly, the MADS box transcription factor *FLOWERING LOCUS C* (*FLC*) which acts as a potent repressor of flowering time could also suppress the *FT* and *SPL* genes (Deng et al., 2011; Matsoukas et al., 2012). Therefore, a molecular link between AHL and FLC in the repression of the *SPLs* and *FT* is predicted (Supplementary Fig. 9). GA is known to accelerate flowering by degradation of DELLA proteins (Yu et al., 2012). We showed that AHL15 reduces transcription of genes that encode the rate-limiting enzyme in the synthesis of GA biosynthesis (Karami et al., 2020a, chapter 2), therefore, regulation of GA biosynthesis by AHL15 is another possibility of suppressing the flowering time by AHL15 (Supplementary Fig. 9). Taken together, we suggest that AHL proteins act as flowering repressors by down-regulating many genes in different pathways controlling flowering (Supplementary Fig. 9). More detailed investigation of the relationship between AHL proteins and the different flowering pathways is required to elucidate which interactions are truly relevant.

SPLs promote reproductive identity of axillary meristems by repressing *AHL15* expression

In Arabidopsis, following the floral transition the main inflorescence meristem (IM) is converted into a floral meristem after producing two to three cauline leaves. The AMs formed in axils of these cauline leaves directly become IM that produce a few lateral cauline leaves before being converted to a floral meristem (Supplementary Fig. 8). In contrast, the AMs in the axils of cauline leaves of *p35S:miR156* or *spl9 spl15* and *p35S:AHL15* plants start in the vegetative phase and are converted to IM only after producing several rosette leaves (Supplementary Fig. 8). This heterochronic shift in the development of AMs leading to the formation of aerial rosettes in *p35S:miR156* or *spl9 spl15* plants is associated with the up-regulation of *AHL15*. Moreover, we have previously shown that the development of aerial rosettes from AMs in axils of cauline leaves of the *soc1 ful* double mutant (Melzer et al., 2008) is associated with and dependent on upregulation of *AHL15* expression (Karami et al., 2020a, chapter 2). Consistent with the finding that SPL proteins promote *SOC1* and *FUL* expression (Wang et al., 2009) and our own results, we postulate that SPLs prevent the aerial rosettes formation by upregulating *SOC1* and *FUL*, which subsequently leads to repression of *AHL15* expression (Supplementary Fig. 9).

A consequence of maintaining AMs in the vegetative phase, following the floral transition in *p35S:miR156, spl9 spl15, p35S:AHL15* or *soc1 ful* plants, is that this increases the life span of the plant and extends the period during which a plant is able to produce fruits and seeds. This heterochronic growth and development of AMs has been reported in Arabidopsis ecotypes such as Sy-0 (Poduska et al., 2003). A dominant allele of *FLC* has been reported as a key factor that underlies the aerial-rosette phenotype and increases the life span in Sy-0 (Poduska et al., 2003). Detailed studies on the genetic link between *FLC* and *AHL*s should provide more insight into aerial-rosette phenotype in Arabidopsis ecotypes such as Sy-0.

AHL gene families have been identified in many plant species (Zhao et al., 2014; Karami et al., 2020b). Along with the results obtained in tobacco, we suggest that the role of *AHL* genes in controlling developmental switches and through that plant longevity and life history strategy is likely to be conserved to in many other plants.

Methods

Plant material and growth conditions and phenotype analysis

All Arabidopsis mutant- and transgenic lines used in this study are in the Columbia (Col-0) background. The *ahl15*, *ahl19*, *p35S:AHL15*, *p35S:AHL15-GR*, *pAHL15:GUS*, *pAHL15:AHL15*, *pAHL15:AHL15-ΔG*, *p35S:amiRAHL20 and ahl15/+ pAHL15:AHL15-ΔG* plant lines has been described previously (Karami et al., 2020a,b). The *spl9 spl15*, *p35S:miR156*, *p35S:MIM156*, *pSPL9:rSPL9-GR*, *pSPL2:rSPL2-GUS*, *pSPL9:rSPL9-GUS*, *pSPL10:rSPL10-GUS*, *pSPL11:rSPL11-GUS*, *pSPL13:rSPL13-GUS* and *pSPL15:rSPL15-GUS* plant lines were obtained from the Nottingham Arabidopsis Stock Centre (NASC). The reporter lines *pmiR156A:GUS, pmiR156B:GUS and pmiR156C:GUS* has been described previously (Yu et al., 2015). Plant lines and F1, F2 or F3 plants from crosses were PCR genotyped using primers described in the Supplementary Table 1. Seeds were directly sown on soil in pots and grown at 21°C, 65% relative humidity, and 16 hours (long day: LD) or 8 hours (short day: SD) photoperiod. One exception: SD was10 hours for the top panel of supplementary Fig. 1A. To score aerial rosette leaves production by AMs, wild-type, mutant or transgenic plants were transferred to larger pots about 2 weeks after flowering. *Nicotiana tabacum* cv SR1 Petit Havana (tobacco) wild-type or *p35S:AHL15-GR* plants (Karami et al., 2020a, chapter 2) were grown in medium-sized pots at 25 °C, 70% relative humidity, and a 16 hours photoperiod. For dexamethasone (DEX, Sigma-Aldrich) treatment, Arabidopsis and tobacco plants were sprayed with 20 and 30 µM DEX, respectively. Leaf size was measured directly using a ruler.

The number of juvenile leaves (without abaxial trichomes) was scored once they appeared, and detected by eye. For imaging of leaf shape, fully expanded leaves were removed, attached to cardboard with double-sided tape, flattened and photographed with a Nikon D5300 camera. Leaf images were optimized and changed into black and white images and assembled using Adobe Illustrator cc2017. Potted plants were photographed with a Nikon D5300 camera. All measurements were statistically analyzed and plotted into graphs in GraphPad Prism 8.

Plasmid construction and transgenic Arabidopsis lines

To generate the constructs *pFD:AHL15* and *pANT:AHL15*, 3 kb regions upstream of the ATG initiation codon of the *FD* (AT4G35900) and *ANT* (AT4G37750) genes were amplified from ecotype Columbia (Col-0) genomic DNA using the forward (F) and reverse (R) PCR primers indicated in Supplementary Table S1. The resulting fragments were first inserted into pDONR207 by BP reaction, and subsequently cloned upstream of the genomic fragment containing the *AHL15* transcribed region in destination vector *pGW-AHL15* (Karami et al., 2020b) by LR reaction. To generate the *pFD:miR156*, first *pGW-miR156* was generated by replacing the *AHL15* fragment in *pGW-AHL15* for a *Kpn*I and *Spe*I fragment containing the *miR156* transcribed region. The *FD* promoter fragment was subsequently recombined from pDONR207 into the resulting *pGW-miR156* construct by LR reaction. All binary vectors were introduced into *Agrobacterium tumefaciens* strain AGL1 by electroporation (den Dulk-Ras and Hooykaas, 1995) and Arabidopsis Col-0 and *ahl15* plants were transformed using

the floral dip method (Clough and Bent, 1998). The resulting plant lines and F1, F2 or F3 plants from crosses were PCR genotyped using primers described in the Supplementary Table 1.

Histochemical staining and microscopy

Histochemical staining of plant tissues for β-glucuronidase (GUS) activity was performed as described previously (Anandalakshmi et al., 1998). Tissues were stained for 4 hours at 37°C, followed by chlorophyll extraction and rehydration by incubation for 10 minutes in a graded ethanol series (75, 50, and 25 %). GUS stained tissues were observed and photographed using a LEICA MZ12 microscope (Switzerland) equipped with a LEICA DC500 camera.

Quantitative real-time PCR (qPCR) analysis

RNA was isolated from rosette base nodes, and the basal part of inflorescence stems (about 0.5 cm above rosette base) using the RNEasy© kit (Qiagen). First-strand cDNA was synthesized using the RevertAid RT Reverse Transcription kit (Thermo Fischer Scientific). Quantitative PCR was performed on three biological replicates along with three technical replicates using the SYBR-green dye premixed master-mix (Thermo Fischer Scientific) in a C1000 Touch© thermal cycler (BIO-RAD). CT values were obtained using Bio-Rad CFX manager 3.1. The relative expression level of genes was calculated according to the $2^{-\Delta\Delta Ct}$ method (Livak and Schmittgen, 2001).

The miRNAs abundance was quantified using 1µg of RNA in a reverse transcription reaction by using SnoR101 reverse primer and a miRNA-specific RT primer. Expression was normalized using the *β-TUBULIN-6* gene, analyzed and plotted into graphs in GraphPad Prism 8. Three biological replicates were performed, with three technical replicates each. The primers used are described in Supplementary Table 1.

References

Abe, M., Kobayashi, Y., Yamamoto, S., Daimon, Y., Yamaguchi, A., Ikeda, Y., Ichinoki, H., Notaguchi, M., Goto, K., and Araki, T. (2005). FD, a bZIP protein mediating signals from the floral pathway integrator FT at the shoot apex. Science (80-.). **309**: 1052–6.

Anandalakshmi, R., Pruss, G.J., Ge, X., Marathe, R., Mallory, A.C., Smith, T.H., and Vance, V.B. (1998). A viral suppressor of gene silencing in plants. Proc. Natl. Acad. Sci. U. S. A. **22**: 13079--13084.

Aukerman, M.J. and Sakai, H. (2003). Regulation of flowering time and foral organ identity by a microRNA and its APETALA2 -like target genes. Genetics **15**: 2730–2741.

Clough, S.J. and Bent, F. (1998). Floral dip: a simplified method for Agrobacterium-mediated transformation of *Arabidopsis thaliana*. Plant J. **16**: 735–743.

Corbesier, L., Vincent, C., Jang, S., Fornara, F., Fan, Q., Searle, I., Giakountis, A., Farrona, S., Gissot, L., Turnbull, C., and Coupland, G. (2007). FT protein movement contributes to long-distance signaling in floral induction of Arabidopsis. Science (80-.). **18**: 1030–3.

Daxinger, L., Hunter, B., Sheikh, M., Jauvion, V., Gasciolli, V., Vaucheret, H., Matzke, M., and Furner, I. (2008). Unexpected silencing effects from T-DNA tags in Arabidopsis. Trends Plant Sci.: 13, 4–6.

Demura, T. and Ye, Z.-H. (2010). Regulation of plant biomass production. Curr. Opin. Plant Biol. **13**: 299–304.

Deng, W., Ying, H., Helliwell, C.A., Taylor, J.M., Peacock, W.J., and Dennis, E.S. (2011). FLOWERING LOCUS C (FLC) regulates development pathways throughout the life cycle of Arabidopsis. Proc. Natl. Acad. Sci. **2011**: 1–6.

den Dulk-Ras, A. and Hooykaas, P.J. (1995). Electroporation of Agrobacterium tumefaciens. Methods Mol. Biol. **55**: 63–72.

Fouracre, J.P. and Scott Poethig, R. (2019). Role for the shoot apical meristem in the specification of juvenile leaf identity in Arabidopsis. Proc. Natl. Acad. Sci. U. S. A. **116**: 10168–10177.

Franco-Zorrilla, J.M., Valli, A., Todesco, M., Mateos, I., Puga, M.I., Rubio-Somoza, I., Leyva, A., Weigel, D., García, J.A., and Paz-Ares, J. (2007). Target mimicry provides a new mechanism for regulation of microRNA activity. Nat. Genet. **39**: 1033–1037.

Fujimoto, S., Matsunaga, S., Yonemura, M., Uchiyama, S., Azuma, T., and Fukui, K. (2004). Identification of a novel plant MAR DNA binding protein localized on chromosomal surfaces. Plant Mol. Biol. **56**: 225–239.

He, J., Xu, M., Willmann, M.R., McCormick, K., Hu, T., Yang, L., Starker, C.G., Voytas, D.F., Meyers, B.C., and Poethig, R.S. (2018). Threshold-dependent repression of SPL gene expression by miR156/miR157 controls vegetative phase change in *Arabidopsis thaliana*. PLoS Genet. **14**: 1007337.

Huijser, P. and Schmid, M. (2011). The control of developmental phase transitions in plants. Development **138**: 4117–4129.

Karami, O., Rahimi, A., Khan, M., Bemer, M., Hazarika, R.R., Mak, P., Compier, M., van Noort, V., and Offringa, R. (2020a). A suppressor of axillary meristem maturation promotes longevity in flowering plants. Nat. Plants **6**: 368–376.

Karami, O., Rahimi, A., Mak, P., Horstman, A., Boutilier, K., Compier, M., Van der Zaal, B., and Offringa, R. (2020b). An Arabidopsis AT-hook motif nuclear protein mediates somatic-to-embryonic cell fate conversion coinciding with genome duplication. bioRxiv. **Nature com**:

https://www.biorxiv.org/content/10.1101/2020.01.03.

Lim, P.O., Kim, Y., Breeze, E., Koo, J.C., Woo, H.R., Ryu, J.S., Park, D.H., Beynon, J., Tabrett, A., Buchanan-Wollaston, V., and Nam, H.G. (2007). Overexpression of a chromatin architecture-controlling AT-hook protein extends leaf longevity and increases the post-harvest storage life of plants. Plant J. **52**: 1140–1153.

Livak, K.J. and Schmittgen, T.D. (2001). Analysis of relative gene expression data using real-time quantitative PCR and the 2(-Delta Delta C(T)) Method. Methods **25**: 402–408.

Matsoukas, I.G., Massiah, A.J., and Thomas, B. (2012). Florigenic and antiflorigenic signaling in plants. Plant Cell Physiol. **53**: 1827–1842.

Matsushita, A., Furumoto, T., Ishida, S., and Takahashi, Y. (2007). AGF1, an AT-hook protein, is necessary for the negative feedback of AtGA3ox1 encoding GA 3-oxidase. Plant Physiol. **143**: 1152–1162.

Melzer, S., Lens, F., Gennen, J., Vanneste, S., Rohde, A., and Beeckman, T. (2008). Flowering-time genes modulate meristem determinacy and growth form in *Arabidopsis thaliana*. Nat. Genet. **40**: 1489–1492.

Ng, K.-H., Yu, H., and Ito, T. (2009). AGAMOUS controls GIANT KILLER, a multifunctional chromatin modifier in reproductive organ patterning and differentiation. PLoS Biol. **7**: e1000251.

Ozturk, N., Singh, I., Mehta, A., Braun, T., and Barreto, G. (2014). HMGA proteins as modulators of chromatin structure during transcriptional activation. Front. Cell Dev. Biol. **2**: 1–9.

Poduska, B., Humphrey, T., Redweik, A., and Grbić, V. (2003). The synergistic activation of FLOWERING LOCUS C by FRIGIDA and a new flowering gene AERIAL ROSETTE 1 underlies a novel morphology in arabidopsis. Genetics **163**: 1457–1465.

Poethig, R.S. (2013). Vegetative phase change and shoot maturation in plants. Curr. Top. Dev. Biol. **105**: 125–152.

Reeves, R. (2010). Nuclear functions of the HMG proteins. Biochim. Biophys. Acta - Gene Regul. Mech. **1799**: 3–14.

Sgarra, R., Zammitti, S., Lo Sardo, A., Maurizio, E., Arnoldo, L., Pegoraro, S., Giancotti, V., and Manfioletti, G. (2010). HMGA molecular network: From transcriptional regulation to chromatin remodeling. Biochim. Biophys. Acta **1799**: 37–47.

Song, Y.H., Ito, S., and Imaizumi, T. (2013). Flowering time regulation: photoperiod- and temperature-sensing in leaves. Trends Plant Sci. **18**: 575–583.

Street, I.H., Shah, P.K., Smith, A.M., Avery, N., and Neff, M.M. (2008). The AT-hook-containing proteins SOB3/AHL29 and ESC/AHL27 are negative modulators of hypocotyl growth in Arabidopsis. Plant J. **54**: 1–14.

Telfer, A., Bollman, K.M., and Poethig, R.S. (1997). Phase change and the regulation of trichome distribution in *Arabidopsis thaliana*. Development **124**: 645–654.

Teotia, S. and Tang, G. (2015). To bloom or not to bloom: Role of micrornas in plant flowering. Mol. Plant **8**: 359–377.

Turnbull, C. (2011). Long-distance regulation of flowering time. J. Exp. Bot. **62**: 4399–43413.

Wang, J.-W., Czech, B., and Weigel, D. (2009). miR156-regulated SPL transcription factors define an endogenous flowering pathway in *Arabidopsis thaliana*. Cell **138**: 738–749.

Wu, G., Park, M.Y., Conway, S.R., Wang, J.-W., Weigel, D., and Poethig, R.S. (2009). The sequential action of miR156 and miR172 regulates developmental timing in Arabidopsis. Cell **138**: 750–759.

Xiao, C., Chen, F., Yu, X., Lin, C., and Fu, Y.-F. (2009). Over-expression of an AT-hook gene, AHL22,

delays flowering and inhibits the elongation of the hypocotyl in *Arabidopsis thaliana*. Plant Mol. Biol. **71**: 39–50.

Xu, M., Hu, T., Zhao, J., Park, M.-Y., Earley, K.W., Wu, G., Yang, L., and Poethig, R.S. (2016). Developmental functions of miR156-regulated *SQUAMOSA PROMOTER BINDING PROTEIN-LIKE* (*SPL*) genes in *Arabidopsis thaliana*. PLoS Genet. **12**: e1006263.

Xu, Y., Wang, Y., Stroud, H., Gu, X., Sun, B., Gan, E.-S., Ng, K.-H., Jacobsen, S.E., He, Y., and Ito, T. (2013). A matrix protein silences transposons and repeats through interaction with retinoblastoma-associated proteins. Curr. Biol. **23**: 345–350.

Yamaguchi, N., Jeong, C.W., Nole-Wilson, S., Krizek, B.A., and Wagner, D. (2016). AINTEGUMENTA and AINTEGUMENTA-LIKE6/ PLETHORA3 Induce LEAFY expression in response to auxin to promote the onset of flower formation in arabidopsis. Plant Physiol. **170**: 283–293.

Yang, L., Conway, S.R., and Poethig, R.S. (2011). Vegetative phase change is mediated by a leaf-derived signal that represses the transcription of miR156. Development **138**: 245–249.

Yang, L., Xu, M., Koo, Y., He, J., and Poethig, R.S. (2013). Sugar promotes vegetative phase change in *Arabidopsis thaliana* by repressing the expression of MIR156A and MIR156C. Elife **2**: e00260.

Yu, N., Niu, Q.-W., Ng, K.-H., and Chua, N.-H. (2015). The role of miR156/SPLs modules in Arabidopsis lateral root development. Plant J. **83**: 673–685.

Yu, S., Cao, L., Zhou, C.-M., Zhang, T.-Q., Lian, H., Sun, Y., Wu, J., Huang, J., Wang, G., and Wang, J.-W. (2013). Sugar is an endogenous cue for juvenile-to-adult phase transition in plants. Elife **2**: e00269.

Yu, S., Galvão, V.C., Zhang, Y.-C., Horrer, D., Zhang, T.-Q., Hao, Y.-H., Feng, Y.-Q., Wang, S., Schmid, M., and Wang, J.-W. (2012). Gibberellin regulates the Arabidopsis floral transition through miR156-targeted SQUAMOSA promoter binding-like transcription factors. Plant Cell **24**: 3320–32.

Yun, J., Kim, Y.-S., Jung, J.-H., Seo, P.J., and Park, C.-M. (2012). The AT-hook motif-containing protein AHL22 regulates flowering initiation by modifying FLOWERING LOCUS T chromatin in Arabidopsis. J. Biol. Chem. **287**: 15307–16.

Zhao, J., Favero, D.S., Peng, H., and Neff, M.M. (2013). *Arabidopsis thaliana* AHL family modulates hypocotyl growth redundantly by interacting with each other via the PPC/DUF296 domain. Proc. Natl. Acad. Sci. **110**: E4688–E4697.

Zhao, J., Favero, D.S., Qiu, J., Roalson, E.H., and Neff, M.M. (2014). Insights into the evolution and diversification of the AT-hook Motif Nuclear Localized gene family in land plants. BMC Plant Biol. **14**: 266.

Zhou, J., Wang, X., Lee, J.-Y., and Lee, J.-Y. (2013). Cell-to-cell movement of two interacting AT-hook factors in Arabidopsis root vascular tissue patterning. Plant Cell **25**: 187–201.

Acknowledgements
We are grateful to Scott Poethig for providing different *SPL* and *miR156* related lines also Nam-Hai Chua for providing *pmiR156-GUS* reporter lines. We are grateful to Ward de winter, Jan Vink, Nick Surtel and Mariel Lavrijsen for their supports.

Author contribution
A.R., O.K. and R.O. conceived the project, designed the experiments and analysed and interpreted the results. A.R. performed all the experiments. O.K. and R.O. supervised the project. A.R., O.K. and R.O. wrote the manuscript. All authors read and commented on versions of the manuscript.

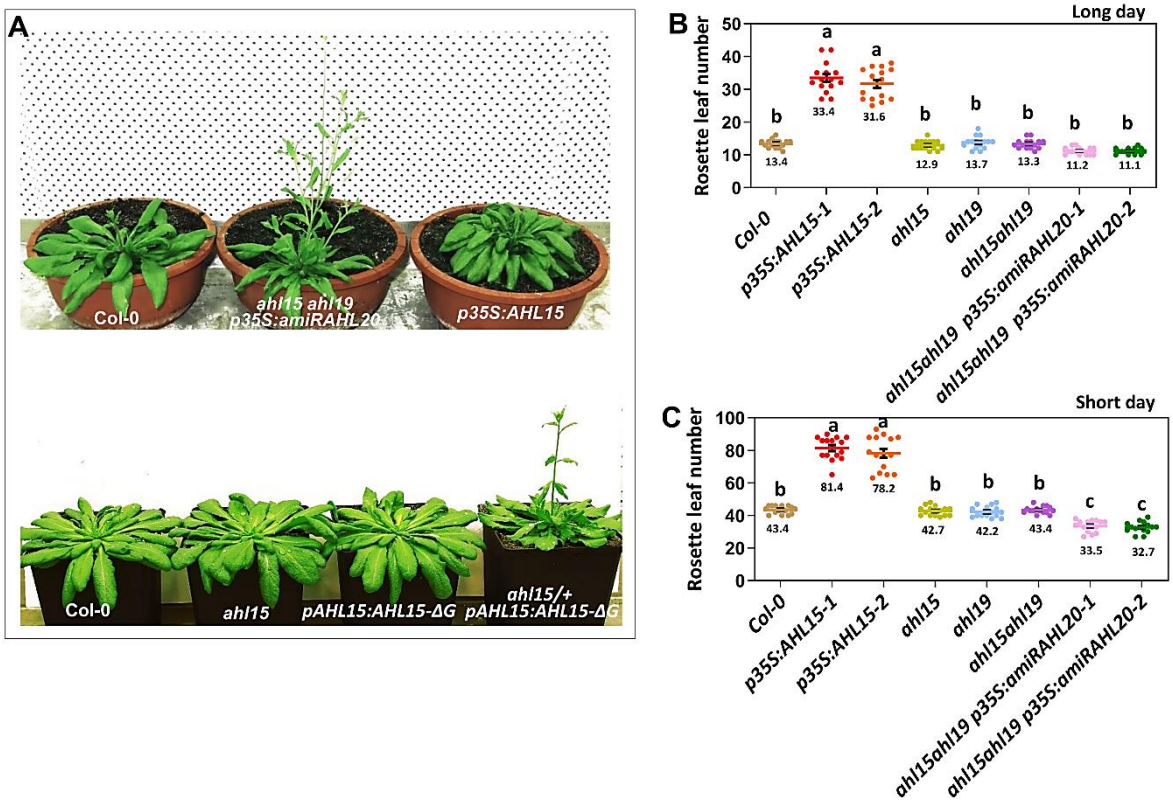

Supplementary Fig. 1 *Arabidopsis AHL15* and close homologs redundantly regulate flowering time. (**A**) Phenotype of a 8-weeks-old wild-type (Col-0), *ahl15 ahl19 p35S:amiRAHL20* or *p35S:AHL15* plant grown under SD (10-hour photoperiod) conditions (top) or of a 10-weeks-old wild-type (Col-0), *alh15*, *pAHL15:AHL15-ΔG* or *ahl15/+ pAHL15:AHL15-ΔG* plant grown under SD (8-hour photoperiod) conditions (bottom). (**B**, **C**) The number of rosette leaves produced until flowering by wild-type (Col-0), *p35S:AHL15*, *ahl15*, *ahl19*, *ahl15 ahl19*, or *ahl15 ahl19 p35S:amiRAHL20* plants grown under LD (**B**) or SD (**C**) conditions. Colored dots indicate the number of rosette leaves per plant (n = 15 biologically independent plants) per line, horizontal line and the number below this line indicate the mean and error bars indicate the s.e.m. Different letters indicate statistically significant differences ($P < 0.01$) as determined by a one-way ANOVA with Tukey's honest significant difference post hoc test.

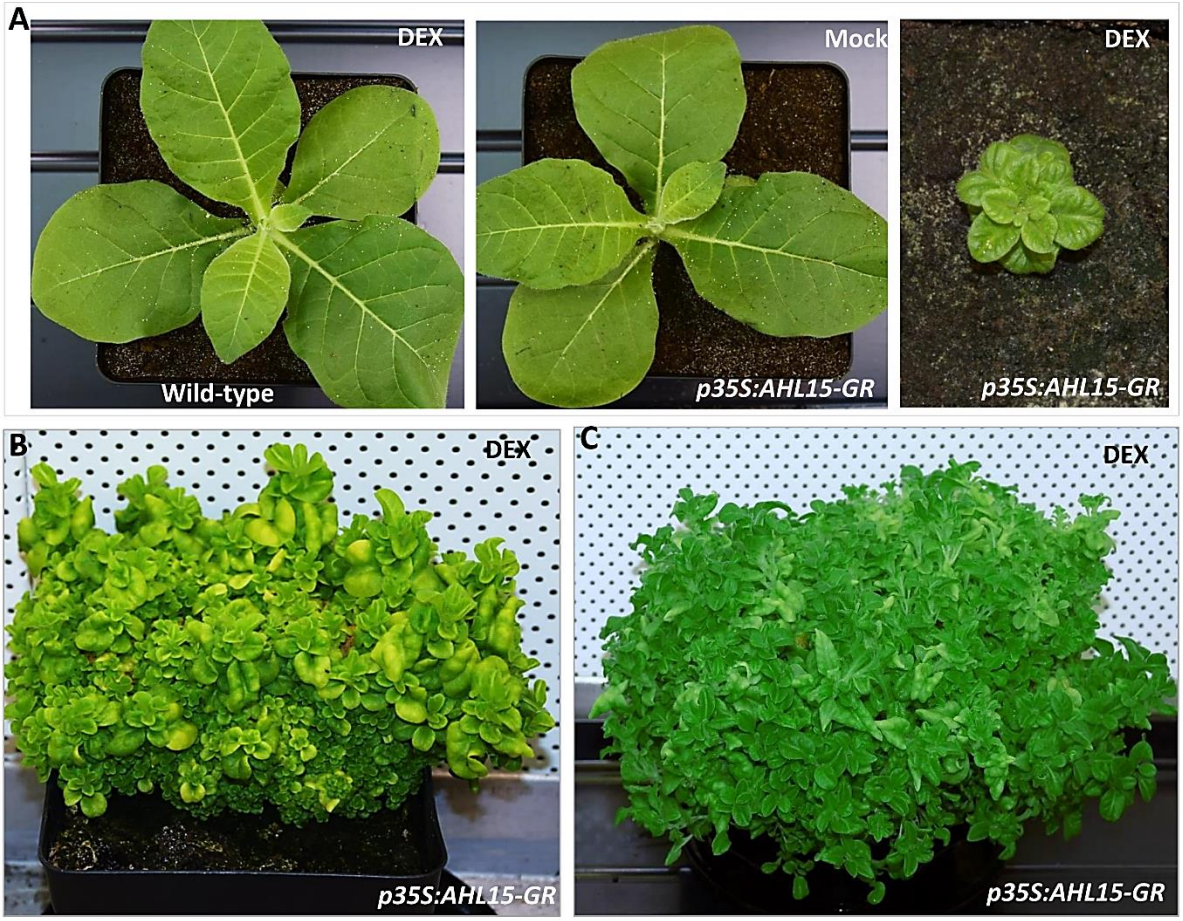

Supplementary Fig. 2 Extreme delay of the VPC by heterologous *AHL15* expression in tobacco. (**A**) Shoot morphology of a one-month-old wild-type (left) or *p35S:AHL15-GR* (middle and right) plant sprayed with water (Mock, middle) or sprayed with 20 μM DEX (DEX, left and right). (**B**, **C**) Extreme delay of the VPC in a six-month-old (**B**) or a one-year-old *p35S:AHL15-GR* (**C**) plant sprayed every week with 20 μM DEX.

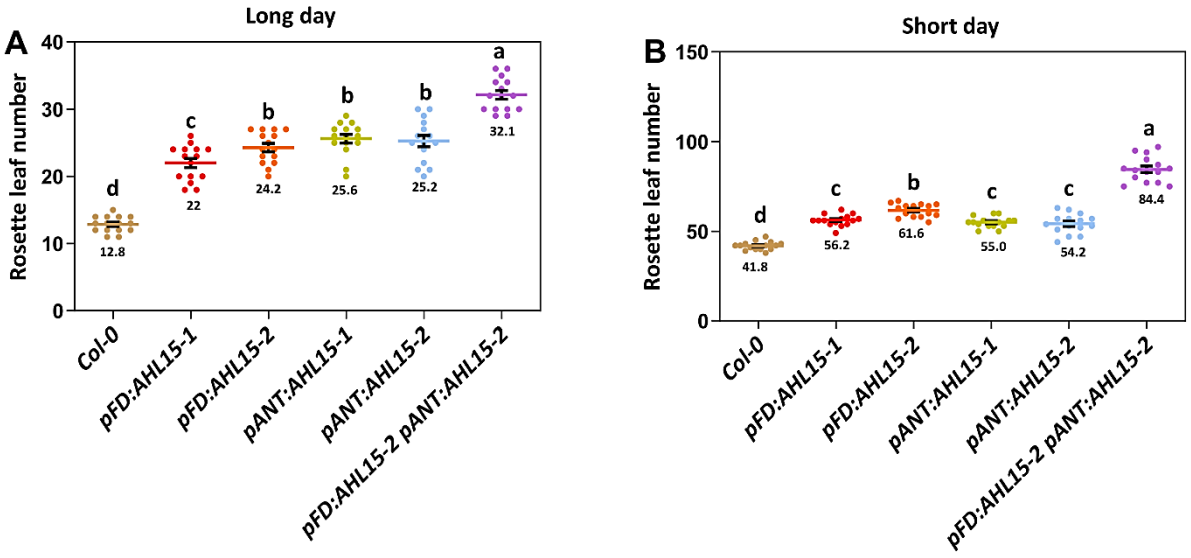

Supplementary Fig. 3 The effect of SAM- and young leaf-specific *AHL15* overexpression on flowering time. (**A**, **B**) The number of rosette leaves produced until flowering by wild-type (Col-0), *pFD:AHL15*, *pANT:AHL15* and *pFD:AHL15 pANT:AHL15* plants grown under LD (**A**) or SD (**B**) conditions. Colored dots indicate the number of rosette leaves per plant (n = 15 biologically independent plants) per line, horizontal line and the number below this line indicate the mean and error bars indicate the s.e.m. Different letters indicate statistically significant differences ($P < 0.01$) as determined by a one-way ANOVA with Tukey's honest significant difference post hoc test.

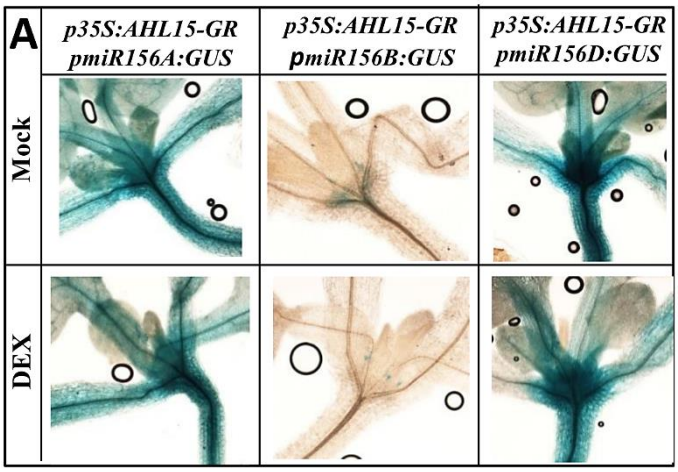

Supplementary Fig. 4 *AHL15* does not affect the expression of *miR156A,B,D*. (A) Histochemical staining for GUS activity in 2-week-old seedlings transgenic for *p35S:AHL15-GR* and *pmiR156A:GUS*, *pmiR156B:GUS* or *pmiR156C:GUS* following treatment with water (Mock, top) or DEX (bottom).

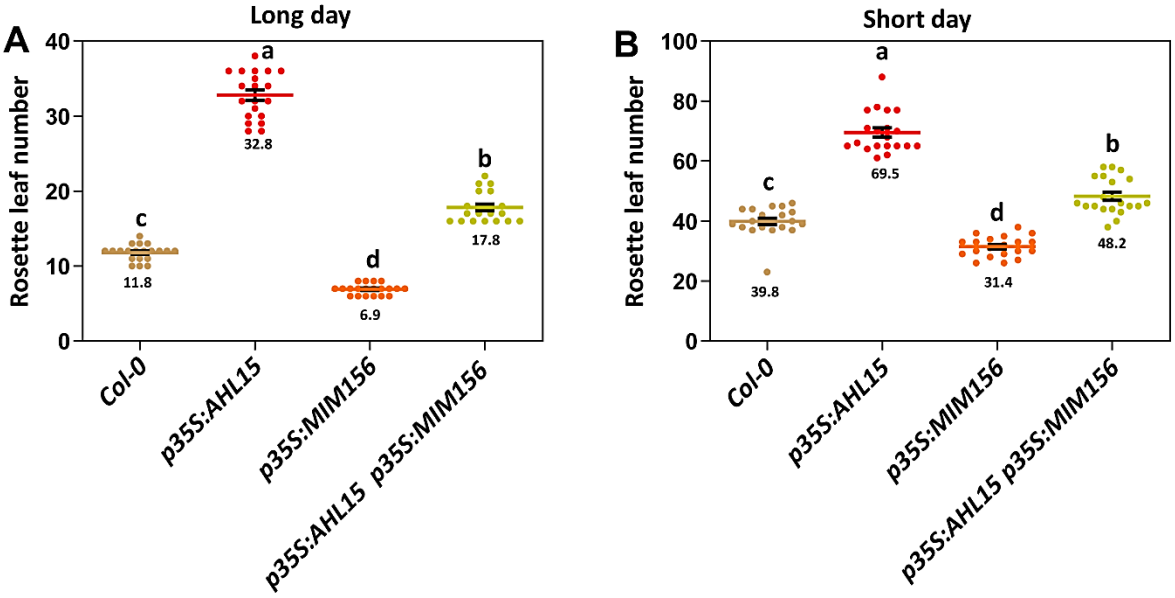

Supplementary Fig. 5 AHL15 and SPLs antagonistically control flowering time. (**A**, **B**) The number of rosette leaves produced until flowering by wild-type (Col-0), *p35S:AHL15*, *p35S:MIM156* and *p35S:AHL15*, *p35S:MIM156* plants grown under LD (**A**) or under SD (**B**) conditions. Colored dots indicate the number of rosette leaves per plant (n = 15 biologically independent plants) per line, horizontal line and the number below this line indicate the mean and error bars indicate the s.e.m. Different letters indicate statistically significant differences (P < 0.01) as determined by a one-way ANOVA with Tukey's honest significant difference post hoc test.

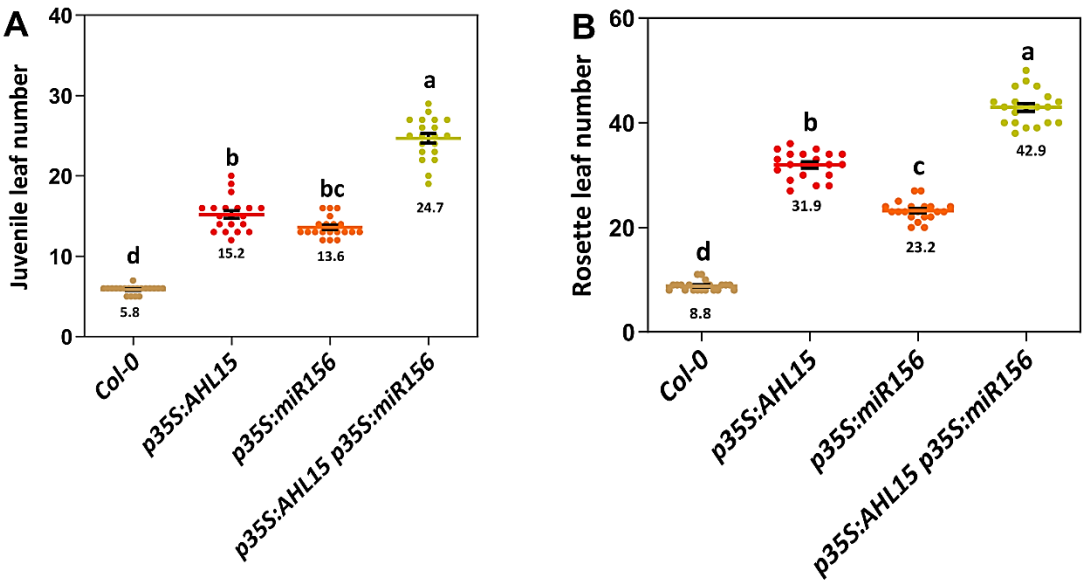

Supplementary Fig. 6 AHL15 and SPLs control the VPC and flowering time through parallel pathways. (**A**, **B**) The juvenile leaf number (leaves without abaxial trichomes) (**A**) and the number of rosette leaves produced until flowering (**B**) in wild-type, *p35S:AHL15*, *p35S:miR156* and *p35S:AHL15 p35S:miR156* plants grown under LD conditions. Colored dots indicate the number of leaves without abaxial trichomes (**A**) and the number of rosette leaves (**B**) per plant (n = 15 biologically independent plants) per line, horizontal line and the number below this line indicate the mean and error bars indicate the s.e.m. Different letters indicate statistically significant differences (P < 0.01) as determined by a one-way ANOVA with Tukey's honest significant difference post hoc test.

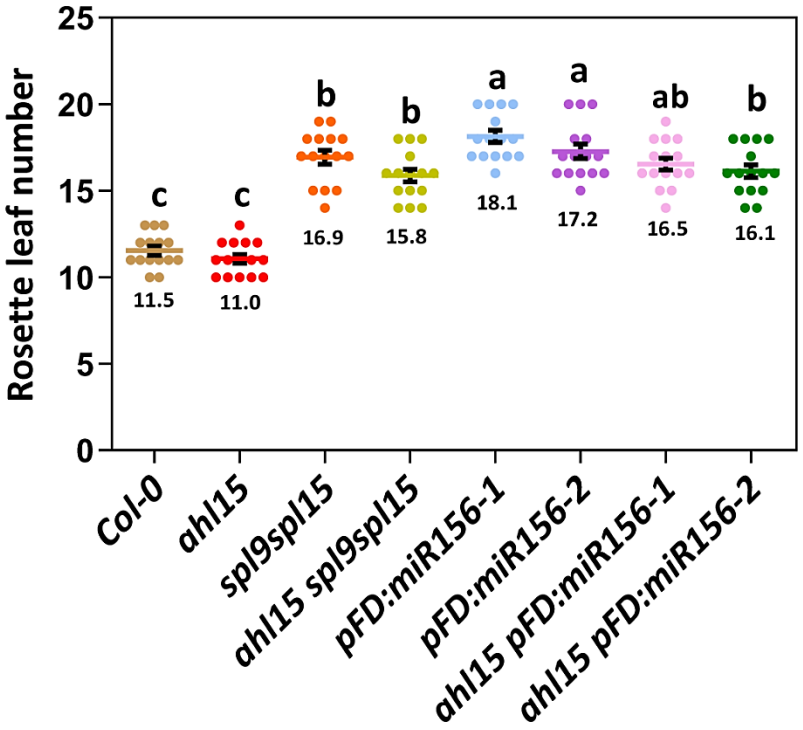

Supplementary Fig. 7 Delay of flowering by *spl* loss-of-function is largely *AHL15*-independent. The number of rosette leaves produced until flowering by wild-type (Col-0), *ahl15*, *spl9 spl15*, *ahl15 spl9 spl15*, *pFD:miR156*, *ahl15 pFD:miR156* plants grown under LD conditions. Colored dots indicate the number of rosette leaves per plant (n = 15 biologically independent plants) per line, horizontal line and the number below this line indicate the mean and error bars indicate the s.e.m. Different letters indicate statistically significant differences ($P < 0.01$) as determined by a one-way ANOVA with Tukey's honest significant difference post hoc test.

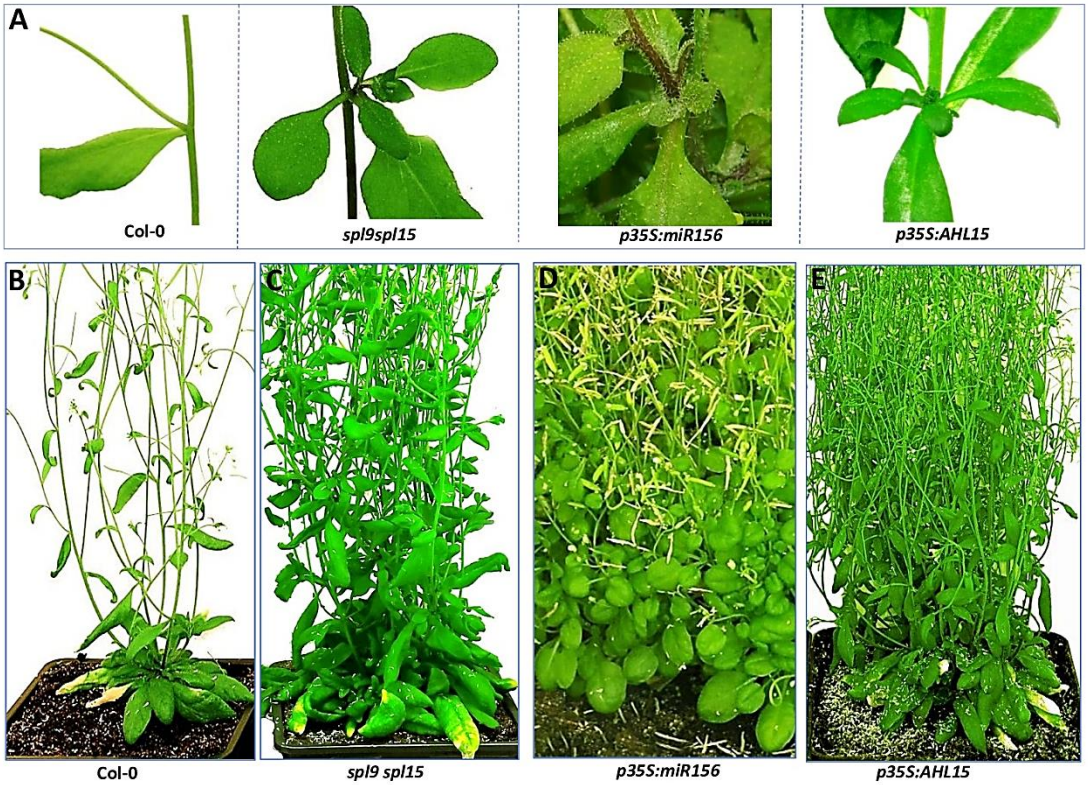

Supplementary Fig. 8 Aerial rosettes in Arabidopsis by reduced *SPL* expression or *AHL15* overexpression. (**A**,**B**) A detail of the first node of an inflorescence (**B**) and the complete shoot phenotype of a flowering wild-type (Col-0), *spl9 spl15*, *p35S:miR156* or *p35S:AHL15* plant grown under LD conditions.

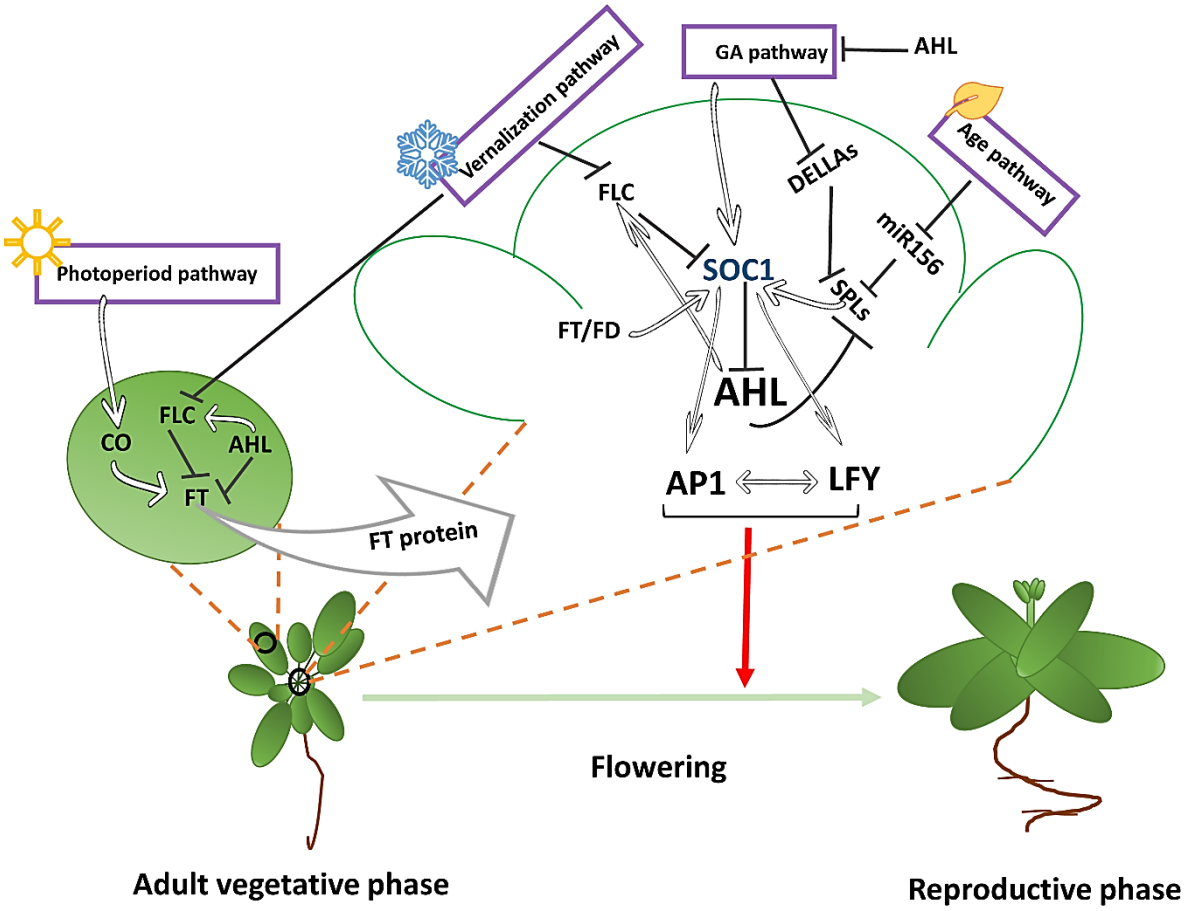

Supplementary Fig. 9 The position of AHLs in the network of pathways controlling flowering in Arabidopsis. In the vernalization pathway, cold treatment leads to stable repression of *FLC* transcription. The MADS box protein FLC determines the cold-period-dependent timing of flowering in Arabidopsis by repressing the expression of the floral integrator genes *FT* and *SOC1*. *FT* expression is induced in leaves by the photoperiod pathway through the accumulation of CO under long days. The FT protein subsequently travels to the SAM, where it physically interacts with FD to activate *SOC1*, which subsequently activates *AP1* and *LFY* (Song et al., 2013) .AHLs are integrated into the vernalization pathway and the photoperiod pathway by activating FLC or directly repressing *FT* expression (Yun et al., 2012). In the age pathway, an age-dependent decline in miR156/miR157 levels allows an increased production of the SPL transcription factors, which activate the transcription of *SOC1* and other floral integrators (not shown). AHLs are integrated into the age pathway by repression of *SPL* expression. The phytohormone GA independently promotes flowering through activation of *SOC1* (and *SPL* expression). AHLs by repression of GA biosynthesis are integrated into the GA pathway. The subsequent activation of the downstream floral meristem identity genes, such as *LFY* and *AP1*, completes the floral transition.

Supplementary Table 1. Primers used for cloning, genotyping and qRT-PCR

Name*	Sequence (5' to 3')	Purpose
KpnI -miR156-F	CAGGTACCGTAAGACACGTGTAGAAATC	*pFD:miR156* construct
miR156-R-SpeI	GGGTGAAGCACATTAGATACTAGTACC	
pFD-F	GGGGACAAGTTTGTACAAAAAAGCAGGCTGGCCCTCTCTACTTGATTTAG	*pFD:AHL15* construct
pFD-R	GGGGACCACTTTGTACAAGAAAGCTGGGTATGGAAAAGAGAACAGAAGTGAAC	
pANT-F	GGGGACAAGTTTGTACAAAAAAGCAGGCTCATACGCTTGGAAGGGATAAG	*pANT:AHL15* construct
pANT-R	GGGGACCACTTTGTACAAGAAAGCTGGGTAGGTTTCTTTTTTTGGTTTCTGC	
miR156-RT-PCR	GTCGTATCCAGTGCAGGGTCCGAGGTATTCGCACTGGATACGACGTGCTCA	
miR157-RT-PCR	GTCGTATCCAGTGCAGGGTCCGAGGTATTCGCACTGGATACGACGTGCTCT	
At snoR101-R-qPCR	AGCATCAGCAGACCAGTAGTT	
spl9-F	TGGTTCCTCCACTGAGTCATC	*spl9* genotyping
spl9-R	GCTCATTATGACCAGCGAGTC	
spl15-F	TGTTGGTGTCTGAAGTTGCTG	*spl15* genotyping
spl15-R	TCCACCGAGTCTTCTTCACTC	
SALK_040729-F	GTCGGAGAGCCATCAACACCA	*ahl15* genotyping
SALK_040729-R	CGACGACCCGTAGACCCGGATC	
qAHL15-F	AAGAGCAGCCGCTTCAACTA	*qRT-PCR AHL15*
qAHL15-R	TGTTGAGCCATTTGATGACC	
qAHL19-F	CTCTAACGCGACTTACGAGAGATT	*qRT-PCR AHL19*
qAHL19-R	ATATTATACACCGGAAGTCCTTGGT	
qAHL20-F	CAAGGCAGGTTTGAAATCTTATCT	*qRT-PCR AHL20*
qAHL20-R	TAGCGTTAGAGAAAGTAGCAGCAA	
qmiR157-F	GCGGCGGTTGACAGAAGATAG	*qRT-PCR miR157*
qmiR157-R	GTGCAGGGTCCGAGGT	
qmiR156-F	GCGGCGGTGACAGAAGAGAGT	*qRT-PCR miR156*
qmiR156-R	GTGCAGGGTCCGAGGT	
qβ-TUBULIN-6-F	TGGGAACTCTGCTCATATCT	*qRT-PCR β-TUBULIN-6*
qβ-TUBULIN-6-R	GAAAGGAATGAG GTTCACTG	
qSPL2-F	TTTCCGATACCGAGCACAATAG	*qRT-PCR SPL2*
qSPL2-R	TACGGGTTGGAGGTTGCTTGAGG	
qSPL9-F	AATTGGCGACTCAAACTGTG	*qRT-PCR SPL9*
qSPL9-R	CTGAAGAAGCTCGCCATGTA	
qSPL10-F	CAGACAAAGGTGTGGGAGAATGCTC	*qRT-PCR SPL10*
qSPL10-R	TAGGGAAAGTGCCAAATATTGGCG	
qSPL11-F	AGTCCAAGTTTCAACTTCATGGCG	*qRT-PCR SPL11*
qSPL11-R	GAACAGAGTAGAGAAAATGGCTGC	
qSPL13-F	GCTCGAGAACCGCATCGTT	*qRT-PCR SPL13*
qSPL13-R	CCCGTAAAAAACTGTCTCAACTGCT	
qSPL15-F	TGAATGTTTTATCACATGGAAGCTC	*qRT-PCR SPL15*
qSPL15-R	TCATCGAGTCGAAACCAGAAGATG	

*, F: forward; R: reverse.

Chapter 4

A novel pathway controlling cambium initiation and -activity via cytokinin biosynthesis in Arabidopsis

Arezoo Rahimi[1] **,Omid Karami**[1] **, Tobias de Werk**[1]**, Angga Dwituti Lestari**[1]**, Dongbo Shi**[2]**, Thomas Greb**[2]**, and Remko Offringa**[1]

[1] Plant Developmental Genetics, Institute of Biology Leiden, Leiden University, Sylviusweg 72, 2333 BE Leiden, The Netherlands

[2] Department of Developmental Physiology, Centre for Organismal Studies (COS), Heidelberg University, 69120 Heidelberg, Germany

Abstract

Plant secondary growth, also referred to as wood formation, includes the production of secondary xylem, which is derived from meristematic cambium cells embedded in vascular stem tissues. Here we identified an important role for the *Arabidopsis thaliana* (Arabidopsis) *AT-HOOK MOTIF CONTAINING NUCLEAR LOCALIZED 15 (AHL15)* gene, encoding a transcriptional regulator, in controlling vascular cambium activity. Secondary xylem development was significantly reduced in inflorescence stems of the Arabidopsis *ahl15* loss-of-function mutant, whereas general or vascular meristem-specific *AHL15* overexpression led to enhanced secondary xylem formation. Moreover, *AHL15* appeared to be required for the enhanced secondary xylem formation in the Arabidopsis double loss-of-function mutant of the *SUPPRESSOR OF OVEREXPRESSION OF CONSTANS 1* (*SOC1*) and *FRUITFULL* (*FUL*) genes. Our findings uncover a novel pathway in which AHL15 induces vascular cambium activity downstream of the transcription factors SOC1 and FUL by promoting biosynthesis of the hormone cytokinin. *AHL15* thus governs the rate of secondary xylem production that differentiates between herbaceous and woody plant stems.

Keywords: Secondary growth, *AHL15*, *SOC1*, *FUL*, cytokinin, Arabidopsis

Introduction

Throughout their lifespan, plants can dynamically change their growth and development in response to environmental signals, and this allows them to adapt and survive adverse conditions. In many flowering plants, but especially in woody plant species, stems show two distinct developmental growth processes. The increase in stem length and the establishment of the primary vascular meristem that is arranged into vascular bundles in young stems are known as primary growth. Each bundle contains a primary vascular meristem, or procambium, that generates primary xylem towards the center and primary phloem towards the periphery of the stem(Fischer et al., 2019). Later in development, when primary stem growth is completed, the procambium and its neighbouring interfascicular parenchyma cells (between the vascular bundles) differentiate into the cambial meristem, eventually forming a continuous cylinder of stem cells in the primary plant stem. This then initiates the process of secondary growth, during which the cambial meristem continuously generates secondary xylem usually towards the inside of the stem, and secondary phloem towards the outside of the stem, resulting in radial stem expansion(Jouannet et al., 2015).

Secondary vasculature production is performed by cambial initials located at the center of the cambial zone that undergo two types of cell divisions: i) periclinal cell divisions giving rise to proliferating derivatives called phloem and xylem mother cells, and ii) anticlinal cell divisions supporting the increase in circumference of the cambial zone(Tonn and Greb, 2017). The vascular cambium is an important meristem. On the one hand, it produces vascular tissues that transport water and nutrients throughout the plant body. On the other hand, through secondary growth, it provides mechanical support for the plant body by generating lignified wood cells. The rate of cell division in stem cells of the vascular cambium determines the amount of secondary growth and, thus, whether and how much wood is formed. In view of the use of wood as building material and renewable energy source, there is an obvious demand for an understanding of the genetic mechanisms that control the cambium activity.

The model plant Arabidopsis is herbaceous, but it can undergo secondary growth in the hypocotyl, root, or stem depending on the growth conditions(Ragni and Greb, 2018; Fischer et al., 2019). In contrast to woody plants that already produce a ring of xylem in young stems, Arabidopsis plants produce only a limited amount of xylem without forming a xylem ring in young stems. Secondary growth does occur in older Arabidopsis inflorescence stems and is generally quantified by the number of secondary xylem cell files produced by cambial cell divisions in the interfascicular part of the stem (the area between two bundles)(Nieminen et al., 2015; Fischer et al., 2019).

Most of our current understanding of secondary growth comes from studies in Arabidopsis. These studies have revealed a number of molecular factors and genetic components, including phytohormones and transcription factors, that are involved in the establishment and proliferation of cambium cells(Oh et al., 2003; Fischer et al., 2019). The TDIF-PXY-WOX signaling pathway is the best-studied signaling pathway that controls cambium activity. The peptide ligand CLE41/44/TRACHEARY ELEMENT DIFFERENTIATION INHIBITORY

FACTOR *(*TDIF*)* is synthesized in the phloem and seems to diffuse through the apoplastic space to cambium cells, where it binds to its cognate receptor PHLOEM INTERCALATED WITH XYLEM *(*PXY*)*. PXY subsequently promotes the proliferation of cambium cells by activating the expression of the cambium-specific *WUSCHEL-RELATED HOMEOBOX* genes *WOX4* and *WOX14(*Etchells and Turner, 2010; Hirakawa et al., 2010; Wang et al., 2019). The WOX4 transcription factor promote stem cell proliferation by interacting with the GRAS domain transcription factor HAIRY MERISTEM 4 (HAM4)(Zhou et al., 2015).

Cambium activity is also known to be regulated by the flowering genes *SOC1* and *FUL* and a hormonal signaling network(Bhalerao et al., 2016; Immanen et al., 2016; Brackmann et al., 2018; Fischer et al., 2019). In the Arabidopsis *soc1 ful* double loss-of-function mutant xylem formation is significantly enhanced, resulting in the formation of a xylem ring even in young inflorescence stems(Melzer et al., 2008). This suggests that SOC1 and FUL repress cambium ring formation and secondary growth, however, what is downstream of these transcription factors is still unknown. In addition, the plant hormone cytokinin has been highlighted, in parallel to the TDIF-PXY-WOX pathway, as a major positive regulator of vascular cambium cell proliferation during secondary growth(El-Showk et al., 2013). Isopentenyl transferase (IPT) enzymes are mostly responsible for cytokinin biosynthesis. The Arabidopsis *ipt1,3,5,7* quadruple mutant completely lacks cambial activity, but this can be rescued by treatment with exogenous cytokinin(Miyawaki et al., 2006; Matsumoto-Kitano et al., 2008). Moreover, the expression of a cytokinin catabolic gene in *Populus alba* (poplar) led to a remarkable decrease in cambial cell divisions and thinner trunks(Immanen et al., 2016). By contrast, increasing cytokinin levels in poplar stems by overexpressing *IPT7* under the wood-specific *LMX5* promoter strongly stimulated cambial cell divisions and biomass production(Immanen et al., 2016). In addition, it was shown that secondary growth in \Arabidopsis roots is dependent on the cytokinin-responsive transcription factor AINTEGUMENTA (ANT) and the D-type cyclin CYCD3;1, which are both expressed in the vascular cambium(Dewitte et al., 2007; Randall et al., 2015). Despite this increasing knowledge, the connection between the different players and the exact signals that initiate the formation of the cambium ring and regulate the amount of secondary growth, and thus differentiate between woody and non-woody species, remain unclear.

Here we identified a new role for the Arabidopsis *AHL15* gene as an important regulator of vascular cambial activity and secondary xylem formation. AHL15 is part of a plant-specific protein family, containing a single AT-hook DNA binding motif and a Plant and Prokaryote Conserved (PPC) domain(Fujimoto et al., 2004; Zhao et al., 2013). *AHL15* homologs have been implicated in several aspects of plant growth and development in Arabidopsis, including flowering time and hypocotyl growth(Street et al., 2008; Xiao et al., 2009), flower development(Ng et al., 2009), vascular tissue differentiation(Zhou et al., 2013), and gibberellin biosynthesis(Matsushita et al., 2007). In addition, we have recently shown that *AHL15* and family members play key roles in plant embryogenesis(Karami et al., 2020b) and –longevity(Karami et al., 2020a). Apart from promoting plant longevity, we also discovered that *AHL15* enhances secondary growth. A more detailed analysis indicated that *AHL15* regulates vascular cambium initiation and -activity in Arabidopsis by linking the action of the

upstream flowering genes *SOC1* and *FUL* to the downstream cytokinin biosynthesis genes *IPT3, IPT7* and *LONELY GUY 4* (*LOG4*).

Results

AHL15 promotes secondary growth in Arabidopsis inflorescence stems

In contrast to woody plants that already produce a ring of xylem in young stems, herbaceous plants, such as Arabidopsis, produce only a limited amount of xylem without forming a xylem ring in young stems. Secondary growth does occur in older Arabidopsis inflorescence stems and is generally quantified by the number of secondary xylem cell files produced by cambial cell divisions in the interfascicular part of the stem (the area between two bundles) (Nieminen et al., 2015; Fischer et al., 2019). In the Arabidopsis *soc1 ful* double loss-of-function mutant, however, xylem formation is significantly enhanced, resulting in the formation of a xylem ring even in young inflorescence stems (Melzer et al., 2008). In addition, *soc1 ful* mutant plants show extended longevity by the maintenance of vegetative growth from axillary meristems (AMs) (Melzer et al., 2008).

Recently, we have shown that overexpression of the Arabidopsis *AHL15* gene (*p35S:AHL15*) also increases plant longevity (Fig. 1A), similar to *soc1 ful* plants, and that *AHL15* acts downstream of the SOC1 and FUL transcription factors in maintaining AMs in the vegetative phase (Karami et al., 2020a, Chapter 2). In view of these data, we analyzed whether *AHL15* overexpression could also promote secondary growth and xylem formation in *p35S:AHL15* inflorescence stems. One-month-old *p35S:AHL15* stems displayed a significant increase in xylem formation compared to wild-type stems (Fig. 1B). In 2- and 3-month-old *p35S:AHL15* stems secondary xylem formation continued, whereas it stopped in 2-month-old wild-type stems (Fig. 1B, C). These results suggested that AHL15 can trigger cambium activity and thereby enhance secondary growth in Arabidopsis inflorescence stems. Arabidopsis inflorescence stems normally produce more secondary xylem than secondary phloem (Altamura et al., 2001).

Lignin staining showed that inflorescence stems of one-month-old *p35S:AHL15* plants produced more lignified xylem cells in the interfascicular region than those of wild-type plants (Fig. 1E, F). In contrast, *ahl15* loss-of-function mutant stems contained significantly less lignified xylem cells at interfascicular region than wild-type stems (Fig. 1E, F), even though *ahl15* plants developed and flowered like wild-type plants (Fig. 1D). Introduction of the *pAHL15:AHL15* genomic clone into the *ahl15* mutant background completely restored the secondary xylem growth to wild-type levels (Fig. 1E, F), indicating that the reduction in the xylem cell number was caused by *ahl15* loss-of-function.

Previous studies have shown that expression of a mutant AHL protein (AHL15-ΔG), from which the conserved six amino-acid sequences (GRFEIL) in the PPC domain was deleted, in the heterozygous *ahl15/+* mutant background leads to a dominant-negative effect that overcomes the functional redundancy between the different *AHL* family members (Zhao et al., 2013; Karami et al., 2020a). Whereas *pAHL15:AHL15-ΔG* plants showed wild-type development, as previously reported (Karami et al., 2020a, Chapter 2), *ahl15/+ pAHL15:AHL15-ΔG* plants developed even less secondary xylem (Fig. 1D) compared to

ahl15 plants (Fig. 1E, F). The diameter of *ahl15* stems was already smaller than wild-type stems, but *ahl15/+ pAHL15:AHL15-ΔG* stems remained even smaller in size (Supplementary Figure 1). Except for the difference in cambium activity, mutant stems showed the same structure and tissue organization as wild-type stems (Supplementary Figure 2). These results show that *AHL15* plays an important role in increasing cambium activity and secondary growth in Arabidopsis inflorescence stems, and that like with developmental processes such as embryogenesis and AM maturation (Karami et al., 2020a, 2020b), it acts partially redundant with other *AHL* genes.

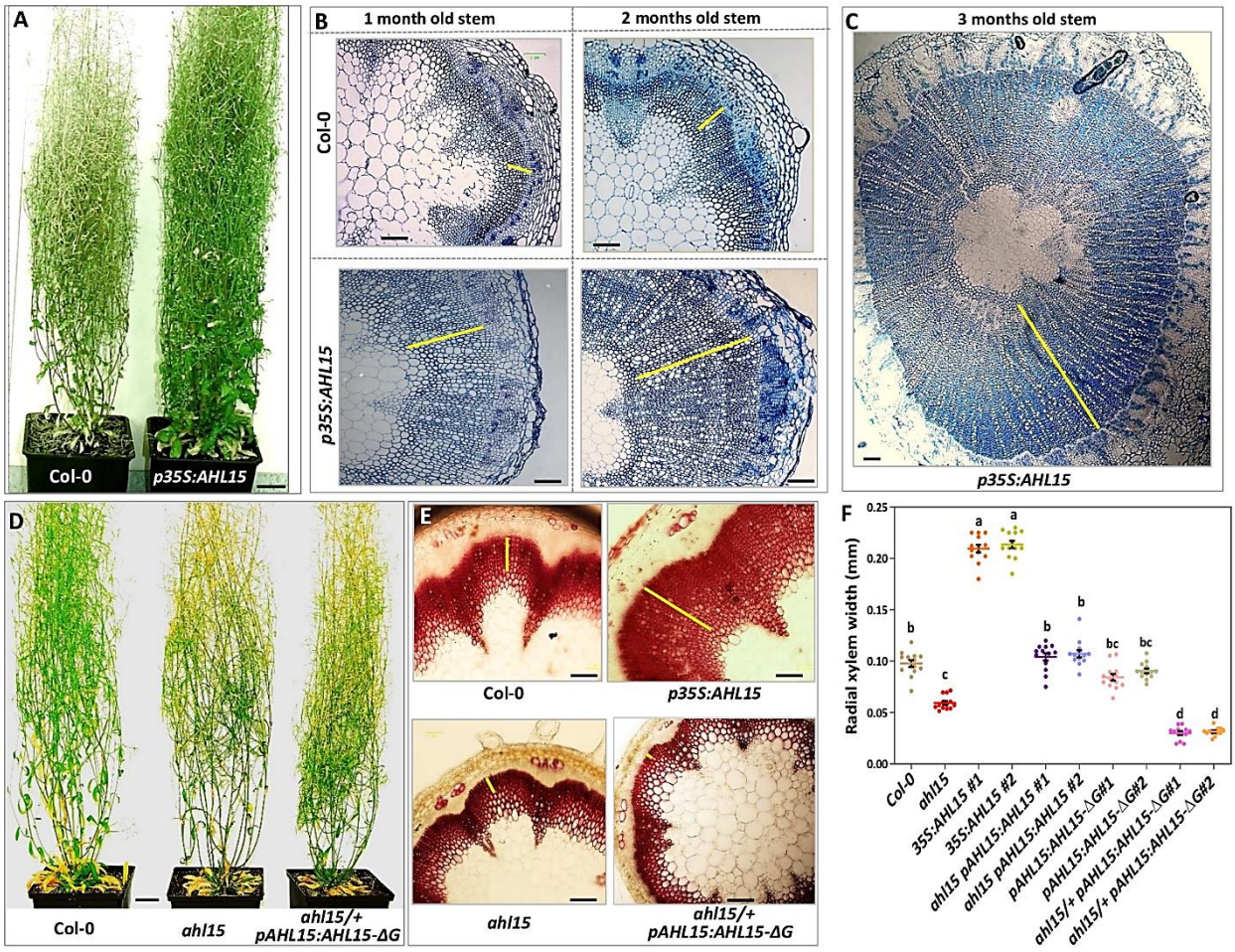

Fig. 1| *AHL15* promotes secondary growth in Arabidopsis inflorescence stems. (**A**) Plant shoot phenotype of a three-month-old wild-type and *p35S:AHL15* plants. (**B**) Toluidine blue-stained cross-sections of most-bottom base of a one-month-old (left panel) or two-month-old (right panel) inflorescence stem of wild-type and *p35S:AHL15* Arabidopsis plants. (**C**) Toluidine blue-stained cross-sections of most-bottom base of a three-month-old *p35S:AHL15* inflorescence stem. (**D**) Shoot phenotypes of two-month-old wild-type (left), *ahl15* (middle) and *ahl15/+ pAHL15:AHL15-ΔG* mutant (right) plants. (**E**) Phloroglucinol-stained fresh cross-sections of most-bottom base of a one-month-old wild-type (upper panel left), *p35S:AHL15* (upper panel right), *ahl15* (lower panel left), and *ahl15/+ pAHL15:AHL15-ΔG* (lower panel right) inflorescence stems. (**F**) Quantification of the secondary xylem width (most-bottom base) in interfascicular part of one-month-old wild-type, *p35S:AHL15*, *ahl15* and *pAHL15:AHL15 ahl15*,*pAHL15:AHL15-ΔG* and *ahl15/+ pAHL15:AHL15-ΔG* main inflorescence stems. Colored dots indicate the average secondary xylem width of 3 random interfascicular region of an individual stem independent plants (n = 9), all the secondary xylem width are presenting the width average per line, horizontal lines indicate the mean and error bars indicate the s.e.m. Different letters indicate statistically significant differences ($P < 0.01$) as determined by a one-way ANOVA with Tukey's honest

significant difference post hoc test. The yellow bars in (**B**), (**C**) and (**E**) mark the xylem width in the interfascicular cell domain. Scale bars indicate 2 cm in (**A**) and (**D**) and 0.06 mm in (**B**), (**C**) and (**E**).

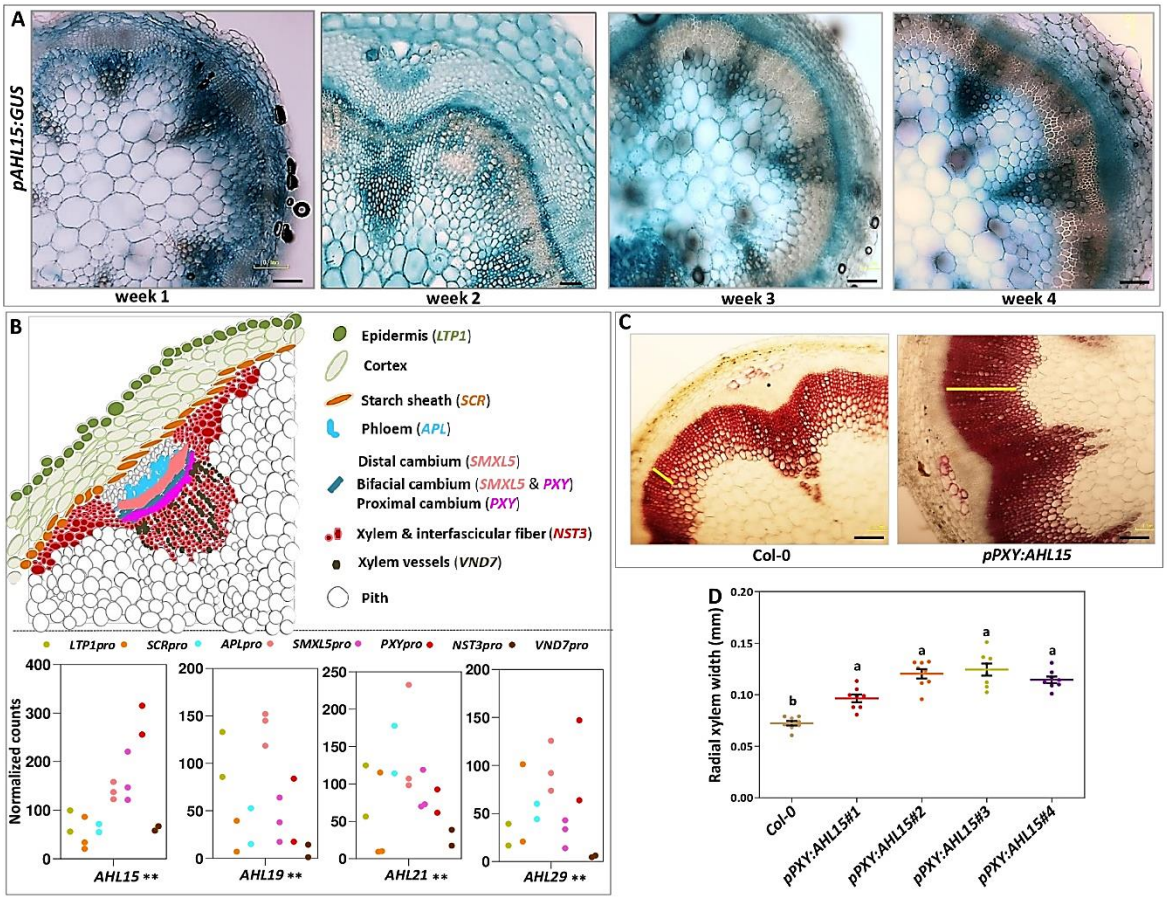

Fig. 2| Along with unique expression pattern of *AHL15* in cambium area with other *AHLs*, Cambium-specific *AHL15* expression promotes secondary xylem formation (**A**) Cross-sections of most-bottom base of a one-,two-, three- and four-week-old inflorescence stems presenting the expression pattern the *pAHL15:GUS* reporter line (promoter activity). (**B**) Schematic representation of part of a cross section of an inflorescence stem, including the vascular bundle and the interfascicular regions, in which different stem tissues and the tissue-specific expression domains of genes used for stem transcriptome profiling are indicated (*NST3* (fibers), *VND7*(xylem vessels), *PXY* (proximal cambium), *SMXL5* (distal cambium), *APL* (phloem), *SCR*(starch sheath), *LTP*1(epidermis cells) (upper panel)). Co-expression of *AHL15*, *AHL19, AHL21* and *AHL29* genes at cambium and bundle domains. (lower panel). Normalized read counts of the *AHL* genes in the tissue-specific gene expression atlas generated by combining fluorescence-activated nucleus sorting (FANS) using the promoter-H4-GFP fusions of the indicated marker genes (*NST3*, *VND7*, *PXY*, *SMXL5*, *APL, SCR* and *LTP1*) and combining FANS and laser-capture microdissection with next generation RNA sequencing (Shi et al., 2020). Colored dots indicate the values of two or three biological replicates of RNA isolation obtain by FANS, Normalized gene read counts of the indicated genes among seven different tissues displayed for each replicate individually. *, ** indicates $p < 0.05$ and 0.01, respectively in LRT (Shi et al., 2020). (**C**) Phloroglucinol-stained fresh cross-sections of most-bottom base of a one-month-old wild-type (left) and *pPXY:AHL15* (right) inflorescence stems. The yellow bars mark the xylem width in the interfascicular cell domain. (**D**) Quantification of the secondary xylem width (most-bottom base) in interfascicular part of one-month-old wild-type and *pPXY:AHL15* main inflorescence stems. (5 individual lines). Colored dots indicate the average secondary xylem width of 3 random interfascicular region of an individual stem independent plants (n = 7), all the secondary xylem width are presenting the width average per line, horizontal lines indicate the mean and error bars indicate the s.e.m. Different letters indicate statistically significant differences ($P < 0.01$) as determined by a one-way ANOVA with Tukey's honest significant difference post hoc test. Scale bars in (**A**) and (**C**) indicate 0.06 mm.

SOC1/FUL-repressed cambium-specific *AHL15* expression regulates secondary growth

The above results suggested that *AHL15* is expressed in the vascular cambium area where it regulates cambial cell division activity. Histochemical staining of plants having the *AHL15* promoter β-glucuronidase (GUS) reporter (*pAHL15:GUS*) in wild-type background indicated that *AHL15* is expressed in almost all tissues in 1-week-old inflorescence stems (1-week after bolting) (Fig. 2A), but that the expression became progressively restricted to the vascular and interfascicular cambium zone during stem maturation (Fig. 2A). Interestingly, *AHL15* expression was completely absent from the secondary xylem, whereas it remained expressed in the primary xylem and xylem fibers of the inflorescence stem (Fig. 2A).

In order to confirm that *AHL15* is expressed in the vascular cambium, we extracted the expression pattern of clade-A *AHL* genes from tissue-specific gene expression atlas generated from different Arabidopsis stem tissues (e.g., xylem vessels, fibers, the proximal and the distal cambium, phloem, phloem cap, pith, starch sheath, and epidermis cells; see Fig. 2B) by combining fluorescence-activated nucleus sorting and laser-capture microdissection with next-generation RNA sequencing (Shi et al., 2020). The extracted *AHL15* expression from this data belonging to the second bottom-most internode of Arabidopsis stem (about 2 weeks after bolting) (Fig. 2B) showed a high level of similarity with the activity pattern of the *pAHL15:GUS* reporter in 2-week-old inflorescence stem up to 4-week old stems. The expression of *AHL15* in the *PXY* and *SUPPRESSOR OF MAX2 1-LIKE PROTEIN 5* (*SMXL5*) cambium sub-domains, the areas where cell division is taking place (Shi et al., 2019), further supported the role of *AHL15* in promoting vascular cambium activity. In line with the functional redundancy between *AHL* genes in promoting cambium activity, we also found *AHL19*, *AHL20*, and *AHL29* to be expressed in the *PXY* and *SMXL5* cambium sub-domains (Fig. 2B).

Altogether, the seemingly overlapping expression of *AHL* genes in the stem cambium zone supports their role in the regulation of cambium activity. To establish whether *AHL* expression in the Arabidopsis vascular cambium is rate-limiting for secondary growth, we expressed *AHL15* under control of the cambium-specific *PXY* promotor (*pPXY:AHL15*) (Fisher and Turner, 2007). Lignin stained one-month-old *pPXY:AHL15* stems showed a significant increase in secondary xylem development compared to wild-type stems (Fig. 2C, D). These results indicate that in wild-type Arabidopsis, secondary growth and xylem development are limited by *AHL* expression, and that cambium-specific enhancement of *AHL15* expression is sufficient to promote cambium activity. Apart from the enhanced cambium activity, *pPXY:AHL15* plants developed and flowered like wild-type plants (Supplementary Figure 3), confirming that the effect of locally enhanced *AHL15* expression on cambium activity is direct, and not caused by changes in developmental timing.

Previously, we have shown that *AHL15* expression is repressed by binding of the SOC1 and FUL MADS-box transcription factors to its up- and downstream genomic regions, and that alleviation of this repression in the *soc1 ful* double mutant leads to delayed maturation of AMs, resulting in the mutant aerial rosette phenotype (Karami et al., 2020b, Chapter 2). Comparison of *soc1 ful* double mutant with *soc1 ful ahl15* triple mutant stems showed that the high secondary xylem production in *soc1 ful* stems was dependent on the presence of a functional *AHL15* gene. The interfascicular secondary xylem formation was reduced to wild-

type levels in the *soc1 ful ahl15* triple mutant (Fig. 3A, B). This is in line with the previously observed enhanced expression of *AHL15* in *soc1 ful* mutant AMs (Karami et al., 2020b, Chapter 2). The co-expression of *AHL15* with *SOC1* and *FUL* in the *PXY* and *SMXL5* cambium sub-domains (Fig. 3C) further supports the negative regulation of *AHL15* by *SOC1* and *FUL* in cambium related domains, which limits secondary growth in the herbaceous wild-type Arabidopsis.

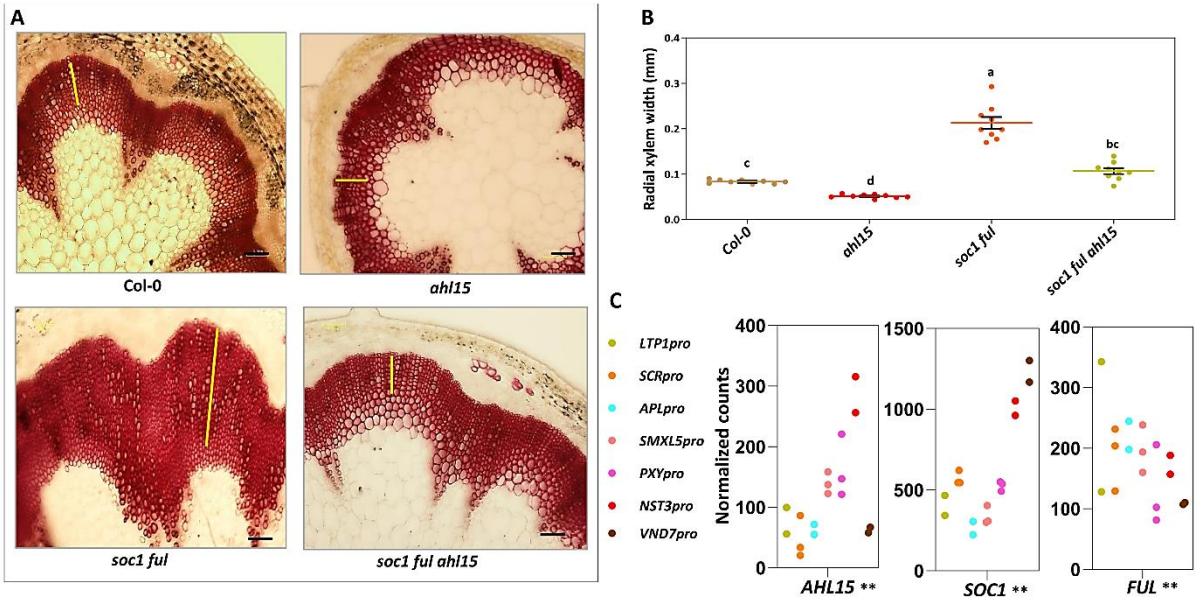

Fig. 3| *AHL15* is required for enhanced secondary xylem formation in the *soc1 ful* double mutant. (**A**) Phloroglucinol-stained fresh cross-sections of most-bottom base of a one-month-old wild-type (upper panel, left), *ahl15* (upper panel, right), *soc1ful* (lower panel, left) and *soc1ful ahl15* (lower panel, right) inflorescence stems. The yellow bars mark the xylem width in the interfascicular cell domain. (**B**) Quantification of the secondary xylem width (most-bottom base) in interfascicular part of one-month-old wild-type, *ahl15*, *soc1ful* and *soc1ful ahl15* main inflorescence stems. Colored dots indicate the average secondary xylem width of 3 random interfascicular region of an individual stem independent plants (n = 9), all the secondary xylem width are presenting the width average per line, horizontal lines indicate the mean and error bars indicate the s.e.m. Different letters indicate statistically significant differences ($P < 0.01$) as determined by a one-way ANOVA with Tukey's honest significant difference post hoc test. (**C**) Co-expression of *AHL15*, *SOC1* and *FUL* genes at cambium and bundle domains. Colored dots indicate the values of two or three biological replicates of RNA isolation obtain by FANS. Normalized gene read counts of the indicated genes among seven different tissues displayed for each replicate individually. *, ** indicates $p < 0.05$ and 0.01, respectively in LRT (Shi et al., 2020). Scale bars indicate 0.06 mm.

AHL15 promotes secondary growth by increasing cytokinin biosynthesis

In Arabidopsis inflorescence stems, secondary growth is initiated by the occurrence of interfascicular cambium, leading to the formation of a cambium ring. The initial cell divisions marking the starting point of interfascicular cambium formation can be readily observed in one-week-old wild-type stems, but are absent in one-week-old *ahl15* loss-of-function stems (a noticeable feature of this mutant), despite a normal organization of the mutant stem tissues (Fig. 4A). In contrast, one-week-old *p35S:AHL15* inflorescence stems already showed a cambium ring consisting of several layers of cells in the interfascicular region (Fig. 4A). These results indicate an important role for *AHL15* in cambium initiation and the promotion of cambial cell divisions. Previous studies have highlighted that the cell division rate in the procambium and cambium is regulated by the plant hormone cytokinin (Matsumoto-Kitano et al., 2008; Immanen et al., 2016). To test the involvement of cytokinin in the AHL15-enhanced cell divisions, we compared the expression of cytokinin response reporter *pTCS:GFP* (Zürcher et al., 2013) in wild-type, *ahl15* or *p35S:AHL15* inflorescence stems during cambium development. In very young (2-day-old) stems, only a weak *pTCS:GFP* expression could be detected in the procambium zone of stems of all three genetic backgrounds, indicating that *AHL15* does not modulate the cytokinin response in these very young stems stage (Fig. 4B, left images). However, three days later, when *pTCS:GFP* signals started to appear in the interfascicular regions of wild-type stems, *pTCS:GFP* expression was still limited to the procambium in *ahl15* stems, whereas *p35S:AHL15* stems displayed a ring of *pTCS:GFP* signal colocalizing with the cambium ring already present in these stems (Fig. 4B, middle images). These overlapping rings of cambium and *pTCS:GFP* expression also became visible in 10-day-old wild-type stems, and were even stronger in *p35S:AHL15* stems (Fig. 4B, right images). In 10-day-old *ahl15* stems, however, *pTCS:GFP* expression remained restricted to the cambium in the vascular bundles (Fig. 4B, right images). These results suggested that AHL15 might regulate cambium initiation and promote the cambial cell division rate in Arabidopsis stems by altering cytokinin biosynthesis or -response.

To analyze the effect of *AHL15* on cytokinin biosynthesis, the expression of the cytokinin biosynthesis genes *IPT7*, *IPT3*, *LONELY GUY4* (*LOG4*) and *LOG5* (Matsumoto-Kitano et al., 2008) was compared between wild-type and *ahl15* mutant stems. Our qPCR experiments showed that the expression of *IPT3, IPT7*, and *LOG4* was significantly reduced in *ahl15* stems (Fig. 4C), suggesting that *AHL15* acts by activating these cytokinin biosynthesis genes in the cambium area. This was further confirmed by the co-expression of *AHL15*, *IPT3*, *IPT7*, *LOG4*, and *LOG5* in the *PXY* and *SMXL5* cambium sub-domains (Supplementary Fig. 4).

To verify that the reduced secondary xylem formation in *ahl15* mutant stems was caused by a reduced cytokinin biosynthesis, we introduced the *Agrobacterium tumefaciens IPT* gene under the control of the cambium-specific *PXY* promoter (*pPXY:IPT*) in the *ahl15* mutant background (Robson et al., 2004; Van Der Graaff et al., 2001). The presence of the *pPXY:IPT* construct significantly increased the width of interfascicular lignified xylem in *ahl15* stems, bringing it back to wild-type or even higher levels (Fig. 4D-E). Our data demonstrate that local expression of *AHL15* assisted by that of redundantly acting *AHL* genes determines the initiation and activity of interfascicular cambium and thereby the secondary growth of Arabidopsis inflorescence stems by promoting cytokinin biosynthesis.

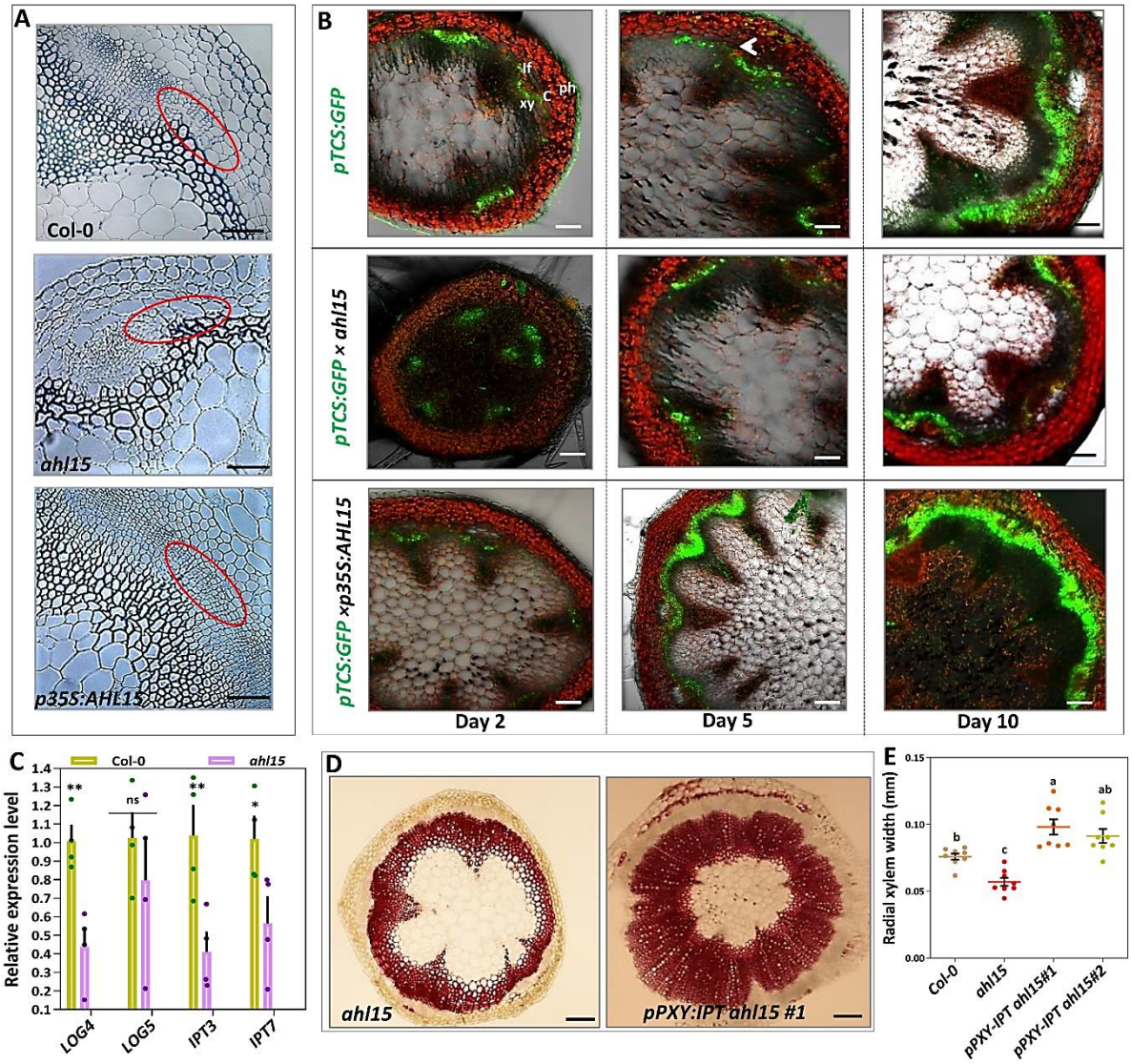

Fig. 4| Cytokinin acts downstream of *AHL15* to promote cambium activity. (**A**) Toluidine blue-stained cross-sections of most-bottom base of one-week-old wild-type (upper), *ahl15* (middle) and *p35S:AHL15* (lower) inflorescence stems. The red circle marks the cambium cell division area in the interfascicular region which is absent in *ahl15* mutant. (**B**) Confocal images showing the expression of the *pTCS:GFP* cytokinin response reporter cross-sections of most-bottom base of two-, five- and ten-day-old wild-type (upper panel)(arrow indicate the cambium cell division start point in wild-type), *ahl15* (middle panel) and *p35S:AHL15* (lower panel) inflorescence stems. (**C**) Relative expression of the cytokinin biosynthesis genes *LOG4*, *LOG5*, *IPT3* and *IPT7* by qPCR analysis in the base of ten-day-old wild-type and *ahl15* inflorescence stems. Dots indicate the values of three biological replicates per plant line, bars indicate the mean and error bars indicate the s.e.m. Asterisks indicate significant differences between wild-type and *ahl15* plants (*P < 0.05, **P < 0.01, ns (not significant)), as determined by a two-sided Student's *t*-test. (**D**) Phloroglucinol-stained fresh cross-sections of most-bottom base of one-month-old *ahl15* (left) and *ahl15 pPXY:IPT* (right) inflorescence stems. (**E**) Quantification of the secondary xylem width (most-bottom base) in interfascicular part of one-month-old wild-type, *ahl15* and *ahl15 pPXY:IPT* (2 independent lines) main inflorescence stems. Colored dots indicate the average secondary xylem width of 3 random interfascicular region of an individual stem independent plants (n = 9), all the secondary xylem width are presenting the width average per line, horizontal lines indicate the mean and error bars indicate the s.e.m. Different letters indicate statistically significant differences (P < 0.01) as determined by a one-way ANOVA with Tukey's honest significant difference post hoc test. Scale bars indicate 0.05mm in A,B and 0.15 mm in D.

AHL15 promotes secondary growth independent of the PXY-WOX pathway

In Arabidopsis inflorescence stems, the *WUSCHEL HOMEOBOX RELATED 4 (WOX4)* and *WOX14* genes have been shown to promote the rate of cell division in the vascular cambium (Denis et al., 2017; Etchells et al., 2013; Campbell et al., 2016). Inflorescence stems from the *wox4 wox14* double mutant develop significantly less secondary xylem in the interfascicular regions (Etchells et al., 2013). In view of the co-expression of *WOX4*, *WOX14*, and *AHL15* in the *PXY* and *SMXL*5 cambium sub-domains (Fig. 5A) and the fact that loss-of-function mutant inflorescence stems show similar defects in cambium development, we investigated the genetic interaction between *AHL15* and *WOX4/WOX14* in controlling secondary xylem growth. Introduction of *pPXY:AHL15* into the *wox4 wox14 pxy* mutant background did not lead to enhanced secondary growth (Fig. 5B). This result indicated that *AHL15* is not responsible for promoting cell division downstream of *WOX4* and *WOX14*, but instead that the PXY-WOX4/14 pathway is required for AHL15 action. However, the *pWOX4:GFP* reporter, which normally labels the vascular bundles and the cambium cells in wild-type stems (Suer et al., 2011), did not show a clear difference in *ahl15* mutant inflorescences stems, indicating that the *WOX* genes are not downstream of AHL15 (Fig. 5C). Based on these experiments, we conclude that PXY-WOX and AHL15-IPT are parallel pathways that are mutually required to promote cell division in the interfascicular cambium of Arabidopsis inflorescence stems.

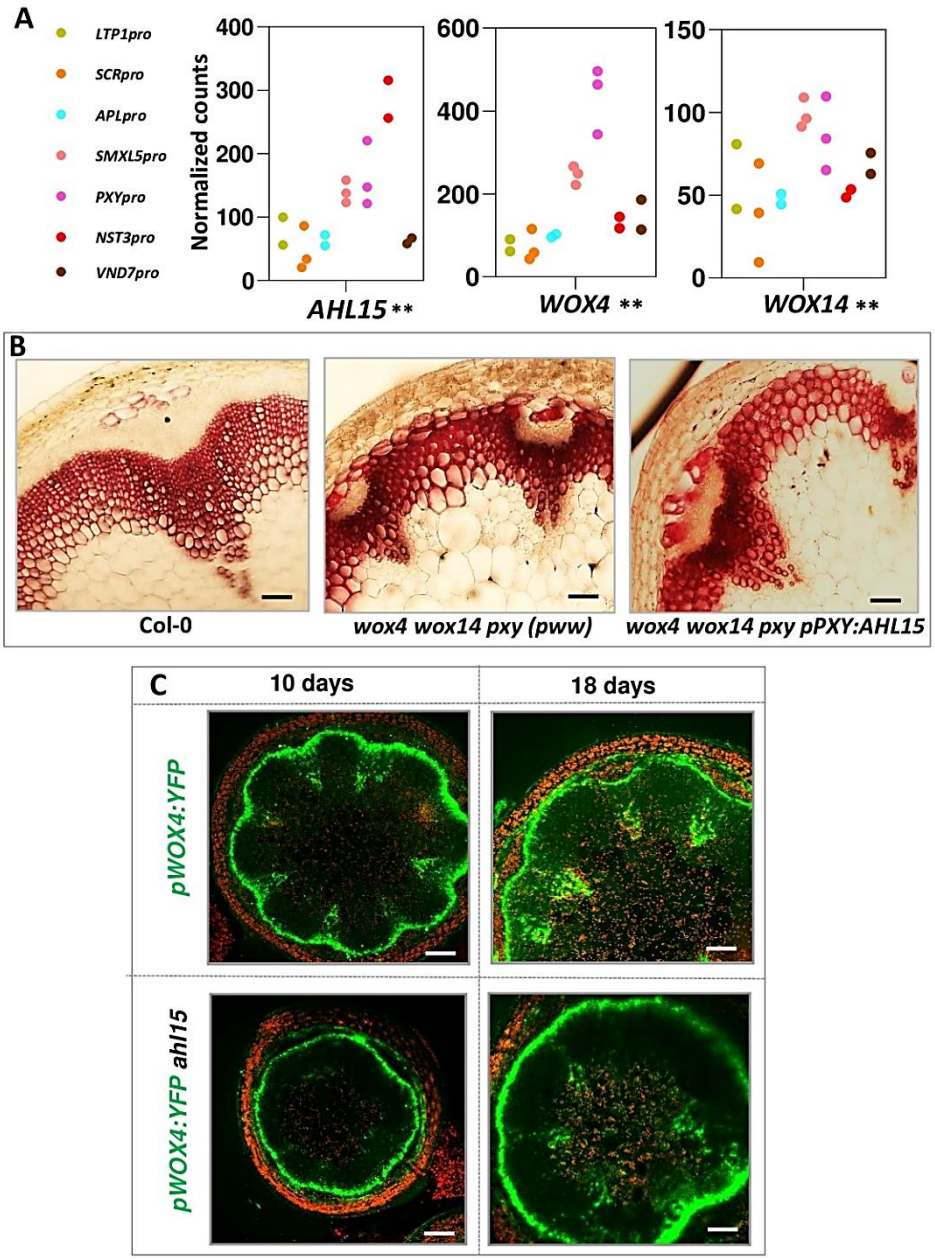

Fig. 5| *AHL15*-cytokinin and *PXY-WOX4,14* represent two parallel pathways regulating cambium activity. (**A**) Co-expression *AHL15*, *WOX4 and WOX14* at cambium and bundle domains. Colored dots indicate the values of two or three biological replicates of RNA isolation obtain by FANS. Normalized gene read counts of the indicated genes among seven different tissues displayed for each replicate individually. *, ** indicates p < 0.05 and 0.01, respectively in LRT (Shi et al., 2020). (**B**) Phloroglucinol-stained fresh cross-sections of most-bottom base of one-month-old wild-type (left) and *pxy wox4 wox14* (middle) and *pPXY:AHL15 pxy wox4 wox14* (right) inflorescence stems. (**C**) Confocal analyses shows activity of *pWOX4-GFP* at 10 and 18-day-old wild-type (up panel) and *ahl15* (low panel) stem. Scale bars indicates 0.06 mm in B and 0.09 mm.

***AHL15*-increased cytokinin biosynthesis possibly also promotes lateral branching.**

In our previous study, we have shown that the level of *AHL15* expression in AMs regulates their maturation from the vegetative to the reproductive phase. Enhancing *AHL15* expression by growing Arabidopsis plants in short-day conditions or placing the gene under the control of a stronger (AM-specific) promoter, delayed this maturation, resulting in increased vegetative development. Apart from this enhanced vegetative development, which prolongs plant longevity, we noticed that plants with enhanced *AHL15* expression also showed more branching (Karami et al., 2020b, chapter 2). The outgrowth of AMs into axillary buds and lateral branches depends on their activation from dormancy, which is known to be inhibited by the plant hormones auxin and strigolactones and to be promoted by cytokinin (Aguilar-Martínez et al., 2007; Gonzalez-Grandio et al., 2017). The Arabidopsis *MYB DOMAIN PROTEIN 2* (*AtMYB2*) gene was shown to inhibit the outgrowth of axillary buds at later stages of development by reducing the endogenous cytokinin levels (Guo and Gan, 2011). In view of the position of cytokinin biosynthesis downstream of AHL15 in promoting wood formation, we investigated whether this hormone also acts downstream of *AHL15* in lateral branching. The *ahl15* loss-of-function mutant showed a significant reduction in the number of AMs in the axils of cauline leaves growing out into lateral buds and developing lateral branches (Fig. 6A, B) (Aguilar-Martínez et al., 2007). In contrast, when we expressed *AHL15* under control of the *AtMYB2* promoter, transgenic plants produced significantly more lateral branches compared to wild-type plants (Fig.6 C, D). Expression analysis by qPCR showed that the cytokinin biosynthesis genes *IPT3*, *IPT7*, and *LOG5* were significantly up-regulated in the basal node of 6-week-old (6-week after germination) *pMYB2:AHL15* plants (10 days after flowering) compared to wild-type plants (Fig.6 E). These results suggest that *AHL15* similarly promotes lateral branching as it enhances secondary growth by increasing cytokinin biosynthesis.

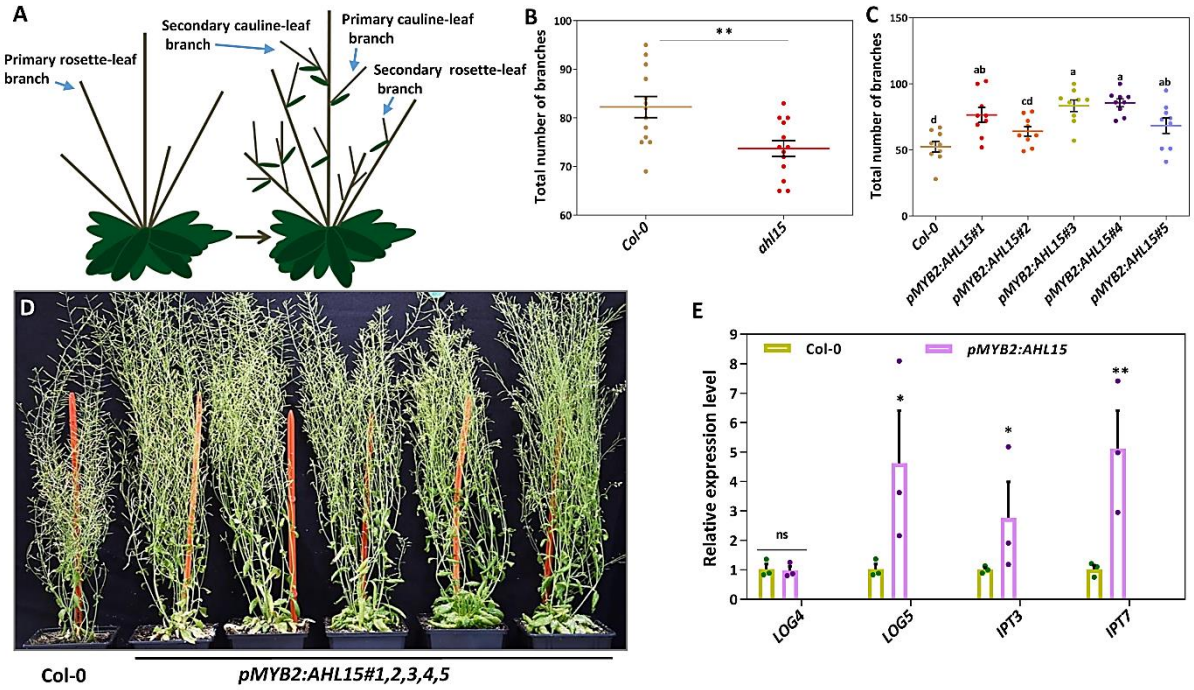

Fig. 6| *AHL15* promotes lateral branching most likely by activating cytokinin biosynthesis. (**A**) Schematic representation of the Arabidopsis architecture of lateral branches. (**B**,**C**) Quantification of the total number of lateral branches in three-month-old wild-type and *ahl15* plants (B) or in two-month-old wild-type and *pMYB2:AHL15* plants (5 independent transgenic lines) (**C**). The asterisks in (**B**) indicate a significant difference ($P < 0.001$) as determined by two-sided Student's *t*-test. Colored dots indicate the number of lateral branches per plant (n = 14 (in **B**) or 10 (in **C**) biologically independent plants), horizontal lines indicate the mean and error bars indicate the s.e.m. Different letters indicate statistically significant differences ($P < 0.01$) as determined by a one-way ANOVA with Tukey's honest significant difference post hoc test. (**D**) Shoot phenotype of two-month-old wild-type and *pMYB2:AHL15* plants (5 individual transgenic lines). (**E**) Relative expression of the cytokinin biosynthesis genes *LOG4*, *LOG5*, *IPT3* and *IPT7* by qPCR analysis in the ten-day-old stem base (basal node) of wild-type compare to *pMYB2:AHL15* plants (*$P < 0.05$, **$P < 0.01$, ns (not significant)), as determined by a two-sided Student's *t*-test.

Discussion

Understanding the molecular mechanisms regulating the activity and functioning of vascular cambium is fundamentally important because the woody biomass in plants derives from the activity of the vascular cambium. The cell division rate of the stem cells of the vascular cambium plays a crucial role in secondary growth: how active the stem cells are in the cambial zone can determine the amount of secondary growth or wood formation (Campbell et al., 2016; Chiang and Greb, 2019). Although previous studies have provided the first insight into the molecular basis regulating cambial activity, our fundamental insight into how initiating and regulated cambial stem cell activity has remained largely unknown.

In this study, we present the role of *AHL15* as a novel regulator in the control of interfascicular cambium activity and secondary xylem formation in Arabidopsis. In particular, in inflorescence stems of *ahl15* loss-of-function mutant plants, we observed a delay in cambium initiation and formation from parenchyma cells and a significant reduction in the

amount of secondary xylem formed. By contrast, inflorescence stems of *AHL15* overexpression plants developed an increased amount of secondary xylem. Our data suggest that the *AHL15* gene is a positive regulator of cambial cell proliferation and thereby an important determinant of secondary xylem formation in Arabidopsis inflorescence stems.

AHL15 belongs to a large family of *AHL* genes in Arabidopsis that have a high degree of functional redundancy among family members (Xiao et al., 2009; Zhao et al., 2013). In line with our recent observations on the redundant action of *AHL15* and other *AHL* genes in controlling axillary meristem maturation (Karami et al., 2020a, Chapter 2), and embryogenesis (Karami et al., 2020b), the results presented here suggest that *AHL* genes also act redundantly in regulating interfascicular cambium activity. The overlapping expression of *AHL15*, *AHL19*, *AHL20*, and *AHL28* in the *PXY*/*SMXL5*-marked cambium region of inflorescence stems is in line with their redundant role in controlling cambial cell proliferation. Despite this redundancy, and as observed for axillary meristem maturation (Karami et al., 2020a, Chapter 2), *AHL15* seems to play a key role in this process, since secondary growth is significantly reduced in the *ahl15* loss-of-function mutant background.

The cell division in the cambial zone is known to be controlled by both genetic and hormonal factors (Immanen et al., 2016; Oles et al., 2017; Fischer et al., 2019). Based on the current model, the TDIF-PXY-WOX and cytokinin/auxin pathways act in parallel to regulate cell division in the vascular cambium (Fig. 7) (Fischer et al., 2019). In the first pathway, the TDIF peptide, belonging to the CLE family of peptides, is produced in the phloem and subsequently transferred to the cambium where it binds to the PXY receptor-like kinase. Upon peptide binding, PXY activates the expression of the cambium-specific transcription factors WOX4 and WOX14, which promote cell proliferation in the cambium (Fig. 7). Our results show that AHL15 promotes the timing of cambial cell initiation, proliferation, and maintenance afterward in parallel to and dependent on the TDIF-PXY-WOX pathway by increasing the expression of cytokinin biosynthesis genes (Fig. 7). Interestingly, it has been shown that the cambial cell division and secondary xylem production are significantly increased upon elevated cytokinin levels in the stem of poplar trees (Immanen et al., 2016).

We have previously shown that the MADS-box transcription factors SOC1 and FUL repress AHL15 expression by directly binding to the AHL15 upstream and downstream regions (Karami et al., 2020b, Chapter 2). In addition, we show here that the enhanced secondary growth in the *soc1 ful* double mutant inflorescence stems is dependent on the presence of a functional *AHL15* gene, indicating that SOC1 and FUL also act as repressors of secondary growth upstream of *AHL15* (Fig. 7). We conclude that PXY-WOX and SOC1/FUL-AHL15-IPT are parallel pathways that are mutually required to promote cell division in the interfascicular cambium of Arabidopsis inflorescence stems.

It has been reported that AHL3-AHL4 heterodimers control the boundary between the procambium and xylem axis in Arabidopsis roots (Zhou et al., 2013). Single and double loss-of-function mutants of *AHL3* and *AHL4* display ectopic protoxylem vessels and ectopic metaxylem vessels in the procambial region adjacent to the xylem axis (Zhou et al., 2013). Since the cytokinin response is altered in the *ahl4* loss-of-function mutant and similar vascular defects have been observed for cytokinin-defective mutants (Zhou et al., 2013), this confirms the strong relationship between *AHL* genes and cytokinin in cambium initiation and cell division, and in the resulting xylem formation.

How exactly cytokinin promotes cambial cell divisions is still not understood. Cytokinin likely influences the cell cycle of the cambium stem cells. Because cytokinin and auxin usually work together, cytokinin may exert its effect on the cambial cell division by reducing the concentration of auxin in cambium cells by up-regulating the levels of PIN auxin efflux carriers (Šimášková et al., 2015). However, this should be confirmed by future studies.
Interestingly, we also observed a role for *AHL15* in promoting lateral branching, as loss-of-function resulted in a reduced number and overexpression in an increased number of lateral branches. AM-specific *AHL15* overexpression led to enhanced expression of the cytokinin biosynthesis genes *LOG5, IPT3*, and *IPT7*, which makes it tempting to speculate that cytokinin is also downstream of *AHL15* in this process. It has been reported that cytokinin promotes shoot branching by repressing BRC1 expression, which activates axillary buds (Dun et al., 2012; Ferguson and Beveridge, 2009)`However, more recently, cytokinin was also suggested to promote PIN PM abundance and thereby to enhance auxin efflux in axillary buds (Waldie and Leyser, 2018). It is, therefore, likely that *AHL15* and cytokinin act in the same pathway in regulating cambium and axillary meristem activity.
In conclusion, our studies show that *AHL* genes positively regulate both cambium activity and axillary meristem outgrowth in Arabidopsis, downstream of the SOC1 and FUL transcription factors and upstream of cytokinin biosynthesis. Our findings represent an important step forward in our understanding of the increased vascular cambium activity and shoot branching in *soc1 ful* mutant plants. In particular, our findings show that it is possible to increase secondary growth without affecting the flowering time and fruit and seed development of plants, which will eventually be helpful for plant biomass improvement.

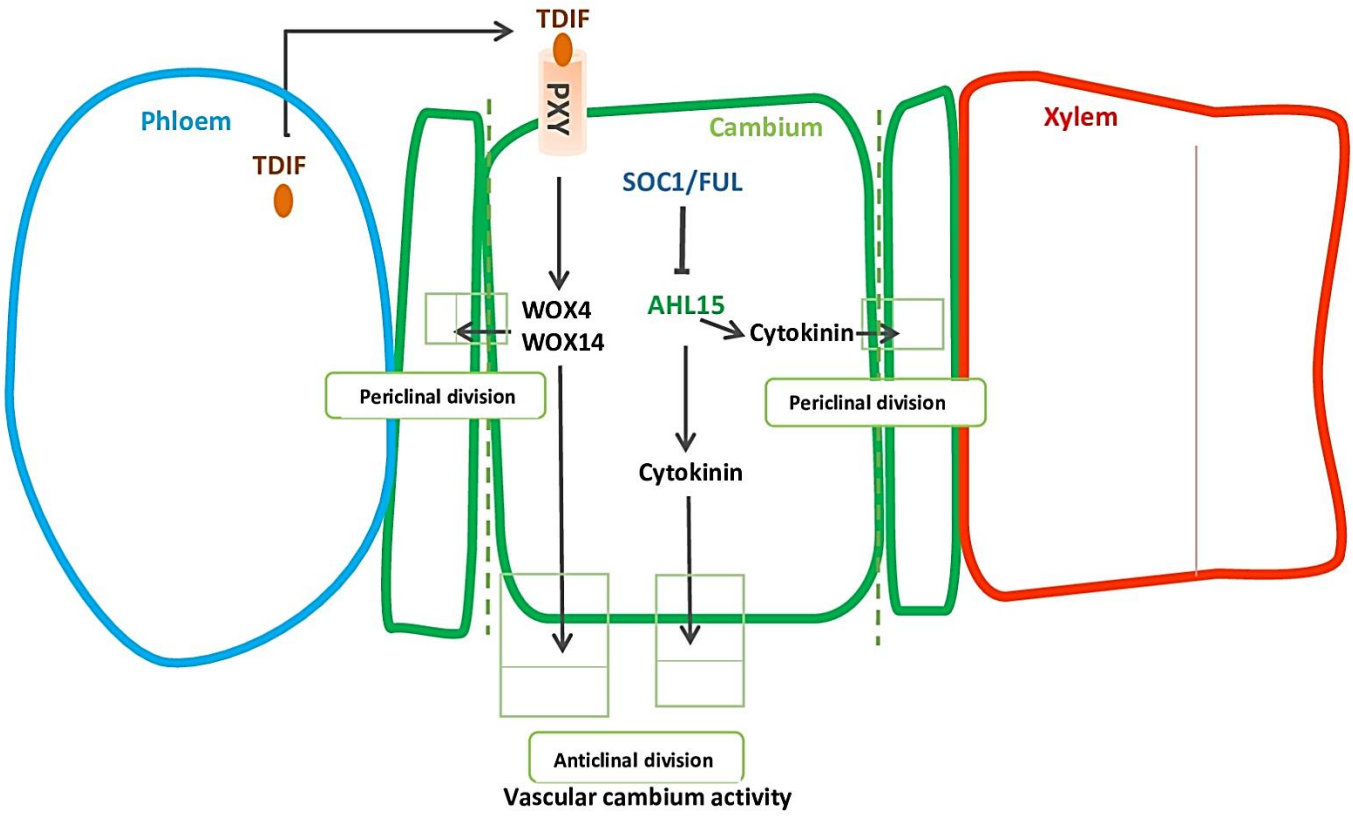

Fig. 7| Proposed model for *AHL15* and its key role in promoting cambium activity. Schematic drawing of the cambium area showing the phloem (blue), cambium (green), and xylem (red) cell types. Peptide TDIF is synthesized in the phloem and travels through the apoplastic space to the cambium cells, where it binds to the PXY receptor. PXY subsequently promotes the proliferation of the cambium cells by activating the expression of *WOX4* and *WOX14*. In a parallel pathway, the MADS box transcription factors SOC1 and FUL limit cambium activity by repressing *AHL15* expression. AHL15 in turn promotes both the periclinal and anticlinal cell division activity of the cambium by enhancing the expression of cytokinin biosynthesis genes. Blunt-ending lines indicate repression, arrows indicate promotion.

Methods

Plant material, growth conditions, and transgenic *Arabidopsis* lines

All Arabidopsis mutant- and transgenic lines used in this study are in the Columbia (Col-0) background. The *ahl15* mutant and the *pAHL15:AHL15*, *pAHL15:GUS*, *ahl15/+ pAHL15:AHL15-ΔG* transgenic lines (Karami et al., 2020b, Chapter 2) and the *p35S:AHL15* transgenic line (Karami et al., 2020a) were previously described. The *soc1-6 ful-7* double mutant (Melzer et al., 2008), the *pxy wox4 wox14* mutant and the *pTCS:GFP* (Bruno and Jen, 2008) and *pWOX4:YFP* (Suer et al., 2011) reporter lines were obtained from the Nottingham Arabidopsis Stock Centre (NASC). Seeds were surface sterilized with 40% bleach solution followed by four times washing with sterile water and germinated, after three days incubation at 4°C, on ½ MS (Murashige and Skoog, 1962) medium containing 1% sucrose, 0.7% agar at 21°C and a 16 hours photoperiod. Two-week-old seedlings were transferred to soil and grown at 21°C, 65% relative humidity and a 16 hours (long day: LD) photoperiod, and potted plants were photographed with a Nikon D5300 camera.

Plasmid construction

To generate the *pPXY:AHL15* and *pMYB2:AHL15* constructs, upstream regions of approximately 3 kb from the ATG initiation codon of the *PXY (AT5G61480)* or the *MYB2(AT2G47190)* genes were amplified from ecotype Columbia (Col-0) genomic DNA using the forward (F) and reverse (R) PCR primers indicated in Supplementary Table 1. The resulting fragments were first recombined into pDONR207 by a BP reaction and subsequently cloned upstream of the *AHL15* cDNA fragment in previously made destination vector *pGW-AHL15* (Karami et al., 2020b, Chapter 2) by a LR reaction according to Gateway cloning procedures (Clonetech). To generate the *pPXY:IPT* construct, the *AHL15* gene in the *pPXY:AHL15* construct was replaced by a *Kpn*I and *Xba*I flanked fragment containing the *IPT* gene from *Agrobacterium tumefaciens* (Van Der Graaff et al., 2001). All binary vectors were introduced into *Agrobacterium tumefaciens* strain AGL1 by electroporation (den Dulk-Ras and Hooykaas, 1995). Subsequently, Arabidopsis Col-0, *ahl15*, and *wox4wox14pxy* plants were transformed using the floral dip method (Clough and Bent, 1998).

RNA preparation and quantitative real-time PCR (qRT-PCR)

RNA was isolated from rosette base nodes, and the basal part of inflorescence stems (about 0.5 cm above rosette base) using the RNEasy© kit (Qiagen). First-strand cDNA was synthesized using the RevertAid RT Reverse Transcription kit (Thermo Fischer Scientific). Quantitative PCR was performed on three biological replicates along with three technical replicates using the SYBR-green dye premixed master-mix (Thermo Fischer Scientific) in a C1000 Touch© thermal cycler (BIO-RAD). CT values were obtained using Bio-Rad CFX manager 3.1. The relative expression level of genes was calculated according to the $2^{-\Delta\Delta Ct}$ method (Livak and Schmittgen, 2001), and expression was normalized by using the *β-TUBULIN-6* gene as a reference, analyzed and plotted into graphs in GraphPad Prism 8. The primers used for each gene are described in Supplementary Table 1.

Histology and microscopy

To analyze stem secondary growth and lignification, the base part (bottom-most) of the main inflorescence stem was cut and sectioned freshly using a razor blade (Wilkinson Sword) (very thin-fresh free-hand cross-sections), which were kept on the ice up to the staining in 3% phloroglucinol-HCL (0.3 g phloroglucinol, 10 ml absolute ethanol, 5 ml 37 % HCL), using a protocol from Mitra & Loqué 2014 (Pradhan Mitra and Loqué, 2014). Sections were further analyzed under a light microscope (Nikon eclipse Ci-E/Ci-L). The secondary xylem (SX) width was measured with ImageJ in the way three randomly selected interfascicular parts of the individual stem were measured and divided by 3 to have SX width per stem. For embedded sections, the basal part (bottom-most) of the 1or 2 -month old main inflorescence stem segments at least 1cm in length (including the stem base) were harvested and were fixed overnight in 4 % formaldehyde in a 50 mM phosphate solution. The stems were dehydrated in a graded ethanol series (70 %, 80 %, 90 %, 96 %, 100 %) and embedded in epoxy resin molds. Sections (3-4µm) cut by rotary microtome (Leica RM2265) were stained with 0.01 % aqueous toluidine blue, before being analyzed under a light microscope (Nikon eclipse Ci-E/Ci-L).

Histochemical β-glucuronidase (GUS) staining was performed as described previously (Anandalakshmi et al.,1998). The stem segments were cut one centimeter above the basal part and placed in the vial tubes containing cold acetone 90% on ice, after vacuum infiltration and keeping them on ice the protocol followed with two-time washing and vacuum infiltration afterward transferring to GUS staining solution (containing X-gluc), at the end staining reaction was allowed to proceed around 2 hours at 37°C in the dark. After rehydration in a graded ethanol series (75, 50, and 25 %), the stained tissues were cut freshly by razor blade (very thin-fresh free-hand cross-sections) and observed and photographed using a light microscope (Nikon eclipse Ci-E/Ci-L). For quantitative analyses, at least seven plants were analyzed for each data point. Cellular and subcellular localization of GFP and YFP protein in fresh hand section stem on microscopy slide covered with coverslip were visualized using the confocal laser scanning microscope (ZEISS-003-18533) with a 534 laser, 488 nm LP excitation and 500-525 nm BP emission filters for GFP and YFP signals. All Photo-based measurements performed in ImageJ then analyzed and plotted into graphs in GraphPad Prism 8.

Shoot branching quantification

Branches were counted either in 2 or 3-month-old plants. As a measure of axillary meristem activity, all branching instances were counted, as presented in Fig. 6A, primary rosette-leaf branches, secondary-cauline leaf branches, and secondary rosette-leaf branches counted and considered as a total number of branches per plant. Counted numbers analyzed and plotted into graphs in GraphPad Prism 8.

Transcriptome profiling of stem tissues

Based on what has been described by Shi et al., 2020, the free-hand cross-sections of the second bottom-most internode of one-month-old Arabidopsis inflorescence stems prepared. Sections belong to different GFP tagged promoter reporter lines (*NST3pro:H4-GFP, VND7pro:H4-GFP, PXYpro:H4-GFP, SMXL5pro:H4-GFP, APLpro:H4-GFP, SCRpro:H4-*

GFP, LTP1pro:H4-GFP) corresponding for xylem and interfascicular fiber, xylem vessels, proximal cambium, distal cambium, phloem region, starch sheath and epidermis respectively. GFP positive and negative nucleus confirmed by confocal microscopy, nucleus isolated (15,000 nuclei per sample), and sorted (three replicate for each sample type). After performing RNA isolation, cDNA library prepared for next-generation sequencing. FANS-derived datasets present in this chapter as an expression of a particular gene in transcriptome data stand for normalized gene read counts of the indicated genes among seven different tissues displayed for each replicate individually. *, ** indicates $p < 0.05$ and 0.01, respectively in likelihood-ratio test (LRT), null hypothesis to be rejected in the LRT is that among the seven different tissues, genes have similar expression. Read counts analyzed and plotted into graphs in GraphPad Prism 8.

Acknowledgements

We thank N. Savant and F. van der Klauw, for generating *PXY-AHL15* and *PXY-IPT* constructs respectively, Gerda Lammers and Merijn de Bakker for their help with microscopy. We are grateful to Ward de winter, Jan Vink, Nick Surtel and Mariel Lavrijsen for their supports.

Author contributions

A.R. designed and performed the majority of the Arabidopsis experiments, with contributions from T.W, A.L. T.W analyzed the *IPTs* expression level, A.L analyzed the *PXY-AHL15*. O.K. and R.O supervised the project. D.S and T.G generated the transcriptome profiling of stem tissues. A.R., O.K. and R.O. wrote the manuscript.

References

Aguilar-Martínez, J.A., Poza-Carrión, C., and Cubas, P. (2007). Arabidopsis BRANCHED1 acts as an integrator of branching signals within axillary buds. Plant Cell **19**: 458–472.

Altamura, M.M., Possenti, M., Matteucci, A., Baima, S., Ruberti, I., and Morelli, G. (2001). Development of the vascular system in the inflorescence stem of Arabidopsis. New Phytol. **151**: 381–389.

Anandalakshmi, R., Pruss, G. J., Ge, X., Marathe, R., Mallory, A. C., Smith, T. H., and Vance, V.B. (1998). A viral suppressor of gene silencing in plants. Proc. Natl. Acad. Sci. **95**: 13079--13084.

Baucher, M., El Jaziri, M., and Vandeputte, O. (2007). From primary to secondary growth: Origin and development of the vascular system. J. Exp. Bot. **58**: 3485–3501.

Bhalerao, R.P., Fischer, U., and Turner, S. (2016). Environmental and hormonal control of cambial stem cell dynamics. J. Exp. Bot. **68**: 79–87.

Brackmann, K. et al. (2018). Spatial specificity of auxin responses coordinates wood formation. Nat. Commun. **9**: 875.

Bruno, M. and Jen, S. (2008). Cytokinin and auxin interplay in root stem-cell specification during early embryogenesis. Nature **4**: 1094–1097.

Campbell, L., Turner, S., and Etchells, P. (2016). Regulation of vascular cell division. J. Exp. Bot. **68**: 27–43.

Chiang, M.H. and Greb, T. (2019). How to organize bidirectional tissue production? Curr. Opin. Plant Biol. **51**: 15–21.

Clough, S.J. and Bent, F. (1998). Floral dip: a simplified method for Agrobacterium-mediated transformation of Arabidopsis thaliana. Plant J. **16**: 735–743.

Denis, E., Kbiri, N., Mary, V., Claisse, G., Conde e Silva, N., Kreis, M., and Deveaux, Y. (2017). WOX14 promotes bioactive gibberellin synthesis and vascular cell differentiation in Arabidopsis. Plant J. **90**: 560–572.

Dewitte, W., Scofield, S., Alcasabas, A.A., Maughan, S.C., Menges, M., Braun, N., Collins, C., Nieuwland, J., Prinsen, E., Sundaresan, V., and Murray, J.A.H. (2007). Arabidopsis CYCD3 D-type cyclins link cell proliferation and endocycles and are rate-limiting for cytokinin responses. Proc. Natl. Acad. Sci. U. S. A. **104**: 14537–14542.

den Dulk-Ras, A. and Hooykaas, P.J. (1995). Electroporation of Agrobacterium tumefaciens. Methods Mol. Biol. **55**: 63–72.

Dun, E.A., Germain, A. de Saint, Rameau, C., and Beveridge, C.A. (2012). Antagonistic action of strigolactone and cytokinin in bud outgrowth control. Plant Physiol. **158**: 487–498.

El-Showk, S., Ruonala, R., and Helariutta, Y. (2013). Crossing paths: Cytokinin signalling and crosstalk. Dev. **140**: 1373–1383.

Elo, A., Immanen, J., Nieminen, K., and Helariutta, Y. (2009). Stem cell function during plant vascular development. Semin. Cell Dev. Biol. **20**: 1097–1106.

Etchells, J.P., Mishra, L.S., Kumar, M., Campbell, L., and Turner, S.R. (2015). Wood formation in trees is increased by manipulating PXY-regulated cell division. Curr. Biol. **25**: 1050–1055.

Etchells, J.P., Provost, C.M., Mishr, L., and Turner, S.R. (2013). WOX4 and WOX14 act downstream of the PXY receptor kinase to regulate plant vascular proliferation independently of any role in vascular organisation. Dev. **140**: 2224–2234.

Etchells, J.P. and Turner, S.R. (2010). The PXY-CLE41 receptor ligand pair defines a multifunctional pathway that controls the rate and orientation of vascularcell division. Development **137**: 767–774.

Ferguson, B.J. and Beveridge, C.A. (2009). Roles for auxin, cytokinin, and strigolactone in regulating shoot branching. Plant Physiol. **149**: 109.135475.

Fischer, U., Kucukoglu, M., Helariutta, Y., and Bhalerao, R.P. (2019). The dynamics of cambial stem cell activity. Annu. Rev. Plant Biol. **70**: 293–319.

Fisher, K. and Turner, S. (2007). PXY, a Receptor-like Kinase Essential for Maintaining Polarity during Plant Vascular-Tissue Development. Curr. Biol. **17**: 1061–1066.

Fujimoto, S., Matsunaga, S., Yonemura, M., Uchiyama, S., Azuma, T., and Fukui, K. (2004). Identification of a novel plant MAR DNA binding protein localized on chromosomal surfaces. Plant Mol. Biol. **56**: 225–239.

Gerttula, S., Zinkgraf, M., Muday, G.K., Lewis, D.R., Ibatullin, F.M., Brumer, H., Hart, F., Mansfield, S.D., Filkov, V., and Groover, A. (2015). Transcriptional and hormonal regulation of gravitropism of woody stems in populus. Plant Cell **27**: 2800–2813.

Gonzalez-Grandio, E., Pajoro, A., Franco-Zorrilla, J.M., Tarancon, C., Immink, R.G.H., and Cubas, P. (2017). Abscisic acid signaling is controlled by a BRANCHED1/HD-ZIP i cascade in Arabidopsis axillary buds. Proc. Natl. Acad. Sci. U. S. A. **114**: E245–E254.

Van Der Graaff, E.E., Auer, C.A., and Hooykaas, P.J.J. (2001). Altered development of Arabidopsis thaliana carrying the Agrobacterium tumefaciens ipt gene is partially due to ethylene effects. Plant Growth Regul. **34**: 305–315.

Guo, Y. and Gan, S. (2011). AtMYB2 regulates whole plant senescence by inhibiting cytokinin-mediated branching at late stages of development in Arabidopsis. Plant Physiol. **156**: 1612–1619.

Hirakawa, Y., Kondo, Y., and Fukuda, H. (2010). TDIF peptide signaling regulates vascular stem cell proliferation via the WOX4 homeobox gene in Arabidopsis. Plant Cell **22**: 2618–2629.

Immanen, J. et al. (2016). Cytokinin and auxin display distinct but interconnected distribution and signaling profiles to stimulate cambial activity. Curr. Biol. **26**: 1990–1997.

Jouannet, V., Brackmann, K., and Greb, T. (2015). (Pro)cambium formation and proliferation: Two sides of the same coin? Curr. Opin. Plant Biol. **23**: 54–60.

Karami, O., Rahimi, A., Khan, M., Bemer, M., Hazarika, R.R., Mak, P., Compier, M., van Noort, V., and Offringa, R. (2020a). A suppressor of axillary meristem maturation promotes longevity in flowering plants. Nat. Plants **6**: 368–376.

Karami, O., Rahimi, A., Mak, P., Horstman, A., Boutilier, K., Compier, M., Van der Zaal, B., and Offringa, R. (2020b). An Arabidopsis AT-hook motif nuclear protein mediates somatic-to-embryonic cell fate conversion coinciding with genome duplication. bioRxiv. **Nature com**: https://www.biorxiv.org/content/10.1101/2020.01.03.

Livak, K.J. and Schmittgen, T.D. (2001). Analysis of relative gene expression data using real-time quantitative PCR and the 2(-Delta Delta C(T)) Method. Methods **25**: 402–408.

Matsumoto-Kitano, M., Kusumoto, T., Tarkowski, P., Kinoshita-Tsujimura, K., Václavíková, K., Miyawaki, K., and Kakimoto, T. (2008). Cytokinins are central regulators of cambial activity. Proc. Natl. Acad. Sci. U. S. A. **105**: 20027–20031.

Matsushita, A., Furumoto, T., Ishida, S., and Takahashi, Y. (2007). AGF1, an AT-hook protein, is necessary for the negative feedback of AtGA3ox1 encoding GA 3-oxidase. Plant Physiol. **143**: 1152–1162.

Melzer, S., Lens, F., Gennen, J., Vanneste, S., Rohde, A., and Beeckman, T. (2008). Flowering-time genes modulate meristem determinacy and growth form in Arabidopsis thaliana. Nat. Genet. **40**: 1489–1492.

Miyashima, S., Sebastian, J., Lee, J.Y., and Helariutta, Y. (2013). Stem cell function during plant vascular development. EMBO J. **32**: 178–193.

Miyawaki, K., Tarkowski, P., Matsumoto-Kitano, M., Kato, T., Sato, S., Tarkowska, D., Tabata, S., Sandberg, G., and Kakimoto, T. (2006). Roles of Arabidopsis ATP/ADP isopentenyltransferases and tRNA isopentenyltransferases in cytokinin biosynthesis. Proc. Natl. Acad. Sci. U. S. A. **103**: 16598–16603.

Ng, K.-H., Yu, H., and Ito, T. (2009). AGAMOUS controls GIANT KILLER, a multifunctional chromatin modifier in reproductive organ patterning and differentiation. PLoS Biol. **7**: e1000251.

Nieminen, K., Blomster, T., Helariutta, Y., and Mähönen, A.P. (2015). Vascular cambium development. Arab. B. **13**: e0177.

Oh, S., Park, S., and Han, K.H. (2003). Transcriptional regulation of secondary growth in Arabidopsis thaliana. J. Exp. Bot. **54**: 2709–2722.

Oles, V., Panchenko, A., and Smertenko, A. (2017). Modeling hormonal control of cambium proliferation. PLoS One **12**: 1–21.

Poulios, S. and Vlachonasios, K.E. (2018). Synergistic action of GCN5 and CLAVATA1 in the regulation of gynoecium development in Arabidopsis thaliana. New Phytol. **220**: 593–608.

Pradhan Mitra, P. and Loqué, D. (2014). Histochemical staining of Arabidopsis thaliana secondary cell wall elements. J. Vis. Exp.: e51381.

Ragni, L. and Greb, T. (2018). Secondary growth as a determinant of plant shape and form. Semin. Cell Dev. Biol. **79**: 58–67.

Randall, R.S. et al. (2015). AINTEGUMENTA and the D-type cyclin CYCD3;1 regulate root secondary growth and respond to cytokinins. Biol. Open **4**: 1229–1236.

Robson, P.R.H., Donnison, I.S., Wang, K., Frame, B., Pegg, S.E., Thomas, A., and Thomas, H. (2004). Leaf senescence is delayed in maize expressing the Agrobacterium IPT gene under the control of a novel maize senescence-enhanced promoter. Plant Biotechnol. J. **2**: 101–112.

Rybel, B.D., Mähönen, A.P., Helariutta, Y., and Weijers, D. (2015). Plant vascular development : from early specification to differentiation. Nat. Rev. Mol. Cell Biol. **17**: 30–40.

Shi, D., Jouannet, V., Agustí, J., Kaul, V., Levitsky, V., Sanchez, P., Mironova, V. V, and Greb, T. (2020). Tissue-specific transcriptome profiling of the Arabidopsis thaliana inflorescence stem reveals local cellular signatures. bioRxiv **preprint d**: https://doi.org/10.1101/2020.02.10.941492.

Shi, D., Lebovka, I., Lopez-Salmeron, V., Sanchez, P., and Greb, T. (2019). Bifacial cambium stem cells generate xylem and phloem during radial plant growth. Dev. **146**: 1–8.

Šimášková, M. et al. (2015). Cytokinin response factors regulate PIN-FORMED auxin transporters. Nat. Commun. **6**.

Street, I.H., Shah, P.K., Smith, A.M., Avery, N., and Neff, M.M. (2008). The AT-hook-containing proteins SOB3/AHL29 and ESC/AHL27 are negative modulators of hypocotyl growth in Arabidopsis. Plant J. **54**: 1–14.

Suer, S., Agusti, J., Sanchez, P., Schwarz, M., and Greb, T. (2011). WOX4 imparts auxin responsiveness to cambium cells in arabidopsis. Plant Cell **23**: 3247–3259.

T, M. and F, S. (1962). A revised medium for rapid growth and bio assays with tobacco tissue cultures. Physiol. Plant. **15**: 473–497.

Tonn, N. and Greb, T. (2017). Radial plant growth. Curr. Biol. **27**: R878–R882.

Waldie, T. and Leyser, O. (2018). Cytokinin targets auxin transport to promote shoot branching. Plant Physiol. **177**: 803–818.

Wallner, E.-S., Jouannet, V., and Greb, T. (2019). SUPPRESSOR OF MAX2 1-LIKE 5 promotes secondary phloem formation during radial stem growth. **JAN**: 14670.

Wang, N., Bagdassarian, K.S., Doherty, R.E., Kroon, J.T., Connor, K.A., Wang, X.Y., Wang, W., Jermyn, I.H., Turner, S.R., and Etchells, J.P. (2019). Organ-specific genetic interactions between paralogues of the PXY and ER receptor kinases enforce radial patterning in arabidopsis vascular tissue. Dev. **146**: 10.1242.

Xiao, C., Chen, F., Yu, X., Lin, C., and Fu, Y.-F. (2009). Over-expression of an AT-hook gene, AHL22, delays flowering and inhibits the elongation of the hypocotyl in Arabidopsis thaliana. Plant Mol. Biol. **71**: 39–50.

Zhao, J., Favero, D.S., Peng, H., and Neff, M.M. (2013). Arabidopsis thaliana AHL family modulates hypocotyl growth redundantly by interacting with each other via the PPC/DUF296 domain. Proc. Natl. Acad. Sci. **110**: E4688–E4697.

Zhou, J., Wang, X., Lee, J.-Y., and Lee, J.-Y. (2013). Cell-to-cell movement of two interacting AT-hook factors in Arabidopsis root vascular tissue patterning. Plant Cell **25**: 187–201.

Zhou, Y., Liu, X., Engstrom, E.M., Nimchuk, Z.L., Pruneda-Paz, J.L., Tarr, P.T., Yan, A., Kay, S.A., and Meyerowitz, E.M. (2015). Control of plant stem cell function by conserved interacting transcriptional regulators. Nature **517**: 377–380.

Zürcher, E., Tavor-Deslex, D., Lituiev, D., Enkerli, K., Tarr, P.T., and Müller, B. (2013). A robust and sensitive synthetic sensor to monitor the transcriptional output of the cytokinin signaling network in planta. Plant Physiol. **161**: 1066–1075.

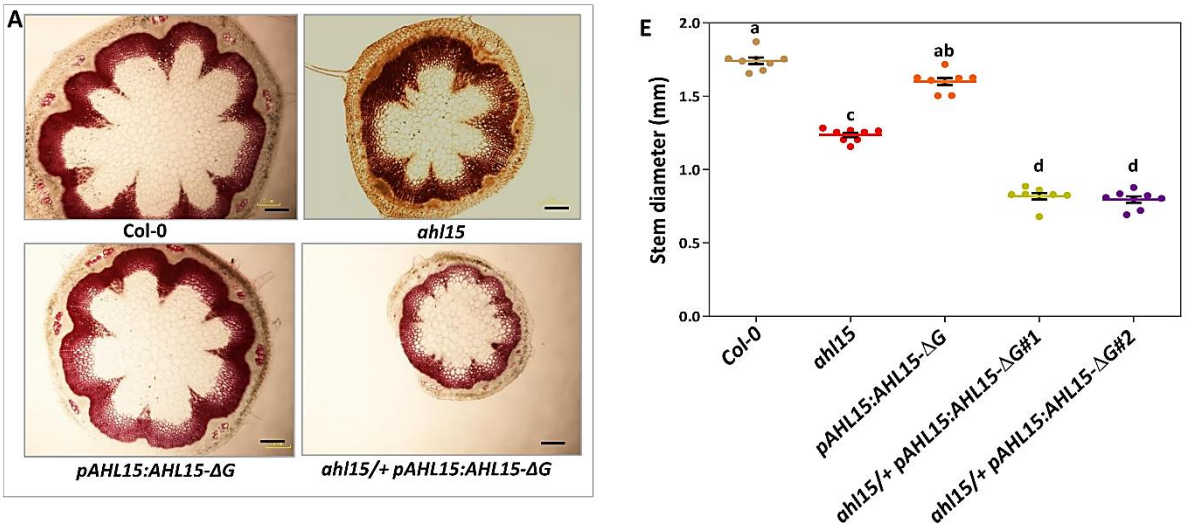

Supplementary Figure 1| *AHL* genes are essential for secondary growth of Arabidopsis inflorescence stems. (A) Phloroglucinol-stained fresh cross-sections of most-bottom base of one-month-old wild-type (up panel, left), *ahl15* (up panel, right), *pAHL15:AHL15-ΔG* (down panel, left), and *ahl15/+ pAHL15:AHL15-ΔG* (down pane, right) inflorescence stems. (B) Quantification of the stem diameter in one-month-old stem wild-type, *ahl15*, *pAHL15:AHL15-ΔG*, and *ahl15/+ pAHL15:AHL15-ΔG* plants. Colored dots indicate the number of lateral branches per plant (n = 14 (in B) or 10 (in C) biologically independent plants), horizontal lines indicate the mean and error bars indicate the s.e.m. Different letters indicate statistically significant differences ($P < 0.01$) as determined by a one-way ANOVA with Tukey's honest significant difference post hoc test. Scale bars indicate 0.15 mm.

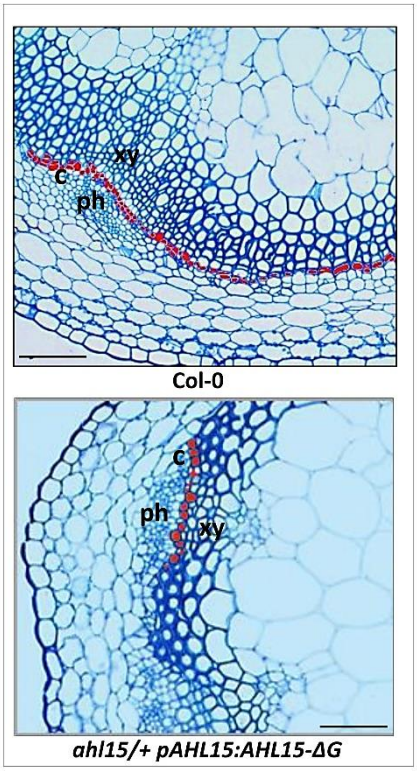

Supplementary Figure 2| *ahl15/+ pAHL15:AHL15-ΔG* displays normal and organized structure of bundle and interfascicular region compare to wild-type along with delay in cambium initiation. Toluidine blue-stained cross-sections of most-bottom base of two-week-old wild-type (upper) and *ahl15/+ pAHL15:AHL15-ΔG* (lower) inflorescence stems. The red dots mark the cambium/procambial cells in the interfascicular and bundle regions of wild-type and *ahl15/+ pAHL15:AHL15-ΔG* respectively. Scale bars indicate 0.05mm.

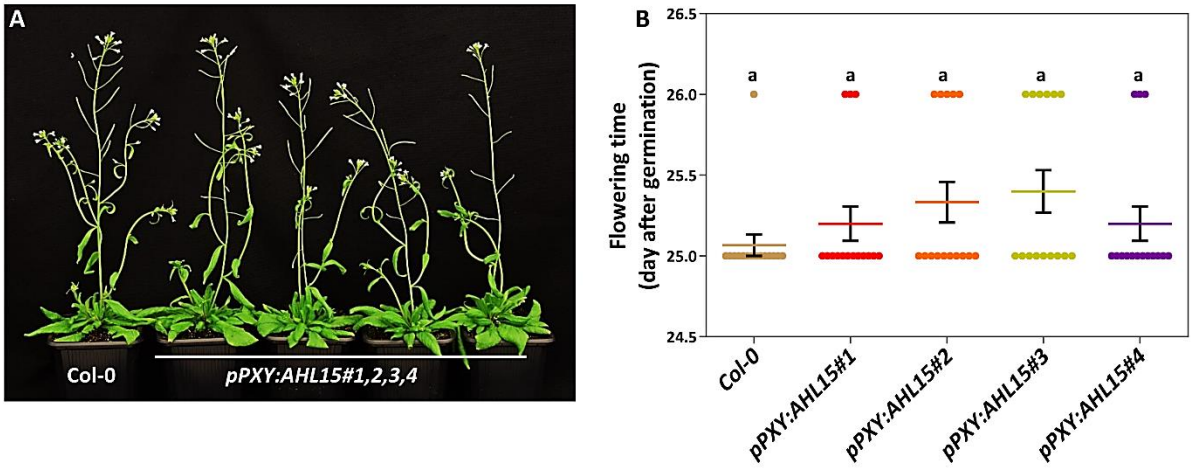

Supplementary Figure 3| Cambium-specific *AHL15* overexpression does not affect branching or flowering time in Arabidopsis. (A) The shoot phenotype of 5-week-old wild-type and *pPXY:AHL15* (4 independent lines) plants. (B) Quantification of the flowering time of wild-type and *pPXY:AHL15* plants, as presented in (A). Colored dots indicate the flowering time of individual plants in days after germination (n = 15 independent plants per line), horizontal lines indicate the mean and error bars indicate the s.e.m. Different letters indicate statistically significant differences ($P < 0.05$) as determined by a one-way ANOVA with Tukey's honest significant difference post hoc test.

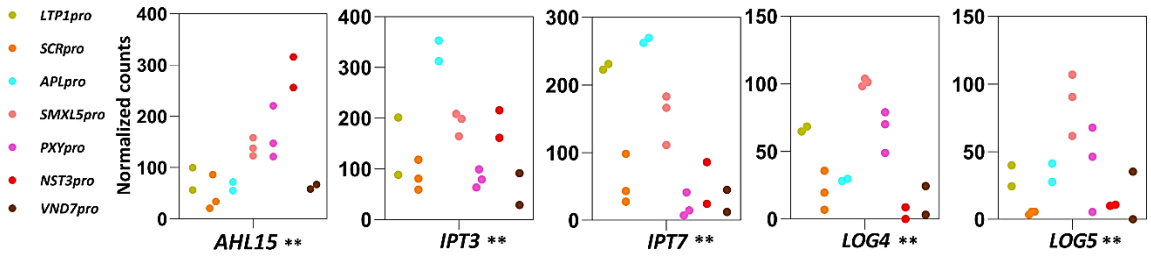

Supplementary Figure 4| *AHL15* and cytokinin biosynthesis genes are co-expressed in the cambium domain. Co-expression of *AHL15* with *IPT3*, *IPT7, LOG4* and *LOG5* at cambium and bundle domains. Colored dots indicate the values of two or three biological replicates of RNA isolation obtain by FANS. Normalized gene read counts of the indicated genes among seven different tissues displayed for each replicate individually. *, ** indicates $p < 0.05$ and 0.01, respectively in LRT (Shi et al., 2020).

Supplementary Table 1. Primers used for cloning, genotyping and qRT-PCR

Name*	Sequence (5' to 3')	Purpose
PXY-Promoter-F	GGGGACAAGTTTGTACAAAAAAGCAGGCTGCCATACTGTCATCTTGTACCAG	*pPXY:AHL15 construct*
PXY-Promoter-R	GGGGACCACTTTGTACAAGAAAGCTGGGTACGTAGCTTTTAGAAAGAAATTA	
KpnI-IPT-F	AAAGGTACCATGGACCTGCATC	*pPXY:IPT construct*
IPT-XbaI-R	AAATCTAGA CTAATACATTCCGAACG	
MYB2-Promoter-F	GGGGACAAGTTTGTACAAAAAAGCAGGCTCGGACGAGATTGTGGGTTCTAC	*pMYB2:AHL15 construct*
MYB2-Promoter-R	GGGGACCACTTTGTACAAGAAAGCTGGGTATTCTTATAAAGAAACTTTAAATG	
q IPT3-F	GTGGATGCGACTCCAGTCTT	qRT-PCR *IPT3*
q IPT3-R	CACTAGACACCGCGACAACT	
q IPT7-F	GACGCCACTGAGGTGTTCTT	qRT-PCR *IPT7*
q IPT7-R	TGGGCTCTACTTCCACTTCC	
q LOG4-F	GGTTTGCTTTGTAATGATTTCTGGG	
q LOG4-R	ACTTCCTTAGATGGGCAAAACACGC	qRT-PCR *LOG4*
q LOG5-F	TCAAACCATCTCAGCGTCAC	qRT-PCR *LOG5*
q LOG5-R	AGGGCAATCTCAGTCTGCAT	

*, F: forward; R: reverse.

Summary

Plant architecture has distinct forms in different plant species, but also within a species the final architecture of a plant is determined by its gradual development and changes therein induced by environmental conditions during the plant's life cycle. Higher plants have the ability to continually produce new organs and tissues during their lifetime. This unique ability is provided by pools of stem cells organized in so-called meristems. Primary meristems located at apices of the plant body are involved in elongation of the main plant axes, whereas secondary meristems in lateral positions play a role in branching and axis thickening. This meristem activity leads to the development of stems, leaves, branches, and inflorescences. **Chapter 1** of this thesis reviews current advances in our understanding of the molecular mechanisms that regulate plant meristems and their developmental phase transitions. Two main developmental phase transitions are distinguished during post-embryonic plant development. Upon germination, development starts with the juvenile seedling phase, and during the juvenile to adult vegetative phase transition (1) the plant acquires reproductive competence, allowing the plant to subsequently undergo the vegetative to reproductive phase transition (2), which ends with gametogenesis. The shoot apical meristem (SAM) is presented as the main regulator of these developmental phase changes. But also the importance of the shoot axillary meristems (AMs) located in axils of leaves is discussed, as AMs support the formation of secondary shoots (branches) and are important determinants of plant longevity. **Chapter 1** also discusses the procambium and cambium meristems, which continuously generate the major plant vascular tissues, xylem and phloem, via asymmetric periclinal cell divisions. The regulatory mechanisms and factors behind cambium meristem initiation and dynamics are shortly described. Following the reproductive phase and seed set, ageing monocarpic plants (flower only once) undergo senescence, which eventually leads to plant death. In contrast, polycarpic plants (flower more than once) maintain a number of vegetative AMs to support subsequent cycles of growth and to prolong their life span. The structure and function of the *Arabidopsis thaliana* (Arabidopsis) *AT-HOOK MOTIF NUCLEAR LOCALIZED* (*AHL*) gene family is introduced in **chapter 1**, and that of family member *AHL15* described and studied more in detail in **chapter 2**. *AHL15* in Arabidopsis encodes a nuclear protein containing a single DNA-binding AT-hook motif in the N-terminal part and plant- and prokaryote-conserved (PPC) domain at the C-terminus. The PPC domain contributes to physical interaction with other AHLs or nuclear proteins, whereas the AT-hook motif interacts with DNA at AT-rich stretches. In **chapter 2** we show a novel role for *AHL15* as a suppressor of AM maturation, as demonstrated by the reduced longevity phenotypes of single *ahl15* or multiple *ahl* loss-of-function mutants. In contrast, high expression of *AHL15* suppresses AM maturation, resulting in increased longevity in monocarpic Arabidopsis and *Nicotiana tabacum* (tobacco). Detailed analysis and observation showed that *AHL15* function is essential for suppression of AM maturation in the long living, polycarpic Arabidopsis *soc1 ful* double mutant. As expected, *AHL15* acts directly downstream of the flowering genes *SOC1* and *FUL* and in part by suppressing the biosynthesis of the growth- and ageing hormone gibberellic acid. We further compared the expression of the *AHL* gene family in Arabidopsis with that of its close polycarpic relative *Arabidopsis lyrata*. Surprisingly, the expression of several *AHL* genes (*AHL15*, *AHL17*, *AHL19*, *AHL20*, and *AHL27*) was significantly higher in rosette nodes of flowering *Arabidopsis lyrata* plants compared with seedlings, which was not the case in Arabidopsis, suggesting that differential regulation of *AHL* genes in AMs results in different life histories.

Chapter 3 discusses ageing in flowering plants, defined by different developmental phase transitions. The switch from the juvenile to the adult vegetative phase, also referred to as the vegetative phase change (VPC), is marked in Arabidopsis by changes in leaf morphology, with small, round juvenile leaves lacking abaxial trichomes turning into adult leaves that are elongated, serrated, and carry trichomes on the back side of the leaves. During the juvenile-to-adult transition, *miR156/157* expression gradually decreases, and that of their target *SQUAMOSA-PROMOTER BINDING PROTEIN-LIKE* (*SPL*) genes increases to promote plant ageing. An *ahl15* loss-of-function mutant showed early VPC. In contrast, high expression of *AHL15* delayed VPC and flowering in Arabidopsis and tobacco. Expressing *AHL15* under control of a SAM-specific promoter revealed that AHL15 changes the VPC and flowering time by a direct effect on the SAM. AHL15 appeared to repress *SPL* expression independent of the miRNA pathway, and SPLs in turn suppress *AHL*s, suggesting a negative feedback loop between *AHL15* and *SPL*s. Overall, in **chapter 3** we identified a new branch of the ageing pathway in Arabidopsis, in which the longevity-promoting AHL15 protein represses ageing independent of *miR156/157*. **Chapter 4** of this thesis focuses on *AHL15*'s effect on Arabidopsis vascular cambium activity and secondary growth. Detailed analysis showed that in an *ahl15* loss-of-function mutant, interfascicular secondary growth is significantly reduced. In contrast, *AHL15* overexpression remarkably increases secondary xylem formation. A more detailed analysis revealed the unique expression pattern of *AHL15* in the Arabidopsis cambium ring. To confirm this pattern, we expressed *AHL15* under a cambium-specific promoter, *pPXY*, resulting in enhanced secondary-xylem formation in *pPXY:AHL15* stems compared to wild type stems. More interestingly, we confirmed that *AHL15* function is necessary for extensive wood formation in the *soc1ful* double mutant. As explained in **chapter 2,** *AHL15* is downstream of SOC1 and FUL. Close observations of the mechanisms for low or high secondary xylem in *ahl15* loss-of-function or *AHL15* overexpression lines, respectively, showed involvement of cytokinin, a central regulator of cambium activity and secondary growth. In our gene expression analysis, levels of the *IPT* cytokinin biosynthesis genes were low in *ahl15* and high in *pPXY:AHL15*, indicating that AHL15, by increasing cytokinin biosynthesis, enhances secondary xylem in Arabidopsis. Our findings support a novel cambium regulation pathway, in which *AHL15* acts downstream of SOC1 and FUL and upstream of *IPT* and *LOG* genes to enhance cambium activity and wood formation in the Arabidopsis stem. In addition, we show that the SOC1/FUL-AHL15-cytokinin pathway is also involved in the regulation of AM activity.

Samenvatting

De architectuur van planten kent verschillende vormen in verschillende plantensoorten. Maar ook binnen één soort wordt de uiteindelijke architectuur van een plant bepaald door de geleidelijke ontwikkeling en veranderingen daarin veroorzaakt door omgevingsfactoren tijdens de levenscyclus van de plant. Hogere planten kunnen tijdens hun leven voortdurend nieuwe organen en weefsels aanmaken. Dit unieke vermogen wordt geleverd door stamcellen die in zogenaamde meristemen georganiseerd zijn. Primaire meristemen aan de apicale uiteinden van de plant verzorgen de lengtegroei van de plant, terwijl secundaire meristemen in laterale posities een rol spelen bij vertakking en verdikking. Deze meristeemactiviteit leidt tot de ontwikkeling van stengels, bladeren, takken en bloeiwijzen. **Hoofdstuk 1** van dit proefschrift bespreekt de huidige kennis van de moleculaire mechanismen die de meristemen in planten en hun ontwikkelingsfaseovergangen reguleren. Tijdens post-embryonale ontwikkeling worden twee belangrijke faseovergangen onderscheiden. Na ontkieming begint de ontwikkeling van de plant met de juveniele zaailingfase en tijdens de overgang van de juveniele naar volwassen vegetatieve fase (1) verwerft de plant reproductieve competentie, waardoor de plant vervolgens de vegetatieve naar reproductieve faseovergang kan ondergaan (2). De reproductieve fase eindigt met gametogenese. Het scheut apicale meristeem (SAM) staat bekend als de belangrijkste regulator van deze ontwikkelingsfaseovergangen. Maar ook het belang van de axillaire meristemen (AMn) in de oksels van bladeren wordt besproken, omdat AMn de secundaire scheuten (vertakkingen) vormen en bepalend zijn voor de levensduur van de plant. **Hoofdstuk 1** bespreekt ook de procambium- en cambiummeristemen, die via asymmetrische periclinale celdelingen de belangrijkste vaatweefsels van planten, xyleem en floëem genereren. De regulerende mechanismen en factoren achter cambium meristeeminitiatie en -dynamiek worden kort beschreven. Na de reproductieve fase en zaadzetting ondergaan monocarpe planten (bloeien slechts één keer) veroudering, wat uiteindelijk tot de dood van de plant leidt. Daarentegen houden polycarpe planten (bloeien meer dan eens) een aantal AMn in de vegetatieve fase, en dit stelt hen in staat om in de daaropvolgende groeicyclus weer uit te groeien en daarmee hun levensduur te verlengen. De structuur en functie van de *Arabidopsis thaliana* (Arabidopsis) *AT-HOOK MOTIF NUCLEAR LOCALIZED* (*AHL*) genfamilie wordt geïntroduceerd in **hoofdstuk 1**, en die van familielid *AHL15* wordt beschreven en in meer detail bestudeerd in **hoofdstuk 2**. *AHL15* codeert voor een nucleair eiwit met een AT-hook motief in het N-terminale deel en een in planten en prokaryoten geconserveerd (PPC) domein aan het C-terminale uiteinde. Het PPC-domein draagt bij aan fysieke interactie met andere AHL- of nucleaire eiwitten, terwijl het AT-hook motief AT-rijke stukken in het DNA bindt.

In **hoofdstuk 2** laten we een nieuwe rol zien voor AHL15 als onderdrukker van de maturatie van AMn, zoals blijkt uit de verkorte levensduur van enkelvoudige *ahl15*- of meervoudige *ahl*-verlies-van–functie mutanten. Hoge expressie van *AHL15* onderdrukt daarentegen AM maturatie, wat resulteert in een langere levensduur van monocarpe Arabidopsis en *Nicotiana tabacum* (tabak). Gedetailleerde analyses toonden aan dat *AHL15* essentieel is voor het onderdrukken van AM-rijping in de langlevende en polycarpe Arabidopsis *soc1 ful* dubbelmutant. Zoals verwacht werkt *AHL15* direct stroomafwaarts van de bloeigenen *SOC1* en *FUL* en gedeeltelijk door de biosynthese van het groei- en verouderingshormoon gibberelline te onderdrukken. Een vergelijking van de expressie van de *AHL* genfamilie in Arabidopsis en in de verwante polycarpe soort *Arabidopsis lyrata* liet zien dat de expressie van een aantal *AHL* genen (*AHL15*, *AHL17*, *AHL19*, *AHL20* en *AHL27*) significant hoger was in rozetknoppen van bloeiende *Arabidopsis lyrata*-planten in vergelijking met zaailingen. In Arabidopsis bleek

daarentegen de expressie van dezelfde genen juist laag in AMn en hoger in zaailingen. Dit suggereert dat differentiële regulatie van *AHL* genen in AMn bepalend is voor de langlevendheid en de reproductiestrategie van planten.

Hoofdstuk 3 bespreekt de veroudering bij bloeiende planten gekenmerkt door de verschillende ontwikkelingsfaseovergangen. De overgang van de juveniele naar de volwassen vegetatieve fase, ook wel de vegetatieve faseverandering genoemd, wordt in Arabidopsis gemarkeerd door veranderingen in de bladmorfologie, waarbij kleine ronde jonge bladeren zonder abaxiale trichomen veranderen in volwassen bladeren die langwerpig en gekarteld zijn, en trichomen op de onderkant dragen. Tijdens de overgang van het juveniele naar volwassen stadium neemt de expressie van *miR156 / 157* geleidelijk af en die van de *SQUAMOSA-PROMOTER BINDING PROTEIN-LIKE* (*SPL*) doel genen toe, wat de veroudering van planten bevordert. Een verlies-van-functie *ahl15* mutant liet een vroege vegetatieve faseverandering zien, terwijl hoge expressie van *AHL15* de vegetatieve faseverandering en bloei in Arabidopsis en tabak vertraagde. Door *AHL15* onder controle van een SAM-specifieke promotor tot expressie te brengen, kon worden aangetoond dat *AHL15* de vegetatieve faseverandering en bloeitijd kan veranderen door een direct effect op de SAM. AHL15 bleek de expressie van *SPL* genen onafhankelijk van *miR156 / 157* te onderdrukken, en SPL eiwitten bleken op hun beurt de expressie van *AHL* genen te onderdrukken. Er is dus een reciproke negatieve feedback tussen *AHL15* en *SPL* genen. Concluderend hebben we in **hoofdstuk 3** een nieuwe tak van de verouderingsroute in Arabidopsis ontdekt, waarin het AHL15 eiwit de levensduur van de plant verlengt door veroudering onafhankelijk van *miR156 / 157* te onderdrukken. **Hoofdstuk 4** van dit proefschrift focust op het effect van AHL15 op de vasculaire cambiumactiviteit en de secundaire groei in Arabidopsis. Gedetailleerde analyse toonde aan dat in een *ahl15* verlies-van-functie mutant de interfasculaire secundaire groei aanzienlijk is verminderd. Daarentegen leidt overexpressie van *AHL15* tot een opmerkelijke verhoging van secundair xyleemvorming. Een meer gedetailleerde analyse liet zien dat *AHL15* in de cambium-ring tot expressie komt. Cambium-specifieke expressie van *AHL15* onder de *pPXY* promoter resulteerde in een verhoogde vorming van secundair xyleem. Interessant genoeg bleek *AHL15* ook verantwoordelijk te zijn voor de verhoogde houtvorming in de langlevende *soc1 ful* dubbel mutant. Zoals beschreven in **hoofdstuk 2**, staat *AHL15* onder controle van de SOC1 en FUL transcriptiefactoren. Een verdere analyse van het mechanisme verantwoordelijk voor weinig of veel secundair xyleem in respectievelijk *ahl15* verlies-van-functie mutanten of *AHL15* overexpressielijnen toonde aan dat het plantenhormoon cytokinine ook in dit geval als centrale regulator van cambiumactiviteit en secundaire groei functioneert. De expressie van de *IPT* cytokinine biosynthesegenen was laag in de *ahl15* mutant en hoog in *pPXY: AHL15* planten, wat aangeeft dat AHL15 secundaire xyleemvorming in Arabidopsis stimuleert door de cytokininebiosynthese te verhogen. Onze resultaten leggen een nieuw mechanisme voor de regulatie van secundaire groei in planten bloot, waarbij SOC1 en FUL de expressie van *AHL15* onderdrukken, en AHL15 op zijn beurt de cytokininebiosynthese stimuleert om daarmee cambiumactiviteit en houtvorming in Arabidopsis-stengels te bevorderen. Tevens laten we zien dat de SOC1/FUL-AHL15-cytokinine-route ook betrokken is bij de regulering van AM-activiteit.

Curriculum vitae

Arezoo Rahimi was born on January 18, 1987, in Dehgolan/Laylakh (Iran). After graduating from the Khadijeh high school at Dehgolan (Iran) in 2006, she studied general biology at the University of Razi (Kermanshah, Iran), where she obtained her BSc degree in 2011. She continued her studies at the Faculty of Science of Tehran Science and Research University (Sanandaj branch, Iran), where she received her MSc degree in plant cellular and molecular genetics in 2013. For her master project (2013), she studied the involvement of the Arabidopsis *AT-HOOK MOTIF CONTAINING NUCLEAR LOCALIZED 15* (*AHL15*) gene in auxin activity and plant ageing in the Plant Developmental Genetics group of Prof. dr. Remko Offringa at the Institute of Biology Leiden (IBL), Leiden University, The Netherlands. In September 2015, she started her PhD research under the supervision of Prof. Dr. Remko Offringa. During her PhD research, she focused on the functional analysis of *AHL* genes in Arabidopsis, as is described in this PhD thesis with the title 'Novel role of the *AT-HOOK MOTIF NUCLEAR LOCALIZED 15* gene in Arabidopsis meristem activity and longevity'. From September 2019 on, she is working as a postdoc in the laboratory of Dr. Salma Balazadeh at the IBL.

Acknowledgment

The journey of a PhD study is full of challenges, wishes, frustrations, charms, and hopes. This four years period of time is made by those people who made me smile or upset, but they are all appreciated since I became stronger and stronger.

Foremost, I would like to express my sincere gratitude to my supervisor **Prof. Remko Offringa**, for allowing me to work in his lab for my master internships, which were the starting point of my real scientific life, and for his continuous support and guidance during my PhD study and research.

My special thanks is going to **Dr. Omid Karami** for his support during my master and PhD studies. I learned a lot from you, Omid.

I appreciate **Ward de Winter** (the heart of department) for his endless help. I will never forget your help while I had the back pain during lab work. Also thanks to **Gerda Lamers** for her help with microscopy, and to **Jan Vink**, **Marielle Lavrijsen** and **Nick Surtel** for their technical support.

To my students and lab mates of the Plant Developmental Genetics group, and also other members of the plant cluster, thanks for fun and support.

My thanks also go to my 2nd promotor **Prof. Paul Hooykaas** for his scientific feedback and kind support.

I want to thank Hein (receptionist), for his smiles and positive energy at the beginning of day.

I acknowledge the people who mean a lot to me, my parents, my father who is no longer alive to see what I achieved, but for sure he is aware of that, my mother **Fati goli** for her selfless love.

I'm thankful to my mother and family-in-law for their support.

Thanks to my brother for his care, dedicated efforts and encourages which contributed a lot to the completion of my thesis.

I owe deep thanks to a very special person, my beloved husband, who understands me like no other, who supports my every dream. I am just happy to have you by my side.

Arezoo Rahimi, Leiden
September 2020